Development of Guidance for Air Flow Network Modelling to Improve Domestic Decentralised Mechanical Extract Ventilation Design

Energy Systems Research Unit

University of Strathclyde, Glasgow, United Kingdom

Thesis submitted for the degree of Doctor of Philosophy

Muhammad Zaeem Farooq

muhammad.zaeem@strath.ac.uk

29th May 2024

Declaration

This thesis is the result of the author's original research. It has been composed by the author and has not been previously submitted for examination which has led to the award of a degree.

Signed: Zaeem

Date: May 29, 2024

Acknowledgements

I would like to express my deepest gratitude to my supervisor, Dr Paul Tuohy, for his guidance and support throughout these years. My heartfelt thanks also go to my colleagues in offices JW605 and JW804, as well as the ESRU staff, particularly Dr Aizaz Samuel, Dr Jon Hand, Dr Daniel Costola, and Dr Mohammed Reda, who all contributed greatly to my professional development and academic progress.

I am especially grateful to Prof Tim Sharpe for offering me opportunities to participate in research projects on domestic ventilation—experiences that truly helped me grow as a researcher. The insights and expertise of my colleagues Barbara Lantschner and Dr Linda Toledo enriched my work; in particular, Dr Toledo’s mentorship consistently motivated me to push forward.

I would also like to extend my appreciation to my colleagues at the University of Sheffield, particularly Dr Abigail Hathway, whose perspectives and guidance benefited my PhD research in numerous ways.

On a personal note, my parents have shown exceptional patience, kindness, and understanding. Their support and well-wishes have been a foundation stone of my journey. To my brothers, especially Umer, thank you for all the encouragement, support, and kindness you’ve shown. Lastly, I would like to thank my wife and daughters for their understanding, love, and the many ways they have helped me through this journey.

Without all of you, this work would have been immeasurably more difficult. Thank you.

Abstract

The current domestic decentralised mechanical ventilation (dMEV) design, mandated by Scottish Building Regulations section 3.14, is aimed at providing occupants with adequate ventilation.

However, studies have shown that in practice dMEV systems do not serve the intended purpose, with issues in design and construction process, and occupant interactions.

This thesis directly addresses deficiencies in the ventilation design process. The use of Airflow Network (AFN) methods in design are common in non-domestic but not in domestic design. This is largely due to the perceived complexity of AFN modelling as well as a lack of standardised guidance of domestic applications.

The primary aim of this thesis was to investigate the application of AFN in domestic design, establish a knowledge base and methods, and make recommendations and propose guidance for effective utilisation of AFN in domestic ventilation design.

A literature review was carried out into current domestic ventilation performance, the use of AFN for ventilation design, standards and regulations, and relevant research, which highlighted poor performance, gaps, and ambiguities, plus a lack of studies directly relevant to the domestic design paradigm.

A dataset was sourced from a domestic dMEV monitoring study which included design, construction, occupant behaviour, and carbon dioxide (CO_2) monitoring. The monitoring was for two distinct periods, one with normal occupancy (logged through an occupant diary) and one with specified settings for occupant-controlled components.

A modelling study was designed to investigate the application of AFN using this dataset as a reference point. Different configurations of AFN model and underpinning equations and parameter settings were investigated, reflecting the ambiguities found in literature, statistical analysis applied, and useful insights generated. The key results indicate that with an appropriately configured AFN, there is a significant increase in the model's accuracy. The main findings suggest that the errors for the metabolic CO2 concentration can be up to 53%.

The literature and the findings from the modelling study were both used to inform a set of recommendations and provide guidance on effective application of AFN to address the deficiencies in current design methods with a higher accuracy

The primary focus in the thesis was the use of AFN in design for the provision of adequate ventilation using a dMEV system. However, applicability of the findings for the wider

application of AFN for overheating and energy performance and applicability for different system types such as MVHR were discussed.

This work contributes to the field by presenting guidance to assist modellers in conducting effective AFN-based ventilation design studies, directly addressing critical gaps in current practices. Limitations of the research include reliance upon a single dataset and this study would require broader validation across different building types and ventilation systems. Future work can focus on the expansion of applicability of AFN methods to other system types such as Mechanical Ventilation with Heat Recovery (MVHR) and exploring their role concerning overheating and energy performance issues.

Contents

List of Figures

List of Tables

List of Acronyms

ADF	Approved Document F
AFN	Airflow Network
AIM	Alberta Infiltration Model
ASHRAE	American Society of Heart Refrigeration and Air Conditioning Engineers
ASTM	American Society for Testing and Materials
BES	Building Energy Simulation
BS	Building Standards
BSD	Building Standards Division
BSI	Building Standards International
CFD	Computational Fluid Dynamics
CIBSE	Chartered Institute of Building Service Engineers
CV(RMSE)	Coefficient of Variation of the Root Mean Squared Error
DCLG	Department for Communities and Local Government
dMEV	Decentralised Mechanical Extract Ventilation
DSY	Design Summer Year
EPW	Energy Plus Weather
GBG	Good Building Guide
IAQ	Indoor Air Quality
IC	Influence Coefficient
IEQ	Indoor Environmental Quality
IPMVP	International Performance Measurement and Verification Protocol
ISO	International Standards Organisation
IZO	Interzone Opening
LBL	Lawrence Berkeley Laboratory
MAE	Mean Absolute Error
MAPE	Mean Absolute Percentage Error
MBE	Mean Bias Error
MVHR	Mechanical Ventilation with Heat Recovery
NMBE	Normalized Mean Bias Error
NR	Noise Reduction
PMV	Predicted Mean Vote
POE	Post Occupancy Evaluation
PPM	Part Per Million
PS	Stack Pressure
PVC	Polyvinyl Chloride
RH	Relative Humidity
SBS	Sick Building Syndrome
SD	Standard Deviation
SEAM	Statistical Effective Area Model
SGDV	Supporting Guidance for Domestic Ventilation
SP	Sound Pressure
STC	Sound Transmission Class
TL	Transmission Loss
TM	Technical Memoranda
TMY	Typical Met Year
TRY	Test Reference Year
TSL1	Technical Standard L1
TUS	Time Use Survey
TV	Trickle Vent
UC	Undercut
VOC	Volatile Organic Compound
WHO	World Health Organisation

Chapter 1 Introduction

People spend over 90% of their time indoors and a significant proportion of this time in their bedrooms (Katsoyiannis & Cincinelli, 2019). The indoor air quality (IAQ) experienced by the occupants of a space can have implications on their health (NICE, 2020). In a domestic setting, larger proportion of the time is spent in bedrooms, while sleeping, and night-time IAQ effects the next day performance of an individual (Strøm-Tejsen et al., 2016). Ventilation performance of any space has also gained higher importance due to the recent COVID-19 pandemic. (Buonanno et al., 2020) suggests higher ventilation rates can mitigate the risk of transmission. However this measure would increase the energy usage of the buildings which subsequently would affect the targets to reduce carbon emissions (UNFCCC, 2015). There should be a balance set for IAQ and carbon emissions of the domestic stock.

To propose enhancements to ventilation design and other various assessments, building energy simulation (BES) techniques are employed by designers, engineers and architects (J. Clarke, 2007). Theory behind airflow physics and its application in BES is well documented in CIBSE documentations: (CIBSE, 2021) and (CIBSE AM10, 2005) however these guidance need an update to provide straightforward and unambiguous details to effectively model the flow and pressure components (Baeumle & Hunt, 2018).

1.1 Background

Energy efficient dwelling design is widely adopted to meet carbon emission cut targets set by the governments. For example, UK aims to reduce these emissions by 77% by 2035 as compared to 1990 levels (UK Government, 2023). This strategy of dwelling design leads to various indoor environmental quality (IEQ) issues due to the increased insulation and airtightness measures. The key metrices include indoor thermal quality, lighting quality, indoor air quality (IAQ) and indoor acoustics quality. These factors are crucial for occupants' wellbeing and comfort (Al horr et al., 2016; Gonzalo et al., 2022; Mewomo et al., 2023; Wu et al., 2023). The ventilation provision affecting IAQ which subsequently impacts the health of the occupants is the primary focus of this thesis.

In the UK houses, ventilation strategies are generally classified into natural ventilation, mechanical ventilation or combination of both (Scottish Government, 2017). Natural ventilation relies on passive flow of air through windows and vents. Mechanical systems include centralised and decentralised inlet or extract ventilation. This work focuses on decentralised mechanical extract ventilation (dMEV) systems, commonly implemented in modern airtight buildings. However, the flow components such as trickle vents, windows, doors, door undercuts and extract fans are commonly part of all ventilation designs.

With the implementation of airtight building design, buildings standards have set provision for minimum ventilation in domestic buildings. For instance in England and Wales, a minimum ventilation rate of 0.3 l/s/m^2 of internal floor area or 13 l/s if volume flow of air for one room dwelling is suggested (HM Government 2010). Similarly, the Scottish Regulations recommend a minimum trickle vent effective flow area of 11,000 mm^2 in habitable rooms (Scottish Government, 2023).

Trickle vents are small slit openings which can be closed off when required. However, the building regulations suggest keeping them open to allow extract fans in the wet rooms to assist background ventilation. These regulations are further discussed in detail in Chapter 3. The dMEV system relies on continuous mechanical extraction in wet rooms and background ventilation through trickle vents in habitable room, creating a planned airflow path throughout the dwelling as shown in the figure below:

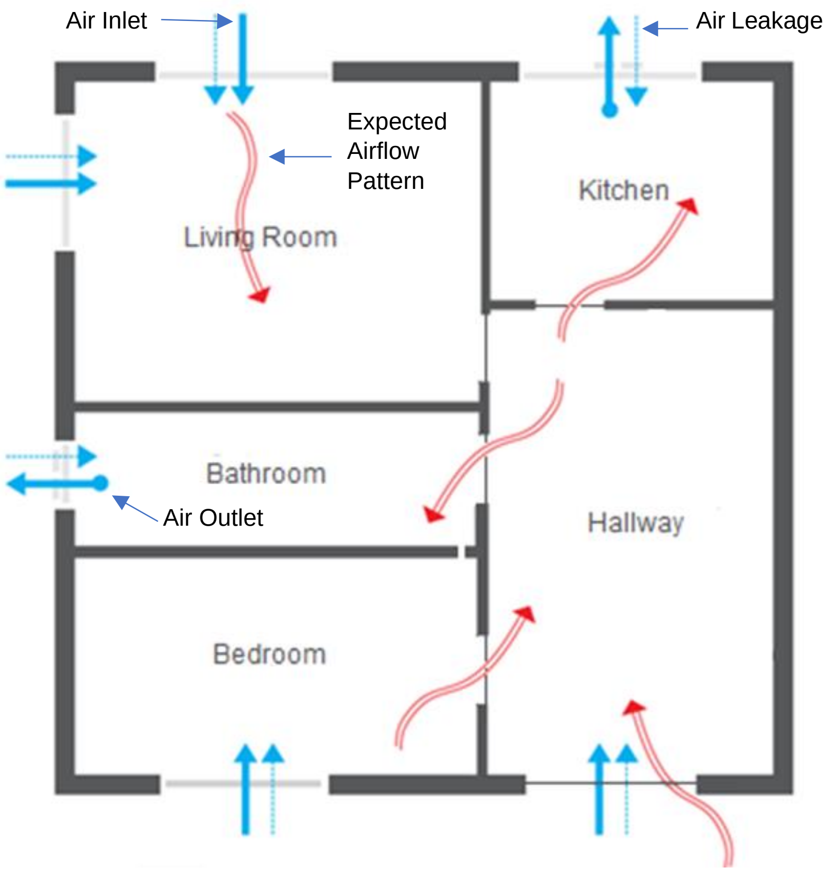

Figure 1.1: Flow inlets (trickle vents), pathways, and extract points of a typical one-bedroom single storey house.

Such a ventilation design relies on the occupants' discretion to operate. Secondly building design and construction practices has a gap as well. For example T. Sharpe et al. (2015) shows how door undercuts can be blocked off by carpets, cutting off whole air flow path which runs from trickle ventilators to door undercuts (if door is closed) to constant running extracts in the wet rooms. In such scenarios, even if occupants keep trickle vents open as well as keep extracts on constant running mode, this decentralised mechanical extract ventilation (dMEV) design is failed. This points towards the fragility of this system. However, this fragility can be reduced by introducing shorted or low resistive pathways from inlet to the outlet. For this purpose, acoustic interzone openings are available. A detailed discussion is presented under section 2.8.

Assessing the performance of different ventilation systems often involves measuring metabolic CO_2 concentrations in dwellings. These measurements are used as an indicator of IAQ because it's a readily measurable tracer gas representing occupancy levels. However, there are limitations to solely rely on CO_2 as it does not account for pollutants such as volatile organic compounds (VOCs) or particulate matter, which effect IAQ and occupant's health.

Post occupancy evaluations of built environment of dwellings can help to provide data for deductive and inductive analysis. Data from these studies can inform models to predict ventilation performance under various scenarios, aiding in the development of effective ventilation strategies.

Building airflow design can be assessed through simulation and modelling techniques such as computational fluid dynamics (CFD) and AFN. Such techniques are effective as they can predict working of a ventilation design – in design stage as well in post occupancy evaluations. Air flow modelling is mainly done either by CFD simulations or air flow network (AFN) methods. Both strategies are validated and are in practice. CFD can be more accurate as it divides the zones into several control volumes creating a mesh. Ekren et al. (2017) used CFD in ventilation evaluation study where they assessed effectiveness by changing the locations of the vents and extract fans. But this method is heavy on resources, time, and effort.

AFN methods can predict flow rates, pressures, and contaminant concentrations using a network of airflow paths and nodes, solving mass and energy balance equations. AFN can model metabolic activities of in conjunction with mass balance approaches. While AFN may be less detailed than CFD, it is efficient enough for modelling whole building airflow, making it suitable for this study's scope (Gu, 2007). AFN can sufficiently model trickle vents, door gaps, and dMEV systems, which are integral components of the ventilation strategy under investigation. However, the use of correct flow equations and coefficients is deemed important. Furthermore, AFN assumes well mixed air within zones and may not capture localised airflow patterns (while CFD can), which is a limitation to consider (L. Wang & Chen, 2007).

This work will use the AFN method to develop models involving airflow and indoor CO_2 concentrations, incorporating weather (boundary conditions) and occupancy patterns (internal loads). The aim is to provide insights into various modelling approaches. The modelling investigation shows simplistic vs proposed modelling and simulation results. Simplistic approaches would define flow components without a justification for the equation and coefficients use. For example, use of default discharge coefficient of 0.6 to model a slot opening including trickle vents (Arendt et al., 2017; Karava et al., 2004). Also, the weather and occupancy load are defined without due consideration of regulatory documents, for example an averaged weather dataset to assess building performance in extreme conditions (Bocanegra-Yanez, 2018). By comparing the impact of these approaches on the outcomes, this investigation ultimately contributing towards a guidance for effective ventilation strategies in energy efficient dwellings – specifically equipped with dMEV.

1.2 Problem Statement

Vastly implemented dMEV system is inefficient to main safe indoor air quality (IAQ) levels hence modelling techniques can be used to propose a working ventilation system. However, current airflow modelling guidance do not provide modellers to effectively model air flow passages hence resulting in a higher error in the simulation outputs. The reliance on the uninformed tunning of inputs to reduce discrepancy between simulation and monitoring outputs results in a not-fit-for-purpose design.

1.3 Research Question

How to conduct an effective AFN modelling study to devise improvements in a dMEV ventilation design?

1.4 Aims and Objectives

The overall aim of the work is to investigate ventilation performance in domestic buildings and propose guidelines to be used in AFN simulation for ventilation design.

For the accomplishment of this aim following set of objectives are defined:

1. To understand domestic ventilation design limitations and occupant's influence on its effectiveness.
2. To identify the shortcomings and ambiguities in building airflow modelling practices.
3. To compare solutions of simplistic and proposed airflow modelling approaches alongside validation testing with measured values.
4. To formulate guidance for "close-to-reality" AFN simulation which will help to suggest an effective ventilation design in dwellings.
5. To propose an alternative solution for adequate ventilation provision to the occupants – concerning the widely adopted and current decentralised mechanical extract ventilation (dMEV) system.

1.5 Scope of the Research

This thesis focuses on state-of-the-art dMEV design in UK residential settings, using indoor CO_2 levels as a proxy for ventilation efficacy. Whole house AFN modelling is employed with occupancy simulated only in the main bedroom, analysing outputs like pressure differentials, flow rates, and CO_2 concentrations to investigate modelling strategies.

1.6 Thesis Approach

In this section, the approach is presented in four stages, with the corresponding chapter of this thesis indicated. This is done by the help of a visually summarised flow chart (Figure 1.2) which outlines the thesis approach with an indication of these stages. These stages are subsequently detailed.

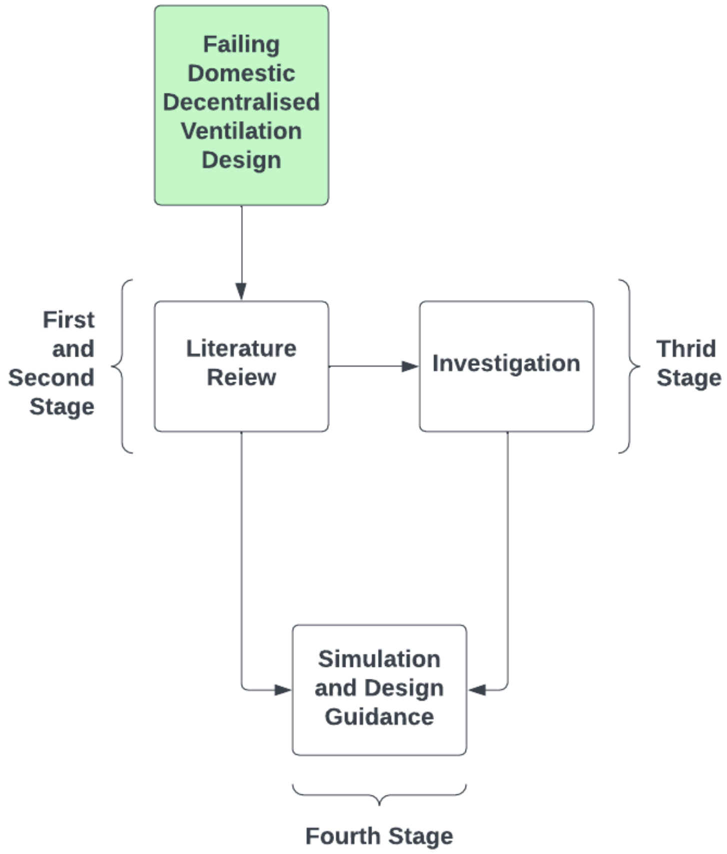

Figure 1.2: Thesis approach as per stages elaborated in the section. The flow chart highlights the inspiration behind the undertaken study i.e., failing dMEV design in a domestic setting.

The first stage (described in Chapter 2) involves a literature review which provides grounds to explore the problem, map possible solutions, and thereby addresses the aim of this thesis. This review examines the following:

- The mention of indoor air quality field investigations which allows to assess implications of inadequate ventilation provision.

- A critique of the literature dealing with experimental and numerical airflow measurements and solutions via the airflow pathways, part of the current dMEV design.
- The AFN simulation techniques in practice and validity of their inputs to the models.
- Statistical approaches to evaluate the validity and variance of different modelling approaches.

At the end of first stage, the review outcomes are presented which are aimed to be utilised in conjunction with proposed statistical analysis methodology, feeding into an AFN modelling guidance.

<u>The second stage</u> (outlined in Chapter 3) reviews current ventilation design guidance in combination with post occupancy evaluation surveys and data. This involves the following steps:

- A review of the ventilation design in the Scottish Building Regulation Handbook.
- A comparison and critique of ventilation design amongst various regulatory and standard documents.
- An evaluation of design guides/regulatory documents in conjunction with post occupancy evaluation studies highlighting design shortcomings and performance gap issues.
- Highlighting the insufficiency of guidance from the CIBSE Application Manual 10 (AM10) to conduct a domestic ventilation design and modelling study.

<u>The third stage</u>, (presented in Chapter 4 with results discussion in Chapter 5) outlines an AFN modelling methodology which investigates and applies the proposed approaches.

- A step-by-step approach is taken in which complexity in the model is added sequentially.
- A CO_2 concentration solution is used to assess the performance of the modelling approach.
- Physical and statistical analyses are employed together to highlight the factors affecting the simulation outputs.

<u>The fourth stage</u> (explained in Chapter 6) combines the literature review findings and modelling study data to present AFN modelling guidance which is aimed to complement the existing literature. An example is presented using the guidance to demonstrate the improvements to the ventilation design.

1.7 Outcomes and Contribution

This thesis makes the following original contributions to the field of residential ventilation design and modelling:

Critical Evaluation of Ventilation Design Guidelines: Through a comprehensive critique of current ventilation design practices, particularly within the Scottish Building Regulations and other regulatory documents, this research aims to identify specific shortcomings and performance gaps in existing dMEV systems. It highlights the insufficiency of guidance from the CIBSE Application Manual 10 (AM10) for conducting effective domestic ventilation design and modelling studies.

Integration of Monitored Data with Modelling Approaches: By utilising post occupancy monitoring dataset, the study bridges the gap between real world ventilation performance and simulation models.

Development of a Sequential/Iterative AFN Modelling Methodology: A step-by-step AFN modelling methodology is proposed, where complexity is added sequentially. This approach allows for systematic investigation of modelling strategies. This helps in assessing the influence of various modelling parameters on simulation outputs, specifically CO_2 concentrations.

Application of Combined Physical and Statistical Analyses: The research evaluates the validity and variance of different AFN modelling approaches by employing both physical and statistical analyses.

Development of AFN Modelling Guidance: The thesis presents clear and practical guidance for modelling integral AFN elements. This guidance is designed to complement existing literature and addresses the non-prescriptive nature of current modelling practices.

1.8 Proposal of Improved Ventilation Design

An example application of the developed AFN modelling guidance is provided which highlights enhancements to ventilation design capable of maintaining safer indoor CO_2 concentration levels during winter months.

1.9 Overall Methodology

This section has outlined the methodological framework employed to investigate the aim and objectives described in section 1.4. The research is systematically sub-divided into several stages shown in Figure 1.3. Each stage is defined to ensure a comprehensive approach towards the exploration of improved ventilation provision in the UK domestic settings, the assessment of AFN modelling methods, and the application of an alternative ventilation design.

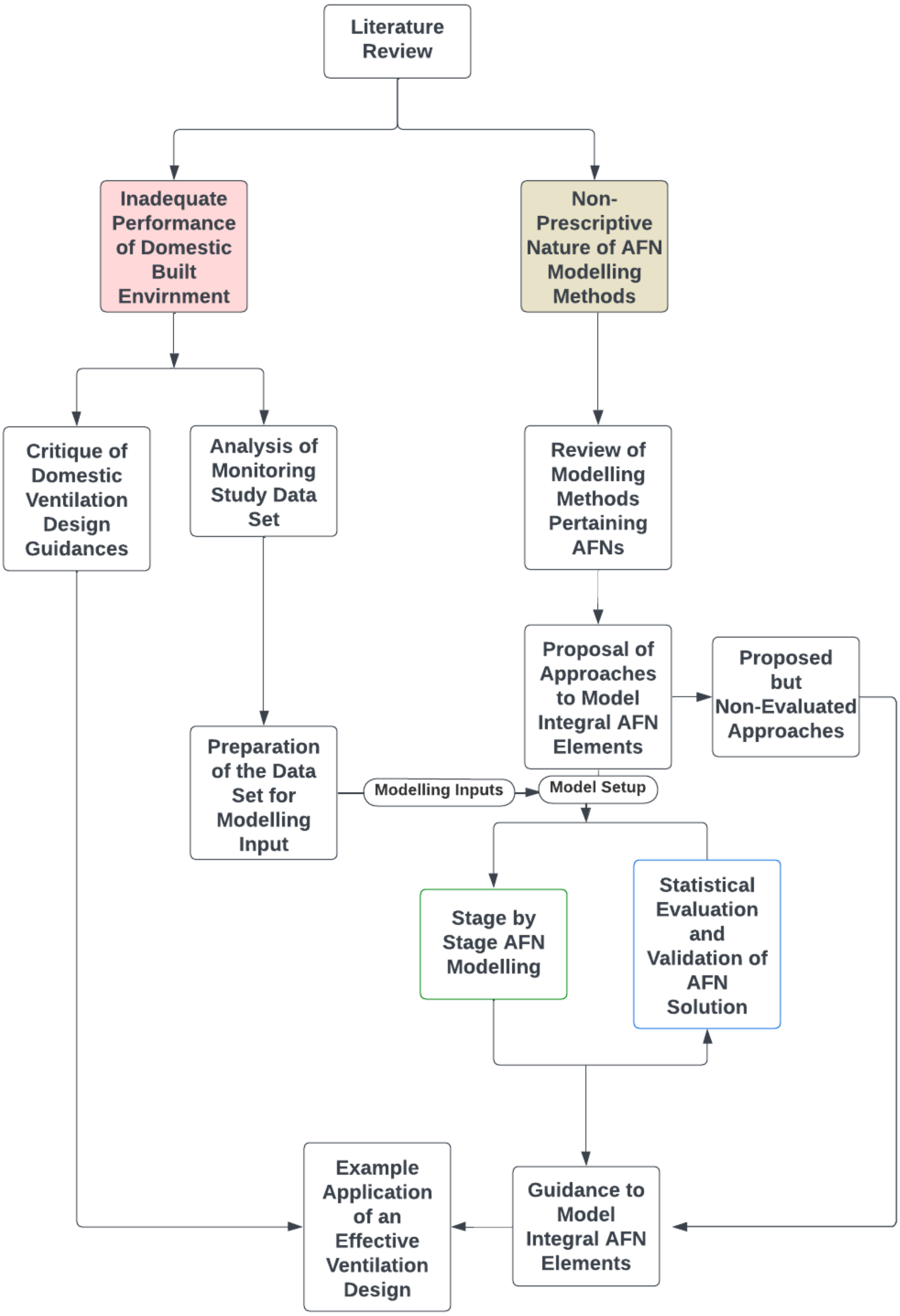

Figure 1.3: Overall Methodology

This research work commences with an extensive **Literature Review** to highlight the importance of ventilation, the lack of optimum performance of current ventilation design specially in the Scottish newly built dwellings, the critique of building regulatory guidelines and non-prescriptiveness of existing knowledge on AFN modelling. Critical insights gained from the literature would inform the **inadequacy of performance of domestic built environment** and **non-prescriptiveness of AFN modelling methods**.

The **critique of domestic ventilation design guidance** elaborates possible causes for the failure of domestic ventilation design. From this critique, design improvements are recommended, and the performance gap is presented. A **review of modelling methods pertaining to AFN** produces a set of approaches to conduct a simulation study for ventilation design. A subset of these approaches is investigated by employing a field study dataset which is represented by the "**proposal of approaches to model integral AFN elements"** in the overall methodology flow chart.

The rest of the approaches which are indicated, with the help of critical review, are presented as **proposed but non-evaluated approaches**. These are noted as beneficial for further study and advanced analysis.

Prior to utilising the dataset, the appropriateness of their use is analysed. This step, called the **analysis of monitoring study dataset** confirms if these data are representative of the ventilation inadequacies highlighted in the literature review. The representative monitoring dataset undergoes **preparation for the modelling input** which involves the categorisation of available modelling inputs, geometry set up, weather, occupancy gains and schedules, and specifications of airflow components.

The application of the proposed approaches for airflow elements undergoes physical and statistical analysis in a stage-by-stage manner, providing a dual perspective on the viability, performance and influence of each method on the simulation results. Both analyses help to formulate guidance to model the AFN flow elements by assessing the influence of modelling parameters.

Following the literature review and the analysis of modelling results, the **guidance to model integral AFN elements** is presented. This aims to complement existing modelling manuals and provide architects, designers, and engineers with unambiguous guidance. It is used in conjunction with a critique of domestic ventilation design to present an **example application of effective ventilation design** which is aimed to be capable of safer indoor CO_2 concentration levels.

The overall methodology stages outlined here, represent a structured approach that not only highlights the shortcomings of existing ventilation design but also investigates the different approaches of AFN modelling. A **statistical evaluation of the AFN solution** is presented in section 2.12.7 while the **stage by stage AFN modelling** investigation methodology is presented in Chapter 4.

Chapter 2 Literature Review

This literature review starts with the assessment of number of factors which influence the indoor air quality of built environment. Ventilation design of a domestic stock is proposed to be evaluated via building energy simulations (BES) Later, inputs essential to solve air flow solution are reviewed producing set of modelling methods to be evaluated via AFN simulation case study. Structure is aimed to cover wide range of aspects, each integral to understating following:

- **Importance of ventilation** (2.1): What is the relationship between ventilation, indoor air quality and health of the occupants? How current design guidance and practices have insufficient functional efficacy?
- **Influence of occupant's behaviour on ventilation performance** (2.2): How different behavioural aspects of the occupancy can cause design to fail. What are the motivations and barriers behind certain decisions pertaining ventilation?
- **Airflow dynamics in domestic settings** (2.5 -2.9): How adventitious and purpose provided ventilation components contribute towards airflow? What are physical aspects of these flow paths? What are uncertainties in modelling of such paths?
- **Occupancy Loads** (2.10): How is occupancy data collected? What are important aspects of its modelling in BES regarding ventilation study? What are uncertainties in assessing internal gains, presence, and influence on ventilation efficiency of the dwelling?
- **Boundary conditions** (2.11): How weather data is responsible for wind induced pressures? What are the available typical/representative weather data sets available to use for design studies. What are the translative elements of wind pressure in building energy simulations.
- **Model calibrations and validation methods** (2.12): Which statistical metrices are suitable to assess a model's validity? How do we use these metrices to conduct a sensitivity study? What are the acceptance criteria for a simulation model output? How statistical approach can aid in investigating the variance due to a range of physical inputs and parameters?

An extension of the literature review is presented in Chapter 3 which adds to the current design strategies and shortcoming affecting the building performance specifically in the Scottish context.

The literature review was shaped to systematically explore the fundamental factors which would affect AFN modelling for a domestic building ventilation design. This required an investigation into a range of topics, including:

- The relationship between ventilation, indoor air quality, and occupant health.
- The impact of occupant behaviour on ventilation efficiency.
- The physical and dynamic characteristics of airflow in domestic settings.
- The effects of environmental boundary conditions, such as weather data and terrain.

Additionally, previously, simplified assumptions for coefficient inputs in orifice and power law equations as well as uninformed usage of flow equations without catering to the need to suit the directionality of the airflow. Furthermore, this review would bring-in detailed guidance on selecting weather databases (such as TMY, TRY, and DSY) for specific purposes as well as advises on terrain adjustments, thereby enhancing the contextual accuracy of ventilation models.

Knowledge gained from addressing the questions in each category of the literature review is used to propose a methodology for this AFN study which investigates the influence of vital input parameters. This investigation is aided by a proposed statistical approach, combined with a focus on the physical aspects of the AFN solution.

2.1 Performance of Domestic Ventilation

2.1.1 Ventilation, IAQ and Health

To establish the need of an improved ventilation design in domestic dwellings, first step is to detail possible health effects due to the insufficient ventilation rates leading to low IAQ. The relationship between both the factors is clear and has been investigated in various studies. Fisk et al. (2009) worked on developing a correlation between ventilation rates and the occurrence of sick building syndrome (SBS) suggesting up to 23% increase in SBS symptoms as ventilation rate halves from 10 to 5 l/s/p. The increases in ventilation rates effectively reduce this risk and provide control against the increase of dust mites, mould, and other allergic agents and these findings were established by the reviews by Wargocki et al. (2002) and Sundell et al. (2011).

The European Standard BS EN 15251:2007 (replaced by BS EN 16798-1:2019 (BSI, 2019)) was critically assessed by (Aganovic et al. 2017). It was found that with the provision of ventilation rates of less than 14 l/s/p, concentrations exceed the threshold limits defined by the acceptable values for CO_2 and TVOCs (discussed in the next section).

In the literature CO_2 is debated to be categorised as a pollutant or just a proxy for ventilation rates. Abdul-Wahab, (2011) elaborated those higher levels of CO_2 cause dizziness, nausea and headaches. Experimental study by Satish et al. (2005) describes how excess levels of CO_2 effect human decision making however conclusion of the study is left for further research for the assessment of viable ventilation rates. It was shown that, for high CO_2 concentrations of 2500 and above, the decision-making performance of individuals decreased. A similar classroom study was done by Wargocki et al. (2017) and an inverse relation was found between classroom performance and CO_2 concentrations.

IAQ problems due to poorly ventilated buildings are also pointed out by World Health Organisation (WHO) in World Health Organisation, (2009) and World Health Organisation, (2010). Former details effect of dampness on respiratory health of the building residents and later underlines 9 pollutants which accumulate in living spaces due to low ventilation rates and results in pervasiveness of respiratory diseases and allergies. ASHRAE, (2007) sets limit of 700ppm of indoor CO_2 concentration above ambient levels for acceptable indoor air quality in addition to the mention of a number of other pollutants' concentration levels. Ahmed Abdul–Wahab et al. (2015) tabulates and discusses indoor pollutant's limits set by various international organisations including WHO which also sets safe CO_2 concentration levels at 1000 ppm. This study shows how the excess levels of these pollutants from the thresholds can be hazardous.

Domestic environment was further assessed by Air Quality Expert Group, (2022) and pollutants such as VOCs, NO2 and PMs were found to be prevalent to alarming levels. These levels tend to rise during daily household activities mainly during cooking and cleaning. Vardoulakis et al. (2020) highlighted that the PMs level surge is mainly due to the outdoor air and specially in the cases where natural ventilation (without filtration) is dominant, the demographics of the buildings matter.

As a support measure, improving IAQ would help elderly and vulnerable to resist contagious diseases. In a recent study, a statistical model developed by Afshari, (2020) declares better IAQ helping in lowering the mortality rate, alongside the severity and prevalence of COVID-19 virus in aging patients. Moreover, focusing on the building ventilation design, Kurnitski et al. (2020) prepared REHVA COVID-19 guidance report for workplaces which is also sought to be useful for residential spaces. Report suggests continuous ventilation at higher rates when building is occupied and at lower rates when there is no occupancy. Frequent use of windows is one of the important suggestions to lower the chances of viral transmission. The transmission potential of such viruses also needs to be incorporated in current UK building regulations and improvements are to be made in existing dwellings. Finally, according to the presented literature, adverse health and behavioural effects are well established due to insufficient ventilation rates.

2.1.2 Monitoring and IAQ Evaluation Studies

To assess the ventilation rates and accumulation of contaminants, various monitoring studies have been undertaken. A recent study was conducted by Ministry of Housing, (2019) to monitor houses for air quality and ventilation rate in accordance with Approved Document F (McKay et al., 2010). Monitoring was done for total volatile organic compounds (TVOCs), formaldehyde, NO2, CO and Radon levels as well as Relative Humidity (RH) and CO_2 levels. Detailed monitoring of 7 houses indicated higher levels of TVOCs and CO_2 in 4 houses exceeding 400 µg/m^3 and 1100ppm respectively. These levels are higher than WHO limits set of TVOCs (300 µg/m^3) and CO_2 (1000ppm). Results from the report further show a correlation between concentrations of TVOCs and CO_2 levels. This correlation is also discussed by Chatzidiakou et al. (2015) where concentration levels of various contaminants are assessed by studying the concentration levels of CO_2 alone as a proxy as it leads to dilution of contaminants as well as gives an insight about the ventilation rates of the occupied space. However, space under study must be occupied as metabolic rate or activity level is directly related to the CO_2 concentration. Where CO_2 concentration source i.e., metabolic activity levels by occupancy can be quantified it is possible to use CO_2 as proxy to evaluate ventilation performance of a living/working space.

CO_2 as a proxy was also used to assess ventilation of 41 newly built dwellings which were fitted with trickle vents in living spaces and dMEV fans in wet rooms concludes that ventilation design and building practices have a major gap. Additionally, this also refers how background ventilation is not sufficient which is proven by above the limits CO_2 concentration rates (T. Sharpe et al., 2019). The extract fans inducing pressure differential were also not providing enough volume flow rates which caused reduced background ventilation. Window opening is highly recommended in such scenarios which would include limitations due to thermal comfort, acoustics and safety.

In a recent study focussed on dMEV performance by Toledo et al. (2023) highlighted that a large proportion of the dwellings had higher levels of CO_2 and dMEV in combination with trickle vents as inlets are not sufficient to ensure safe IAQ.

Newly built passive house dwellings were reviewed for their IAQ performance by Rojas et al. (2024) and it was found that with the inclusion of mechanical supply and extraction, CO_2 are below 1500 ppm for most of time but a surge is scene in PM levels specially during cooking.

Few & Elwell. (2021) compared two dwellings where window opening behaviour changed. The authors pinpointed the accepted ventilation rate of 0.5 ach and concluded that with longer opening of windows, the required safe ventilation rates could be achieved ensuring ample IAQ. The quantification of window's efficiency for ventilation provision was carried out by Von Grabe et al. (2014). Total of 6 most used window opening mechanisms were appraised in a lab-based tracer gas experiment. CO_2 decay rate also termed as CO_2 removal rate is compared for same opening area. Vertical pivot and turn windows performed in a similar manner while horizontal pivot window was by far best performing window. Tilt/awning window which is lowest performing window type, provides best airtightness when closed as compared to slide windows hence is mostly recommended window type in construction practice (Van Den Bossche & Janssens, 2016). CO_2 removal rate evaluation shows how it is important to choose between window types to be used in frequently occupied areas of the house for purge ventilation.

Monitoring studies based on IAQ as well as ventilation rates and design have concluded that the current building regulations and practice is insufficient to provide ample indoor air quality. Background TV ventilation is proven to be insufficient on its own unless windows are opened, or other additional measures are taken. Safer levels of IAQ are recorded in case of occupant intervention such as window opening but this is subjected to various external factors including safety, heat loss, noise, and pollution. Hence there is need for a working ventilation design providing sufficient ventilation rates which does not depend on occupant's attention and perception.

2.2 Occupant's Influence on Ventilation Performance

Apart from the ventilation design of the building, another important aspect to gain better indoor air quality is the use of the ventilation components by the occupants. There are motivations and barriers which would affect the operation of the ventilation components. Various questionnaire survey studies as well post occupancy evaluation (POE) studies are evaluated, and the two important factors (motivations and barriers) can be highlighted serving the purpose of this part of the literature review.

Occupiers' perception about indoor air quality (IAQ) plays vital role in determination of ventilation performance of a building. The absence of air quality monitors and lack of knowledge about IAQ and ventilation strategies can lead to serious health issues (Wong-Parodi et al., 2018). Comfort, habits, intentions, and control are the deciding factors for any individual to operate the ventilation and can be basis of a motivation or barrier (D'Oca et al., 2016).

2.2.1 Motivations

Sharpe et al. (2015) interviewed the occupants regarding the possible driving factors for the increased ventilation. The majority, i.e., 75% of 200 respondents stated that thermal comfort is their main reason to open windows in their living spaces. Secondary motivations were indoor humidity and smell. In addition, habits and social norms also account for motivation for opening windows or operating ventilating systems at higher ventilation rate. T. Sharpe et al. (2019) suggest that occupants tend to take increased ventilation measures right before they start the cooking. Similar behaviour was recorded by Few et al. (2024) in which cooking smells mainly led occupants to operate their extraction and other flow components.

Toledo et al. (2023) showed that occupants were drawn towards turning on their extract fans as well as the trickle vents upon indication of high CO_2 levels on their main bedroom monitors. Furthermore, in the interviews, participants expressed that by checking the indoor temperature on the monitor, there was a change in perception of thermal comfort, and they tend to open the flow components if high CO_2 is indicated.

Placement of windows and their opening mechanism is another important factor. People tend to open the windows more frequently which are accessible. Moreover, the type of windows, for example top hung windows which provides shelter in case of rain are preferred to be opened more by the occupants. It is expressed in a review by Izadyar et al. (2020) that the windows offering a smaller flow area are tend to be open for longer as compared to larger windows.

Bruce-Konuah, (2014) also assessed the window opening behaviour by the staff in university offices which is greatly motivated by indoor temperatures. This study also suggested that, how CO_2 monitor readings can be highly encouraging for occupants to operate ventilation components in an indoor space. The same was found by Toledo et al. (2023) and bedrooms installed with the monitors performed better.

2.2.2 Barriers

The awareness of indoor air quality is a major factor which would urge occupants to open windows and operate ventilation components allowing a higher flow rate. There is generally a lack of knowledge regarding pollutants in the indoor environment. Zhao et al. (2016) interviewed domestic and commercial users of buildings and 41% of the respondents stated that indoor air quality does not have any effect on their health and productivity.

Despite the occupant's awareness to open windows for fresh air and increased ventilation, weather conditions such as wind and rain can compel occupants to keep them shut. According to (T. Sharpe et al. 2015) 59% of 200 domestic household respondents expressed that the main barrier for them to opening windows for fresh air is heat loss and security. Other major factors found by Roetzel et al. (2010) include wind gushes, the location of the building, type of the window installed and the availability of overhangs.

Occupants have also shown concern towards the mechanically running systems. T. Sharpe et al. (2019) interviewed the residents of 41 houses and found that the residents had a major problem with the noise from their constant running extract fans which led them to turn them off completely. The same study also highlighted that occupants were not aware of the installed trickle vents, and more than the half stated that they did not feel the need to open them. This highlights a major problem of awareness regarding the working of installed ventilation systems.

Amongst the residents of areas which are closer to establishments like bars, cafes and restaurants, a major concern apart from heat loss is the disturbance that might be created due to the noisy outdoors. Torresin et al. (2019) detailed the acoustic issues from either indoor or outdoor sources faced by the occupants.

Based on the literature, the main concerns requiring immediate attention are:

- Heat loss.
- Weather
- Knowledge of the working of ventilation systems.
- Lack of motivation due to limited awareness about indoor pollutants.
- Noise from the continuous running of fans/extractors.
- Noise from the disturbing outdoors.

Literature cited in this part of review was used to formulate a category framework (Figure 2.1) which can be used to assess the possible actions that occupants may or may not take to fulfil the minimum ventilation provision criteria. Furthermore, this will also be helpful for behavioural insights, design implementation, policy, and quantitative and qualitative assessments. These actions can be translated into computer models where the specifications of the building envelop, flow of air, temperature, internal heat gains and occupancy schedules form an integrated framework. The upcoming sections will first assess the current modelling techniques and then a literature review on the components of the models is presented.

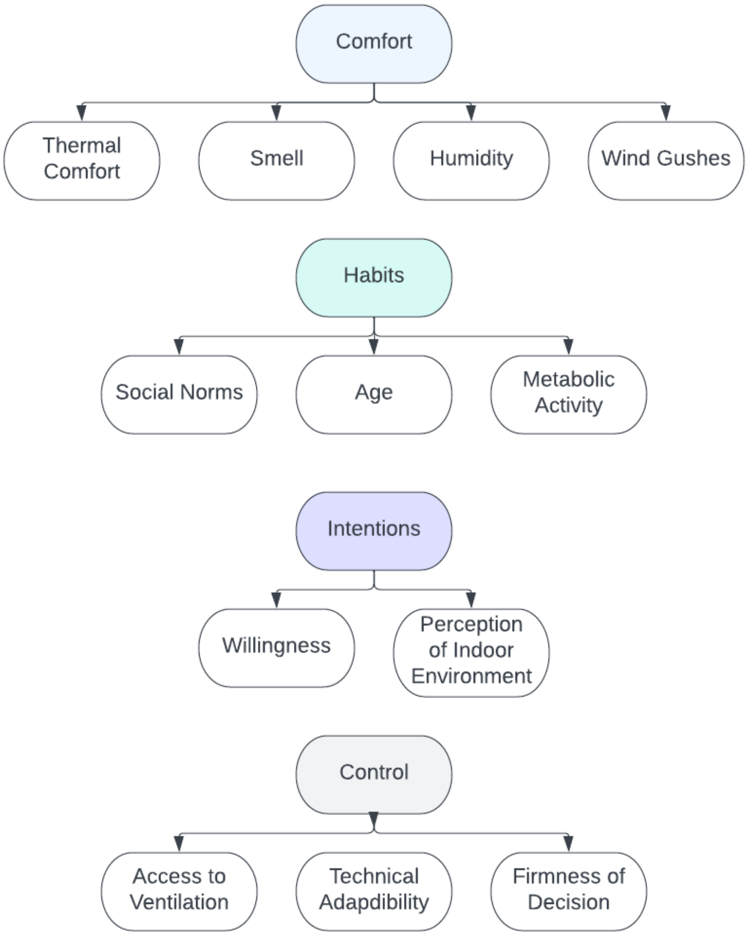

Figure 2.1: Factors governing human-building interaction.

2.3 Comparative Review of Calculation Methods for Building Simulation

This section presents a comparative review of various calculation methods which are used in building simulation with a focus on the evolution from simplified models to more complex approaches. The aim is to highlight the advantages and disadvantages of these methods.

One of the straightforward approaches in building simulation is the use of analytical models such as the Passive House Planning Package (PHPP) and the Standard Assessment Procedure (SAP) (Moutzouri, 2011). These models utilise predefined equations and empirical data to estimate energy consumption, heating and cooling loads. While these tools are user-friendly and straightforward to use, their reliance on generalised assumptions does not capture the complexity of indoor environments.

The simplest computational approach is the single zone model, which assumes a uniformly mixed environment within the building with no variations in temperature or air velocity on a set node (ASHRAE Fundamentals Handbook, 2021). This model was primarily used in early building energy simulation software due to its computational simplicity and ease of implementation. However, it oversimplifies the indoor environment by assuming uniform conditions and neglects dynamic factors. Consequently, it is not deemed suitable to study a building's performance with multiple zone featuring varied indoor and boundary conditions (Musser & Yuill, 1999).

To address the limitations of the single zone model, the multi-zone models were developed (Allard et al., 1990; W.S. Dols, 2015a). This approach divides the building into multiple interconnected zones where each zone is treated as a node, assuming well mixed air within each zone. The multi-zone model offers a closer to reality representation of indoor environment compared to the single zone model by accounting for variations in temperature, air velocity, and pollutant concentrations between zones. It is more suitable for simulating buildings with multiple rooms and varying usage patterns. The multi zone model is also well suited to integrate purpose designed ventilation components and extract fans as found in state-of-the-art dMEV system. However, this approach assumes well mixed air within each zone, neglecting air stratification and local variations. Additionally, it also overlooks the influence of airflow momentum and turbulence, limiting its accuracy for such scenarios (Lu et al., 2020)

Computational Fluid Dynamics (CFD) offers a significant advancement by accurately analysing the three-dimensional temperature and airflow distribution within a space, where it utilises numerical methods to solve the Navier-Stokes equations. This is done by incorporating airflow momentum and turbulence modelling to provide a more realistic representation of indoor environment (Tan, 2005). CFD can provides detailed analysis of temperature profiles, airflow patterns, and contaminant dispersion (Shree et al., 2019). It allows the analysis of complex scenarios such as natural ventilation, displacement ventilation, and other assessments concerning indoor air quality and ventilation performance. However, CFD simulations are computationally demanding and often require significant processing power and time. They also require specialised expertise to set up and interpret simulation results. The accuracy greatly varies depending upon the quality of input data, such as boundary conditions, grid resolution and turbulence models.

Recognising the computational limitations of full-scale CFD, researchers have developed simplified CFD techniques with an aim to balance accuracy with computational efficiency. Examples include Fast Fluid Dynamics (FFD) and State-Space Fluid Dynamics (SFD) (Q. Wang et al., 2017). These methods utilise simplified algorithms and numerical schemes to solve the governing equations using lesser computing resources and hence enabling faster simulations. Such techniques are suitable for applications where real-time or near real-time analysis is required with a condition of highly accurate input data. However, they are less accurate than full-scale CFD, especially for complex airflow scenarios and also require careful validation against experimental data to ensure reliability.

The choice of calculation method for building simulation depends on the specific application, desired level of accuracy as well as on the available computational resources. Analytical models like PHPP and SAP are valuable for preliminary energy assessments and regulatory compliance, but they may not offer the necessary detail for dynamic IAQ analysis or complex ventilation strategies. On the other hand, simplified models like the single zone are overly simplistic to capture spatial variations in CO_2 concentrations and air quality. The multi-zone model is identified as a suitable approach for studies focusing on modelling occupancy effect such as CO_2 build-up used as a proxy for good IAQ and assessing the performance of purpose designed ventilation components such as trickle vents and extract fans which are part of a dMEV system. It provides a balance between computational efficiency and the ability to model dynamic factors, proving it an effective tool for simulating indoor environments with varying occupancy and ventilation scenarios. While CFD offers the most detailed level of analysis, its computational demands make it less practical for routine simulations in this context. Simplified CFD techniques provide a middle ground but may not be necessary when the multi-zone model sufficiently addresses the simulation requirements (L. Yang et al., 2014). As research progresses, enhancements to multi-zone models and their integration with other simulation techniques such as Building Information Modelling (BIM) may further improve their accuracy and applicability in building simulation (Kwok, 2021).

2.4 Overview of Multizone AFN Models

In the AFN models, a building is considered as an interconnected collection of zones. These interconnections form the flow paths which are coupled with flow components. A combined energy and mass transportation calculation is done by the coupling which is explained by (Hensen, 1995). State of the art modelling tools use mass balance approach in which steady state flow of incompressible air in a building network, governed by specific boundary conditions i.e., wind pressure and temperature (Singh & Sharston, 2022). The network calculates fluid flow starting with an initial estimation of unknown pressure. These pressures are then iteratively adjusted to gain mass balance at each node. However, there are set of assumptions inherent in the numerical solution. The concept of well mixed zone refers to the assumption that a defined zone is considered perfectly mixed. This means that temperature, air velocity, humidity and pollutant concentrations are assumed to be unform in the zone (Johnson et al., 2012). This approach also neglects the momentum effect of the air movement which is suggestive of still air conditions in the zone (L. (Leon) Wang & Chen, 2008).

The AFN approach is implemented in the literature by using single zone and multizone models. Single zone model of a building is a simplified approach which assumed well mixed conditions for the whole building. Multizone on the other hand divides zones by having multiple representative nodes (Lorenzetti, 2002).

The accuracy of input variables is governed by the representation of boundary conditions, flow components, and internal loads. External nodes represent the boundary conditions and usually connected with an internal node to solve for the pressure difference across a component. Equation below expresses the arithmetic of the pressure difference solution where P_{wind} is pressure due to wind on external nodes, P_{room} is internal node pressure and PS is stack pressure due the placement of the flow component.

$$\Delta P = P_{wind} - P_{room} + PS \qquad 2.1$$

Wind pressure is governed by a pressure coefficient C_p, room pressure is unknown while PS depends upon the height, density of the fluid, and direction of flow.

A brief overview of the solution via AFN is presented here which highlights the importance of a pressure difference solution, an equation set to represent the flow components and their location and relative placement.

Forthcoming sections of the literature review will discuss the component equations and their setups, boundary conditions and internal loads specific to the scope of this study. The components are mandatory part of most of the buildings specially installed with an extract fan coupled with passive airflow intake from trickle vents as well as uncontrolled airflow due to infiltration. For this purpose, the following sections would detail equations and modelling of infiltration, trickle vents, door undercuts, larger interzone opening passages including windows and extract fans. Additionally, the boundary conditions such as weather and pressure coefficients are discussed along with internal loads i.e., occupancy. The critical analysis of available equation sets and approaches is presented and as an output a grand discussion is provided to feed into guidance to model for better ventilation provision both for as-designed as well as as-built dwellings.

2.5 Flow Through Cracks

To model infiltration as part of the AFN, the air leakage characteristics of cracks are incorporated via an equation set. The translation of these characteristics is aided by coefficients which rely on crack geometry and airflow types. It is impossible to obtain these characteristics due to a large variation in the possible forms of cracks (Allard et al., 1990). To present a clear approach in modelling cracks, it is first necessary to determine the typical geometry of a crack and its representation via an equation. For this purpose, the experimental and analytical studies are referenced in this section which then lead to present a discussion on a suitable equation and its inputs to model infiltration.

Cracks in the built environment are categorised as adventitious openings which are normally less than 10mm in height approximately (Standard, 1991). This dimension is often termed as width and perceived as the vertical dimension while length is the horizontal dimension of such a crack for which length>height. These flow pathways are responsible for uncontrolled infiltration and exfiltration from the dwellings. Analytical models referenced in Cockroft, (1979) and J. A. Clarke, (2001) set the height limits as 10 and 12mm respectively. The implications of these dimensions are discussed later under upcoming subsection 2.5.2. It is also aimed in this study to standardise the use the term height for the vertical dimension of any opening including the cracks to refrain from any ambiguity.

A flow through adventitious openings is frequently calculated using power law or quadratic equations, as both have empirical and experimental validity. It is important to discuss both equations and evaluate their application in AFN tools.

2.5.1 Power Law versus Quadratic

To evaluate the airtightness of the built environment, Nevander & Kronvall, (1978) described the relationship between airflow through a building due to pressure differences as a power law relation (equation 2.2). Later, Sherman, (1980) explained that flows through adventitious openings are dominated by viscous forces at very low pressures and $Q \propto \Delta P$ while at high pressures, they are dominated by inertial forces and $Q \propto \sqrt{\Delta P}$. Etheridge (1984) criticised the use of power law equations on the basis that flows through building pathways also show quadratic relations with the change in pressure which is represented by the quadratic equation (2.3) which was formulated by Thomas & Dick, (1953). They suggested that at higher pressure differences power law offered better agreement with the measured data while at lower pressure differences, quadratic equations were more suitable; however, they also suggested the careful use of flow coefficients and exponents in power law equation, when used. This refers to the fact that the difference measured between the solution of both equations was based on the coefficient inputs.

On the other hand, M. W. Liddament & Diff, (1987) compared both equations at pressure range of 0-50Pa and suggested that power law provided a better representation of airflow through cracks even at lower ΔP. At higher pressures, i.e., 5Pa-50Pa, both equations showed identical results. Walker et al. (1998) also suggested the use of power law for the representation of airflow by field and numerical studies. Later, Chiu & Etheridge, (2002) evaluated error by the infiltration calculations by power law which are two to three times greater than for quadratic equations at lower pressures i.e., 4-10Pa. This study involved CFD calculations which compare both airflow models. Zheng & Wood, (2020) obtained experimental data and compared them with the curve fitting values from both equations, which suggested the use of power law.

$$Q = C \times (\Delta P)^n \qquad 2.2$$

$$\Delta P = aQ + bQ^2 \qquad 2.3$$

Literature shows that the use of both equations for the estimation of flow through openings allows for laminar, developing, and turbulent flows. Quadratic equations are more analytic as they separately inform turbulent and laminar flow i.e., aQ expresses frictional losses due to laminar flow and bQ^2 relates to exit losses due to turbulent flow. In a building envelope, airflow leaks are not fully developed and, due to the complex geometry of cracks, it is highly difficult to predict flow regime through such passages. Moreover, these passages are present in the form of a parallel and series combination. Study by Walker et al. (1998) suggested that in such scenarios, quadratic equations are unable to accurately solve flow rates. CFD study by Etheridge involved two and four bend crack geometries which are probably present in a building envelope but when data is limited; such complexity cannot be applied in infiltration modelling. To enhance accuracy of AFN solutions for infiltration modelling, complex geometries of cracks can be modelled by using flow coefficient and exponent values from blower door data. Alternatively typical values from large databases could be used. These values are inputs in power law equation.

ASHRAE Fundamentals Handbook, (2021) lists two infiltration models which predict the airflow through cracks i.e., basic model and enhanced model. The basic model is mainly known as the LBL infiltration model Sherman & Grimsrud, (1980) while the enhanced model is known as AIM-2 model (Walker & Wilson, 1990). Both models are also implemented in the Energy Plus simulation tool and called the effective area model and flow coefficient model respectively (Energy Plus Documentation, 2020). Both the models are vastly applied by implementing power law equation with appropriate coefficients.

Based upon the sufficient validity of the use of power law equation at various pressure ranges, availability of data and its implementation in the simulation tools, the review backs the use of power law equation to model infiltration in an AFN model.

2.5.2 Flow Coefficient (C) and Flow Exponent (n) in the Power Law

In the equation 2.2, Q is the flow rate through a crack due to a pressure difference ∆P. Flow coefficient C and its dimensions l/s*Pa^n shows that it is dependent upon flow exponent n which varies between 0.5 (turbulent flow) and 1 (laminar flow).

Fan pressurisation methods allow estimation of airtightness of a building. Quantitative results from these tests are empirically analysed to determine flow exponent which allows to calculate the flow coefficient. These numbers provide an estimation of nature of crack geometry and flow type through the cracks respectively (M. Liddament, 1986).

The value of n=0.65 was concluded by Walker et al., (2013) by analysing data of n values from 6007 measurements of residential dwellings which is very close to the mean of Lawrence Berkeley National Laboratory (LBNL) database i.e., 0.646. Typical values for n and C are also available in M. Liddament, (1986); Orme et al. (1994) which are experimentally examined for 15 different leakage components present in a typical house.

Orme et al. (1998) through experimental procedures informs that flow exponent value depends on the type of crack and overall airtightness of the structure. A porous wall would show deviation in the range 0.5-1.0 while a crack due to a joint will be within the range of 0.5-0.7.

Jose & Perez-Camanyo, (2023) conducted IAQ study concerning infiltration rates in a domestic setting. They also highlighted the assumption that, flow through cracks causing infiltration is neither fully laminar nor turbulent and the leakage area was modelled using n=0.67.

Urquhart et al. (2015) suggests against using n-value beyond the range of 0.62-0.65. IES MacroFlow User Guide, (2014) uses n value to be 0.6 from Orme et al. (1994) for component leakage.

Evidently, as the literature suggests use of n≈0.65, analytical equation set can be employed to determine the characteristics dimension h of the crack. J. Clarke, (2007) suggests input of height of the leakage crack to calculate n value using the analytical equations below:

$$n = 0.5 + 0.5\exp\left(-\frac{h}{2}\right) \quad 2.4$$

$$C = L9.7(0.0092)^{n} \quad 2.5$$

Where h and L is height and length of the crack and this empirical set of relationships.

This model is integrated in ESP-r as a crack flow model (also called component 120). In case of absence of specific coefficients' data for cracks (available from blower door testing) or even to model larger openings up to 10mm (investigated further in 5.2.9), n and C values from this model can be used as approximation to model infiltration; or any purpose provided openings falling in the criteria. The relation between n and h of the crack allows modellers to determine a physical dimension of the crack(s) based on the literature informed n value range (0.6-0.7).

In the literature use of this power law model (eq. 2.4 and 2.5) is found. However, in some studies concerning IAQ, the height of the geometry of the cracks is used without a justification.

For example, for a passive house study, Bocanegra-Yanez, (2018) employed the same crack component 120 with a height equal to 3mm. Ehsan et al. (2010) used 5mm height of the crack in a multizone study to model infiltration. Ferdyn-Grygierek, (2014) does not mention the dimensions taken for the crack or the coefficients to model infiltration in the case study building. While there is indicated guidance available in the literature to comply with, the application related studies do not explicitly give due consideration to crack dimensions.

The other important coefficient in power law equation, Flow coefficient (C), quantifies the rate at which air can flow through a crack at given pressure difference. It is the key parameter in AIM-2 model as the physical presence of the crack is determined by defining a C value. In Orme et al. (1994), values for C are given per m^2 of the crack length for different components.

Variation in the geometry of cracks is well anticipated, and the cited literature emphasises the significance of these inputs to consider in an AFN model.

The review helps to determine a closer range of n=0.65-0.68 to exhibit transitional flow. This value would provide height of the crack which by equation 2.4 is determined to be ~2mm. The value of C is then determined by the n value which increases linearly with the length of the crack (equation 2.5). The length of the crack is user definable and suggested to be equal to the length of crack in the zone. In case of availability of total leakage flow rate for the zone, this length can be adjusted to match the flow rate using the power law equation.

2.5.3 Estimation of Location of Cracks

In the AFN calculations, the location of a flow component affects the prediction of the flow rates and hence an estimation of the locations of adventitious openings is important. However, there is great uncertainty if the modeller does not have access to the site and smoke test data. During the pressure testing surveys which are highly recommended in some countries and mandatory in others, crack locations are not determined as it is not found necessary. Zheng & Wood, (2020) enlists possible leakage locations in a dwelling and such literature can be taken as guidance but a great level of uncertainty could not be tackled. In an AFN application, the height of a component greatly affects the flow hence location of these cracks carries much importance.

Challenges also arise when the cracks need to be defined for windows and doors as cracks can be present all over the frame or on the top or bottom. Addition to this, trickle vent fitting can demonstrate a crack as well. In such cases it becomes difficult in modelling to introduce cracks in the right location. A visual inspection can be helpful to some extent but most of the times modeller does not have access to the building site under study and specially at the design stage. Studies have been found suggesting to model infiltration cracks on two extremities of a façade. Orme & Leksmono, (2002) suggests to model cracks on top and bottom of a façade, H. Li, (2002) suggests placing two strips of horizontally elongated cracks on top and bottom of the façade to introduce stack pressure in the AFN solution. Kravchenko et al. (2022), in their study suggested to present infiltration and exfiltration separately as external leakage area. However, these references lack the comparison of flow rate solution due to distribution of cracks at different heights. The introduction of increased stack pressure would allow greater flow magnitude but it is important to note that this increase will be not be linear under standard modelling conditions (Walker & Wilson, 1998).

Kalamees et al. (2007) studied building leakage pathways via thermography. Higher probability of leakage was found for window fittings, doors and junctions of ceiling and/or floor with external walls. Younes et al. (2012) refers to literature which presents percentage distribution of infiltration leakage categorised by building components. Walls, ceilings, windows and doors contribute mainly towards infiltration of a whole house. Walls has an average of 35%, ceilings 18% and windows and doors contribute at average of 15% towards total infiltration.

AIM-2 model provides approximations for the leakage distribution of the cracks. This distribution is based on different parts of the building envelop such as floor, ceiling, wall and flue leakage. Wills (Wills et al., 2022) applied AIM-2 model in AFN and distributed C value per façade as well as for floor and flue leakage. The height of the wall leakage cracks was at an arbitrary elevation H from the central internal node.

Finally, as the location of these cracks remains uncertain, it is important to assess the effect of solution of flow in AFNs due to difference in crack heights on a façade. Various studies have suggested different approaches however higher probability of cracks on window fittings as well as on wall-ceiling and wall-floor junctions is indicated. Models can be formed via a single dominant crack per zone or distribution over the facades however impact quantification of these approaches is not found in the literature.

2.5.4 Discussion

The review establishes a preference for use of power law equation rather than quadratic equation to model airflow through cracks, especially due to its applicability across the various conditions and availability of empirical in the literature. Cited studies jointly highlight the power law's application to accurately model infiltration, especially when paired with the flow coefficients obtained from blower door tests, databases, or analytical methods. The inputs of power law equation i.e., flow coefficients (C) and exponents (n); research by Walker (Walker et al., 2013) and Liddament (M. Liddament, 1986) suggests a consensus around using $n \approx 0.65$ for a close-to-reality representation of crack flow characteristics.

The literature review also identifies a significant gap in accurate modelling the placement of cracks in AFN models. Review presents an examination of probable crack locations, the precise positioning of cracks in built environment remains a challenge. Locating cracks in a model is based on the level of detail intended and the availability of data, hence either a deterministic or stochastic approach can be used. A deterministic approach would locate cracks at predefined and specific locations. The stochastic method can be used in cases of limited information about the building envelope by the distribution of cracks in a multizone model by placing a unit crack in each zone or assigning to each window fitting. In the case of multiple cracks per façade, as suggested in the AIM-2 model, the distance between these cracks is as much as the height difference between the floor and ground. For a design focused study, a unit crack approach or distributed crack approach can be adopted. However, the impact of distribution of crack on a façade is yet to be evaluated in AFN application. This gap points towards an area for further research, especially in determining the impact of placement of cracks on the AFN solution.

The review highlights the suitability of the power law equation in AFN modelling. Also, it highlights the importance of empirical/analytical data to determine key parameters such as flow coefficients and exponents. Additionally, impact of placement of cracks in AFN model on the solution is not found. As this stays an area of uncertainty, however, an understanding of impact of this setting would enable modellers to take an informed approach.

2.6 Flow Through Slot Shaped Openings

In a building envelope such slot shaped openings are usually purpose provided openings and are visually identifiable. The door undercuts, trickle ventilators or a slight window opening can be included under this category – depending upon their dimensions. This section examines the dimensional criteria of such openings with the help of literature and presents the flow characteristics through such openings. Later, two important flow components of the domestic built environment (i.e., door undercuts and trickle vents) are described, and their modelling is discussed. Towards the end of the section, the potential for investigation flow equations and the respective coefficients is presented.

The flow area is a key performance estimation criterion as it affects the flow regime and resistance of the opening. When calculating the flow through such openings, it is important to consider the opening characteristics as this enables categorisation into crack flow or orifice flow.

According to Cockroft (Cockroft 1979), typical dimensions of these openings are up to 10mm to characterise them as crack flow. Similarly BS 5925 (Standard, 1991) suggests crack openings to be less than 10mm in opening height. In the guidelines for airflow solvers, Hand

(Hand, 2018) suggests such height to be 12mm otherwise such flow should be solved by an orifice flow equation 2.6. A consensus can be seen in a criterion to categorise orifice or crack flow representation through a flow path. The reasoning behind this criterion can be explained basing upon the discussion on flow exponent n and possible flow regime from laminar to turbulent.

For openings large enough to have height of ≥10mm, orifice flow equation can be used which is given as:

$$Q = C_d A \sqrt{\frac{2\Delta P}{\rho}} \tag{2.6}$$

The effective area is represented as:

$$A_{eff} = C_d A \tag{2.7}$$

Where A is geometric area of the opening.

With such larger opening pathways, orifice flow is expected in which the actual flow area and geometrical flow area are not the same. Hence, the ratio of actual flow to theoretical flow is called discharge coefficient C_d. This coefficient is further discussed in detail in the section 2.7.4.

2.6.1 Assessment of Flow Characteristics

There are several studies which experimentally identify n values using blower door testing of small slit openings. Gonzalez (Gonzalez, 1984) and Karava (Karava et al., 2003) suggested the value of n≈0.5 pointing towards a turbulent flow through these openings.

The aerodynamic properties of a flow path or a component can be inferred from laboratory testing as devised in British Standards EN13141 (EN13141-1, 2004). The flow rate is measured for series of pressure differentials and this data is used to determine C_d and/or effective area. In some events when this coefficient is not calculated hence the testing data can be employed to determine the n and C values (W.S. Dols, 2015b).

Literature review suggests that such data is available for purpose provided ventilation devices following a standardised practice.

2.6.2 Flow Thorough Closed Doors

The flow through a closed door is of great importance because in a decentralised system, the extraction of air in a living space takes place via the door undercut, which is regarded as a purpose provided opening. A limited literature is found on the use of door undercuts as purpose provided openings while majority of the studies couple geometric area with C_d=0.6 (Bouvier et al., 2019; G. Guyot et al., 2019). However, some studies evaluated slight door openings or larger cracks of the door. For example Mckeen (Mckeen & Liao, 2019) refers to Klote and Milke (Klote & Milke, 2008) to devise C_d for larger flow paths through the doors in the range of 0.35-0.47.

On the other hand, Omre (Orme et al., 1998) present n and C values for air leakage from closed doors. However, to model a purpose provided door undercut with a definitive geometry, employability of such leakage parameters would require investigation.

Modelling of door undercuts input parameters are unclear from the literature and purpose serving testing data is non-existent.

2.6.3 Flow Thorough Trickle Vents

Trickle vents are purpose provided and aerodynamically tested ventilation devices. This section provides clarification of the use of effective flow area rather than use of geometrical area in combination with an estimated C_d.

Karava Karava, Stathopoulos and Athienitis, (2003) investigated slot ventilators providing an effective flow area of 4000 mm^2. Pressurisation tests assessed the flow through a slot ventilator and the flow exponent was 0.53. A comparison was conducted between the volume flow rate using experimental data, power law and the orifice flow equation. The orifice flow equation was found to overestimate the flow rates due to the use of a generalised C_d of 0.6, while the discharge coefficient for trickle ventilators can be calculated using the following equation:

$$C_d = \frac{measured\ volume\ flow\ rate}{predicted\ volume\ flow\ rate} \times 0.6$$

Using this equation, Karava (Karava et al., 2003) suggested the use of C_d=0.34. However, the errors due to a complex geometrical area would lead to erroneous modelling parameters. Manufacturers of trickle vents provide an effective area which can be used in an orifice flow equation rather than the product of the geometric area and C_d.

In a more detailed experimental study of simple slots of PVC and timber as well as different canopy and mesh screen examine the influence on flow exponent values, Fox, (2008) found for PVC and timber slots of 13mm-16mm height, value for n ranged between 0.47-0.5. Pressurisation tests gave a higher value (+0.2) of n than the depressurisation test due to the canopy and mesh screen installed on the outside of the vent. Another interesting aspect of this study was the n value of the crack formation when the trickle vent was shut, which was calculated at 0.926 confirming a developing and close to fully laminar flow.

Furthermore, using the geometric area to model a trickle vent with a default of C_d=0.6 would result in an erroneous solution of flow due to the installation of canopy and/grille and the physical behaviour of the opening. The geometric area of an example model of trickle vents is calculated as 4832mm^2 while the effective area is given as 4600mm^2 (Titon, 2016.). The geometric area coupled with C_d would yield a much lower flow area causing an underprediction of the flow from the component. Hence, this review places emphasis on the use of manufacturers' testing data to model a trickle vent.

Literature has confirmed that modelling of trickle vents is comparatively a straightforward approach as effective area is available from the most manufacturers. In case manufacturer name/model of the trickle vent is unknown, it is not advised to model them using geometric area of slots using sharp edged orifice discharge coefficient.

2.6.4 Discussion

The literature review suggests that an effective area of flow is an elementary parameter to model a purpose provided opening.

For door undercuts such testing data is not available, especially for standard slots of 10mm in height.

For trickle vents, the mandatory provision of an effective area number is given by the manufacturers. When available, it is straightforward to use this number in the orifice flow equation 2.6.

As indicated from the review, trickle vents and door undercuts have the potential to be erroneously modelled. This is further investigated in the simulation study which aims to quantify the impact of various representations of trickle vents and door undercuts in AFN.

2.7 Flow Through Windows and Other Large Openings

Following the analysis of infiltration cracks and larger slot shaped openings, a section on larger flow apertures is now given. This section details hinged/flapped openings in particular although the general flow behaviour for unflapped larger openings (≥10cm in height) is also described. The definition of a larger flow openings can be presented with the help of literature. Such opening has the capability of bi-directional flow due to differences in temperature between zones (Hensen, 1991). This section also elaborates the limitations of modelling approaches and ambiguity in important inputs such as geometric areas and discharge coefficients. Furthermore, it presents a method from the literature which enables the modelling of such unflapped/flapped openings with better accuracy.

Wind and buoyancy forces are responsible for natural ventilation through windows in a building (Awbi, 2003). The wind pressure coefficients, wind profile, opening areas of windows, C_d and temperature differences ΔT determine the airflow magnitude (Awbi, 1994; Favarolo & Manz, 2005). In the cold weather, dominating flow driving force is buoyancy and stack effect while in summers it's the wind turbulence. In the former scenario, for single-sided ventilation the bottom part of window openings act as inlets while the top part is the outlet. In the later scenario, turbulence, wind direction and speed have the greatest variability which is further combined with stack due to ΔT (D. W. Etheridge & Sandberg, 1996).

To model such openings, ambiguities in the behaviour of the opening and the use of a set of coefficients to simulate the phenomenon leads to greater uncertainty. This part of the thesis discusses the physical aspects of flow through such openings in order to highlight challenges in the modelling process. The following factors are addressed:

- Flow through windows/openings in the event of dominant buoyant forces.
- Flow through windows/openings in the event of dominant wind effect.
- C_d variation basing on the flow scenario and geometry of the window/opening.
- Geometric representation of window.

2.7.1 Flow due to Buoyancy

Under buoyancy driven flow and with the temperature difference between indoors and outdoors, a typical window opening offers a bi-directional flow from the top and bottom parts. The flow areas differ for different opening mechanisms of windows. Six of the most common opening mechanisms are illustrated in Figure 2.2.

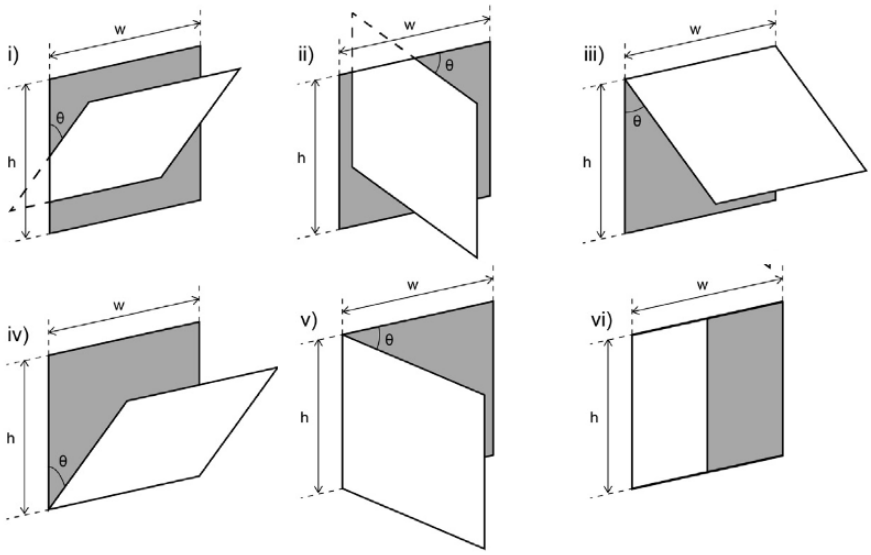

Figure 2.2: Typically fitted window types in dwellings (i) Horizontal Pivot (ii) Vertical Pivot (iii) Awning (iv) Tilt (v) Turn (vi) Slide (CIBSE, 2018)

(i)	(ii)	(iii)	(iv)	(v)	(vi)
Horizontal Pivot	Vertical Pivot	Awning	Tilt	Turn	Slide
Horizontal Centre Hung	Vertical Centre Hung	Top Hung	Bottom Hung	Side Hung	
Horizontal Centre Pivot	Vertical Centre Pivot		Hopper	Casement	

Table 2.1: Naming conventions for different window types.

Window opening mechanisms can be categorised based on the presence of a neutral plane. Horizontal pivots, turn and sliding mechanisms have horizontal neutral planes in the centre which are referred to as symmetrical windows, while awning and tilt mechanisms do not have a definite neutral plane location and are categorised as asymmetrical windows. This helps to define modelling practices for both these kinds of window. Please note that this determination of horizontal plane is under still air conditions.

(Grabe, 2013) investigated the flow behaviour of these windows under buoyancy. A comparison of both window categories shows that for the same opening area and boundary conditions, a tilt window (asymmetric) offers higher resistance than a turn window (symmetric). Furthermore, the neutral plane height of a tilt window was visualised by a smoke test, and it was found that the area of outlet is 2.5 times greater than area of inlet under buoyancy for an opening gap >10cm. Figure 2.3 shows the inlet as red areas and the outlet as orange. For the awning window type, which is the second type of asymmetrical window with a top rather than a bottom hinge, the inlet would be larger than the outlet due to the geometry.

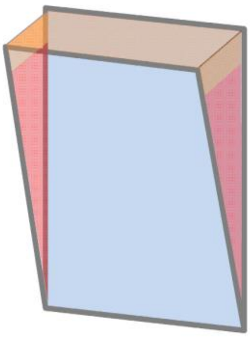

Figure 2.3: Red shaded area represents inlet while orange shows outlet area of a tilt window (Von Grabe et al., 2014).

The Figure 2.4 shows higher flow rates via symmetrical windows when compared to asymmetrical windows. The important takeaway from this study is presence of a neutral plane in a large opening. Also, the resistance of the flow opening varies for the different flow mechanisms. Now the impact of the flow strategy (single sided/cross) on the presence of neutral plane and the pressure distribution profile across the opening is discussed.

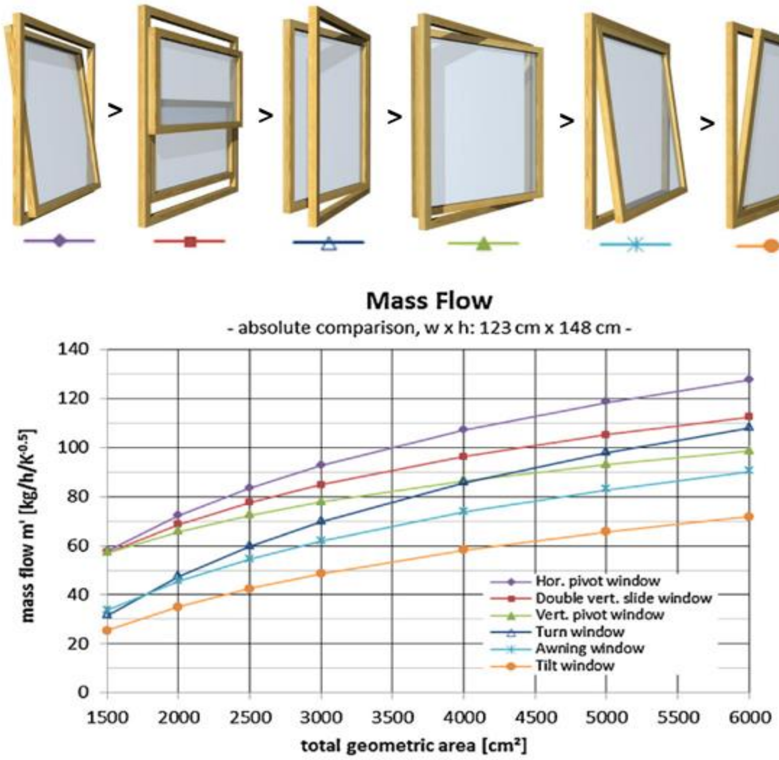

Figure 2.4: Window types and their air flow capacities for different geometric opening areas (Grabe, 2013).

(Heiselberg et al., 2001) details difference in the pressure distribution in case of cross and single sided ventilation through windows in Figure 2.5. This pressure distribution is responsible for the neutral plane placement in the opening. The equation involved in calculating the neutral plane height is discussed in the next section. Here we will keep focus on flow behaviour in case of different window mechanisms by looking at pressure profiles.

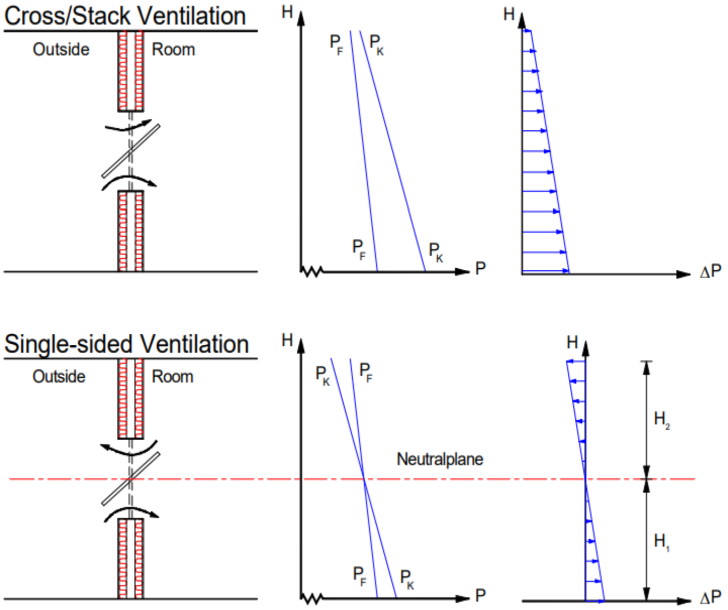

Figure 2.5: Comparison of Single Sided and Cross Ventilation Through a Window Opening

Figure 2.5 shows the pressure profile differs between single-sided and cross ventilation. Cross ventilation allows for higher pressure differential between the indoors and outdoors and the bi-directional flow through the window openings (top and bottom) is overridden. This is because of the unbalanced flow which can be caused by opening more than one window in a room or by the presence of a constant flow by a mechanical extract in the zone (Jones et al., 2014).

Pressure profiles are also visualised by (J. Wang et al., 2017) for different window types under buoyancy. This helps in visualising the neutral plane when there is single sided flow. It is important to note that in Figure 2.6, the awning window is opened inwards hence pressure profile is inverted. The study shows that, for all symmetrical windows, the neutral plane is present at the centre of the geometry while it is not true for asymmetrical windows. Figure 2.6 shows pressure-drop profiles where subscript CI is from window frame centre to indoors and OC is from outdoors to window frame centre.

This conforms with the natural convention theory presented by (Brown & Solvason, 1962) which states that buoyancy alone results in the formation of a neutral plane which is at the centre of the opening, the upper part acts as an outlet while the lower acts as an inlet. The application of Bernoulli's principal further explains this type of movement of air through an opening which allows for density differences between indoor and outdoor air due to the temperature differences at different heights.

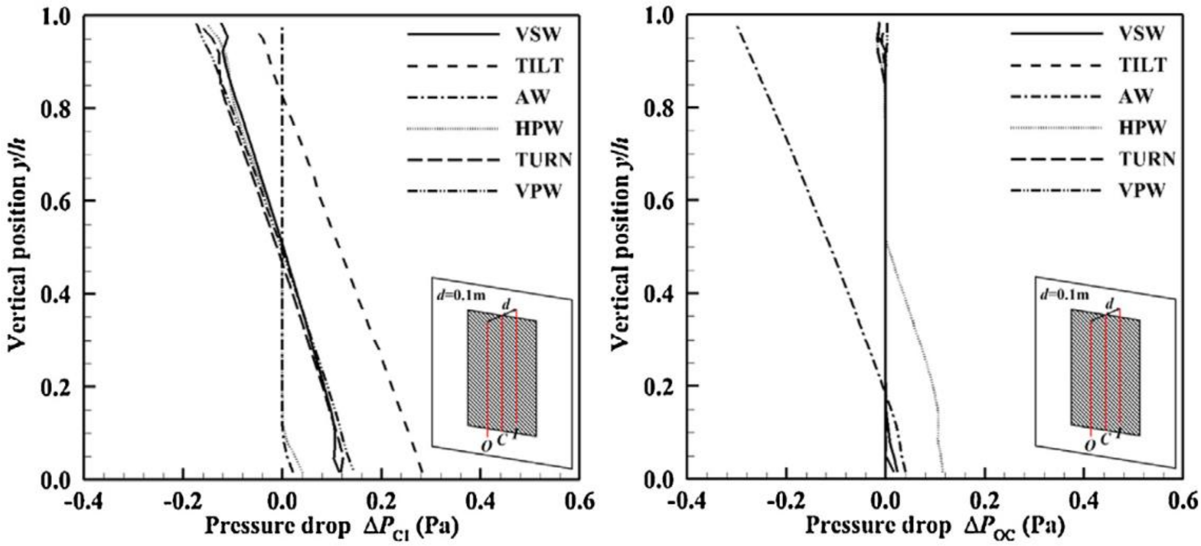

Figure 2.6: Comparison of Pressure Profiles of Vertical Slide, Tilt, Awning, Horizontal Pivot, Turn and Vertical Pivot Windows (J. Wang et al., 2017).

This section has detailed the air movement through different window mechanisms due to the pressure drop across the opening. The experimental and modelling studies cited confirm the presence of a neutral plane at different heights depending upon the flow conditions and opening mechanism and in the case of a large opening greater than 10cm of height. The translation of large flow openings into AFN is discussed in the section 2.7.3.

2.7.1.1 Modelling of Buoyancy Driven Bi-Directional Flow

As previously suggested, different window mechanisms allow different in and outflow of air under different conditions. CONTAM, COMIS and ESP-r offer a very similar approach in which the existence of a neutral plane is calculated where the flow possibility is null. A solution of flow throughout the height of the opening is solved in imaginary and real parts. Real part of the solution means the flow is in positive direction and imaginary part indicates that it's in negative direction. It is important to note that the set of equations discussed here are essentially for simple 2D openings.

For openings with height smaller than 10cm, such a bi-directional flow has null possibility (Hensen, 1991). This assumption also applies when the temperature difference between the air zones is very small i.e., <0.01K hence a unidirectional flow is expected which can be solved by the simple orifice flow equation.

COMIS and CONTAM both offer multi-opening and single opening equations to model bi-directional flow due to density differences. In a multi-opening approach, a set of orifice flow/power law equations are solved at two different heights (high and low). The velocity of the airflow is assumed to be the function of height of the opening and given by:

$$V(h) = \left[\frac{2\big(P_i(h) - P_j(h)\big)}{\rho}\right]^{1/2} \tag{2.8}$$

For single opening model, to compute flow from the top half of the opening, equation above is integrated from height equal to y=0 up to y=h/2.

$$\dot{m} = C_d \int_{y=0}^{y=h/2} \rho W V(y) dy \tag{2.9}$$

Upon solution of the equation above, one opening is at positive and one at negative height (from a reference datum line) is used to solve flow in positive and negative directions. This approach is not sufficient when neutral plane is not present in the centre of the opening.

A more accurate single opening model which defines the neutral height rather than assuming it in the centre of the opening. Neutral height h_n is calculated by:

$$h_n = \left[\left(\frac{P_{i,0} - P_{j,0}}{g(\rho_i - \rho_j)}\right)\left(\frac{P_{j,0} - P_{i,0}}{g(\rho_j - \rho_i)}\right)\right] \tag{2.10}$$

In the equation above, subscripts i and j refers to zone i and j. If density of both zones is equal, the flow is simulated via simple orifice equation.

To model a vertical opening as one component (equation 2.11), ESP-r represents a large enough vertical opening which will allow for density differences due to ∆T at different heights to induce bi-directional flow to depict windows which is derived from the orifice flow equation. However ESP-r user manual “The Cookbook” (Hand, 2018) also suggests to model a large opening via a pair of orifice equations. A closer look at the bi-directional flow component will be presented and limitations of modelling a bi-directional component with a pair of orifice equations will be identified.

Figure 2.7 shows the inputs, reference nodes and setup of the component.

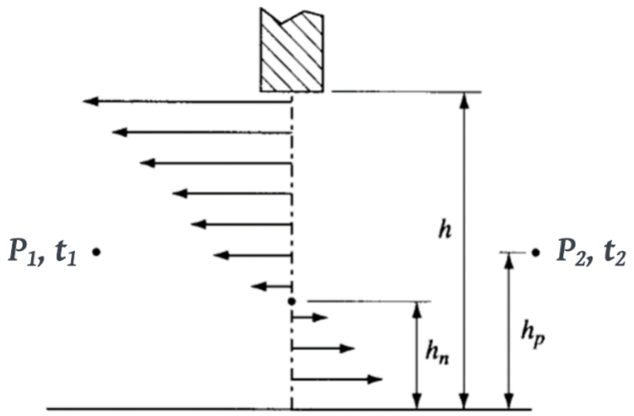

Figure 2.7: ESP-r bi-directional flow component as presented (Cockroft 1979) by and implemented in the tool by (J. Clarke, 2007).

$$Q = \frac{2}{3}\left[C_d W \times h\sqrt{\frac{2}{\rho}}\left(\frac{C_a^{\frac{3}{2}} - C_b^{\frac{3}{2}}}{C_t}\right)\right] \quad 2.11$$

Where C_a, C_b and C_t are given as below:

$$C_a = (1 - r_p)C_t + (P_1 + P_2)$$

$$C_b = (P_1 - P_2) - r_p C_t$$

$$C_t = \frac{g \times P_a h}{R}\left(\frac{1}{t_2} - \frac{1}{t_1}\right)$$

$$r_p = \frac{h_p}{h}$$

$$r_n = \frac{h_n}{h}$$

$$h_n = h\left(r_p - \frac{P_1 - P_2}{C_t}\right) \quad 2.12$$

$$Q = \int_{x=-h_n}^{x=h-h_n} C_d W \times h\sqrt{\frac{g\Delta P x}{R}\left(\frac{1}{T_1} - \frac{1}{T_2}\right)}\, dx \quad 2.13$$

Where, t_2, t_1 ,P_1, P_2, h_p, h_n and h are temperatures, pressures, height from adjacent node to the base of the doorway, neutral height and opening height on either sides where units are (K), Nm^{-1} and m respectively, R is general gas constant $JKg^{-1}K^{-1}$, P_a is atmospheric pressure. Equation 2.12 allows the determination of neutral plane and inputs into the limits of the integration in equation 2.13.

Equation 2.12 also provides the relation between neutral plane height and r_p which is ratio of distance between adjacent node and the bottom of the opening (h_p) and total height h of the opening. The height h_p value is always a positive number as it is used to determine the neutral height h_n and it should not be confused with the placement of the opening with respect to the datum/reference plane. A negative value would yield a negative h_n and thus alters the limits in equation 2.13.

Modelling a bi-directional flow component via multi opening equation has two major caveats. First is the erroneous determination of neutral plane when flow is impeded by pressures other than buoyancy. Second is the overprediction of flow due to height difference between the opening pair. For example, with a side hung flapped opening (e.g., a door), two opening approach would cause overprediction of flow rate when openings are placed at two extremities of the door frame. Patrick Sharpe (P. Sharpe et al. 2021) refers to correction factor for both buoyancy and wind driven flows to be applied to flow equation.

$$C_q = \frac{1}{2}\left[\sqrt{1+\frac{1}{h^*}} + \sqrt{1-\frac{1}{h^*}}\right] \qquad 2.14$$

Where h^* is non-dimensional height equating the ratio $\frac{2(h_n - h_{win})}{h}$, h_n is the neutral pressure height, h_{win} is height of the centre of the window frame and h is distance between the two openings. These AFN equations (orifice and bi-directional flow) used in the solution tools are widely applied and validated to simulate ventilation rates in a building.

Li (Z. Li, 2007) conducted single zone air flow experimental study where flow rate was measured through combination of two openings in a test chamber, one on the wall just above ground level (vertical surface) and other on the ceiling (horizontal surface). Such openings are found in the hallway in a dwelling where there is an entrance door and stairwell offers a horizontal opening. Smoke test detected three flow regimes through these openings and tracer gas technique was used to calculate the flow rates.

- Mode 1: Unidirectional flow through both openings
- Mode 2: Bi-directional flow through vertical opening with outward unidirectional in horizontal opening
- Mode 3: Multi-directional flow in horizontal opening with inward unidirectional in vertical opening.

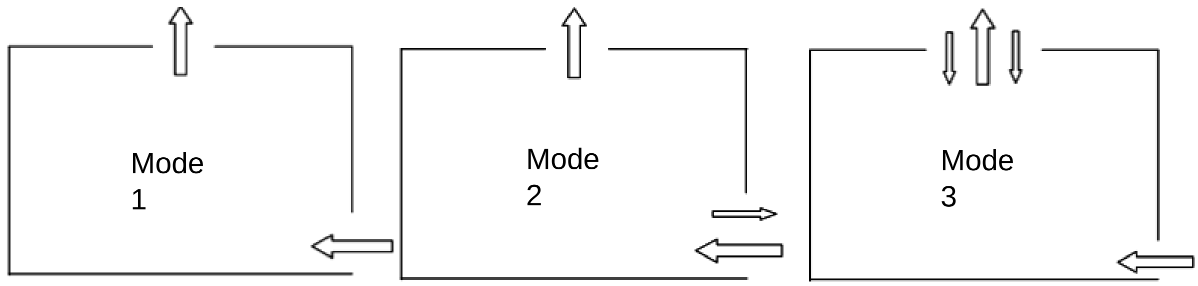

Figure 2.8 : Three Flow Modes/Regimes Detected by Smoke Test (Z. Li, 2007)

The directionality of the flow through a large horizontal openings is also reviewed by Allard (Allard et al., 1990) and cited experimental studies explaining how the flow through horizontal openings rely upon the density difference between the upper and lower zones (connected via a horizontal opening). Walton (Walton, 1989) also suggests the same by taking example of a flow in a stairwell shaft in buildings for such flow (uni/bi/multi-directional).

Johnson (Johnson et al., 2012) evaluated the experiment by Li (Z. Li, 2007) with four simulation tools which are discussed previously. During the experimental work, opening areas and ambient and zone temperatures were varied and total 6 combinations were tested as mentioned in the table below:

	Horizontal Opening Area m^2	**Vertical Opening Area m^2**	**ΔT**	**Flow Mode**
Case A	0.04	0.04	7	1
Case B	0.04	0.16	5.5	1
Case C	0.04	0.36	5.3	2
Case D	0.16	0.04	6.5	1
Case E	0.36	0.04	7.8	1
Case F	1.00	0.04	6	3

Table 2.2 : Experimental Cases for Buoyancy Driven Single Zone Cross Flow Study

The modelling results showed agreement with measured airflow in some cases however the larger opening sizes in this study were not handled well with case C and case F showing issues. ESP-r was used to investigate both orifice flow and bi-directional flow components.

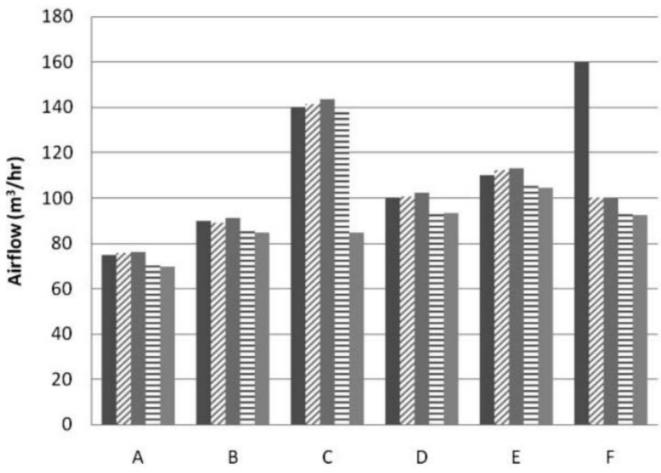

- Measured Energy Plus CONTAM ESP-r Door Component ESP-r Orifice Flow

Figure 2.9: Flow predictions from different modelling tools and set of equations compared with measured data (Johnson et al., 2012).

Limitations of these methods is also highlighted by Wetter (Wetter, 2006) who suggests an error of up to 30% in flow rates when large openings in stairwells are modelled in COMIS.

Peppes (Peppes et al., 2001) also solved the flow in a stairwell via a unidirectional flow equation Q=A.$C_d\sqrt{\Delta\mathrm{TgH/T}}$. It is important to note that for large openings in the case of stairwells, the value of C_d=0.61 when ΔT is small (~1°C) (Wetter, 2006).

Besides the equation representation, calculating the opening area between the stairwell is also ambiguous. Katsumichi (Katsumichi, 2003) elaborated the translation of flow area between the floors as a horizontal planer opening such that the floor area of the stairwell is equal to the area of the horizontal opening.

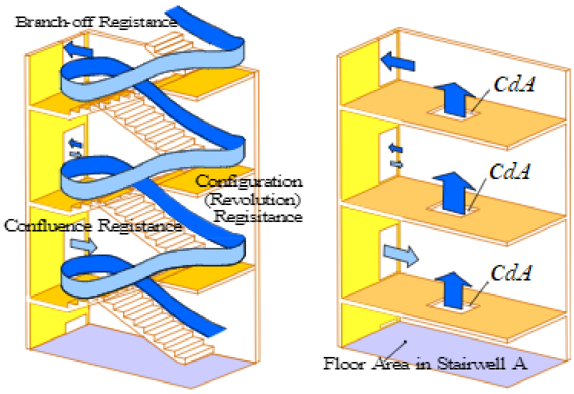

Figure 2.10: Viewing stairwell as horizontal planer openings between floors (Katsumichi, 2003)

A different approach to determine the area by Peppes (Peppes et al., 2001) is by taking a shorter width to calculate the area by not factoring in the floor landing (Figure 2.11).

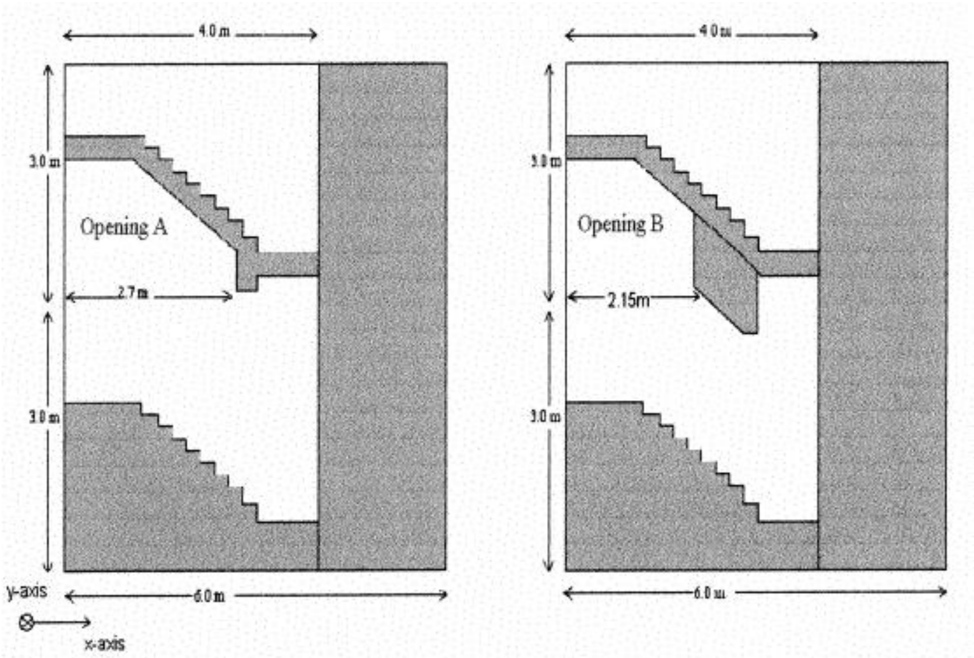

Figure 2.11: Schematics for two different configurations of stairwells and their respective widths to account for in area calculation (Peppes et al., 2001).

In another similar study, Reynolds (Reynolds et al., 1988) study the fluid dynamics in the throat area which is the width equal to the minimum distance between the stairs and the ceiling.

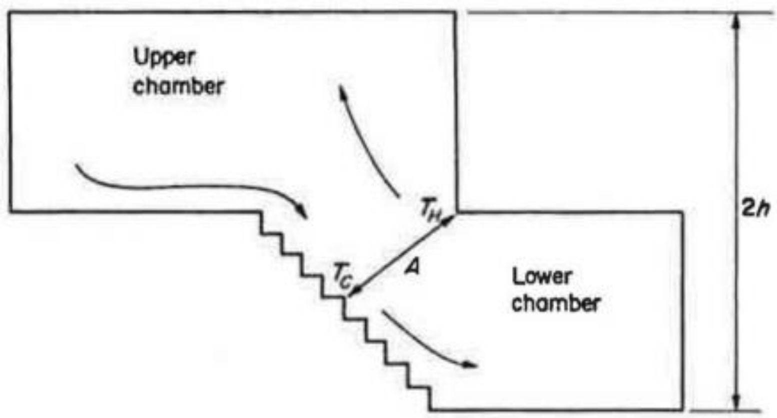

Figure 2.12: The area calculated by measuring the throat (minimum distance between stairs and the ceiling) (Reynolds et al., 1988)

The reviewed studies highlight limitations in modelling horizontal planer openings within AFN tools. The validation study by Johnson (Johnson et al., 2012) reveals that there is inadequate representation of large horiontal openings in AFN tools. Furthermore, Walton (Walton, 1989) suggests varied directionality of flow, while Peppes (Peppes et al., 2001) used a uni-directional equation, and (Dols 2020) suggested the use of power law form of equation. The geometric area representation remains ambigous. However, specifically in modern domestic settings where temperature differences between storeys are small, it would seem that while the accuracy of the modelling stairwells is an area to be resolved, the relatively low resistance to airflow of stairs in comparison with other AFN components should mean that the impact on the overall network is small.

2.7.1.2 Discussion

This part of the review highlights that symmetrical and asymmetrical windows need to be modelled differently for the flow estimation. Additionally, both windows behave differently under varied flow conditions, i.e., buoyancy, wind driven or combined. A simplistic approach to model a symmetrical window would be top and bottom openings with C_d=0.61 and the area equating to the total geometric flow area. Although this approach can overestimate the flow rate, a bi-directional flow component can account for the pressure gradient along the opening height. However, the effective area approximation will still rely on the use of approximate C_d value. The variations in C_d and effective areas of flow are discussed in section 2.7.4.

The approach described to model window opening via two orifice equations as a simplistic approach is not valid for asymmetrical windows. Under still air the pressure distribution along the vertical height of the opening is different for both categories of windows. As suggested in the review, outlet of a tilt window (bottom hinged) had 2.5 times larger outlet area than the inlet area (10cm opening stroke length). Hence the assumption of consistent resistance to flow throughout the opening height would not be correct for windows which are top and bottom hinged.

The review suggests modelling of any vertical opening capable of bi-directional flow (height>10cm) via bi-directional flow component in which neutral plane height is determined due to pressure gradient along the height of the opening. When implementing a simple approach of modelling one large opening via a pair of unidirectional equations, correction factor is implemented which caters the overprediction of flow rates. Both approaches are compared in the upcoming Modelling Study chapter.

In addition, flow through roof windows/horizontal planer openings (such as stairwells) cannot be simulated with an accuracy by any of the mentioned AFN tools for large opening areas. This is worthy of more research and experimentation. However, airflows up to 100m^3/hr were closely simulated by a bi-directional flow component modelled as horizontal openings for the opening area up to 0.36m^2 but the bidirectional flow was not solved. The applicability of these findings to the stairwell openings between the floors suggest that, even though the flow is expected to be either uni/bi or multi-directional, a unidirectional flow component as suggested by (Dols 2020) can be used. Nevertheless, this should be considered as a simplistic approach and further advancement in the accurate modelling of large horizontal planer openings are necessary. Further to the modelling equation selection, an ambiguity in the opening area was also found. However, a sufficiently large area can be modelled such as equal to the floor area in the stairwell. The other input to any flow equation would be C_d value. A small temperature difference between the zones would allow small resistivity to the flow and a sharp-edged orifice value of 0.61 can be used.

2.7.2 Flow due to Wind

Building simulation tools calculate the combined pressure induced due to wind and buoyancy. The equations governing pressure calculation for wind induced flow are presented in this section. Later, the ability of these AFN simulation tools to model wind induced as well as combined wind and buoyancy driven flow is presented. Please note that just like previous section, the studies presented are for general 2D openings.

A prediction of ventilation rates in the presence of wind flow is comparatively complex. The interaction of moving air with the building façade is affected by terrain, surrounding buildings, trees and similar obstructions. This phenomenon alters the wind pressure coefficients due to wind direction and speed. Hence, these variables make any airflow prediction through openings in such facades very uncertain (Mochida et al., 2005). The pressure coefficients are surface averaged to calculate the airflow rates (Swami & Chandra, 1987). Such surface average data contribute to various libraries of building energy simulation programmes and AFN databases. Different pressure coefficient databases are discussed in the section 2.11.6.

To predict airflow rates through openings under wind flow, another simplification is made i.e., assuming the flow under static pressure rather than dynamic pressures. This may lead to an overestimation of the flow rates (Vickery & Karakatsanis, 1987), especially when wind direction is normal to the opening surface.

In real world cases, wind pressure and buoyancy pressures act together on a façade. In the cases where moderate speed wind flows (1-2m/s), wind pressures may dominate the buoyancy pressures (Larsen 2006), which is very common in real life situations. However, AFN solution adds pressures due to buoyancy and wind and airflow rates are calculated with sum of the pressure due to presence of both driving forces.

2.7.2.1 Modelling of Wind Driven Flow

In AFN tools, the local wind velocity (equation 2.15) causes pressure difference which is calculated by Bernoulli's equation. While pressure is given by equation 2.16.

$$V_{local} = V_{station} \times \omega \left(\frac{H}{Z_{met}}\right)^{\alpha} \qquad 2.15$$

Where V_{local} and $V_{station}$ are local and met station wind speeds, ω and α define obstruction due to the building surroundings and terrain and Z_{met} is height of met station which is always taken as 10 meters. The term $\left(\frac{H}{Z_{met}}\right)^{\alpha}$ is wind-reduction factor. Other calculation techniques and their review is presented in section 2.11.5.

Equation 2.16 expresses wind pressure at a point location i on the outside surface where $C_{p,i,d}$ is pressure coefficient for point location i correlating with wind from direction d.

$$P_i = C_{p,i,d}\left(\frac{1}{2}\rho V_{local}{}^{2}\right) \tag{2.16}$$

CONTAM, ESP-r and COMIS use same equation 2.16 to solve for pressure at any location i from wind direction d, where C_p is pressure coefficient, ρ is wind density and V is wind speed at a given height. In CONTAM and ESP-r, C_p is taken from a data file of standard coefficients based on experimental publications while COMIS includes a sub-routine calculator to define a C_p value based on height and direction of wind.

2.7.3 Ability of AFN Solution to Predict Airflow

The following set of validation studies have assessed the numerical solution of experimental data in different simulation tools. It is important to note that these studies only assess the free area opening in the flow equations and do not consider the window mechanisms or flaps. This would allow for an elaboration on the applicability of these solutions to a more generalised context beyond the specific case of flapped openings like windows.

Cross ventilation in a wind tunnel with opening on each side was evaluated in a single zone (Jiang, 2002). Wind speed was kept constant, and measurements of air velocity and wind and leeward pressure coefficients were measured. Flow rate during the experiment was predicted through CFD model. Experimental scenario was simulated in four simulation tools by Johnson (Johnson et al., 2012). Comparison is tabulated below:

CFD Flow Rate	ESP-r	COMIS	CONTAM	Energy Plus	Uncertainty
0.0465 m^3/s	0.035022 m^3/s, 24.8% Error	0.035094 m^3/s, 24.5% Error	0.034978 m^3/s, 24.8% Error	0.034976 m^3/s, 24.8% Error	• Zone Air Movement • Discharge Coefficient of Openings • Windward pressure coefficient

Table 2.3 : CFD vs AFN Simulated Flow Rates for Wind Driven Cross Ventilation Study

It is worth noting that both the studies above are simulated studies, and the comparison only compares CFD estimated flow with AFN estimated flow. A substantial error in the flow rate prediction by all four tools can be due to use of default C_d and a surface averaged C_p.

The aforementioned CFD simulation (Jiang, 2002) was repeated, but this time with just single sided opening, resulting in flow rate of 0.0026 m3/s while all four simulation software were not able to calculate hence resulting in error. This is because the simulation tools require at least two links for an airflow network or if there is a single bi-directional flow component then there should be temperature difference between inside and outside the zone. For this single sided flow simulation study, conditions are isothermal and single sided flow solution via orifice equation is modelled (Johnson et al., 2012).

Larsen (Larsen, 2006) studied cross and single sided flows in two separate experimental studies and Johnson (Johnson et al., 2012) evaluated aforementioned simulation tools for these experiments. The volume flow rates were recorded for three different windspeeds (1, 3 and 5 m/s) and three different temperature differences between ambient and chamber (ΔT=0, ΔT=5 and ΔT=10).

For the cross-ventilation experiment (chamber size: 5.56x5.56x3m; opening size: 0.86x0.15m) all four simulation network models produced same results with negligible difference for each temperature difference (Figure 2.13). For higher temperature they underpredict effect of buoyancy and changes in air flow are negligible. With the increase in windspeed, network models also show discrepancy as shown in the graph below. This can be due to the default value of C_d taken as 0.65 for sharped edged orifice as well as the locations of the openings to simulate the effect of buoyancy and stack. Secondly wind profile information was not available hence sensitivity analysis can be conducted which can show a linear increase in flow rates as wind speed increases. Thirdly the opening height was >10cm and representation of such opening via bi-directional flow would include the impact of ΔT of the pressures.

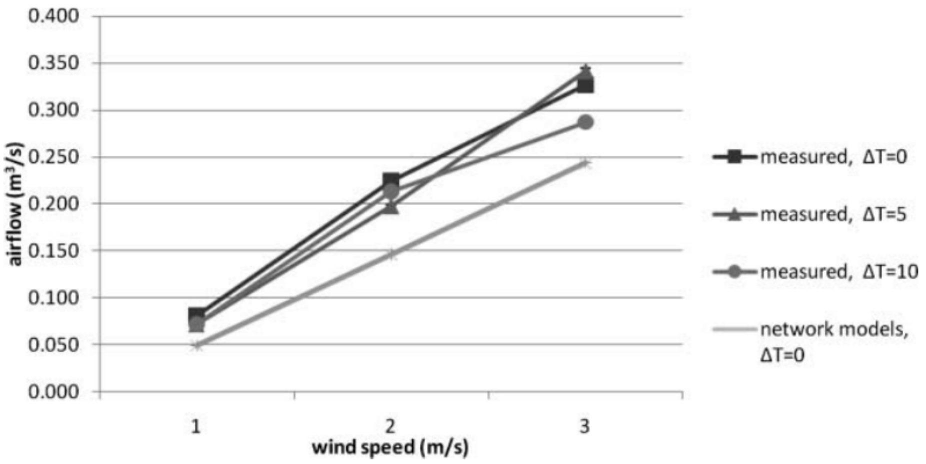

Figure 2.13 : Experimental vs Simulated Results for Cross Flow Driven by Wind Speed and Temperature Difference (Johnson et al., 2012).

Single sided volume flow rate experiment was done in the same chamber with identical boundary conditions as previous experiment but relatively larger opening (size: 0.86x1.4m). Network models again showed superimposed results for each temperature difference. Modelled flow rate remains constant for varying windspeed and this confirms the limitation of AFN solution due to a single opening in the zone and having a constant wind pressure across the entire opening. Yet again the use of equation to model the opening is not expressed.

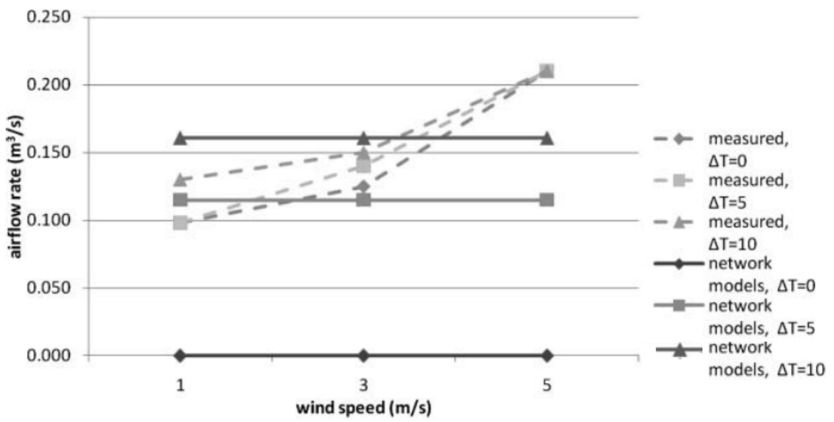

Figure 2.14 : Experimental vs Simulated Results for Single Sided Flow Driven by Wind Speed and Temperature Difference (Johnson et al., 2012).

Its noteworthy that where temperature difference is null i.e., isothermal conditions, simulation tools were not able to converge a solution. Even when there is temperature difference, flow rate does not change with varying wind speed. This is due to the same limitations of single sided flow solution due to no presence of infiltration cracks in the model.

2.7.3.1 Discussion

For single sided flows, it is important to model infiltration in the building along with a flow opening. AFN tools solve airflow basing on mass conservation i.e., the flows in and out of each node are solved by a set of simultaneous nonlinear equations. For just one flow path, the solution will result in error. It is also important for the sake of realistic modelling practices to model infiltration along with a purpose provided opening.

For cross ventilation due to wind, underprediction or overprediction of the flow rate occurred due to the unknown wind profile and discharge coefficient of the openings. Also, as the opening height is greater than 10cm, bi-directional flow component would be a better representation of the opening.

Addition to this, indoor air movement in cross ventilation is caused by a static pressure difference on both the sides as well as the momentum of the incoming air. AFN tools solve for still air in the zone (L. (Leon) Wang & Chen, 2008). Neglecting air momentum effect leads to erroneous prediction of airflows. The significance of this error to evaluate indoor environment is worthy of further analysis. These are however inherent limitations of AFN models. The discrepancy between experimental and simulation results witnessed in the cited studies is due to both input uncertainty and the limitations of the AFN tools.

2.7.4 Variation of C_d for Different Scenarios of Airflow

This section provides the general concept of C_d and presents its variation in case of varied window opening mechanisms. This variation paves way to introduce a more generalised and easier to apply analytical model. For this purpose, free area analytical models are compared and a model capable of translating flapped openings' aerodynamic properties with greater accuracy is presented.

Free area is the maximum flow area offered by the flapped opening frame in the absence of a flap. Such areas are easy to measure. The combination of discharge coefficient and free area would be a simpler method of modelling effective area. Please note that the discharge coefficient used in conjunction with free area would be determined differently compared to a discharge coefficient meant to be used with geometric area.

C_d plays an important part in case of both buoyancy and wind driven flows. It is evident from the literature that the value of C_d is function of Reynolds number (Heiselberg et al., 2015), wind direction (Yi et al., 2019), turbulence/flow regime (Chu et al., 2009) , building geometry which includes sheltering of the window, opening area, window type and ΔP and hence using a generalised value of 0.6 can lead to inaccurate determination of volume flow rates using any set of equations which are based on Bernoulli's principal (Karava et al., 2004). This section will cover the literature concerning experimental evaluation of C_d as function of pressure difference, opening area, wind speed and opening angles.

Before considering the variation of C_d under different circumstances, it is important to highlight the basics of this phenomenon.

When an airflow jet passes through an opening in a building envelope, the jet formed has a cross-section area smaller than the cross-section area of the opening. This phenomenon is called vena-contracta and can be expressed as:

$$C_c = \frac{Area\ of\ jet\ at\ vena - contracta}{Area\ of\ opening} = \frac{a_c}{a} \qquad 2.17$$

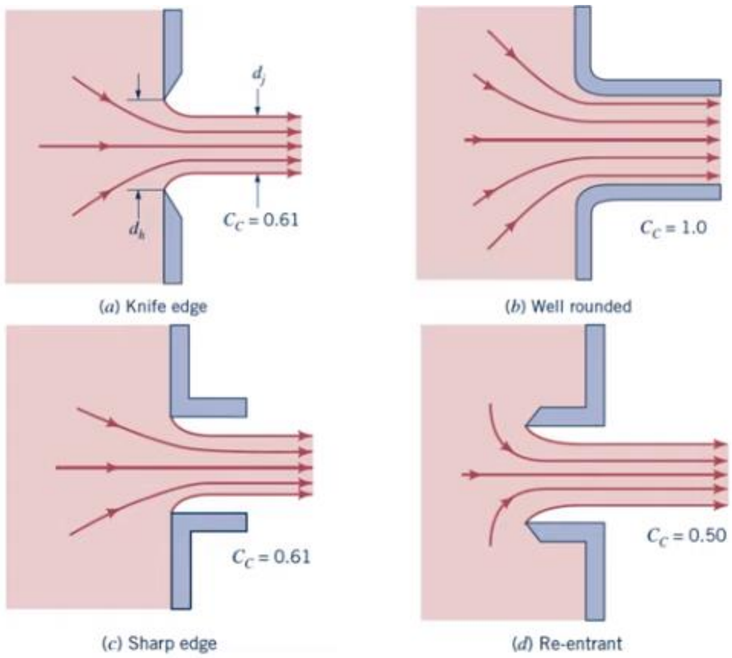

Figure 2.15: Comparison of Free Area and Jet Flow Area and Different Contraction Coefficient for Different Geometries

Similarly, the ratio of velocity at both points is given by coefficient of velocity:

$$C_v = \frac{Velocity\ of\ jet\ at\ vena - contracta}{Theoretical\ velocity} = \frac{v}{\sqrt{2gh}} \qquad 2.18$$

In the same way the actual and theoretical discharges are not equal hence coefficient of discharge is given as:

$$C_d = \frac{Actual\ Discharge}{Theoretical\ Discharge} = \frac{a_c v}{a\sqrt{2gh}} = C_c C_v \qquad 2.19$$

Under the laboratory-controlled environment, simple openings are comparatively straightforward when determining the resistance of the opening towards the flow regarded as C_d.

In the case of varying flow conditions and opening geometries, various studies have been conducted which detail variations in C_d based upon the factors mentioned previously. Heiselberg (Heiselberg et al., 2001) evaluated C_d as a function of ΔP due to the temperature differences associated with the different opening areas of tilt and turn windows. The coefficient values varied with different opening areas and differed for both opening types. Specially, for the turn window, the C_d value varied for smaller pressure differences <10Pa, while for larger ΔP variation was negligible. For smaller ΔP this variation was found in the range of +/-0.15 (Figure 2.16). For tilt windows it was negligible and in the range of +/-0.05 (Figure 2.17). Later Heiselberg (Heiselberg & Sandberg, 2006) extended the study and concluded that inflow and outflow C_d values are not same for the two aforementioned window types and the coefficient value reduced when the flow direction reversed.

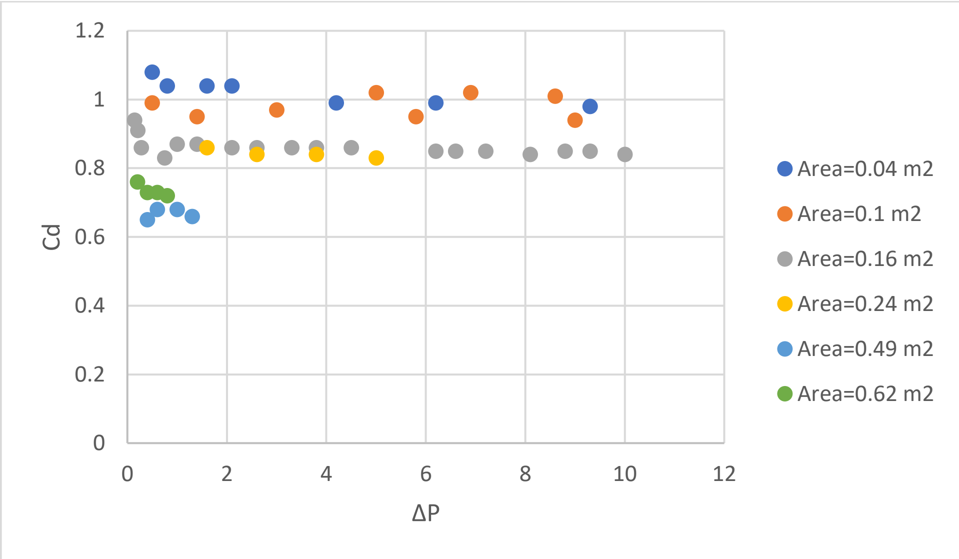

Figure 2.16: Experimental C_d for Turn Window Openings over Various Pressure Differences.

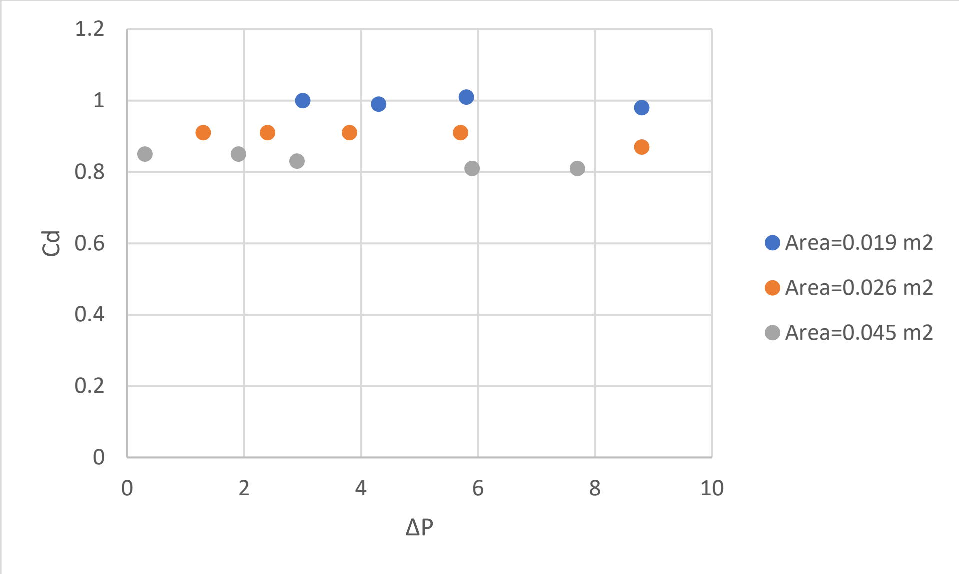

Figure 2.17: Experimental C_d for Tilt Window Openings over Various Pressure Differences.

Under the pure buoyancy driven flows, different windows were analysed by Garbe (Grabe, 2013) where they calculated the flow resistance ζ which is related to C_d by the following relation:

$$C_d = \frac{A\sqrt{\left(\frac{2\Delta P}{\rho}\right)}}{Q} = \frac{1}{\sqrt{\zeta}} \qquad 2.20$$

It is suggested as per Figure 2.18, flow resistance is close to identical for all symmetrical window opening types as well as the inlet of awning and outlet of tilt windows which are deemed as asymmetrical windows. However, the outlet of awning and inlet of tilt offer different resistance to the flows in comparison to other window types as well as amongst themselves. These values show a clear correlation between opening area and discharge coefficients.

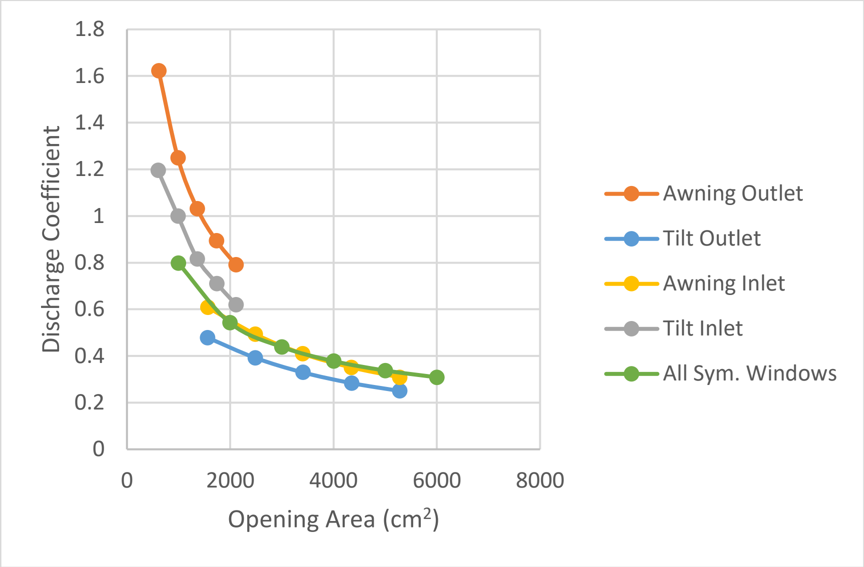

Figure 2.18: Discharge Coefficients Derived from Resistance Coefficients Measured by (Grabe 2013) for Inlet and Outlets of Different Window Types (Asymmetrical) and Geometric Opening Areas. Symmetrical Windows, Tilt Window Outlet and Awning Window Inlet Show Close to Identical C_d values.

This experimental setup has only considered buoyancy driven flow through the windows while in real world scenarios, it is difficult to predict the flow driving forces. Both cross flow study by Heiselberg (Heiselberg & Sandberg, 2006) and single sided buoyancy driven flow study by Garbe (Grabe, 2013) suggest that for tilt windows, inflow C_d> outflow C_d. This is also true for wind driven flow and this was evaluated by Heiselberg (Heiselberg et al., 2015) for centre pivoted window.

Further to the effect of temperature difference on C_d, Ar' is given as:

$$Ar' = \frac{\Delta T}{Q^2} \tag{2.21}$$

The value of C_d is reduced at large temperature differences. This dependency reduces when the area of flow is small. Heiselberg (Heiselberg & Sandberg, 2006) evaluated a turn window area of 0.04m^2 and 0.1m^2.

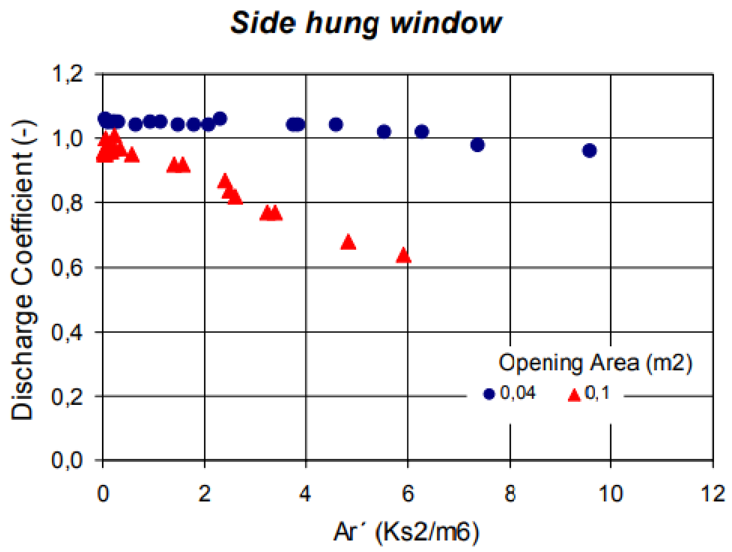

Figure 2.19: Effect of Combination of Buoyancy and Wind Flow on Discharge Coefficient (Heiselberg & Sandberg, 2006).

This phenomenon is evident in window types which offer relative height differences, such as the turn window. For asymmetrical windows this dependency is minimal.

Flow turbulence also played an important part in determining the C_d as well as flow regime. For the opening angle ≤30°, C_d decreased with increases in Reynolds number until Re <10000. This evaluation was for a horizontal pivot window which combines tilt and awning.

$$Re = \frac{\sqrt{A}u}{v} \quad 2.22$$

Where A is geometric opening area, u is average air velocity and *v* is kinematic viscosity. Air velocity ratio (local/reference) is given as function of C_d which ultimately reflects in turbulence in the window opening evaluated by Re.

$$C_d = f\left(\frac{q}{AU_{ref}}\right) = f\left(\frac{u}{U_{ref}}\right) \quad 2.23$$

Fernandes (Fernandes et al., 2020) also evaluated different window mechanisms and angles under cross flow arrangements. Without window flaps and mechanisms, the same opening area behaved as an orifice and gave an ideal value of 0.66. For an awning window opened at a 45° angle, the coefficient of discharge was 0.41 which was close to the value found in literature i.e., 0.45 (Idel’čik, 1966). This is to note that these experiments were conducted in wind tunnel and pressure taps were placed 10cm away from the window opening while Heiselberg (Heiselberg & Sandberg, 2006) mounted these pressure taps right beside them. Moreover, the experimenter used the free area of the window rather than the geometric area.

Such variability in the experimental conduct results in approximation when these values are genialised to model similar openings.

Yang (Yang et al., 2010) conducted wind tunnel tests of a turn opening and calculated C_d. For the constant wind speed and direction and varied opening angle, it showed that, resistance of the opening decreased as the angle is increased. For a small window opening angle of 10°, C_d was 0.12 (based on the free area of the window). (B. Jones & Iddon, 2019) also developed a C_d calculator (BB101) which estimates this value to be 0.19 for the same opening angle.

The flow through a window opening is often due to the combined effect of buoyancy and wind. As mentioned in equation 2.21, Archimedes number evaluates effect of buoyant forces in causing the flow. Etheridge (D. W. Etheridge, 2000) details how this number can be used to evaluate the magnitude of pressure differential caused by buoyancy and wind. This dimensionless number indicates ratio of Grashoff number to the square of Reynolds number. In the equation 2.24, ΔT is temperature difference, D is depth of the room where opening is placed, T_{in} is indoor temperature, H is height of the flow opening and U is wind velocity at the inlet. When Ar<1, flow is primarily due to the wind induced pressure difference and when Ar≥1, flow is mainly caused due to buoyant forces. This metric can help in selection of a C_d number and geometrical representation of a window in AFN.

$$Ar = \frac{g\Delta T H^3}{U^2 D^2} \qquad 2.24$$

A vast variation in C_d is evident due to boundary conditions and the flap mechanism. The next section will present free area models to determine C_d which are aimed to be a comparatively straightforward way of determining the effective area of a window mechanism. This would also eliminate the possibility of erroneous calculations of the geometric area (discussed in section 2.7.5)

2.7.4.1 Analytical and Empirical Models to Estimate C_d

The analytical models rely on experimental data to estimate the resistance offered to the flow by the structure of the window opening. By assessing the frame aspect ratio and opening angle, a C_d value can be determined.

Most of the cited studies in the previous section used geometric areas to determine C_d; this entailed ambiguity as there are various way to measure a window's 3D geometry. An alternative approach defines an easily measurable area and evaluates C_d based on the opening area formed by the opening angle. Equation 2.25 explains C_d to be a function of the width, height and angle of the opening of a window.

$$C_d(\frac{w}{h},\theta) = \frac{Q}{wh}\sqrt{\frac{\rho}{2\Delta P}} \qquad 2.25$$

In the equation above, $\frac{w}{h}$ is the aspect ratio of the window frame and θ is the opening angle.

Jong (de Jong & Bot, 1992) evaluated flow resistivity offered by the window due to its mechanisms and geometry. They evaluated top hinged window and suggested aspect ratio of the opening as well as the window mechanisms both offer resistivity and that needs to be accounted for to determine C_d of such window.

$$C_d = \frac{\mathrm{F}_o}{f_w(\theta)}^{\frac{-1}{2}} \qquad 2.26$$

Where F_o is friction factor of the opening without the flap and dependent upon aspect ratio of the opening and the function $f_w(\theta)$ i.e., window function is given by:

$$f_w(\theta) = \frac{[f_2(\theta)]^2}{f_1(\theta)}$$

Where $f_2(\theta)$ is ratio of geometric area of the opening to the free area of the opening and $f_1(\theta)$ is ratio of friction factor due to the flap to the friction factor of the orifice opening without the flap. These friction factors can be calculated by the fitting curve data basing upon the aspect ratio of the free area:

$$F_o = 1.75 + 0.7\exp\left[-\frac{\frac{L_o}{H_o}}{32.5}\right]; when \frac{L_o}{H_o} > 1$$

$$F_o = 1.75 + 0.7\exp\left[-\frac{\frac{H_o}{L_o}}{32.5}\right]; \ when \frac{L_o}{H_o} < 1$$

In the case where flap is mounted onto the opening, this fiction factor changes as the function of the opening angle of flap. Assuming window is top hinged and has rectangular form factor and aspect ratio is > 1 $f_1(\theta)$ can be given as:

$$f_1(\theta) = \frac{F_w}{F_o} = \frac{1.75 + 0.7\exp\left[-\frac{\frac{L_o}{H_o sin\theta}}{32.5}\right]}{1.75 + 0.7\exp\left[-\frac{\frac{L_o}{H_o}}{32.5}\right]}$$

Now $f_2(\theta)$ is given as

$$f_2(\theta) = \left[\frac{1}{2}\rho(\frac{F_o}{A_o}) \times f_1(\theta)\right]^{1/2} \times \frac{Q}{\Delta P^{1/2}}$$

Bailey (Bailey et al., 2003) worked towards further development on top of the study by Jong (de Jong & Bot, 1992) and suggested a relation for the estimation of C_d for aspect ratios ≥5 basing upon the linear regression of experimental analysis.

$$C_d = -0.198 + 0.157 \ln \theta + 0.00108 \frac{L_o}{H_o} \quad 2.27$$

For aspect ratios ≤5, equation is given by:

$$C_d = \left[1.9 + 0.7exp[-L_o/32.5H_o sin\theta]\right]^{-0.5} \quad 2.28$$

The approach by Jong (de Jong & Bot, 1992) and Bailey (Bailey et al., 2003) gives a closer estimation of the C_d values and this is evaluated by Patrick Sharpe Sharpe et al. (2021). They have reported an error <2.5% which is more acceptable than an error up to 23% by taking the value for the sharp orifice i.e., 0.61. Both of these approaches also take account of the reduced efficiency of side window openings which impact the overprediction by the simple representation of windows via the orifice equation, as based on the correction factor in equation 2.29 where a and b are empirical coefficients. The values for a and b were found to be 0.25 and 1.0 respectively (de Jong & Bot, 1992), and 0.6 and 1.0 (Bailey et al., 2003).

$$f = sin\theta \left[1 + a\frac{H_o}{L_o}\left[cos\theta - 2b\pi\frac{(90-\theta)}{360} sin\theta\right]\right] \quad 2.29$$

Equation 2.29 yields the factor to be multiplied by C_d value calculated by equation 2.28.

It is important to note that these free area models have limitations as experimental procedures to determine C_d are undertaken in idealised conditions.

Patrick Sharpe (P. Sharpe et al., 2021) captured the predictive power of a vast data (including the studies cited above) from analytical, semi empirical and pure empirical models and formulated a statistical/empirical set of equations.

$$B = ae^{-b\left(\frac{w}{h}\right)} + 0.61 \quad 2.30$$

$$M = c(\frac{w}{h} + 1) \quad 2.31$$

$$C_d(\theta) = \mathrm{B}(1 - \mathrm{e}^{-M\theta}) \quad 2.32$$

Equations 2.30-2.32 are used to determine C_d for a certain opening angle of the window with aspect ratio $\frac{w}{h}$. The values for a, b and c are determined through the curve fitting process of experimental data with R^2=0.98 which means that 98% of the variance is observed by the equation set.

To compare the effective area calculated by these models is presented in a common form compared with the idealised discharged coefficient which is given by:

$$C_{d,idealised} = 0.61\frac{Free\ Area}{wh} \tag{2.33}$$

The conditions used to determine $C_{d,idealised}$ include a steady, unidirectional flow between two zones of still air of uniform pressure and density difference is null. Data from different free area models is inputted in equation for $C_{d,idealised}$ and compared against experimental data. The SEAM model had the lowest mean and standard deviation which indicates the predicted effective area is closest to the experimental data. However, data for very small opening angles was limited and model is suggested to be used for opening angle >10°.

This model is applicable to tilt, awning and turn windows by taking account of correct width and height of the window frame. Due to its straightforward application and pertinence to various window mechanisms, this model is included to feed into the guidance to model windows. For slight opening of these windows <10°, this model needs to be updated with greater number of experimental studies concerning cracked opening of windows and doors. Hence this model entails the limitation to calculate C_d for slightly opened mechanisms.

2.7.4.2 Discussion

The literature review identifies that varied angles of opening/opening areas for different window mechanisms offer different resistance to the incoming flow, and this resistance also varies with the flow regime. A modeller can have access to data such as window opening mechanisms, area of flows and obstructions, but weather-related ambiguities, such as ambient pressure data which depends upon wind speed and defines the flow regime, are very difficult to assess.

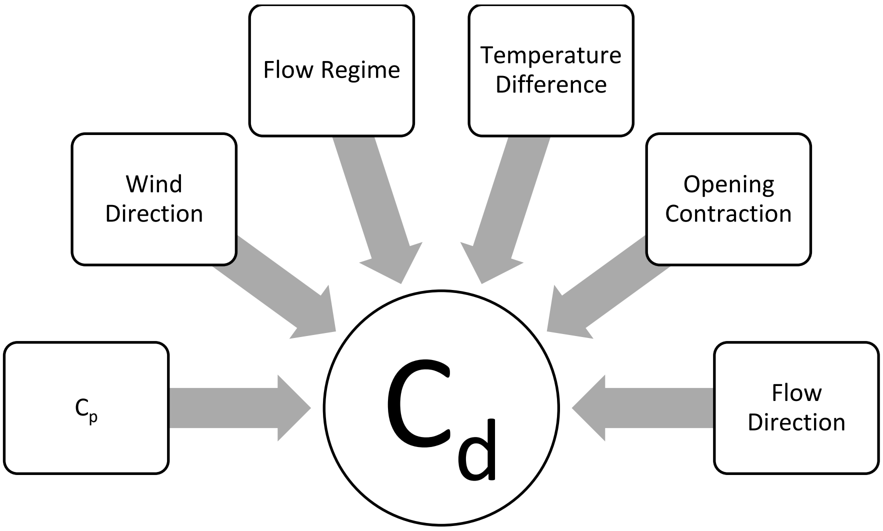

Figure 2.20: Factors defining Coefficient of Discharge in a Model

It is established that flow through a window in real life is uncertain and a generalised C_d of 0.61 can cause an erroneous estimation of flow when using the orifice equation. It is evident from the literature that various factors significantly affect the C_d value meaning it is difficult to take a value from the literature and ensure it does not underpredict or overpredict the airflow values.

The key points from this review of experimental studies can be used to assess appropriate C_d for a certain scenario.

- For different window opening sizes and mechanisms, C_d varies.
- Inflow C_d is greater than outflow C_d; this is true for buoyancy driven flows as well as combined driven flow when buoyant forces dominate.
- For window types replicating doors, large temperature differences can cause C_d to reduce.
- Windows with symmetrical areas of flow can be given be modelled as a single opening with a C_d value however this will change when these windows as a whole or their portions behave as an outlet.

The varied values of C_d from the cited experimental studies show that the coefficient of discharge ranges for different window mechanisms and flow conditions. It is evident that conditions from single sided buoyancy alone have higher C_d values. In a wind driven cross flow these values lie in the range of 0.6-0.87. If we compare cross flow due to wind under isothermal conditions with non-isothermal conditions, the opposing buoyant forces result in a lower C_d number. This is more relevant in domestic ventilation design as rooms are often cross ventilated with an opened internal door. Variability in the determination of C_d paves the way to use SEAM which effectively calculates the effective area of a hinged opening (windows and doors). The mechanisms to which it can apply are vast and involve a straightforward application. However as indicated before, this model cannot replace the actual measured aerodynamic behaviour or flapped openings. However, this model can be used as best approximation in the absence of actual data.

2.7.5 Geometric, Effective and Equivalent Areas of Flow

As SEAM can determine effective areas on the basis of the free area of the window frame and the opening angle, it is still found important to highlight the ambiguities in determining the flow areas.

Trigonometric calculations are tabulated in Table 2.4 to determine geometric area of different window types:

Window Type	Geometric Area
Vertical Slide	$w \times G$
Tilt/Awning	$h(hcos\theta sin\theta + w - wcos\theta)$
Horizontal Pivot	$0.5h(0.5hcos\theta sin\theta + w - wcos\theta)$
Turn	$w(wcos\theta sin\theta + h - hcos\theta)$
Vertical Pivot	$w(0.5wcos\theta sin\theta + h - hcos\theta)$

Table 2.4: Geometric area trigonometric equations for different window opening types.

Caciolo et al. (2011) and J. Wang et al. (2017) use the same geometric area relation as given in Table 2.4 but the former study regard them as effective areas, however these areas do not take account of the aerodynamic performance of the openings hence should be regarded as geometric areas. Furthermore, in the literature, uncertainty lies in the measurement of the effective areas of windows. A tilt window is taken as an example in Figure 2.21.

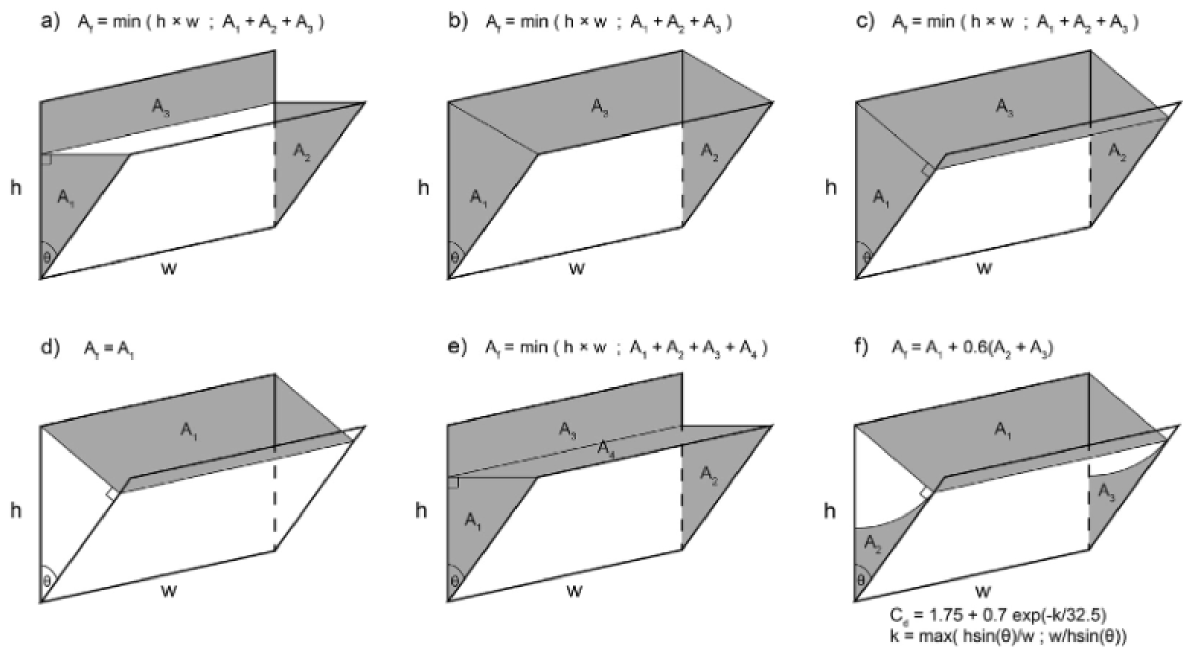

Figure 2.21: Different area calculation methods for tilt window (P. Sharpe et al. 2021).

Figure 2.21, which shows the calculation of geometric area methods, confirms the possible errors in modelling the effective flow area.

The free area is related to the effective area by C_d as a function of opening angle and aspect ratio in equation 2.34:

$$A_{eff} = C_d A_{free}(Angle\ of\ Opening, Height, Width) \qquad 2.34$$

A similar relation for effective and free area basing upon opening aspect ratio and angle of opening is also presented in (Building Bulletin, 2018) which shows variation in C_d for width, height and angle of the window opening.

$$A_{eff} = C_d\big(Angle\ of\ Opening, Aspect\ Ratio\ (h{:}w)\big)\ Height \times Width \qquad 2.35$$

Where we have sharp edged openings and free area is equal to geometric area.

$$A_{eff} = C_d A_f \qquad 2.36$$

A_{eff} is determined by the ventilation equipment manufacturers by using a sealed chamber comprised of a fan, a duct and anemometer which relates to the opening under evaluation. This standard test rig is described by EN13141-1, (2019) and the calculation is based on still air conditions.

Another method is to calculate equivalent area A_{eq} which involves input of C_{d_o} for which sharp edged opening value is taken as 0.62 (hypothetical area of flow with no energy loses). The equation below shows an overall relation between equivalent, effective and free areas of flow.

$$A_{eq} = \frac{C_d A_f}{C_{d_o}} = \frac{A_{eff}}{C_{d_o}} \quad 2.37$$

AIVC	Effective Area: Area derived by assuming the value of the discharge coefficient associated with a sharp-edged orifice, the area varies with the flow rate
CIBSE Guide A	$A_{effective} = C_d A_{free}$ 2.38 $Q = C_d A_{free} \sqrt{\frac{2\Delta P}{\rho}}$ 2.39
EN 13141-1:2019	Free area is the sum of the cross-sectional areas of all unobstructed openings measured on the plane of maximum restriction and at right angles to the flow through the openings. Equivalent area is a sharp-edged circular orifice area which will pass the same airflow rate and at the same applied pressure difference as the product or device being tested.
EN 12101-2:2003	Equivalent area is referred to as the aerodynamic free area.
Approved Document F: Ventilation	Free Area is the geometric area while the effective area is aerodynamically performing area.
IES	Term 'equivalent area' is used and C_d is considered.
CONTAM	Term 'cross sectional area' is used for free area.
Energy Plus	Term 'area' is used to define geometrical area.
ESP-r	Term 'opening Area' is used, and fixed C_d is taken i.e. 0.65 for openings.

Table 2.5: Different Flow Area Terminologies in Guides and Simulation Tools.

The variability of use of different area terminologies across the different designs and simulation guides can cause error in the calculation of flow rates through open windows and other opening passages. It is important to go through the documentation before the calculation process. For example, when defining an opening using "specific airflow opening" in the simulation tool ESP-r, the modeller can assign an area in the equation. It does not explicitly suggest a geometric area or effective area while asks for "opening area" input. The documentation however suggests that it is an effective area by taking the default C_d at 0.65.

The use of different terms for the flow area is evident in the literature as well as in the instructions available for simulation tools. There is no common method to calculate the geometric area of flapped openings. Additionally, the terms to describe the area are contradictory and ambiguous.

2.7.6 Important Considerations to Model Windows

The performance of windows can offer high variability under certain flow conditions and opening mechanisms. This suggests the need for the manufacturer testing of window panels and the availability of such data to accurately model windows for design evaluations. However, in the absence of such facilities and based upon the literature, the following important considerations can be presented to effectively model such openings.

Opening area: Physical models of the opening structures in buildings assume that the window is in the same plane as other components fitted on the façade of the building (Larsen, 2006) and it is validated through CFD studies (Fracastoro et al., 2002). Hence assuming it to be a two-dimensional structure is a well approximated method and the area used to model the window is of high importance. It is also important to consider the window mechanism and any obstructions due to the opening mechanism as well as due to structure of the building. One should be aware of the different opening area terminologies, for example the use of a geometric area where the free area required would result in an underestimation of flow rates.

Flow Equation: For an opening greater than 10cm in height a single bi-directional opening equation is suggested for modelling.

C_d Selection: This review suggests against using C_d=0.61 with the geometric area. A statistical model (SEAM) is presented from recent literature which is capable of handling ambiguity in determining an effective flow area of hinged openings. The input of this model is the aspect ratio of the hinged opening, the free area, and the angle of the opening. The output is C_d which is used with the free area in the orifice flow equation. For the situations where flow obstruction is due to close proximity of frame and flap, this model is not accurate.

2.7.7 Flow Though Doors

As discussed in previous sections which detail the flow through windows, temperature and pressure differentials are responsible for the airflow through an opening. In this section similarities and differences between the flow through doors and windows are highlighted as well as modelling considerations are evaluated via literature review.

Temperature and pressure differences across internal doors are similar to still air conditions (Kalliomäki et al., 2016). Hence, the airflow through doors is due to pressure differences caused by any extracts or opened windows in the room or hallway. With closed windows and trickle vents, and no extraction fans, airflow is supposed to be minute.

The modelling of doors closely resembles the side-hinged turn window mechanism. This leads to the placement of a neutral zone plane which, for symmetrical openings, is in the middle of the opening. Linden (Linden, 1999) explains how the presence of neutral levels allows for a bi-directional flow via a vertical opening due to temperature differences. In the case of internal doors where temperature differences are of a lower magnitude (in case central heating is setup), this flow magnitude can be lower due to its dependency upon ΔT between the zones.

As mentioned earlier, the geometry of the door airflow pathway is similar to the turn window opening mechanism shown in Figure 2.2. However, it is important to account for over and undercuts in a door where the former is a fitting crack and latter is a purpose provided opening. ADF (Approved Document F, 2010) suggests a 10mm undercut in a 76cm wide door to allow for the circulation of air. The overcut is usually smaller than the undercut. Keeping this phenomenon in consideration, the geometric area should be calculated by not just the dimensions of door leaf but also the airflow passage area.

2.7.8 Discussion

The modelling of a door is like the modelling of a symmetrical window. Additional care is required to include door undercut passages, as elaborated in the section 2.6.7. To highlight important considerations when modelling an internal door opening, learnings from the modelling of symmetrical windows will be used to elaborate the presence of a neutral plane in the middle of the opening. Hence, either a bi-directional door component or set of two orifice equations on the top and bottom would closely replicate the airflow through the door opening.

For an internal door, equation 2.11 is best suited as internal pressure gradients can be calculated based upon the flow conditions in adjoining zones. For doors >10°, the effective area from the SEAM analytical model can be used. The second approach to such vertical openings is to model this effective area on the top and bottom of the window frame by taking into account the correction factor to tackle the overprediction of the flow rates (P. Sharpe et al., 2021). The upcoming modelling study chapter will draw comparisons between the single and multi-opening approaches to model a door opening.

2.8 Interzone Flow Components

The interzone flow area and resistance between inlet and exhaust of a ventilation system significantly influence IAQ, supporting the hypothesis that shorter flow paths and/or reduced flow resistance can mitigate high CO_2 levels in main bedrooms (T. Sharpe et al., 2019). Data from this study is further analysed in Appendix 1 further supporting this claim. Basing upon this premise, this section explores the literature to introduce acoustic opening as a viable solution to enable greater air movement between zones. These openings must not compromise the privacy of living spaces. While ensuring no impact on privacy is challenging, the review details the factors which are important in selecting the suitable acoustic opening. This review aims to provide an alternative ventilation design solution by incorporating interzone acoustic openings to improve IAQ in residential living spaces. Hence, it presents a limited list of commercially available, laboratory tested and domestically applicable flow components along with their design data for the AFN modelling.

2.8.1 Acoustic and Airflow Performance of Openings

The important factors determining the performance of an acoustic vent are discussed in this section to evaluate the commercially available ventilation openings providing acoustic performance for noise reduction and privacy.

A large enough opening providing sufficient ventilation rates would also result in noise ingress leading to reduced speech privacy (De Salis et al., 2002).

The Speech Intelligibility Index (SII) parameter varies from 0 to 1 and is calculated using speech to background noise approach and a lower value implies greater speech privacy (Park et al., 2008). SII is advised to be <0.05 for a high level of privacy (Cavanaugh et al., 1962).

To determine the acoustic performance of a ventilation opening, instead of SII, the transmission loss (TL) is used as the design parameter.

$$TL = 10\log(\tau) = 10log\frac{W_{out}}{W_{in}} \tag{2.40}$$

Where τ is the transmission coefficient and the ratio $\frac{W_{out}}{W_{in}}$ is sound energy emitted from the outlet to its incident on the inlet.

TL is related to the noise reduction (NR) factor of openings which relates to the sound pressure levels across the openings.

$$NR = SP_{source} - SP_{receiver} = TL - 10log\frac{A_v}{A_{r,ab}} \tag{2.41}$$

NR is the difference between the source and receiver room sound pressure ($SP_{source} - SP_{receiver}$) which is across any opening. Equation 2.41 links NR with TL concerning opening area A_v and acoustic absorption in the receiver room $A_{r,ab}$. This also shows that transmission loss from the ventilation opening is a key factor in determining the noise isolation between two zones as well as reverberant conditions in the receiver room $A_{r,ab}$.

Based on equation 2.41, Salis (De Salis et al., 2002) studied the transmission loss of a wall when an opening is added. They used the orifice equation to complete the investigation and determine the equivalent area of flow of the opening. They concluded that the provision of an opening in a façade would increase τ. Hence, transmission loss from the opening is the main factor in deciding its acoustic performance. The same study concluded that different lining materials are useful for low, mid and high frequency sounds.

In the context of domestic environment, to introduce such an opening in an internal wall, the relation between the opening area and the wall area with transmission loss is given as:

$$TL_{wall-opening} = 10log\left(\frac{\tau_w \times A_w + \tau_o \times A_o}{A_w + A_o}\right) \qquad 2.42$$

Subscripts w refers to wall while o refers to an acoustic opening. A is area while τ is transmission loss coefficient. The term $\tau_o \times A_o$ must be in a range so that transmission loss is sufficient to provide privacy and low SII.

Both transmission loss and SII do not equate mathematically as they measure different aspects of acoustics; however, an indirect link can be identified in that the high transmission loss of an opening can help create a low SII value. However, industry standards specify the ventilation components by the transmission loss standard, known as Normalised Level Difference, with respect to Energy, Weighted ($D_{n,e,w}$) (Selamet et al., 2005). This standard takes account of the real-world conditions of the rooms where such acoustic openings are placed. These conditions include sound absorption and reverberation. Another experimental standard is sound transmission class (STC) which is a single number rating provided in ASTM 413 (ASTM, 2013). It is a measure of transmission loss at various frequencies (typically 125-4000Hz). These transmission loss measurements are compared against a standard reference contour, and a higher STC indicates better sound insulation. However, $D_{n,e,w}$ provides real-world normalised value and STC provides a standardised laboratory based assessment although both are related through the calculation of the transmission loss of an opening.

In an experimental study by Hopkins (Hopkins, 2004) the acoustic performance of lined duct type ventilation openings were investigated and the results were discussed and their application was evaluated by Bibby (Bibby, 2011). A comparison between performances was conducted via the area ratio parameter (equation 2.43) by simplifying it as the ratio of resistivity to flow and resistivity to sound.

$$Area\ Ratio = \frac{Airflow\ Equivalent\ Opening\ Area}{Sound\ Equivalent\ Opening\ Area} = \frac{AEO}{SEO} \qquad 2.43$$

This ratio implies that the sound power transmission and airflow rate are in direct relation to the opening size (Bibby & Hodgson, 2014).

Different sound absorption measures were implemented in a 2.264m by 0.2m opening, and these configurations gave different C_d and τ values. Sound absorption materials, such as PVC film, was tested with and without bends and grilles. It was concluded that grilles do not decrease τ but would offer a smaller C_d value.

This section offered an understanding of the important parameters to look for when choosing an acoustic opening for a room or domestic setting. Alongside the acoustic performance, the airflow performance of the opening is also discussed.

2.8.2 Commercially Available Acoustic Openings

Building on the understanding of key factors that influence the performance of acoustic vents, commercially available flow components and their functionality are also discussed. By the end of this section, we aim to filter out a limited set of acoustic vents for later modelling, and to evaluate their ventilation performance. As far as acoustic performance is concerned, transmission loss ($D_{n,e,w}$) is considered a key selection metric, although the practical implications of sound proofing are not modelled nor quantified.

The overdoor grille developed by Renson (Renson, 2023) is an undercut alternative that offers better sound reduction. This can also be used in combination with a door undercut to provide an added flow area between two zones. This component does not compromise privacy and provides 28dB of sound reduction. Figure 2.22 shows cross section dimensions of the flow component. The double bend opening has an 11mm characteristic dimension and is fitted over a 35mm door leaf; however, it is also compatible for thicker door leaves of 40mm.

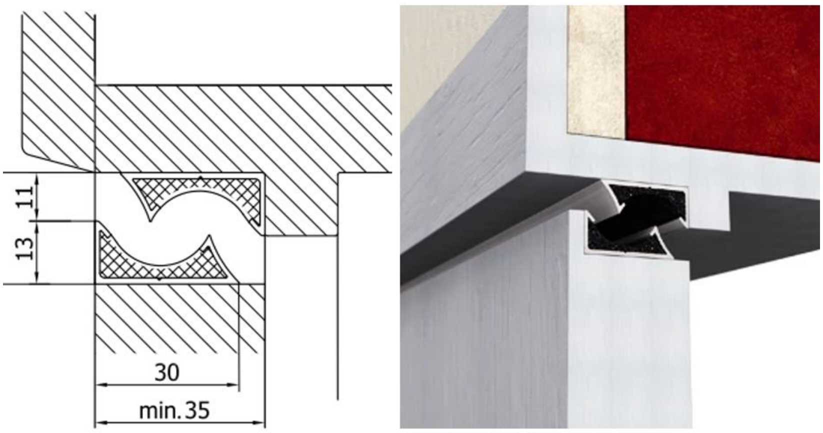

Figure 2.22: Cross section and 3D graphic for overdoor grille flow component (Renson, 2023).

Laboratory testing in accordance with EN13141-1, (2004) is represented in Figure 2.23 can be used to determine flow characterisitcs n and C by plotting base 10 log of variables thereby providing a straightline. The slope of this straightline would provide n while C can be calculated using the intercept value.

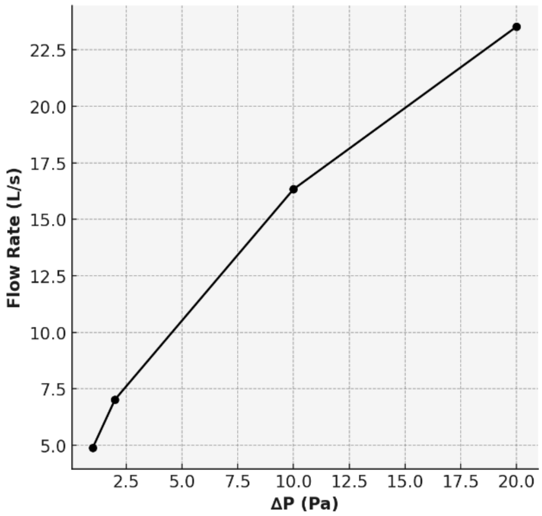

Figure 2.23: Flow vs ΔP in laboratory testing.

Equation 2.44 is in the form of power law providing the flow solution for the opening for a range of ΔP values and it will be used to model over door openings. Q is in l/s.

$$Q = 4.89 \times \Delta P^{0.53} \tag{2.44}$$

Another 'between zone' flow component is Passivent (Passivent, 2019). This noise reduction is suited for a mid range sound spectrum of 500-2000Hz and is suited for hotel bedroom usage as well as other commercial purposes. Transmission loss for a 320x320mm unit is 34dB, and airflow tesing is conducted following the same standard precedures as specified for the previous opening component. The opening without grilles allows for the optimal effective area however, grilles reduce this area by 25%.

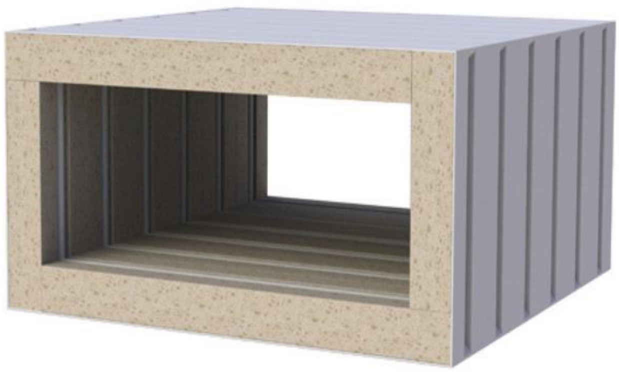

Figure 2.24: Passivent acoustic opening without grilles (Passivent, 2019).

The range of acoustic silencer components that can be integrated with other openings in a wall (including free openings) were developed and tested by Gilberts Blackpool (Gilberts, 2022). A 100mm depth silencer can provide 21dB of sound transmission loss with a 30% free area for the opening. For example, 0.5m^2 of free area will have effective area of 0.15m^2.

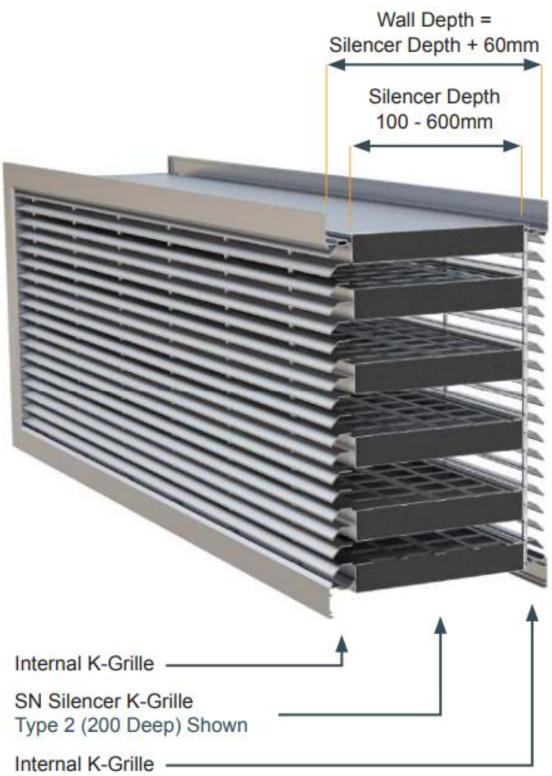

Figure 2.25: Gilberts acoustic silencer component (Gilberts, 2022).

From the flow components tested by Hopkins (Hopkins, 2004), the highest transmission loss for sound was recorded for a PVC lined opening with C_d=0.31, while the lowest transmission loss was recorded for same sized opening with non PVC lining and C_d=0.68. Although these openings are not commercially available and were only tested for regulatory purposes, the design data can be used to model and compare the airflow performances of these openings.

Using their identified flow performance specifications, these four interzone acoustic openings will be investigated for their performance in the AFN study in Chapter 5. On the basis of this performance investigation, the most suitable opening will be included in the example application of an improved ventilation design presented in Chapter 6.

2.8.3 Discussion

Interzone flow components has the potential to significantly impact IAQ by facilitating interzone air movement, hence reducing high CO_2 levels in areas like main bedrooms. Shorter flow paths and reduced flow resistance, as supported by T. Sharpe et al. (2019) and further analysed in Appendix 1, can mitigate elevated CO_2 concentrations. Introduction of acoustic openings can be tested for their viability to enhance airflow without compromising privacy. Key parameters are transmission loss (TL) and discharge coefficient C_d in selecting suitable openings. The selected acoustic openings will be further investigated in the AFN study to identify the most effective design for improving IAQ through enhanced ventilation strategies in the main bedrooms.

2.9 Flow Through Extract Fans

The extract fans are used in spaces such as kitchens and wet rooms to remove stale air along with excess moisture, and pollutants and replace them with fresh air from outside via opened doors, windows, and trickle vents. These spaces have higher levels of humidity, odours, and pollutants leading to health issues as well as damage to building materials. Extract fans work by creating a negative pressure in the space which allows controlled flow of air from outdoors to indoors (Fox, 2008).

In kitchens, extract fans are important for removing cooking fumes, steam, and odours which can accumulate during cooking. Without sufficient ventilation, these pollutants and odours can spread throughout the house (Riffat, 1991). Extract fans in kitchens are typically installed to work with the hob or stove and are designed to operate at higher airflow rates to effectively remove the pollutants. Different building regulations either combine extract fans with a passive stove hood or installed them in a ductless filter fitted hood.

In wet rooms, such as bathrooms and utility rooms, extract fans are important for reducing the accumulation of moisture due to showering, bathing, and laundry, which can prompt the growth of mould and mildew. Such growth can lead to a range of health problems and structural damage if not properly controlled. Extract fans in wet rooms are typically installed in the ceiling (in combination with ducts) or a wall and are set to operate at lower airflow rates than those in the kitchens. Thus, extract fans are widely used in various parts of a domestic setup, especially in wet rooms, to tackle high humidity levels. Additionally, they help to create a consistent airflow between the living spaces (Kolokotroni & Littler, 1995).

This review refers to the Scottish Building Regulations which present a ventilation design depending upon the extract fans installed in the wet rooms. These extract fans when modelled to assess the performance of ventilation design, different approaches can be employed. These approaches are detailed and translation of fan flow characteristics into AFN modelling is presented and compared.

2.9.1 Scottish Building Regulations and Extract Fans

The current building regulations place greater emphasis on the ventilation performance of domestic low energy building stock. Scottish Building Regulations (Building (Scotland)

Regulations, 2019) suggest, as a mandatory standard for ventilation, that a building must be capable of providing sufficient air exchange rate which ensures health of the occupants and structural safety of the building.

As buildings are now more airtight, it is recommended that a mechanical ventilation is installed with heat recovery, particularly where the infiltration rate is <$3m^3/h/m^2$ @ 50Pa. For building with lower airtightness levels, decentralised mechanical extract ventilation (dMEV) system is suggested. These extract fans (constant running) work in combination with trickle ventilators.

The minimum (continuous mode) and maximum (purge/boost mode) extract rates are given in the Table 2.6.

Room	**Minimum dMEV Extraction**	**Maximum dMEV Extraction**
Kitchen	6 l/s	13 l/s
Utility Room	4 l/s	8 l/s
Bath/Shower Room	4 l/s	8 l/s
Toilet	3 l/s	6 l/s
Designated Drying Area	4 l/s	8 l/s

Table 2.6: Min and max extraction rate for continuous dMEV (Scottish Government, 2017).

The role of extraction fans in the decentralised ventilation design of a whole house is elaborated. The required flow rates expected from these constantly running fans are presented in the Table 2.6. For a ventilation design study, these flow rates are modelled by simulation tools and are further discussed in the next section.

2.9.2 Numerical Representation of Airflow Through Extract Fans

The modelling of airflow though domestic extract fans represents a single sided flow (Bradwell, 2014). The basic approach to model a constant running fan is given in (Hensen, 1991):

$$m = \rho \times a \qquad 2.45$$

Where m is the mass flow rate for a fluid of density ρ and a is the constant volumetric flow rate. The density of the fluid is evaluated by the temperature at the zone node for an extract fan. This equation is easy to use when the modeller has access to measured/design flow rate data.

Fan manufacturers also provide the static pressure vs flow rate curve (fan curve) for a range of tested airflows. Following is an example from a known manufacturer Greenwood's info page for the fan model Unity CV2.1 (*Continuous Extract / dMEV Regulation-ready fan designed to deliver Guaranteed Installed Performance*, 2016).

Performance - Free Air

Speed Setting	Airflow performance (l/s)		Sound pressure level @ 3m dB(A)	Energy consumption (W)	
	Bathroom (default)	Kitchen (default)		Min	Max
Low speed	6	8	As low as 11dB(A)	0.5	6.6
High speed	8	13			
Maximum speed	30	30			

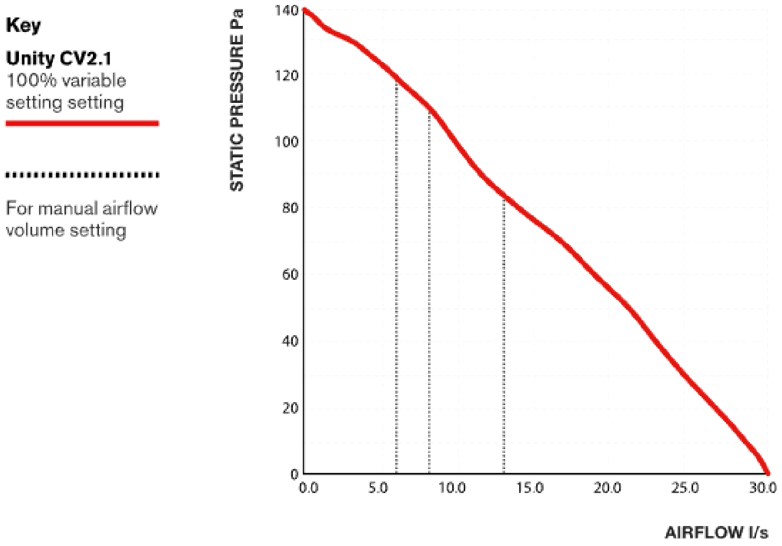

Figure 2.26: Manufacturer tested pressure - volumetric flow curve.

Using this data, the flow inducer component can be implemented which uses a fan pressure-volume curve or system curve information which is also detailed in (Hensen, 1991). The polynomial equation of this component is given as:

$$\Delta P = a_0 + a_1\left(\frac{m}{\rho}\right) + a_2\left(\frac{m}{\rho}\right)^2 + a_3\left(\frac{m}{\rho}\right)^3 \tag{2.46}$$

Where ΔP is the total pressure difference, m is the mass flow rate, ρ is density of the fluid and a_i are the fit coefficients. The user must specify four points of flow and pressure so that $Q_{min} \leq \frac{m}{\rho} \leq Q_{max}$. This information can be extracted from manufacturer's testing data as provided in the Figure 2.26.

In COMIS it is possible to input 3 to 12 pair points of measured flow rate at a pressure difference and solution for the curve fitting (Feustel, 1999).

This piece of review presents two main approaches to model constant running extract fans. Both have their own indicated advantages and selection of one equation over the other is further discussed.

2.9.3 Discussion

Commonly used constant flow and fan inducer component equations which are capable of simulating flow through the extract fan are presented. The constant flow component is straightforward to input the flow rate to be extracted and the direction of the flow can be defined in a nodal setup. For the fan inducer component, fan curve data can be translated into a polynomial curve to determine the flow coefficients. However, the interpolation of the curve can provide appropriate flow coefficients to restrict the calculation for the fan inducer equation at a certain flow rate. Nonetheless, polynomial models can predict non-physical behaviour outside their valid range of solutions, for example, when the prediction of flow rates that are not achievable by the fan is done by extrapolation of the polynomial curve. For a design study aiming to test the ability of an extraction fan to maintain safe IAQ levels in living spaces, a simple constant flow equation can be used by modelling the component for a particular volume flow rate, or schedules/controls can be implemented for the intermittent extraction of the space. While for a more accurate study where sufficient fan curve information is available, flow inducer equation is recommended to account for whole system performance.

2.10 Occupancy and Its Translation in Building Simulation

Occupancy modelling involves an accurate prediction of how a space will be used. These usage patterns directly impact the energy efficiency, comfort and IAQ. This review aims to highlight the following:

- Methods of collecting occupancy data for modelling.
- Relation between occupancy and CO_2 generation.
- Translating CO_2 generation in BES tools and the equation sets used for modelling.
- Presentation of an interconnected framework of internal gains, occupants' presence, and their influence on building usage (highlighting the complexity of human behaviour and its effect on the operation of the building).

This review aims to identify the complexities of occupancy modelling however suggests further effort to be put in to develop a framework to effectively model it in AFN.

2.10.1 Collecting Occupancy Data

It is essential to monitor and assess the number of occupants and their activity levels to model correct internal gain levels in BES tool. The most common methods used for such evaluation are surveys and interviews. Information is gathered on the number of occupants, their activities, preferences, age, sex, and so forth. Gupta (Gupta & Chandiwala, 2010) conducted survey for post occupancy evaluation study targeting thermal comfort. The limitations of their study were lack of real time data and the possible subjectivity and privacy concerns of occupants. Aragon (Aragon et al., 2019) collected data from English households by interviewing participants and analysed a large data set of time-based occupant diaries. The daily diaries were used which were more effective as they captured daily routines and activities, although there were issues with the reliability of self-reported data, issues with intrusiveness and the burden on participants, which are reflected in the collected data and the limited temporal resolution. Despite these downsides, when time-use occupant diaries are used in conjunction with other data collection sets, e.g., CO_2 concentration and hygrothermal values, the potential inaccuracies can be minimised. Sharpe (T. Sharpe et al., 2015, 2019) conducted post occupancy evaluation of low energy houses. The collected data of occupancy diaries was used in combination with indoor CO_2 values, hygrothermal readings and onsite surveys. O'Brien (O'Brien et al., 2017) studied the translation of occupancy into building simulation tools by comprehensively examining occupant diversity in 16 offices; they suggested that larger sample sizes are better representation of data.

Both surveys and occupant diaries along with statistical approach to determine patterns and trends to predict occupant behaviour provide a snapshot of activities but lack real time and study specific data. Hasan (Hasan et al., 2016) asked occupants to use wearable devices to determine their metabolic rates. A very high resolution of 1 min to push data from a wearable device to a computing system ensuring least uncertainty. Moreover, the use of global positioning system location data provided information on whether an occupant was in the building or had left. However, such data collection posed issues for the privacy of occupants, and it was difficult to recruit individuals who would agree to the collection of such data 24/7. Other than this, further issues of compliance and adoption were present as the success of this method relied on the consistent wearing of such devices, including their recharging and maintenance. The use of such devices in combination with occupant diaries would be quite accurate as this combination would also capture routine activities such as showering, cooking, sleeping, and the use of ventilation components, i.e., doors, windows, trickle vents and extractors. Pivac (Pivac et al., 2019) used both wearable devices for metabolic rate data as well as daily diaries to undertake the thermal comfort study. However, the sample size was limited to eight participants, although the data quality was significantly better compared to the studies discussed previously.

Apart from the presence and activity levels of the occupants, their interaction with the ventilation components also carries high weightage. As discussed under the heading 2.2, that occupants significantly influence the effective ness of home ventilation systems depending upon their awareness and understanding; additional factors are also detailed which would serve as barriers or motivations to operate the ventilation components. It is very much important to keep an account of such behaviours as habits like closing doors and using curtains can impede airflow (T. Sharpe et al., 2015). When modelling for behaviours, occupants' interviews are a good resource to include in the scenario-based modelling studies.

The studies discussed here show different methods of monitoring occupancy numbers, the spatial presence of occupants, and their activity levels. Increasing the diversity and size of the study samples would help improve the generalisation of data. It is also found important that the procedures should comply with privacy and data protection, and occupants are required to be taken into confidence specially when using invasive tools like wearable devices.

2.10.2 Occupancy Levels and CO_2 Generation

The outdoor CO_2 concentrations are normally recorded between 380ppm and as high as 500ppm in dense urban areas (Persily & Gorfain, 2004; Satish et al., 2011). Indoor concentrations are mainly due to the exhaling of CO_2 by the occupants and these levels can be taken as a proxy for the ventilation performance of a building.

Exhaled air consists of 4% CO_2 and the normal breath rate of a healthy adult is 15 breaths per minute which increases depending upon the activity level (Voigt & Pelikan, 2010). The consumption of oxygen and release of CO_2 are used as an indirect measurement of the metabolic rate of a person. BS 5925 (Standard, 1991) takes the production rate of 0.00004M l/s where M is taken as a metabolic rate in watts. This rate depends upon the activity level as well as the age and gender. The following equation relates the generation of CO_2 with the metabolic rate where P is CO_2 generation rate (l/s), M is the metabolic gain (Wm^{-2}) and A is the body surface area (m^2) area (CIBSE, 2018):

$$P = 4 \times 10^{-5} \times MA \qquad 2.47$$

Ashrae Standard 62.1 (2019) presents a chart (Figure 2.27) to relate oxygen consumption (l/min), breathing rate (1/min), and physical activity (met) which are categorised as very light, light, and moderate work by a human.

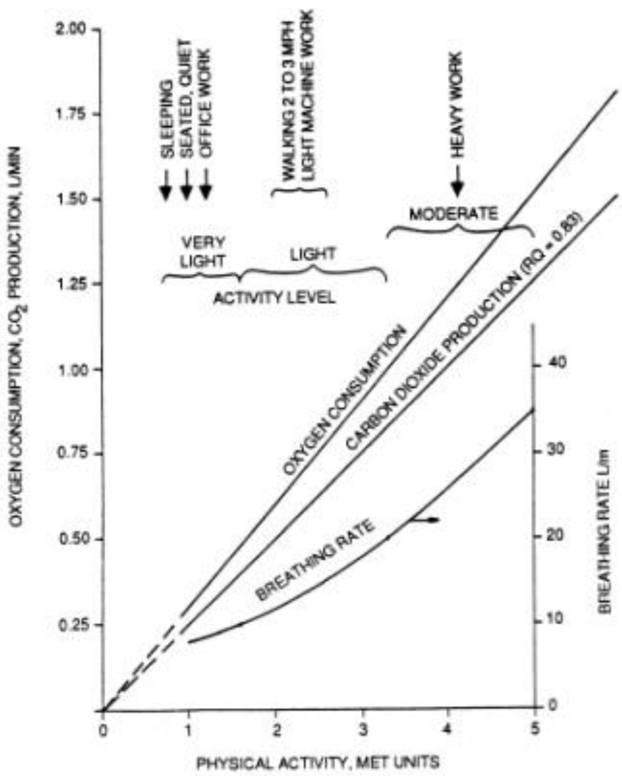

Figure 2.27: Chart to determine activity level and relation between oxygen consumption, breathing rate and physical activity.

A person seated quietly is valued at 1 and the heat generation associated with this level of activity is taken as 1 MET=58.2 W/m^2 while the average body area of the human body is taken as 1.8m^2 (CIBSE, 2021).

2.10.3 Modelling of Occupancy

This part of the thesis will focus on current modelling techniques to translate occupancy schedule in air flow network simulations and the generation of CO_2 from those occupants based upon their metabolic rates. The focus of this study is to translate the reported number of occupants and diary-based occupant activity into an AFN simulation tool.

BES tools have the ability to schedule occupancy throughout the simulation period (Fabi et al., 2011). The occupants are assigned with metabolic rates also known as occupancy loads (C. Yang et al., 2010). The metabolic rates are given in MET and the heat generation in Watts. However, it is important to assess the activity type of the occupant, or errors can emerge up to ±50%. This concern is also noted in the CIBSE Guide A but through the careful evaluation of occupant activities this error can be as low as ±20% which is an acceptable limit.

These metabolic rates are input in the thermal model and used as the source in an AFN tool as a linear function (Samuel & Strachan, 2006). The CO_2 generation equation relating metabolic rate is given in ASHRAE Fundamentals Handbook, (2021) and used in Energy Plus Documentation, (2020). Equation 2.48 relates emission of CO_2 and consumption of O2 by an occupant with respiratory quotient RQ. This is the ratio between consumption of O2 (V_{O2}) and the generation of CO_2 (V_{CO2}).

$$V_{CO2} = RQ \times V_{O2} \quad 2.48$$

$$V_{O2} = \frac{0.00276 A_{du} M}{0.23RQ + 0.77} \quad 2.49$$

$$V_{CO2} = RQ \frac{0.00276 A_{du} M}{0.23RQ + 0.77} \quad 2.50$$

Using equation 2.50 one can determine generation of CO_2 (l/s) for given metabolic rate M, height H and body mass W where $A_{du} = 0.202 H^{0.725} W^{0.425}$.

ESP-r maintains an operations file with internal heat gains including the heat generated as a result of the metabolic activity of the occupants. These gains can be scheduled for the duration of occupancy and are input as a source of CO_2 generation (Samuel & Strachan, 2006).

Assessment of these internal gains as metabolic rates is complex and involves the consideration of thermos-physiology models to be used. Rida (Rida, 2020) focuses on indoor temperature and metabolic rates provide latent and sensible heat loads. This is useful when detailed occupant information is available along with their activity levels and types.

In both Energy Plus and ESP-r, CO_2 generation is a function of the human metabolic rate. The determination of metabolic rates is more complex but typically a database is consulted. In cases where data is limited or simplified approach to occupancy modelling is acceptable, a standardised set of values can be referred. These values are consistently recognised and can be found in ASHARAE and CIBSE guidance documents (ASHRAE Fundamentals Handbook, 2021; CIBSE, 2021).

2.10.4 Causes of Uncertainty in Occupancy Modelling

A greater level of uncertainty arises when limited or no occupancy data are available (Burman et al., 2012). The dynamic and stochastic nature of human behaviour makes this estimation deceptive. Figure 2.28 can help us understand the interconnected nature of variables linked with occupancy. The occupant's presence, internal gains and occupant's influence on building operation are directly linked with the modelling inputs (Feng et al., 2015). Where this information is not available standard schedules in simulation programmes are used with some estimation of occupancy number and spatial information. CIBSE TM59 (Bonfigli et al., 2017) provides the occupancy profiles for residential buildings ranging from a studio apartment to a 3-bedroom house and suggests activity levels in kitchen, living room and bedrooms. This includes the use of appliances and associated gains.

The use of generalised human body factors, activity levels and schedules may lead to increased uncertainty and error when determining the building performance. Various statistical approaches can be taken to reduce this error. For example, simple time series analysis to study trends of other variables as proxy such as CO_2 concentrations and energy metering and data regression techniques i.e., simple linear regression, multiple linear regression, and logistic regression (Jin et al., 2016; Kim et al., 2019). With the advancements in computational power, complex statistical and probabilistic methods such as Markov models, Bayesian approach and neural network prediction techniques are also used by modellers (Flett & Kelly, 2021; Page et al., 2008).

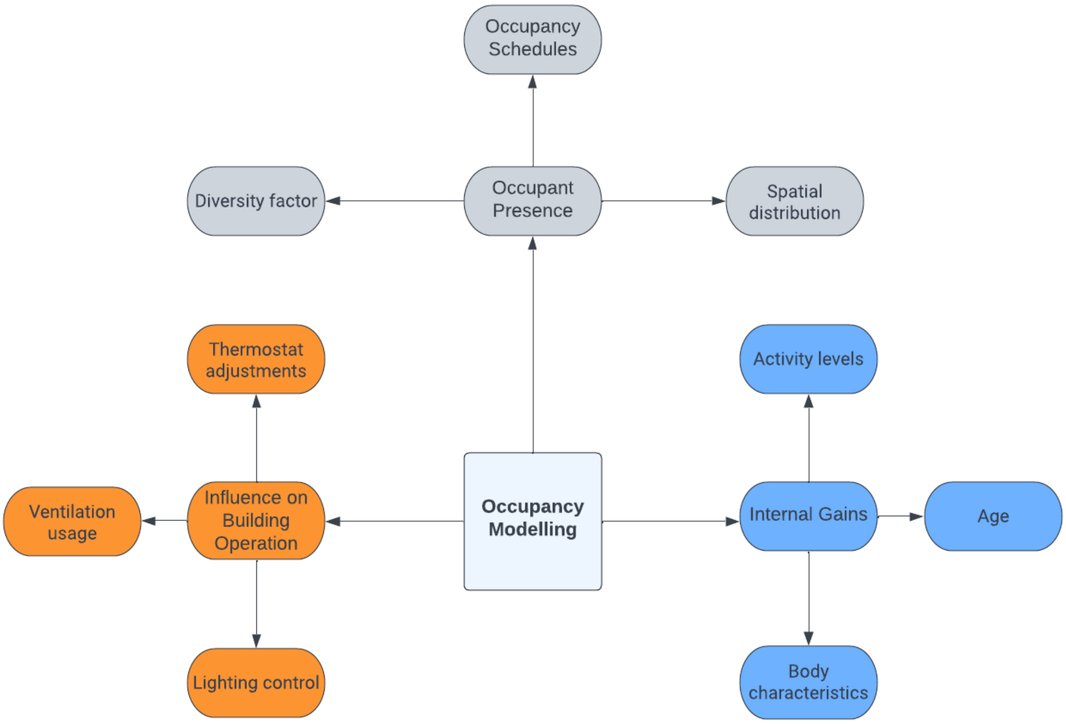

Figure 2.28: Mind mapped factors for occupancy modelling.

The Internal metabolic gains depend upon the body characteristics, age, and activity levels of the occupants. The numbers are interrelated, and the estimation starts with activity levels and body characteristics of an occupant. Metabolic rates for different building types and age group are given in (ISO8996, 2004; Havtun & Bohdanowicz, 2011; ISO7730, 2005) which can be directly used in modelling of occupants of a specific building in the absence of real time measured data. The body surface area can be taken from Dubois & Dubois, (1989) to be used in equation 2.50. However, it is advisable to use ASHRAE and CIBSE documented metabolic gains to model various activities of occupants by keeping an account of their demographics. Depending upon the purpose of the modelling investigation, a higher or lower estimation of the metabolic rates can be taken via an informed decision involving sensitivity analysis.

Modelling the occupant's presence in a zone is a dynamic variable hence translating this into a model is difficult. Page (Page et al., 2008) presented a model capable of producing statistical pattern using Markov chain. First order Markov chain method is also used by Richardson (Richardson et al., 2008) which allows occupancy status at a time t based on the previous time step t-Δt. Both approaches require some input of estimation of occupancy. Flett (Flett & Kelly, 2021) uses UK Time use survey data (TUS) (Ipsos-RSL & of National Statistics, 2003) containing 20000 occupant diaries with a 10 min resolution and uses a smaller dataset of 5000 diaries for the verification of model outputs. Application of Markov chain provides low statistical errors and can be used in a building simulation tool. It is important to consider the type of study being conducted. For indoor environmental assessments, it would be ideal to apply Markov chain method on a large database of indoor CO_2 concentrations recorded alongside occupant diaries. One of the significant issues with low level Markov chain model is that they are unable to categorise the type of activity and the spatial arrangement of occupants in a household unless detailed diary data is provided (Kanthila et al., 2021).

The spatial distribution in a domestic environment is evident to be well predicted in a typical household basing upon the TUS data or an alternative occupant diary database (Richardson et al., 2008). However, it is straightforward for a modeller to estimate the spatial distribution of occupants if they are modelling sleep hours CO_2 generation in the main bedroom to study ventilation effectiveness even when occupant diaries are not available.

Another uncertainty is present when modelling occupancy specially for indoor environment is use of cookers when they are fuelled by natural gas. Sharpe (T. Sharpe et al., 2019) shows CO_2 spikes in kitchen up to 3000ppm when average of the zone is 1100ppm. Similarly, pets also contribute to indoor CO_2 concentrations and should be accounted for when designing the built environment. The house pets have very similar metabolic chemical reaction taking place as humans. Using equation 2.47, one can estimate metabolic heat gain for any living organism using the body surface area. Hence it is recommended to keep account of additional CO_2 concentration sources when undergoing a design study for built environment.

Occupants' influence on the built environment is of high interest as this information can be used to study energy efficiency (Schweiker, 2017), thermal comfort (Haldi & Robinson, 2011), indoor air quality (Liu et al., 2018), the operation and control of building (S. Wei et al., 2014) and design and demand side management (Cominola et al., 2018).

Occupants' influence modelling either depends upon high resolution onsite behavioural data or use of probabilistic methods to estimate from existing perception of occupants' regarding their energy usage, thermal comfort, indoor air quality etc. Techniques like deterministic, stochastic and agent-based methods are employed to model occupant's behaviour on building operation (D'Oca et al., 2016; Lee & Malkawi, 2014). However deterministic models represent models using fixed schedules and pre-defined profiles. Stochastic models are useful when they are based on large datasets. Agent based models can capture the complexity of occupant behaviour, but this method also relies on availability of data and requires high computational resources.

2.10.5 Discussion

The review of the occupancy modelling highlights a vast variability and uncertainty in data collection, factors entailing variability in metabolic gains and variable scheduling and spatial presence of occupants in a domestic setting. Where it is much advised to use accurately measured data for mentioned three variables, literature review also suggests use of standard inputs when no or limited data is available.

In the context of IAQ assessment of domestic setting, sufficiently accurate assessment of CO_2 generations from occupants is possible by incorporating standard metabolic rates from ASHRAE and CIBSE guides. These rates should be able to reflect correct range of activities in accordance with the individual characteristics. These rates should be taken as an approximation and should be altered depending upon the focus of the simulation investigation. For example, a study concerning ventilation with no data about occupants' metabolic activity, a higher estimation above given rates in the guides can be used. The model input should be dynamic in a sense that it is able reflect typical spatial presence of the occupants in a typical household. Trends of presence of occupants can be inferred from TM59 and TUS data. In case, atypical scenarios are required to be assessed, probabilistic models are suggested to be employed. This review sufficiently points towards the need for an integration of these advanced models into current modelling tools. The cited literature included advanced occupant data collection techniques and general aspects of modelling are explained. It is however advised, in instances where no or limited data is available, the cited standard guidance can be used.

2.11 Weather Data in Building Simulations

The representation of relevant weather conditions can help a modeller to assess the performance of a building including its environmental factors and energy consumption. Various databases have been developed ranging from historical, real-time, and synthetic weather data and have their pros and cons of their use based upon the type of study conducted. These databases are further incorporated into building simulation tools. This review will highlight the importance of weather data, the features of different databases, the pros and cons of using these databases by referring to the literature, and the current representation of weather in modelling tools. The conclusion identifies out a suitable type of weather database for a ventilation design assessment.

2.11.1 Relevance of Weather Representation in AFN Modelling

Weather boundary conditions in a simulation model are very important as they affect the outputs such as energy consumption (Auffhammer & Mansur, 2014), occupant comfort (Amasyali & El-Gohary, 2021), day light availability, natural ventilation potential (Sakiyama et al., 2021) and renewable energy generation (Qadir et al., 2021).

Specific to AFN modelling for ventilation design, the accurate representation of weather conditions specifically ambient temperature, wind speed and direction determines the air flow through an opening in a façade. Wind pressure equation given below expresses relation between wind speed and pressure coefficient C_p.

$$P_{wind} = \left(\frac{1}{2}\rho v^2 C_p\right) \qquad 2.51$$

Where C_p is pressure coefficient for wind direction at a time step, P_{wind} is surface pressure due to wind, ρ is density of air and V is wind speed in m/s relating to wind direction angle.

The stack pressure due to difference in ambient and indoor temperature is $\rho gh(\Delta T)$ where ambient temperature is important factor to evaluate ventilation due to buoyant forces.

Wind speed and ambient temperature are core inputs in AFN modelling as far as boundary conditions are concerned. These values from the weather databases are used to calculate wind and stack induced pressures, consequently resulting in simulated airflow in a zone.

2.11.2 Historical Weather Data

Historic weather data is available in the form of archives collected by on ground weather stations and satellite systems Where such data are available in a raw format, it is important to convert this into a system acceptable structure after data processing and the data gaps are filled via interpolation techniques. Kasam (Kasam et al., 2014) presented statistical methods to interpolate missing information in weather data files. Quality assessment of data is important for reliable and accurate application in building simulation. Further to this, when using historical weather data, it is important to look at the temporal resolution as they are available as hourly, daily or annual intervals. The selection would be based on the type of application and simulation tool used. However, it is important to have a database with a higher resolution. Spatial coverage is another aspect in datasets where localised or global values of weather variables are available. For a general building design solution, localised data are worthy enough to study climate research, large scale regional/global data sets are more relevant (Brönnimann et al., 2019; Sakiyama et al., 2021).

Historical localised weather datasets provide opportunities to understand weather patterns and atypical situations although standardised databases are also required. These data sets are then processed in such a way to form synthetic weather databases and are available for use after standardisation. The process of standardisation ensures compatible formatting of the data structures.

2.11.3 Synthetic Weather Data

Historical data sets lack predictive nature for building simulation calculations. Even though they provide atypical weather values which are important to model worst case scenarios, the overall trend for whole-year values is missing. Historical weather data is used to generate synthetic weather data sets such as Typical Meteorological Year (TMY). These sets are produced by statistical processing of 30 years of historical weather data presented by Hall (Hall et al., 1978). For example, the weighted average of all January months from 30 year would form a January month in TMY database. Wang (W. Wang et al., 2021) compared TMY with local weather station recorded and on-site measurement data and concluded that TMY and local station average windspeeds were higher than on-site measurement data. This refers to the terrain and sheltering factors causing wind hinderance.

TMY datasets are also used to develop Energy Plus files (EPW) which are extensively used in various simulation tools including Energy Plus, ESP-r etc. EPW files are formatted and standardised using specific headers to be read by simulation tools while having TMY data in the backend (Energy Plus Documentation, 2020).

Dry Bulb Temperature (°C)
Wet Bulb Temperature (°C)
Wind Speed (ms^{-1})
Wind Direction (° from north)
Atmospheric Pressure (bar)
Radiation (Wm^{-2})
Precipitation (mm)
Global horizontal solar radiation (Wm^{-2})

Table 2.7: Required Weather Parameters Fetched by ESP-r System from EPW File (J. Clarke, 2007)

These hourly EPW files can be used to determine energy performance of a building as well as ventilation performance for all seasons in a typical year.

In addition to forming a typical year for weather, a test reference year (TRY) is also generated from processed historical data. It represents an average year scenario rather than typical year in case of TMY. In TRY extreme high and low temperatures are eliminated and resultant year data is a mild year (Crawley et al., 2015). However later updated by CIBSE in the development of TRY data for the UK, Design Summer Year (DSY) was presented to assess overheating of buildings which is not same as a TRY but a probabilistic design year relating expected frequency and severity of high temperature and discussed by an example simulation in (Virk & Eames, 2016) :

DSY1	Moderately Warm Spell
DSY2	Short and Intense Spell
DSY3	Long and Less Intense Spell

CIBSE used ISO 15927-4 (International Organization for Standardization, 2005) which considered three primary daily indices, i.e., mean dry bulb temperature, total global radiation (horizontal), and mean relative RH, while wind characteristics were taken as a secondary variable. A later update in the methodology by Levermore (Levermore & Parkinson, 2006) considered wind speed primary rather than RH, which gave more weight to the wind parameters.

The use of synthetic databases to represent weather does provide sufficient grounds to evaluate building performance through the key to determining the adoption of the weather database type.

2.11.4 Actual Weather Data

When the simulation study period and location of the building is known, the most accurate method to represent weather is to use actual data from the closest weather station. It is not as accurate as on-site measurements of the variable but when such facilities are not available, the use of real time values eliminate more uncertainty than using statistically generated, typical or representative data. Both on-site measurements and data from the closest weather stations can be regarded as real time weather data as both relate to the site under study and the data time period is the same for monitoring as well as the simulation study period (Casini, 2022).

However, if the simulation period is in the past and historical weather data files are available for the study time, one could simply use that database. By focussing on design upgrades or guidance, studies using actual weather data would not account for extreme conditions nor future weather patterns which are changing at an unprecedented pace.

2.11.5 Wind Reduction Factor

Wind speed at the 10m height of metrological station is different from the local wind speed for which simulation study would be conducted. For this purpose, wind reduction factor is introduced to calculate wind speed at a given reference level for which pressure coefficients are used. To evaluate the wind reduction, there are several wind profile models which are used to solve for wind reduction factor before applying pressure coefficient data to calculate wind pressure on the façade (Hensen, 1991).

Liddament (M. Liddament, 1986) presented power law wind profile where actual wind speed is approximated using the following expression which is also presented in (Standard, 1991):

$$W_r = \frac{U_l}{U_{lo}} = K z_l^a \qquad 2.52$$

Where U_l is local wind speed, U_{lo} is either speed measured in the open countryside or at a certain height i.e., 10 m at the meteorological station, z_l is the local site height while K and a are terrain dependent coefficients which vary for flat, rural, urban, and dense city types.

Bietry (Bietry et al., 1978) and Simiu (Simiu et al., 1980) presented logarithmic wind profiles basing upon the theoretical and experimental findings that wind speed is logarithmically related to the function of height. This model is given as:

$$W_r = \frac{U_l}{U_m} = \frac{U'_l}{U'_m}\left(ln\frac{z_l - d_l}{z_{0,l}} / ln\frac{z_m - d_m}{z_{0,m}}\right) \qquad 2.53$$

And

$$\frac{U'_l}{U'_m} \approx \left(\frac{z_{0,l}}{z_{0,m}}\right)^{0.1}$$

In the equation set above, U_m is wind speed measured at meteorological station at height z_m, U' is atmospheric friction velocity in m/s, z_0 is roughness length and d is displacement length where both factors z_0 and d are terrain dependent. Their typical values are also available for flat, rural, urban, and dense city types.

The third model is from Lawrence Berkeley Laboratory and referenced in (M. Liddament, 1986) and based on a power law:

$$W_r = \frac{U_l}{U_m} = \frac{\alpha\left(\frac{z}{10}\right)^{\gamma}}{\alpha_m\left(\frac{z_m}{10}\right)^{\gamma_m}} \qquad 2.54$$

Terrain based numbers α and γ are given (Table 2.8) as for other two described models.

Here a common scheme can be observed in all three described model, that is, ratio of local wind speed to meteorological station wind speed with consideration of terrain aspects of the local site is used to calculate a number. This number (wind reduction factor) multiplies with the wind speed to calculate pressure in a simulation model. The presented wind reduction calculation models are valid for low rise buildings with up to 3 floors assuming that each floor is 2.4m high (Hopkin et al., 2022).

<table>
<tr><th>Terrain</th><th>K</th><th>a</th><th>z_0</th><th>d</th><th>α</th><th>γ</th></tr>
<tr><td>Open flat country</td><td>0.68</td><td>0.17</td><td>0.03</td><td>0.0</td><td rowspan="2">1.00</td><td rowspan="2">0.15</td></tr>
<tr><td>Country with scattered wind breaks</td><td>0.52</td><td>0.2</td><td>0.1</td><td>0.0</td></tr>
<tr><td>Rural</td><td></td><td></td><td>0.5</td><td>0.7h</td><td>0.85</td><td>0.2</td></tr>
<tr><td>Urban</td><td>0.35</td><td>0.25</td><td>1.0</td><td>0.8h</td><td>0.67</td><td>0.25</td></tr>
<tr><td>City</td><td>0.21</td><td>0.33</td><td>>2.0</td><td>0.8h</td><td>0.47</td><td>0.35</td></tr>
</table>

Table 2.8: Typical terrain values to be incorporated in mentioned 3 wind reduction models (Standard, 1991).

The selection of terrain to use appropriate coefficients in wind reduction calculation equations can be an ambiguous for modellers. Salvati (Salvati et al., 2020) categorises wind reduction based on canyon formation due to high rise dense structure and non-canyon situation i.e., low rise residential blocks and suggests use of power law form of wind reduction model when $H_b/W_c<0.7$ and when $H_b/W_c >0.7$, L_b/W_c should be >20. This gives some clarity of the use of correct terrain type for the given wind reduction models as well limitation of the scenarios where these can be implemented. Here H_b is average height of the buildings, W_c is width of the canyon and L_b is length of the building. These dimensions are elaborated in Figure 2.29 and Figure 2.30.

A similar wind reduction calculation is suggested in (ASHRAE Fundamentals Handbook, 2021) and a table of coefficients is given for different terrains to calculate reduced wind speed at the local site and also implemented in IES-VE (IES MacroFlow User Guide, 2014). However, selection of a terrain remains unclear.

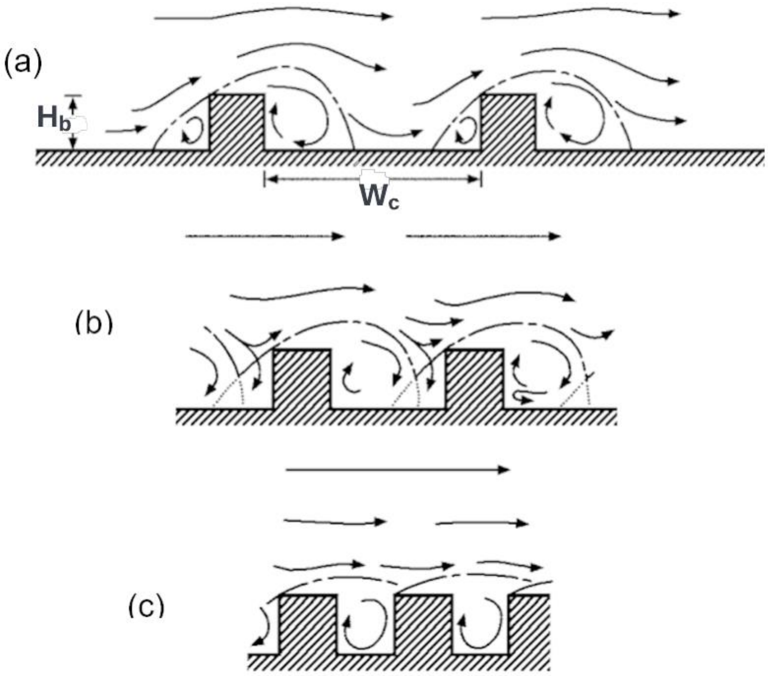

Figure 2.29: Flow hindrance and types of building arrays (Oke, 1988)
(a) Isolated flow (H_b/W_c>0.05) (b) Wake formation of flow (c) Skimming flow

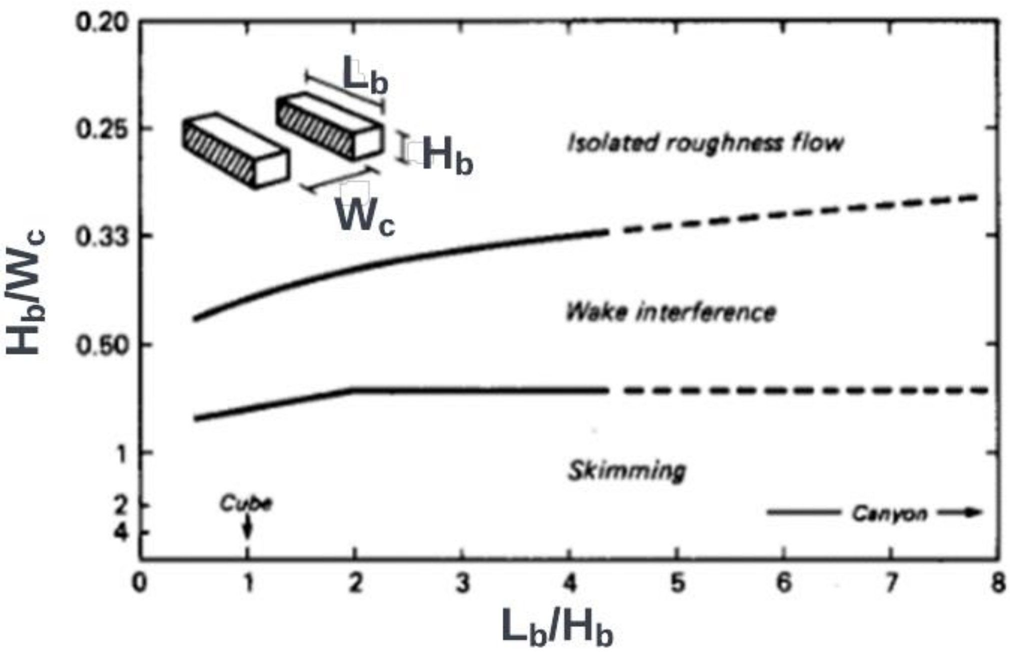

Figure 2.30: Division of flow types in a built area basing upon building structures and dispersion (Oke, 1988).

It is important to elaborate the density and heights of building structures to further understand the terrain type and to use correct set of values to calculate wind reduction. Oke (Oke, 1988) studied the airflow disturbances due to the array of buildings, which suggests that H_b/W_c allows the analysis of area density.

Figure 2.29 infers wind reduction increases as the buildings are more densely situated, while Figure 2.30 allows for a choice between terrain type when the wind reduction factor coefficients are required (shown in Table 2.8). Typically, an open flat country would have very few obstructions and low-rise buildings. Both H_b/W_c (related to a building's height and spacing between buildings) and L_b/H_b (related to a building's proportion) can be used to assess the type of terrain. These ratios will be low for such a terrain. For a countryside with scattered wind breaks, a slightly higher L_b/H_b ratio is applied due to longer buildings like barns, however the H_b/W_c ratio would remain low due to wider spacing between structures. For taller structures in such a terrain, the isolated roughness flow would move towards wake interference. In rural areas, structures would be of varied lengths and moderate heights, hence L_b/H_b would vary but H_b/W_c would suggest a closer interaction of structures. Hence, a transition is possible between the isolated roughness flow and wake interference. In the case of urban areas, a higher H_b/W_c ratio would reflect closer building spacing and a moderate L_b/H_b ratio as the building can be long and tall. The flow regime would span from wake interference to skimming flow. In the case of cities, in central commercial locations, the L_b/H_b ratio would be low due to the vertical design and the H_b/W_c ratio will be high as buildings are taller than their spacing. The flow regime for such a terrain would be skimming at the top levels of buildings and the street level would experience limited wind penetration. This would lead to the formation of canyons. In residential settings situated in dense city areas, L_b/H_b would be higher than the city centre and H_b/W_c would be slightly lower. This is because of the larger green spaces and amenities in such areas. The flow regime would range between the wake interference and skimming flow. However varied wind conditions at the pedestrian level and roofline level would be present.

A definitive range for H_b/W_c for listed terrain types in Table 2.8 were not found in the literature. This leads to uncertainty when selecting an appropriate terrain to input the correct coefficients in the wind reduction equations. However, this review provides some level of guidance to analyse the type of terrain based on H_b/W_c and the possibility of isolated, wake interface or skimming flow. Moreover, the building geometry can be inferred in L_b/H_b which can range from a cube to canyon formations between building structures.

2.11.6 Pressure Coefficients and Weather Data

A pressure coefficient (C_p) is a dimensionless number that is a function of wind induced pressures which depends on wind profile and building characteristics. In building simulation defining boundary conditions which rely on uncertain weather parameters is a challenge and wind interaction with the built environment is the main aspect concerning C_p (Sahal & Lacasse, 2005). Wind tunnel tests and CFD studies are conducted to calculate these numbers but not all simulation studies have access to these facilities due to various constraints. In such scenarios one can refer to literature and design guides or use software tools which provide estimations based on simplified algorithms or consult pressure coefficient databases which are embedded into building simulation tools (Cóstola et al., 2009). This section reports widely adopted three methods to determine input of C_p in AFN modelling.

In simulation studies, time averaged values of C_p, which are obtained from various wind tunnel tests, are used for a building façade (Akins et al., 1980). This can be true for a low rise building but structures with more than 3 floors would exhibit a large error when single average number will be used. The C_p distribution on a wall of a hi-rise for wind incident at 45° shows it varies with the vertical elevation of the windward building façade (Orme et al., 1998). There is separate set of studies tackling C_p values for roofs, but this is not in the scope of this thesis.

Energy Plus uses analytical model for surface averaged C_p values for low rise buildings presented by (Swami & Chandra, 1988):

$$C_{pn} = 0.6\Big[1.248 - 0.703\sin\left(\frac{\alpha}{2}\right) - 1.175sin^2(\alpha) + 0.131sin^3(2\alpha G) + 0.769\cos\left(\frac{\alpha}{2}\right) + 0.07G^2sin^2\left(\frac{\alpha}{2}\right) + 0.717cos^2\left(\frac{\alpha}{2}\right)\Big] \quad 2.55$$

This equation is for low rise buildings where G is a natural log of ratio of building’s length to width. This equation normalises the standard C_p of 0.6 and suggests the range of 0.19-0.91 where normalised C_p varies depending upon wind incident angle but does not take account of shielding. Grosso (Grosso, 1992) took this further to take account of shielding but that resulted in greater complexity because of addition of many variables which are difficult to assess specially for a general application. Later they developed the package CPCALC+ which models local C_p with rectangular floor plans and takes reference height as roof height but lacked backing of high-quality experimental data.

The AIVC database for C_p is mentioned in Appendix 4.A1 of (CIBSE, 2021) and widely implemented in simulation tools like ESP-r and IES-VE. This database combines different measurement studies and takes account of the sheltering of the building, aspect ratio of the structure and wind incident angle.

Another large set of C_p data for various building types was formed by wind tunnel experimental procedures and made available as a tool online by Tokyo Polytechnic University (Tamura, 2012).

In the literature, these three methods of C_p estimation have been evaluated against each other (Muehleisen & Patrizi, 2013; Ramponi et al., 2011) and emphasised the need of an alternative more accurate method. Former study presented new equation to be used which is essentially an update to the equation 2.55 and results show better fit with AIVC database C_p values.

Investigation of these databases is outside the scope of this work however this review highlights a greater impact of this input in AFN models.

2.11.7 Discussion

Concerning a ventilation design study and use of three important weather-related variables are discussed. Following sections will present a clarified proposal of use of weather, wind reduction factor and pressure coefficients to be included as inputs in AFN models.

2.11.7.1 Weather

The selection of a weather database is critical when the design of a built environment is considered and the assistance from simulation is being taken. The focus of mentioned synthetic database is energy usage of buildings and overheating studies. Both TMY and TRY databases are widely used and recommended in various design guides. Crawley (Crawley et al., 2015) concludes TMY to be better option as this includes typical rather than average weather conditions however with a recent update of CIBSE version of TRY and development of DSY along with future weather trends, TRY has been recommended to be used in government building regulations part L (H. M. Government, 2018) as well which is an energy consumption document while Part F which is ventilation oriented; does not mention use of any specific weather database. It is well established from the literature that synthetic weather files are tailored to be used for energy side of investigation while for ventilation aspect, they do not mention a clear standing.

If a design study aims to investigate the possible performance of a building in typical conditions, especially temperature and wind speeds, TMY would be a suggested option. TRY is better suited for averaged conditions. However, for overheating studies, the DSY weather database is suggested for use.

2.11.7.2 Wind Reduction

For a design methods study, different terrains offer varied sheltering effect. The ratio of later and former is wind reduction number. If the weather data is from the local site, then wind reduction would be unity. As per the review, in case of weather data being from site of the study, the wind reduction factor would be unity When the weather data (historical, TMY or actual) is from a weather station, the values from Table 2.8 should be used with care. These values are appropriate to be used in power law or logarithmic wind reduction factors. Power law model is presented in (Standard, 1991) is simplistic to use and can be implemented to the weather data with limited known characteristics of the building terrain.

Terrain type can be inferred from (Oke, 1988) using Figure 2.30 which shows how flow can be hindered due to density of the built area. It is to note that, for a domestic development, height of the low-rise structures is <12.5m (ASHRAE Fundamentals Handbook, 2021). For structures taller than the prescribed height, relevant set of coefficients should be considered. The scatter or the distance between the neighbouring structures and their height would suggest type of the terrain.

2.11.7.3 Pressure Coefficients

As validated C_p databases are commonly used, alternatives like CFD simulations or wind tunnel data would provide a more detailed result but it would require significant resources. Depending on the study's scope, widely used C_p data can suffice, but it is crucial to analyse their impact on simulation outputs so that an informed design decision can be made.

2.12 Model Calibration Methods

Design evaluations dealing with the indoor environment such as contaminant concentrations, indoor temperatures, CO_2 generation by metabolic activity, infiltration, air flow magnitudes etc require some level of calibration to minimise the discrepancy between observation and simulation values (Fabrizio & Monetti, 2015).

This section of the review will discuss:

- Categorisation, ranking and uncertainty entailed in the modelling inputs.
- Residuals in outputs with respect to measured data
- Uncertainties entailed in the modelling process.
- Sensitivity analysis of the inputs to tackle error percentage with measured and simulated data.
- Acceptance criteria of a calibrated model via sensitivity analysis.
- Measuring the impact of inputs on outputs

This assessment provides the suitable statistical error metrices from the literature to check validation of the modelling outputs as per any modelling objective. Also, a statistical analysis framework is presented which would allow to assess the impact of an input on the output - helping to take informed decisions in the modelling process.

2.12.1 Inputs

The data inputs and their sources are identified in a modelling process and adjustments are made as per the motive of a study.

Refsgaard (Refsgaard et al., 2007) suggests an environmental model creation is a multi-stage process entailing various uncertain known and unknown inputs. Mai (Mai, 2023) further provides a detailed stagewise framework and suggests that sensitivity analysis should be confined to the input variables and parameters which are important for the model output.

Source ranking of such variables and parameters proposed by Coakley (Coakley et al., 2012) where they link inputs with sources and defines a hierarchy basing upon certainty of the source, 1 being most certain type of source. This ranking is important as it can help in identifying the possible range of variation in the data from a source. The higher the rank, lower the variation is expected.

Source	Class/Rank
Continuous Measurement/Sensor Data	1
Spot Measured/Physically Verified Data/Interviews	2
Drawings and Manuals	3
Design Documents	4
Guides and Standards	5
Default Values	6
No Available Information	7

Table 2.9: Hierarchy of sources to which input type can be linked and ranked.

2.12.2 Outputs

A model's outputs specify the validity of the data generated when compared against the measured values. In the process of calibrating a model, the initial base case model output is checked against monitored data and inspected either by visual inspection of the graphed data or by the calculation of residuals. This initial check provides a snapshot of accuracy of the model (Royapoor & Roskilly, 2015). The residual value for a measured and simulated output at interval i is given as:

$$r_i = m_i - s_i \tag{2.56}$$

The selection of the temporal interval for these evaluations is important. In a time series dataset, where atypical trends are shown, it is advisable to omit such anomalous data points from the residual analysis (Baba et al., 2022). Moreover, in scenarios requiring the assessment under specified conditions, the measured and simulated values must correspond to the stipulated temporal context. For example, to assess indoor CO_2 concentration accumulation for ventilation design when wind speed exceeds 7 m/s, it is important to extract output data from the analysis representing those intervals where wind speed falls in this criterion. Such considerations would help in an effective cleaning and subjective analysis of the data.

2.12.3 Sensitivity Analysis

In the literature, Morris Method (Morris, 1991) is widely found to rank influential uncertain parameters and variables in multidisciplinary applications (Azevedo et al., 2021; Hove et al., 2023; Menberg et al., 2019; Zhang et al., 2017) while the studies calibrating indoor environment models by assessing CO_2 concentrations reveal that this method is fairly able to help reduce discrepancy in measured and simulated values (Baghoolizadeh et al., 2022, 2023; Hyun et al., 2007). Mentioned applications of this method apply sensitivity analysis. Hyun (Hyun et al., 2007) mentions parameters like flow exponent, C_d, C_p, local terrain, and weather involve high uncertainty and take min, base, and max values from the literature. However, the taken values were general and applied to a specific situation.

According to (Andrea Saltelli, Stefano Tarantola, Francesca Campolongo, 2004) sensitivity analysis (SA) enables:

- Identification and categorisation of influencing variables.
- Understand functions between inputs and outputs.
- Evidential support to any changes made to the model.

A sensitivity analysis of the input parameters can be done on local and global basis (T. Wei, 2013). Local approach is preferred when focus is to deploy enhanced design strategy and a single parameter at a time is assessed while global SA works with several parameters simultaneously and wide range of input variables are explored.

To quantify the effect of change in input on the discrepancy between monitored and simulated values, equation 2.57 is useful to calculate the impact of a change in the input on the model's output (Lam & Hui, 1996).

$$IC = \frac{\Delta OP \div \Delta IP_{BC}}{\Delta IP \div IP_{BC}} \qquad 2.57$$

ΔIP = Change in output value

ΔIP_{BC} = Change in base case input value

ΔIP = Change in input value

IP_{BC} = Input base case value

The calculated influence coefficients in a stage-by-stage modelling approach would allow to determine a rank of least to most impactful inputs.

2.12.4 Statistical Validation

To assess the difference between the simulated/calculated values and monitored/measured values, it is first and important step to pinpoint a metric which gives a clear picture of dependencies of the variables. These quantitative metrics are categorised as: correlation metrices, absolute difference and relative difference metrices (Yu et al., 2006). Hence for the selection of most suitable metric, it is required to determine the pros and cons of different types of metrics.

Correlation metrics explain whether there are linear dependencies in the measured and modelled values. (Benesty et al., 2009) presented the Pearson correlation coefficient which indicates if there is positive (r=+1) or negative (r=-1) linear relationship between measured and simulated set of data.

Absolute metrics were studied by (Royapoor & Roskilly, 2015) i.e., mean bias error (MBE) and mean absolute error (MAE). Former gives information on overestimation or underestimation of the simulation model. Later metric does the same with no cancellation of positive and negative values. MBE and MAE equations are listed below:

$$MBE = \frac{\sum_{i=1}^{n}(m_i - s_i)}{n} \tag{2.58}$$

$$MAE = \frac{\sum_{i=1}^{n}|m_i - s_i|}{n} \tag{2.59}$$

In case error distribution is normal, improved MAE is given as root mean square error (RMSE) detailed by (Chai & Draxler, 2014). It is also stated that use of more than one metric is recommended for variance and overall distribution of results as well as the mean values. RMSE relation is expressed in equation 2.60

$$RMSE = \sqrt{\frac{\sum_{i=1}^{n}(m_i - s_i)^2}{n}} \tag{2.60}$$

Cumulative frequencies are coupled with RMSE absolute metric to get a view of goodness of fitness of data curve by (Belmonte et al., 2019) using equation 2.61.

$$RMSE_f = \sqrt{\frac{\sum_{i=1}^{n}[f_i - f_s]^2}{n}} \tag{2.61}$$

Where f_i and f_s are cumulative frequencies for the data, measured and simulated values respectively.

Relative difference metrices include Normalised Mean Bias Error (NMBE), Modified NMBE and Coefficient of Variation of Root Mean Square Error (CVRMSE). Savage (Savage et al.,

2013) explains how use of absolute metric when there are more than one data sets of same variables can cause unnormalized results and hence comparing them with each other can result in higher error. Hence use of CVRMSE (Equation 2.62) tackles the cancellation effect of negative and positive values and gives better comparison of data sets.

$$CV(RMSE)\% = \frac{1}{\bar{m}}\sqrt{\frac{\sum_{i=1}^{n}(m_i - s_i)^2}{n}} \times 100 \qquad 2.62$$

NMBE and modified NMBE give error estimation ranging from -2 and +2, where negative value depicts underestimation and positive depicts overestimation of simulated data against measured data (Sun et al., 2014).

Mean average percentage error (MAPE) can help environmental models to assess the peak values of contaminants. Percentage errors are calculated at first stage and averages are taken for available intervals.

$$Modified\ NMBE = \frac{2}{n}\sum_{i}\frac{(s_i - m_i)}{(s_i + m_i)} \qquad 2.63$$

$$NMBE = \frac{\sum_{i=1}^{n}(m_i - s_i)}{n \times \bar{m}} \qquad 2.64$$

$$MAPE_{CO2}\% = \frac{1}{n}\sum_{t=1}^{n}\left|\frac{m_i - s_i}{m_i}\right| \qquad 2.65$$

In the equations from 2.58 - 2.65 ; m_i= measured value, s_i = simulated value, n = number of data points and $\bar{m}$ = average of measured data.

These equations provide a range of metrices for calibrating models focussing on environmental studies. It is evident that some metrices (e.g., Pearson correlation) provide information on linear dependencies of the model output while others (e.g., RMSE) provide an overall behaviour of the output.

CV(RMSE) is a relative measure of error which is normalised to the mean of the monitored CO_2 concentrations, it would allow an accurate assessment of AFN's ability to predict CO_2 generated in the modelled zone. Further to this, this metric gives due weightage to large errors as the difference is squared before it is averaged. In the next section the use of CV(RMSE) as a metric in building energy simulation studies is highlighted along with acceptance criteria.

2.12.5 Acceptance Criteria

Error percentages from the aforementioned metrices are checked against the acceptance criteria available in the literature. Coakley, Elharidi and Guyot (Coakley et al., 2012; Elharidi et al., 2017; D. Guyot et al., 2020) use ASHRAE Guidline14 (ANSI/ASHRAE, 2002), IPMVP

(E. V. Organisation, 2012) and Measurement and/or Verification Guidelines (DOE, 2008) which are essentially for energy consumption models and do not provide a criterion for indoor environment parameters like contaminant concentrations, temperature and relative humidity. Sarna and Silva (Sarna et al., 2022; Silva & Henriques, 2021) have used ASHRAE14 criteria for environmental indicators however their threshold error percentages were much lower than the criteria set in the guideline. Paliouras and Foldvary (Paliouras et al., 2015) and (Foldvary, 2016) have used criteria of CO_2 CV(RMSE) at 20% and indoor temperature at 5%. However, for hourly temperature data error percentage <20% was deemed as acceptable limit for the model as higher variability in the data leads to higher CV(RMSE)% (O'Donovan et al., 2019). Coakley (Coakley et al., 2014) sets out a comparison of hourly and monthly model calibration and refers to Guidline14, IPMVP and DOE. CV(RMSE) for building energy simulation models. Hourly data accepts up to 30% of CV(RMSE) while 15% for monthly data.

The acceptance criteria of a metric would rely on the purpose of the analysis and variability of the data. As suggested in the previous passage, temperature and CO_2 have different CV(RMSE) acceptability limits. Also, if purpose of the study is thermal comfort, more weightages would be given to temperature CV(RMSE) but if IAQ is the main concern, CO_2 CV(RMSE) would be main point of focus. Hourly/sub-hourly data is more variable as compared to daily or monthly data as low-resolution data would average out large number of fluctuations which would be part of the hourly data. For this purpose, literature suggests different acceptable CV(RMSE) for different variables and data resolutions.

For a ventilation design study, the widely used CV(RMSE) metric can be used to check difference in CO_2 concentration between measured and simulated data and for indoor temperature. This metric handles the variability in data and normalises the root mean square error by the mean of observed values. If the available data resolution is sub-hourly, a higher estimation of 20-25% of CV(RMSE) would be considered acceptable.

2.12.6 Variance Analysis

Variance analysis is a statistical method used to identify and quantify differences between the simulated and monitored data. Such analysis can be used to determine the difference between different AFN model setups and can help determine the impact of varied inputs on the outputs such as CO_2 concentrations.

A variance analysis often begins with an assumption that data is normally distributed (Box, 1953). This includes the Analysis of Variance (ANOVA), which is used for comparing more than two groups to establish if at least one group mean is statistically different from the rest of the groups. However, ANOVA assumes that the data is normally distributed. When this basic assumption is not met, the results may lead to incorrect inferences about the analysis.

For this purpose, alternatives, such as the Kruskal-Wallis test are used, which do not assume a normal distribution of data and hence are robust against outliers (Vargha & Delaney, 1998). However, unlike ANOVA, in the Kruskal-Wallis test the difference between two sets of data sometimes is not captured. For this purpose, as an initial step to conduct such test, visual and descriptive methods are employed. Visual inspection is the first step and allows the analyst to qualitatively assess the dataset for expected or unexpected patterns or anomalies that might be missed through a standalone statistical analysis. However, this inspection is always done in conjunction with a statistical aid (Kramer et al., 2004). Thus, while the distribution can be assessed via a visual inspection, a visual as well as a statistical measure can help to conduct tests for normality, such as the Shapiro-Wilk test. When applied to a dataset, this test is sensitive to departures from normality (Yazici & Yolacan, 2007). This test would help to determine the type of analysis suitable for the data i.e., ANOVA or Kruskal-Wallis.

After statistically confirming the difference, various pairwise comparison tests (post-hoc) are available to evaluate significant statistical differences between the data in a pair-wise setting when several groups of datasets need to be compared, for example, Tukey's Honest Significant Difference (HSD) Test, Scheffé’s Test, Nemenyi Test, Dunn-Bonferroni Method etc. It is important to choose a test in accordance with the data distribution type. These tests have their respective pros and cons, therefore it is important to determine the type of data and purpose of the analysis before choosing a post-hoc test (Ruxton & Beauchamp, 2008)(Williams & Abdi, 2010). When dealing with large datasets with high variabilities i.e., a common nature of CO_2 concentration data, choosing the right non-parametric post-hoc test is important. For such datasets, Dunn-Bonferroni is a commonly used method which can balance Type I (false positive) and Type II (false negative) errors due to Bonferroni correction (Bitnun & others, 2009).

These post-hoc tests give an indication of statistical difference but are not able to determine the magnitude of difference between the dataset groups for the practical significance. Effect size measurements such as Cliff’s Delta, Rank-Biserial, Cohen’s d etc are therefore considered suitable options. Cliff’s delta provides the probability of one group being larger in value than the other group, but it does not quantify the magnitude in a standard metric such as mean difference (Macbeth et al., 2011)(Tomczak & Tomczak, 2014). Rank-Biserial also lacks direct translation into a standard metric by providing a correlation-based measure which reflects the strength of relationship between the groups. However, Cohen’s d is less intuitive for probabilistic differences; it can directly translate differences into a scale of standard deviation and the magnitude of differences can be categorised into low, medium and large. Wargocki (Wargocki et al., 2017) used Cohen’s d metric to understand the impact of varied indoor CO_2 concentrations on the performance of the pupils. The approach devised in the next section reverses the process by evaluating the effect of change in ventilation parameters on CO_2 concentrations solution by an AFN.

2.12.6.1 Proposed Approach to Variance Analysis

The previous section presented a limited review of approaches to conduct a variance analysis and determine the magnitude of difference between two or more solution data sets.

The process for conducting variance analysis on simulated CO_2 concentrations for AFN modelling begins with a visual inspection, which is an essential qualitative step that provides the groundwork for further quantitative analysis. The subsequent Shapiro-Wilk test ensures that the data are analysed with suitable statistical tools. This is done by distinguishing whether a parametric or non-parametric tests should be applied. Upon confirming the non-normal distribution of data (in case of CO_2), the Kruskal-Wallis test is employed which acknowledges the potential for non-normally distributed data within environmental simulations, and provides valid results even with outliers or skewed data distributions. After confirming the non-normal distribution and statistically different structure of the datasets, the pairwise comparisons using the Dunn-Bonferroni post hoc method allows a pairwise comparison between the groups confirming their significance of difference. This enables the analysis of whether one or more solutions are similar or different.

Up until this point, the magnitude of the difference between the data groups is unknown. Cohen’s d effect size calculation for the pairwise setting of datasets would enable an assessed practical significance of findings, effect size and the direction of the solution. This data can be used to further assess the AFN component modelling parameters via a physical analysis.

2.12.7 Discussion on Statistical Approach to Evaluate AFN Solution

In order to establish an AFN modelling approach that meets the statistical acceptance criteria outlined in sections 2.12.4 and 2.12.5, the application of both physical and statistical methods is carried out step-by-step. This approach allows us to examine how the variation in inputs affect the output. At each stage, we assess IC and CV(RMSE) where possible to assess the impact of these input changes and the model's validation status. In the final stage, the model undergoes an additional evaluation using $RMSE_f$ and CV(RMSE) to ensure the approach's suitability for AFN design studies.

Figure 2.31 provides the layout and sequence of variance analysis in combination with physical analysis and statistical validation. A visual inspection is conducted by qualitative descriptive method. A distribution check is conducted via Shapiro-Wilk test of normality by calculating the W static number. The Kruskal-Wallis test can highlight significant statistical differences between the AFN solution groups. To further quantify and compare this statistical difference a pair-wise comparison, post hoc Dunn's test with Bonferroni correction is conducted. The same pair wise comparison setting is used to evaluate the effect size of AFN solution groups. The heat map of pair wise comparisons assesses influential parameters in the AFN solution which, consequently feed into the physical analysis and the solution is checked for statistical validation.

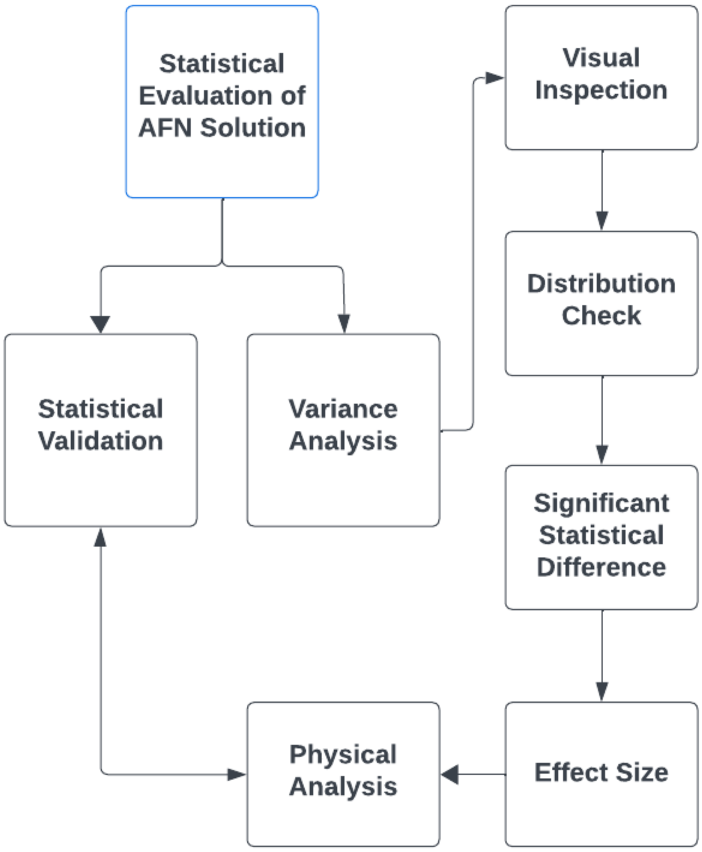

Figure 2.31: Layout of variance analysis framework in combination with physical analysis and statistical validation.

2.13 Important Review Outcomes

Following an in-depth review of the fundamental elements of AFN modelling, a comprehensive discussion is presented which supports the development of a model reliant upon physical and statistical analysis that provides grounds to develop a modelling guidance for ventilation design.

- A power law equation with appropriate coefficients must be used to determine building leakages. The review explains the relevance of these coefficients, emphasising the use of a flow exponent value that is equal to 0.65 which gives a suitable value for the crack height at 2mm. Later, a power law analytical model equation is employed to calculate C based on the user defined length of the crack. The input of the height and length will determine the leakage area for any zone.

- The placement of a crack to model infiltration is also important; a single level crack(s) in a zone can equate to the total leakage area. This specific positioning would result in a lower estimation of flow rates due to the reduced stack pressure which relies on the height of the flow component. The review emphasises the importance of multi-level crack distribution on a wind induced façade, reflecting a realistic infiltration scenario. This scenario will include the effect of buoyant forces on the flow rate calculations in the AFN model.
- The literature review addresses openings which can also be termed as "larger cracks" or "smaller openings". It is emphasised that, any purpose provided opening, such as trickle vents, should be aerodynamically tested. In the absence of such data, a power law analytical model can be used for the openings <10mm in height.
- Although limited information is found in the literature for larger door undercuts, it is advised that to model a door undercut equal to or beyond 10mm of height with a lower value of C_d must be used (i.e., 0.35). The use of standard sharp edged orifice coefficient would overestimate the flow through door undercuts. Thus, it is important to test the possible modelling approaches for such openings. Geometric and effective areas are evaluated in the Modelling Study, and various scenarios will be tested to evaluate the impact of different coefficients and equations to solve flow from these openings.
- To model flapped openings such as windows and doors, variability in their performance under different conditions is acknowledged. Such openings offer significant vertical dimensions and allow for bi-directional flow. A height of 10cm is recommended, and this criterion also applies to un-flapped openings.
- The opening mechanism type, opening angle, and frame aspect ratio determine the flow resistance offered by the window. This resistance also varies with pressure differences due to the wind velocity and angle, and temperature difference between zones. By highlighting substantial differences in the resistivity of the opening due to various factors, it was suggested that analytical models, such as SEAM, to be used to enable better approximation and straightforward inputs. Nevertheless, manufacturers' testing of the component is deemed important for determining the flow characteristics of such openings.
- A large opening area between the stories in multi-level building acts as a horizontal planer opening. The review could not find a suitable equation to solve for multi-directional flow through such openings. However, an approximate approach of using the orifice equation with C_d=0.61 (in case of centrally heated zones such as a dwelling)

is suggested in the literature and suggested here. However, the solution from uni-directional and bi-directional flow equations is compared in the Modelling Study.

- In the current Scottish domestic design of the buildings, the constant running of extract fans is advised to be part of ventilation design. The review highlights the importance of accurately representing fan performance and emphasises on the potential limitations and non-physical behaviour of flow predictions by the polynomial models. It was suggested that, for design studies, a simpler constant flow equation would sufficiently serve the purpose. However, as guidance flow inducer equation is more relevant.
- Occupancy is translated as a load in building simulation models, and in AFN, metabolic gains are modelled based on recorded or typical spatial presence and occupants' activity levels. This translation of gains and schedules for occupancy can be guided by ASHRAE/CIBSE and TM59/TUS data respectively. However, the review calls for a framework for occupant presence, schedules and activities concerning ventilation design.
- The selection of weather data is very important as wind speed, direction and ambient temperature greatly influence the airflow predictions by the models. Two main types of weather databases, TMY and TRY, are found to be suitable for certain evaluation purposes. It was concluded that TMY weather is suitable for a design study, as it enables an assessment of building performance under typical weather conditions. In comparison, TRY weather can account for averaged climatic impacts on the built environment. For specific case of overheating, a DSY weather database can be used.
- Closely related to the weather data, the wind reduction factor is also explored based on site terrain characteristics. The review presents models to quantify the wind reduction, which relies on terrain dependent coefficient sets. A lack of clarity was found regarding the definitions of terrain type. The review aimed to clarify the terrain types based on the structural density and dimensions. The uncertainties in representing pressure coefficients were also reviewed, acknowledging the implications of the dataset selection. The review however advises applying commonly used pressure coefficients with caution.

Based on the findings of the literature review, the following guidance is proposed to inform the application of AFN modelling in ventilation design. Each element of the AFN model has been examined in detail, with recommended approaches summarized below to facilitate practical and accurate modelling. The table categorizes these components and outlines specific guidelines for their implementation in AFN studies.

Category	Component of AFN	Key Guidance/Outcomes
Building Envelope	Building Leakages	Use a power law equation with a flow exponent of 0.65 for building leakages; determine leakage area using user-defined crack dimensions.
	Infiltration	Model infiltration with a single-level crack for total leakage; multi-level cracks are recommended on wind-induced facades to include buoyant forces.
Openings	Small Openings (<10mm)	Purpose-provided openings (e.g., trickle vents) should be aerodynamically tested; use a power law model for openings under 10mm if no data available.
	Door Undercuts	Model door undercuts ≥10mm with a lower discharge coefficient; avoid using standard sharp-edged orifice coefficients.
	Flapped/Unflapped Openings	Model bi-directional flow in windows/doors with height ≥10cm; consider opening mechanism, angle, and frame ratio for flow resistance variations.
	Large Openings (Multi-level)	Use orifice equation with Cd=0.61 for large openings in multi-level buildings; compare uni-directional and bi-directional flow equations in analysis.
Mechanical Ventilation	Mechanical Fans	Represent constant-running extract fans with polynomial models due to limitations.
Occupancy Modelling	Occupancy	Model occupancy as a load; use ASHRAE/CIBSE data for metabolic gains and TM59/TUS for occupancy schedules, with a call for standard frameworks in ventilation design.
Environmental Inputs	Weather Data Selection	TMY weather data is recommended for typical design studies; TRY data for averaged climatic impacts, and DSY for overheating studies.

	Wind Reduction Factors	Apply wind reduction factors based on site terrain; clarify terrain types using structural density and dimensions; use commonly accepted pressure coefficients with caution.
Validation & Verification	Statistical Validation	Adopt a statistical validation approach for CO_2 concentration outputs in AFN models to guide ventilation-focused AFN studies.

Table 2.10: Key outcomes from the literature review categorised for AFN modelling guidance framework.

2.14 Linking Research Gaps to Objectives

The findings from the literature review highlighted significant gaps in domestic ventilation design, airflow modelling practices and current approaches for ample IAQ. To address these gaps, the research objectives laid out in Chapter 1 were carefully designed. The table below provides a concise summary of how the objectives align with the research gaps, and how they progress from problem identification to proposed solutions.

Objective	Gap Identified	How the Objective Addresses the Gap
1. To understand domestic ventilation design and the occupant's influence on its effectiveness	Over-reliance on occupant behaviour and subjective design criteria; insufficient IAQ due to fragile decentralised systems and deficient building regulations.	Identified inadequacies in ventilation design and regulation, highlighting the need for robust, occupant-independent solutions.
2. To identify the shortcomings and ambiguities in building airflow modelling practices	Ambiguities in flow component definitions, unclear modelling methodologies, and insufficient guidance on boundary conditions and weather data selection.	Clarified flow component definitions and proposed methodologies, informing a more standardised and transparent approach to AFN modelling.
3. To compare the solutions for a simplistic and proposed airflow modelling approaches	Discrepancies in current modelling methods (e.g., crack flow vs. orifice equations) and their impact on flow predictions and IAQ.	Conducted comparative simulations to evaluate model accuracy, informing best practices for realistic airflow modelling.
4. To formulate guidance for "close-to-reality" AFN simulations to suggest effective ventilation	Lack of comprehensive guidance for realistic AFN simulations, including node setup, flow path criteria, and boundary condition inputs.	To be addressed in Chapter 5.

5. To propose an alternative solution for adequate ventilation provision (dMEV system)	Current dMEV systems underperform and fail to guarantee safe IAQ under varying conditions, lacking suitable alternative solutions.	

Table 2.11: Alignment of Research Gaps with Objectives and Their Contributions

Chapter 3 Ventilation Design Guides and Evaluation Studies

To develop domestic ventilation design guidance that is assisted by AFN simulation, it is vital to assess current designs in the regulatory documents. This is achieved by exploring the specifications of flow pathways and their described purpose. In this chapter, the Scottish Technical Handbook is taken as reference regulatory document for effective ventilation, and the included elements of flow are reviewed by comparing their representation in other design guides and compliance documents.

Later in this chapter, CIBSE AM10 (CIBSE AM10, 2005) which is a design and calculation guidance document for non-domestic buildings, is taken as a reference. Its applicability is critiqued by addressing ambiguities in the document and by evaluating its applicability to a domestic ventilation design. Although AM10 is primarily designed for non-domestic buildings it remains relevant to designers and modellers as the presented principles and methodologies are broadly applicable.

The summary of this chapter is comprised of two parts, which can contribute towards the development of a design guidance. First part discusses the findings from the review of regulatory documents and second presents the performance gap due to insufficient design and building practices.

3.1 Purpose of Ventilation in Scottish Building Regulations

The purpose of ventilation design, as stipulated in 3.14 of the building standards technical handbook for domestic buildings (Building Standards Division, 2023) is:

> *“Every building must be designed and constructed in such a way that ventilation is provided so that the air quality inside the building is not a threat to the building or the health of the occupants”.*

These Handbooks have been available separately for domestic and non-domestic sectors from 2017 (Scottish Government, 2023) and the following section will discuss guidelines in the ventilation section 3.14 and the underlying specifications of ventilation design. These specifications are also indicated in other regulations, design guides and compliance documents via a review.

3.1.1 Design Air Infiltration and Ventilation System Type

The Handbook advocates the need for greater airtightness levels with more control over ventilation of a building. It calls for balance between the energy usage and ventilation provision and highlights the importance of comfort and structural integrity of the building. Versions 2017, 2019 and 2020 refers to Good Building Guidance for Achieving Airtightness Part 1 (GBG67) (Jaggs & Scivyer, 2006) while version 2023 refers to Supporting Guidance for Domestic Ventilation (SGDV) (Scottish Government, 2017). The latter takes a more scenario oriented rather than a general approach by classifying the airtightness levels. In the first classification, SGDV classifies air permeability as <3 $m^3/hr/m^2$ of building airtightness for mechanical supply and extract ventilation (MEV). The second classification is between 3 and 5 $m^3/hr/m^2$ which is suggested to maintain DMEV (continuous running) ventilation in wet rooms/kitchen via extraction fans. The third classification is >5 $m^3/hr/m^2$ for which DMEV or natural ventilation with intermittent extraction fans or window openings in wet rooms are suggested. The underlying principle behind this categorisation is control over the flow paths which would be effective for the dilution of contaminants and odours throughout the building while maintaining thermal comfort. The aforementioned air infiltration rates classification further devises appropriate extraction rates and trickle vent effective areas to form a ventilation design.

3.1.2 Ventilation Design

The design of airflow in a new built is suggested in the Handbook which includes air inlets (windows, trickle vents), air pathways (internal doors, undercuts) and outlets (extract fans). The specification and placement of these components are of greater importance which finds its roots in UK building design guides and compliance documents. The following sub sections will express their specifications as listed in the Handbook and comparable documentation.

The ventilation strategies from the Handbook are given in the following table which explicitly categorises ventilation strategies based on air permeability of the building.

Ventilation Strategy	**Air Permeability**	**Min Background Ventilator Equivalent Area for Rooms**
Natural with Intermittent mechanical Extract	>5 $m^3/hr/m^2$	4000mm^2
Continuous Extraction (DMEV)	3-5 $m^3/hr/m^2$	11000mm^2
Continuous Supply and Extraction (MEV)	<3 $m^3/hr/m^2$	N/A

Table 3.1: Proposed ventilation systems by design infiltration rate in Scottish Technical Handbook.

The air permeability classifications listed above can be regarded as “tight”, “average” and “leaky”. This phenomenon can further be explained in the figure below. A leakier building would provide ample ventilation rate but less control while an airtight building has greater control but would require careful operation of the ventilation components.

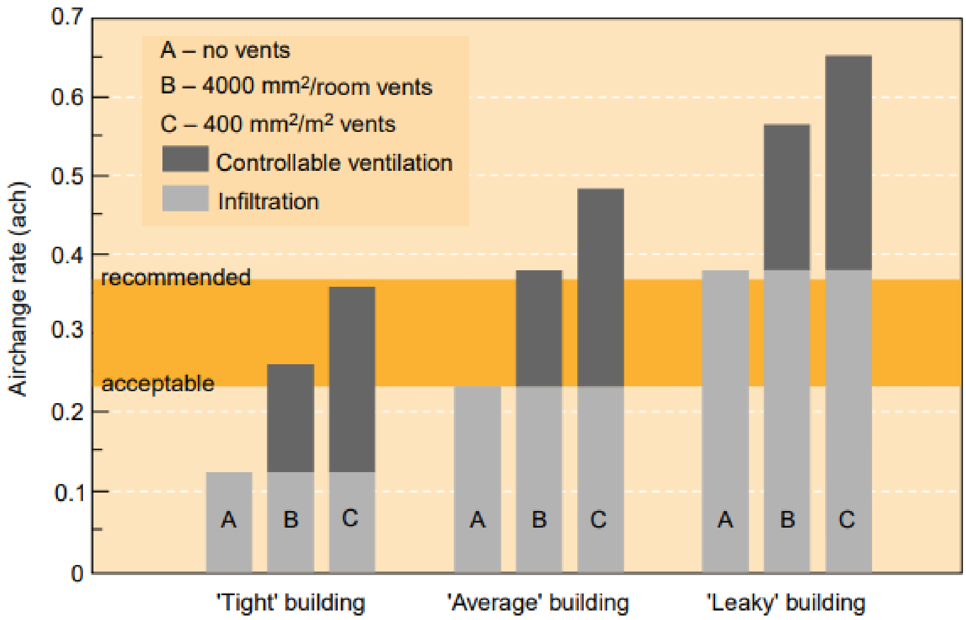

Figure 3.1: Dwelling Airtightness and Trickle Ventilator Flow Area (BRE, 1998)

While the Handbook provides a clear framework for ventilation strategies based on air permeability, there are certain limitations and challenges as well. Achieving airtightness levels below <3 $m^3/hr/m^2$, as recommended for MEV systems, can be particularly difficult in dwellings such as older buildings or retrofits, where existing construction materials and techniques may not support such levels of airtightness. Additionally, achieving airtightness at this level can sometimes lead to unintended consequences, such as increased humidity or condensation risks, hence if ventilation systems are not adequately designed or maintained. Hence a careful consideration of both construction limitations and long-term building performance when implementing these classifications is required. The focal aspect of this classification is energy usage. Biler et al., (2018) explains how trickle vents when not efficiently sized can cause cold draughts and reduces thermal comfort leading towards higher energy usage.

3.1.2.1 Ventilation Requirements

The Handbook describes the specifications of ventilation components in compliance with the regulatory standards. For any kind of ventilation mechanism, minimum ventilation rate is suggested to be 13 l/s for 1 bedroom apartment and addition of 6 l/s per room. This is in agreement with the minimum whole building ventilation rate with one bedroom and 2 occupants as mentioned in the Approved Document Part F (ADF) (UK Government, 2015) and CIBSE KS17 (Clancy, 2011). However instead of addition of 6 l/s as in the Handbook, the cited guides suggest 4l/s addition per room provided that one room adds 1 occupant. The guides mention alternative ventilation rate of 0.3 l/s per m^2 of internal floor area need to be achieved which is 15 l/s in accordance with minimum internal floor areas for a one-bedroom dwelling and 2-person occupancy. Review of different guidance documents focussed on domestic ventilation design has revealed that the Handbook takes more cautious approach and requires greater ventilation rates for similar environments.

Please note that the term used is Gross Internal Floor Area which is defined in the Technical housing standards (DCLG, 2015) as:

> *"The Gross Internal Area of a dwelling is defined as the total floor space measured between the internal faces of perimeter walls that enclose the dwelling. This includes partitions, structural elements, cupboards, ducts, flights of stairs and voids above stairs. The Gross Internal Area should be measured and denoted in square metres (m^2)".*

This definition also complies with the fan pressurisation test methods listed in ISO 9972 (BS EN ISO 9972, 2015) which suggest the same method to calculate the floor area for the heated volume concerning air infiltration measurements. This confirms the uniformity of methods used for the floor area calculation and air tightness measurements. However, the number of occupants is not mentioned in ADF where ventilation rates for additional room is mentioned while the Handbook does specify the occupants.

3.1.2.2 Ventilation Network

To meet the mentioned minimum level of airflow though out a building volume, a decentralised network is formed in which windows and trickle vents are air inlets, door opening/ undercuts are flow paths while extract fans in the wet rooms and kitchen are outlets. The extract fans are responsible to generate a negative pressure in the living spaces and air from outdoors enters via trickle vents and passes through doors/undercuts. This way a full circulation of air takes place in the dwelling. These components are now discussed individually.

Trickle Vents

For an extract driven ventilation system, the background ventilators effective areas for flow according to their calculation method in EN13141 are described in "Geometric, Effective and Equivalent Areas of Flow of Windows" previously in section 2.7.5.

Installation specifications similar to the Handbook are listed in CIBSE Guide B2 (CIBSE, 2016), AM10 (CIBSE AM10, 2005) and ADF (UK Government, 2015) which recommend placing them 1.75m above floor level. As the main purpose of these slots is background ventilation, this height can reduce cold draughts and promote mixing of outdoor air with the indoor air, hence reducing the stratification.

The effective flow area of the trickle vents is given in (Perera et al., 1993), (BRE, 1998), (BS 5925:1991, 2000), AM10, ADF, and the Handbook, which suggest the same area of 4000mm^2 of minimum trickle ventilation per room while BRE, (1994a) suggests 400 mm^2 per m^2 of room area. It is important to note that the Handbook's effective area for a tighter house is 11000 mm^2 per room. Here, the Handbook takes a more scenario oriented and cautious approach.

As the two approaches of suggested trickle ventilation area is seen, BRE, (1998) shows how a larger effective area of trickle vents is important for tighter buildings and highlights that having a standard for tickle ventilation concerning the floor area of the zone can be effective. It provides comparison through a simulation study, of "tight", "average" and "leaky" building air change by defining acceptable and recommended levels. This shows comparison of air change rates in a dwelling with and without trickle vents. For a "tight" building, controllable ventilation is required to achieve acceptable ventilation rates. Also, this graph shows how a leaky, energy inefficient building does not require attention to the provision of controllable ventilation.

Windows

Windows are advised for purge ventilation during the winter months. Like the suggested installation height of trickle vents to overcome stratification, some part of the window opening is suggested to be 1.75m above floor level. The minimum flow area offered by a hinged or pivoted window opening between opening angles of 15-30° should be 1/10th of the floor area of the room, and 1/20th when windows are opened for angles >30°.

The purpose of this area specification is to provide 4 ach of flow to purge the volume of the room. The calculation is based on:

$$Q = \left[C_d \frac{A}{3} \times J(\emptyset) \sqrt{\left(\frac{\Delta \mathrm{T} \times \mathrm{H}_{Vertical}}{\mathrm{T}_{absolute}} \right)} \right] \tag{3.1}$$

Where A is geometric area of the window opening, H is the vertical height of the opening and J is the function of window opening angle ($\emptyset$) given in BS 5925 (BS 5925:1991). The temperature difference is taken as 3°C and the windspeed at 2.1 ms^{-1} in a single sided ventilation setting.

Pennycook (Pennycook, 2009) contributed in the BSRIA guide to advise for the different window mechanisms (both turn and pivoted) by forming a "out of 4" point system for 4 relevant factors i.e., airflow, ventilation control, weather protection and night ventilation. If we test BS5925:1991 (code for practice for building ventilation design) with the BSRIA Guide for Ventilation, those mechanisms which offer greater airflow have less control over ventilation.

Also, it is easy to see the pattern that the windows with lower airflow have greater weather protection. During the winter ventilation, the BSRIA Guide also agrees with the Handbook which refers windows for purge ventilation and advises a greater use of trickle ventilation for thermal comfort and to tackle weather control issues. Figure 3.2 provides an informed guidance for designers to achieve the best suited air purge in winters and in prolonged summer-time usage for a specific ventilation design.

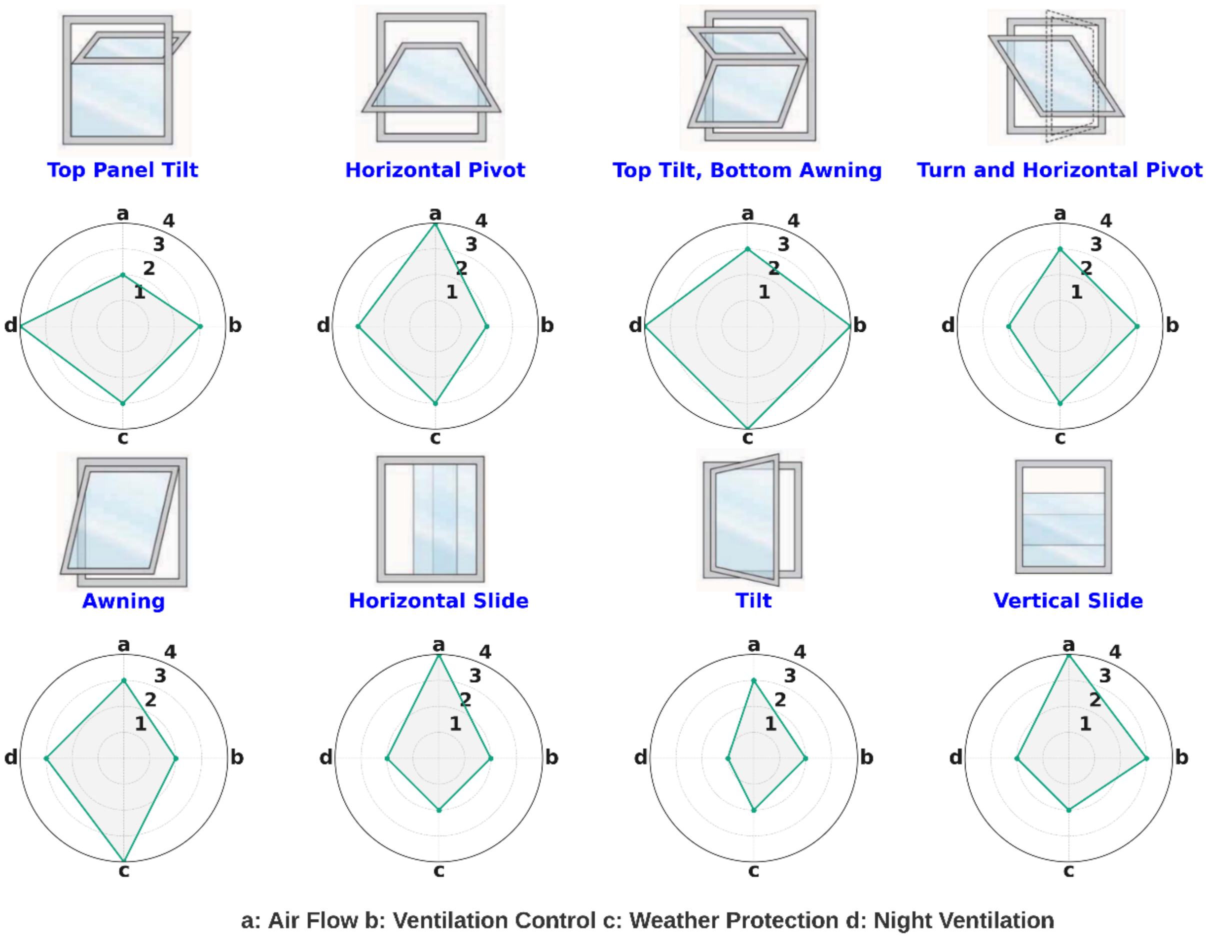

Figure 3.2: Points system for Airflow, Ventilation Control, Night Ventilation and Weather Protection for different window mechanisms by BSRIA (Pennycook, 2009) and regenerated data visualisation by author for this thesis.

The selection of a window mechanism is found to be very important factor for both winter and summer ventilation provisions. Occupants may have their own preferences of windows use during both winter and summer weather conditions. The factors highlighted in the motivations and barriers for occupants section (2.2), can be assessed together with points system elaborated in Figure 3.2 for a suitable selection of window mechanism.

Door Undercuts

The door undercuts allow the airflow from the living spaces to wet rooms and the kitchen which is then extracted by constant running fans. Internal doors are given a clearance area above the finished ground, so the flow path remains unobstructed. The Handbook suggests 10mm gap between the door leaf and the finished floor and this is in agreement with the ADF. CIBSE TM60:2018 (Lelyveld et al., 2018) also refer to ADF for the inclusion of door undercuts as a good practice of ventilation design in homes. Flow between zones is also suggested in the AM10 but due to non-domestic topic of the manual, it recommends open plan and open doorways between zones of the building.

In comparison to other flow elements such as trickle vents and extract fans in a decentralised system, the aerodynamic performance for a 10mm opening of a door undercut is unspecified rather this area is termed as a “free area”. With the assessment of flow performance through door undercuts, an efficient sizing of this component is anticipated. Furthermore, modellers would have accurate data to model these opening pathways and carryout assessment simulations.

Extract Fans

The Handbook stipulates outwards flow rates as mentioned in the table below which are categorised on building infiltration. CIBSE TM60 (Lelyveld et al., 2018) refers to Guide A (CIBSE, 2021) and ADF which agree with the data in table provided. For energy and acoustics, the power consumption of a fan is rated alongside the flow rates, i.e., Watts/Litres/Second, and termed Specific Fan Power (SFP) in SAP (SAP DECC, 2023). While SFP is effective for balancing energy use and performance during the design phase. This metric allows designers to evaluate fan efficiency in relation to airflow rates. However, its actual impact would depend upon ensuring a proper installation, maintenance, and alignment with the ventilation needs.

	Intermittent	**Continuous**	
Room	**Standard (l/s)**	**Normal (l/s)**	**Boost (l/s)**
Kitchen (Elsewhere)	60	6	13
Utility	30	4	8
Bathroom/Shower	15	4	8
Drying Area	15	N/A	N/A
Toilet	6	3	6

Table 3.2: Extract rates in different rooms for intermittent and continuous ventilation systems in all versions.

For a MEV system with supply and extraction mechanisms the flow rates are similar, but the driving force changes to a fully mechanical system with a lower infiltration rate which allows for a greater control over the ventilation. The older versions of the Handbook do not explicitly mention the supply rates but refer to Digest 398 (BRE, 1994b) which recommends supply rates ensuring 4 ach (equal to a purge flow rate through a window opening).

3.2 AM10 Translation to Domestic Ventilation Design and Modelling

The flow elements of a ventilation system in question are now reviewed for their modelling approaches in AM10 guide which is a comprehensive guide that provides detailed methods to implement non-domestic guidance and assesses the potential of natural ventilation based upon network of airflow paths. However, it can be applied to a domestic setting with some conditions. It would be interesting to evaluate a non-domestic guidance to point out important design considerations in a domestic setting. This section is further divided in to two parts, first presents a general critique expressing the ambiguities and incompleteness of the guidance in general (feeding into AFN modelling guidance) and second part particularly presents the gap which would help in the application of AM10 to a domestic AFN simulation (feeding into an effective ventilation design study).

3.2.1 Part 1 – Ambiguities in AM10 for AFN Application

This part highlights important aspects of the document which encourage a level of uncertainty when implementing flow through openings into an AFN model by following AM10.

- It is advised in AM10 that the required airflow is provided through displacement ventilation. This same concept is also presented in the Industrial Ventilation Design Guidebook (MOSER et al., 2001) which details that, in displacement ventilation, air is supplied in a room at low velocity through a low-level opening which is extracted through a higher-level opening (cross ventilation) as this incoming air is heated by the indoor gains and it rises due to buoyancy. These lower and higher-level openings work in combinations which are not always effective. Such scenarios are described theoretically and experimentally by Hunt (Hunt & Coffey, 2010) which inform that the possibility of laminar and turbulent flow due to temperature differences at lower and higher parts of the room and singular dimensionality of flow is not always guaranteed. This can apply to the modelling of stairwells and the multidirectional flow through the large horizontal planer opening formed between the floors in a domestic setting.
- Different terminologies for flow area are discussed in detail in the section “Geometric, Effective and Equivalent Areas of Flow of Windows”. In AM10, three contradictory terms for opening areas are used i.e., effective area, free area, and effective free area

without explicit definitions of these terms which could lead to over or under estimation of air flow rates in a model.

- The sizing of the openings to cater for the required airflow rates and thermal comfort are not mentioned. Specially, being a non-domestic guidance dealing with larger volumes of occupied spaces, this specification is of higher importance (D. Etheridge & Ford, 2008). The document suggests orifice equation to determine single opening size for various flow conditions and leaves the topic open for distribution of flow components and suitable vent sizes. For modelling which concerns a design in a domestic setting, the placement of flow components with definitive effective area and use of suitable equation is found to be very important.

Modellers should resolve these ambiguities by adopting a consistent approach which prioritises informed use of inputs. Terminologies such as effective area, free area, and effective free area should be standardised by referring to detailed definitions. For sizing and distribution of openings, modellers can use iterative AFN simulations and validate with empirical data in order to optimise flow component placement and select equations suited for domestic settings, such as orifice or power law models with context specific parameters.

Part 1 describes how the implementation of AFN modelling to model air flow openings and pathways can be tricky and such comprehensive guidance like AM10 cannot be applied on an "as is" basis without scrutinising the physical parameters of the model.

3.2.2 Part 2 – Applicability to Domestic Ventilation Design

This part will discuss the important considerations of ventilation design which are different for non-domestic and domestic buildings. This would be helpful in developing a design study based on the AFN modelling:

Establishing Required Flow Rates: The guidance document starts by comparing the constant supply of ventilation versus a variable supply (10 l/s) based on the occupied period which would be able to keep CO_2 levels in safe threshold (CIBSE, 2021). Being a non-domestic guidance, it is important to reexamine this ventilation rate as the occupancy patterns vastly differ in non-domestic and domestic settings. Occupancy patterns in domestic environment can be justified as less abrupt as people spend a large part of the day sleeping in their main bedrooms (Adams, 2006). Further activities such as TV watching, cooking and showering are more predictable as compared to a non-domestic setting as it would include a factory, office, theatre etc (Liao et al., 2014). Therefore, establishing the flow rate requirements in certain areas is comparatively straightforward in a domestic setting and less attention to such detail is required.

Sizing of Airflow Components: AM10 suggests sizing of the flow components such as windows in accordance with steady-state calculation methods which fulfil the purpose of the calculations of adequate flow to the indoor environment. It is assumed that the difference between indoor and outdoor is 3K so that the calculations set an upper limit to the requirements. Window types are illustrated, and their preferred usage and effectiveness is detailed. These details can be well related to the data visualised given in (Zero Carbon Hub, 2016b) which is mainly targeted at domestic buildings.

Small sized passive passages of flow such as trickle vents are mentioned in the document and in agreement with most domestic guidance (discussed under heading 3.1.2.2). Other passage type i.e., door undercuts are not discussed at any level of detail. In addition, the sizing of vents in a domestic setting can be based on the area, use and occupancy of a room. Also, occupants of the domestic setting may have more control (decision making) over opening areas compared to a non-domestic setting. Such factors can greatly affect the ventilation design.

Geometry and Flow Path: The AM10 guidance suggests open plan and open doorway (in case of cellular offices) floor planning as in larger volumes, the dilution of contaminants is easier (Chen et al., 2021). Also, it provides rule of thumb for flow strategies based upon the geometry of the room. We can test this rule by looking at a typical double bedroom in a UK house which measures Length 4* Width 2.75* Height 2.4 m according to (DCLG, 2015).

- Single side single opening is recommended for Width≤2H.
- Double opening with height difference for Width≤2.5H.
- Cross ventilation for W≤5H.

If this example room is put to the test, all three criteria are fulfilled which indicates a lack of specificity and adaptability to the variety of layouts, especially in a domestic setting.

It is also important to emphasise that arrows depict flow through these openings in the AM10 however are not representative of actual flow paths as they not only depend on the size and location of these openings but also the distance between these two flow components (D. Etheridge, 2011).

Applying AM10 guidance to smaller domestic spaces presents challenges due to the differences in scale, occupancy patterns, and geometry. The generalised flow rate recommendations in AM10 which are designed for larger non-domestic spaces, may not be appropriate for the lower, more predictable occupancy levels in homes, leading to excessive ventilation or inefficiencies. Additionally, the absence of detailed scaling guidance for trickle vents, door undercuts, and inter-room flow paths can lead to inaccuracies in domestic airflow modelling.

In the upcoming section, through the review of design documents, an account of improvements in the Scottish Handbook is presented aiming for robustness of the ventilation system.

3.3 Recommendations for the Development of Ventilation Design Guidance

In this section the Handbook is reviewed for its applicability. The key elements of ventilation design are presented and critiqued for their effectiveness. Consequently, the performance gaps due to the design and its implementation are presented in the discussion section 3.4.

Infiltration: Sharpe (T. Sharpe et al., 2019) conducted a monitoring campaign and collected information for 41 post 2015 built dwellings and presented data showing their design/locality, and the average air permeability of all dwellings was between 4-5 $m^3/hr/m^2$. However, literature suggests that design air tightness and after construction air tightness can have large discrepancies (Zou et al., 2019). Also, according to the technical note by AIVC, with the passage of time, airtightness tends to vary depending upon any refurbishment works and/or occupants' life styles (Kapsalaki, 2022). The variation in the airtightness of the structure would cause uncontrolled airflow and leading towards inefficient decentralised extraction.

Provision of Trickle Vents: The suggested background/trickle ventilator area is given in Table 3.1. The minimum area for habitable room is consistent amongst all documents however their operational efficiency is questionable (T. Sharpe et al., 2019). The ventilator area suggestion would be beneficial if it was modified as per occupancy or floor area of the room rather than a standardised effective area.

These ventilators when installed in a wet room, it is advised that these should be installed away (0.5m) from extract fans to minimise or curb the short circuiting of air from these ventilators. Finally, when installed in a habitable room, trickle vents are supposed to be placed at least above 1.75m above the floor area as cited from regulatory standards.

Air Short Circuiting and Extract Fans: The survey by Sharpe (T. Sharpe et al., 2019) have reported that in houses installed with dMEV systems, trickle vents were present in bathrooms (17%), kitchens (37%) and open plan kitchens (20%). However, the distance between the trickle vent/possible window opening and extraction unit were not measured. The problem of coexistence of trickle vent and extract is more relevant to the intermittent method; if a house is fitted with an intermittent extract with natural ventilation, such short circuiting would be of a higher magnitude as the extract would offer much higher flow rate than continuously running systems. Hence for a leaky building having an extract fan providing higher flow rate would result in greater short circuiting pressure differential at two points of the building which are close to each other and this would result in worst IAQ when windows are not opened; to dilute the pollutants (SeppĘnen, 2008). ADF (UK Government, 2015) and The Handbook (Scottish Government, 2023) both suggest not having a trickle vent in wet rooms where an extract is installed with a suggestion of having the at least 0.5m apart if they happen to be in the same room.

Zero Carbon Hub Services Guide (Zero Carbon Hub, 2016a) evaluates ADF as a whole and suggests against having a trickle vent in the wet rooms at all basing upon the previously described phenomenon of short circuiting.

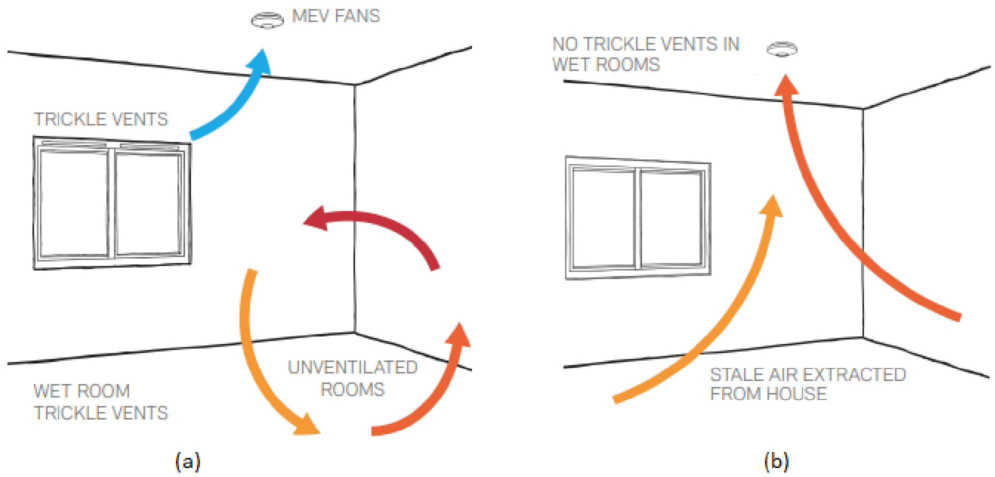

Figure 3.3: Trickle vents presence vs no trickle vents in a wet room with an extract fan installed (Zero Carbon Hub, 2016a).

However, having a trickle vent and extract combination in a wet room can reduce humidity/odours at a higher rate because of the shorter path.

However, the presented review would suggest against having an opened trickle vent in the same room as a constant running extract fans to avoid short circuiting of the flow network in dMEV design.

The survey (T. Sharpe et al., 2019) further showed poor commission of the extract fans such that they were either set at high air flow rate or lower air flow rates. Table 3.2 suggests the extract flow rates in the regulation document while the survey study found they were set at a higher level by up to 15% in most of the houses causing noisy conditions and eventually in 49% of houses these fan units were turned off. These fans usually have an on/off switch that is not usually easy to reach while the normal and boost switches are either fitted within the wet room light switch or separately. It is interesting that in circumstances where fans are turned off from the main switch, the DMEV's constant running extract fan system basically turns into an intermittent system where extractors are on only at a higher rate when wet rooms are being used.

Door Undercuts: The prescribed opening height of the undercut in the guidelines is questioned in the literature (T. Sharpe et al., 2019). The most effective setting to assess their effectiveness would be night-time prolonged occupancy in the main bedroom with trickle vents open, door closed and extract running continuously in the wet rooms and kitchen. Out of 41 monitored dwellings, just 1 was reported to fulfil this recommended setting. Despite these flow settings, the peak CO_2 levels were only 11% of the occupied time below or equal to 1000ppm. However, wet room door undercut was < 5mm in height which further points towards the performance gap found due to the construction practices and failing a ventilation design.

Sharpe (T. Sharpe et al., 2015, 2019) showed that door undercuts in the houses were blocked by carpets or uneven flooring. Another study (Zero Carbon Hub, 2016b) assessed 6 domestic sites consisting of 33 dwellings and none of them consistently met the criteria. Dependence on door undercuts for airflow introduces a high level of fragility to the ventilation design.

Furthermore, the aerodynamics of door undercuts is not mentioned contrary to other vital flow components (trickle vents and extract fans).

Figure 3.4: Insufficient gap left for air to flow throughout the house causing blockage to the flow pathway (T. Sharpe et al., 2019).

Occupier Influence: Various survey and monitoring studies (Cakyova et al., 2021; Saini et al., 2020; T. Sharpe et al., 2015, 2019, 2020) highlight that the inadequate knowledge of IAQ and ventilation can cause a well-designed system to underperform.

Other influential factors include the operation of the building and other construction shortcomings inherited by the occupier as a customer.

Operation factors include the non-use of extract fans, keeping trickle vents closed, and not purging when required, while construction shortcomings would include non-existent door undercuts, airflow short circuits, and noisy fans.

3.4 Discussion

The cited studies suggest two main categories of reasons behind the performance gaps found in the design of the ventilation system i.e., **due to design** and/or the **construction process**. Sections 3.1.1, 3.1.2 and 3.3 are further analysed together to present author's perspective on the review of the Handbook, scientific literature and the guidance documents.

- The Handbook suggests the air permeability bands for which a certain ventilation types are suggested. However, with the decrease in the building's airtightness over time, greater infiltration can cause non-functioning of a whole house ventilation system.
- Air inlets like trickle vents with small air passages would not allow mixing of room air with incoming cold air; being a low velocity intake (Cao et al., 2014).
- For an intermittent fan providing 15 l/s in bathrooms of a volume 20m^3 or 20,000 litres, it would need to run 22 minutes for a complete air change of the space whilst the typical shower time for an adult is 8 minutes (BBC, 2011). A fan must be installed with a humidity sensor. For a dMEV installed system, it would be much longer time for complete air change as "boost" extraction rate is 8 l/s.
- ADF and the Handbook suggest that a trickle vent and extract fan can coexist in a zone when set apart by 0.5m in any ventilation design. A trickle vent would be efficient in such scenario when the quick ventilation of shower area is intended while the fan is in boost mode. If trickle vent would stay open constantly, short circuiting is inevitable specially when the bathroom door is kept closed.
- Window openings are only described as a purge ventilation device and certain angles of openings are suggested for summers conditions when temperature differences are 3°C. Further suggestions are made by the AM10 and the (Zero Carbon Hub, 2016b) for use under different weather conditions which should be catered in the domestic design guidance.
- The generalised approach of the Handbook needs the further investigation of different domestic scenarios such as those governed by building layout, occupancy, weather conditions and flow components.

The cited survey and design studies (Lelyveld et al., 2018; T. Sharpe et al., 2015, 2019; Zero Carbon Hub, 2016a, 2016b) also highlight certain construction issues which include deviations from the design guidance, the quality of workmanship, a lack of coordination between different trades and commissioning issues. These issues are bulleted below:

- The extraction rates provided in the design guidance were not found in most of the buildings. Lower rates result in an insufficient ventilation system while higher rates would compel occupants to turn the continuous running fans off. Additionally, a study which concerns the acoustic comfort of the residents from various demographics can be employed to suggest the set extraction rates from the fans and their acoustics. This approach would ensure that both ventilation efficiency and resident comfort are balanced, leading to more effective and acceptable ventilation solutions in the residential buildings. Mandatory post-installation commissioning and maintenance checks should be implemented to ensure extraction rates meet design specifications.
- The surveys show how the boost switch, at some instances, is provided coupled with the light switch in the bathroom and two individual light and boost switches were found. In the later scenario it is found important to label the switch for occupants' knowledge. A set criterion is required to either have separate or a multifunctional switch. Design standards should provide clear guidance to standardise the placement and labelling of these switches for intuitive occupant use. Regular inspections and stricter enforcement of undercut sizes during construction are necessary to maintain consistent airflow pathways.
- In the presence of on/off switch for extract fans (where these are not hard wired), they were found turned off in a large proportion of houses. This would convert a dMEV system in an inefficient intermittent extract system. Hardwiring extract fans or using automated controls linked to humidity or CO_2 sensors could eliminate the risk of user disengagement.
- A large proportion of the door undercuts were blocked by flooring/carpet as found during the surveys, and suggested door undercuts sizes were not found consistently throughout the buildings. It is well emphasised in this chapter that in a whole house dMEV system, door undercuts should be regarded as an essential element. Regular inspections and stricter enforcement of undercut sizes during construction are necessary to maintain consistent airflow pathways.

These key points are valuable outputs of a multi-category literature review and call for a re-examination of current building regulations for the effective ventilation design of the domestic sector in the UK.

Chapter 4 Modelling Methodology and Case Study Introduction

4.1 Context

Leading from the overall methodology presented in section 1.9 which refers to the non-prescriptive nature of the AFN modelling methods, the proposed approaches to model the AFN components (discussed in the literature review) are applied in conjunction with statistical evaluation (detailed in section 2.12) which would allow to assess the practical implications of these modelling approaches. As an output, it is aimed to present a guidance document helpful in determining a suitable approach for an AFN assisted design study. This procedure would cater the objectives if this work to compare solutions of various modelling approaches and formulate guidance for AFN simulations focussed on ventilation design of domestic buildings. Furthermore, an alternative solution for the adequate ventilation is proposed which concerns the dMEV systems.

4.2 Data Sourcing and Phase Definition

Data is sourced from a monitoring study that includes detailed information about the layout of the houses, dimensions, specifications of the flow components and occupant diaries which document, household activities, sleeping hours and the daily use of flow components. The sensed outputs include indoor CO_2 concentrations, temperature, and relative humidity. Using this monitoring dataset, two distinct phases of occupant behaviour were identified and categorised basing upon standard and interventional ventilation strategies. However, the study faced several data limitations which include a small sample size of 41 dwellings, potential confounding variables such as occupant behaviour and airflow pathways, reliance on as-designed airtightness data for 17 properties along with the challenges with participant recruitment and retention. These constraints show how the complexity of isolating individual factors affects the ventilation effectiveness. These limitations are detailed in the dataset report (T. Sharpe et al., 2019).Using the monitoring dataset, two distinct phases of the occupant behaviour are identified which involved ventilation strategies setup as well as the occupancy durations. The basis of categorisation is standard and interventional ventilation strategies.

Phase I: 6 days standard monitoring period in which occupants were logged having trickle vents open in the main bedroom with closed door offering undercut space. The floor has a wet room fitted with a constant running extract fan and other two unoccupied rooms.

Phase II: Interventional monitoring period in which occupants were asked to implement five different combinations of flow settings in the main bedroom using trickle vents, window, and door during the other six days.

A version system is used for the AFN setups with varying input parameters and modelling setups. Each version presents an output iteration of the AFN, and the results are discussed to inform the modelling guidance. Each version's output's validation is performed by comparing monitored indoor CO_2 concentration data during night-time sleeping hours with the simulated data.

4.3 Monitoring Study and Available Data

Sharpe (T. Sharpe et al., 2019) conducted a monitoring survey of the post 2012 built houses in Scotland for the winter months. Following default features were common for the selected houses:

- Target airtightness between 3 and 5 $m^3/hr/m^2$ @50Pa.
- Trickle vents for the air inlet and extractors in the wet rooms for outlet.
- Minimum effective area of the trickle vent in bedrooms is 2500 mm^2.
- The extract fans integrated in the building design to run continuously and at higher speed (boost) when purge is required.

From an initial survey, a sample of 41 houses was selected for detailed monitoring, including a range of house types and tenures, and was geographically confined for logistical reasons. Researchers conducted an initial walkthrough of each dwelling before sensor installation to confirm the floor plan, assess ventilation components such as trickle vents, door undercuts, and extractors and address any obstructions to airflow.

The monitoring study comprised of 7-day period and intended to collect following data:

- Indoor CO_2 (ppm), RH (%) and Temperature (°C) in bedrooms, living rooms and kitchens. The sensors' model, accuracy and reading resolution figures are provided below.
- Extract fan flow rates in l/s.
- Occupant diaries to include data for occupancy, cooking, sleeping and other household activity hours.

The monitoring survey walkthrough confirmed the floor plan, dimensions, and spot assessment of ventilation components i.e., trickle vents, windows, doors, and extracts. Sensors were installed approximately 1m above the finished floor level and away from direct heat sources, air inlets, or extract vents and away from direct breathing zones of the occupants. Model and accuracy of the sensors are tabulated below from the Tiny Tag's (manufacturer's) data sheet.

Sensor Model	Parameter	Measurement Range	Accuracy	Reading Resolution
TGE-0011	CO2	0 to 5,000 ppm	±(50 ppm + 3% of value)	0.1 ppm
TGU-4500	Temperature	-25°C to +85°C	±0.01°C or better	0.01°C or better
	Relative Humidity	0% to 95% RH	±3.0% RH at 25°C	Better than 0.3% RH

Table 4.1: Sensors models and specifications.

The CO_2 monitoring for the main bedroom for which occupancy is recorded is presented in the Figure 4.1 as an independent analysis by the author. Box plots are ordered by median CO_2 and filtered for the night-time hours (2300-0700). Median is chosen over the mean and max values to show the central tendency of the data.

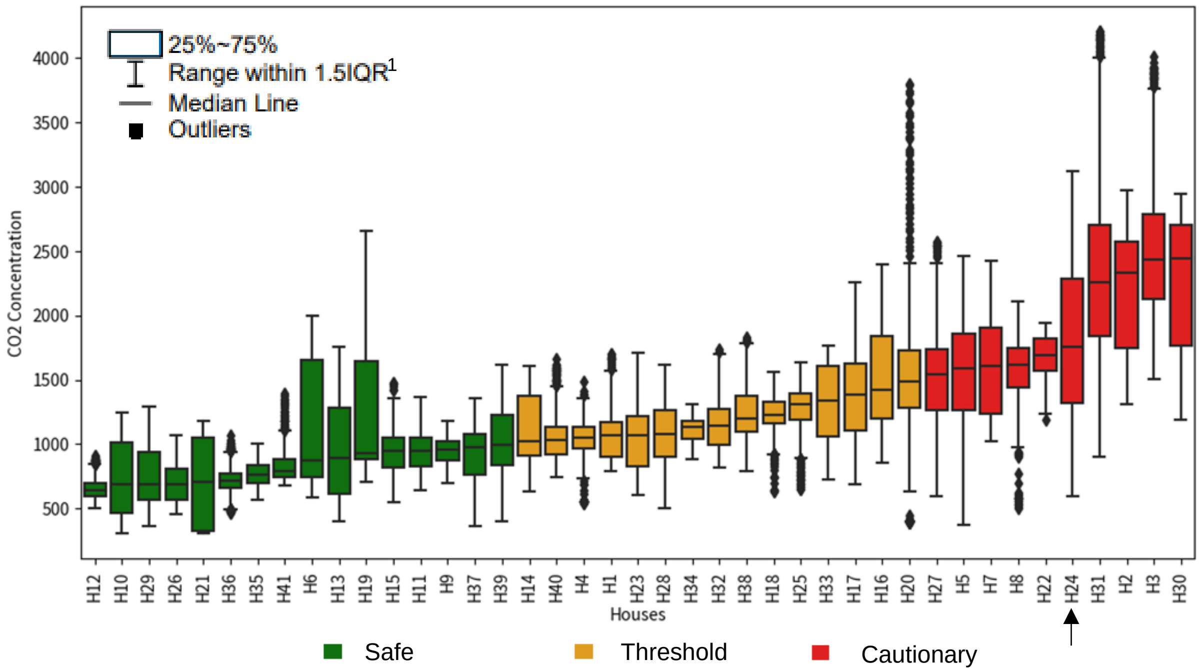

Figure 4.1: Night-time CO_2 concentrations of main bedrooms of 41 houses during sleeping hours 11PM-7AM. Arrow indicates the case study house (H24).

[1] IQR: Inter Quartile Range

This analysis suggests that majority of the bedrooms had median CO_2 concentrations in the "take action" range (>1000ppm), this range is provided in (Scottish Government, 2017).

4.3.1 Analysis of Monitoring Survey Study Data for Appropriateness

CO_2 concentration data from main bedrooms night-time hours is further assessed on the basis of thresholds suggested in the literature.

SGDV document recommends intervening by a crack opening the window if indoor CO_2 concentrations are >1500ppm and opening it further when levels are >2000ppm. This highlights that if concentrations remain in these limits consistently, the stock ventilation design is insufficient.

Another criterion in literature which suggests exposure to high CO_2 concentrations for a longer time period may pose risk to occupants' health. (Maula et al., 2017) suggested that the occupants should not be exposed to consistent CO_2 levels of >2260ppm for more than 4 hours and (Satish et al., 2012) proposed a 2500ppm threshold for 2.5 hours of duration.

In the context of the mentioned criteria, a temporal analysis is conducted by the author, calculating the time (hours) above 1500ppm during the night-time sleeping period and then percentage of time for which concentrations were above 1500ppm. This provides quantitative assessment of the duration as well as the frequency of the instances (hours) when the threshold is violated and presented as scatter Figure 4.2 (a). Then second scatter Figure 4.2 (b) for time above 1500ppm and time above 2260ppm is plotted to further narrow down the houses (bedrooms) which can pose potential risk to the occupants' health. The red line marker at 4-hour mark for the time above 2260ppm identifies such houses (bedrooms). While the yellow line marker excludes houses on the right which have at least of 1 hour of duration of CO_2 concentrations above 1500ppm. It is important to note that this time above certain threshold does not account for the number of nights rather it gives the total number of typical sleeping hours (11AM-7PM).

This analysis filters out the 5 bedrooms which are posing highest levels of risk to its occupants. The monitoring survey study has selected H24 as it has worst-case main bedroom CO_2 levels. The analysis confirms that the selected house is representative of the worst-case scenario of indoor CO_2 concentrations.

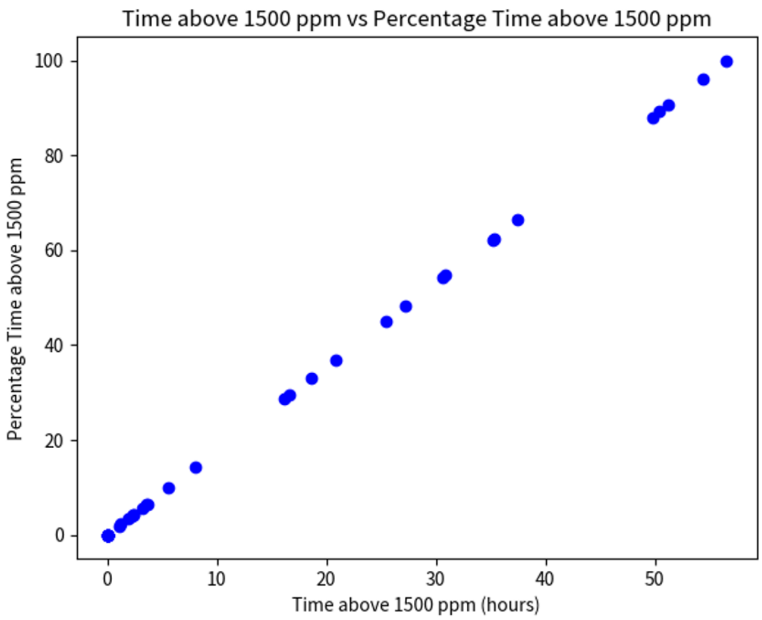

(a)

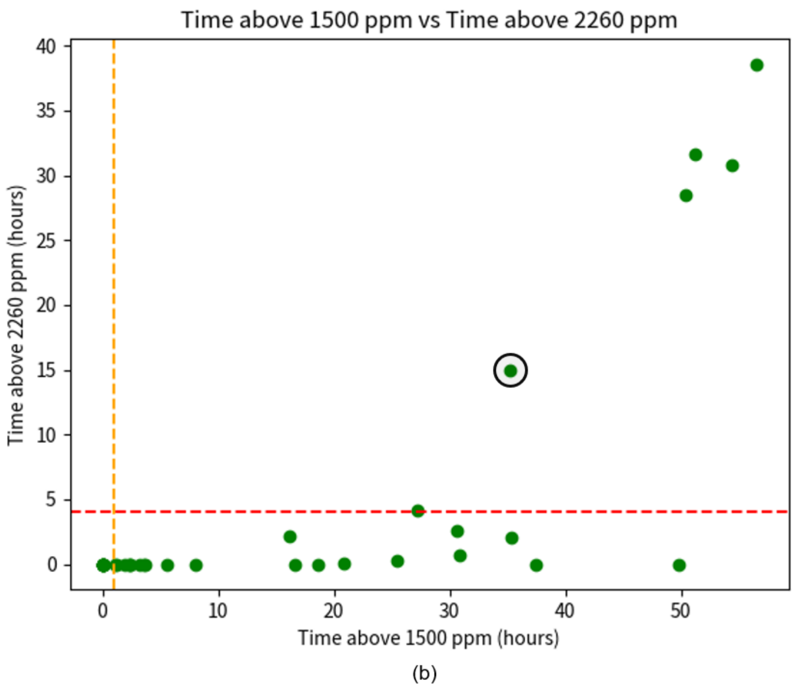

Figure 4.2: (a) Time (hours) above 1500ppm vs Percentage time above 1500ppm (b) Time (hours) above 2260ppm vs time (hours) above 1500ppm. The red marker identifies the houses with more than 4 hours of CO_2 concentrations. The black circle surrounds the data point for case study house.

4.3.2 Relation between CO_2 Concentrations and Design Parameters

It is established in the literature review section 2.1 that low IAQ in domestic environment is an important factor which affects the health and wellbeing of the occupants. Specifically, study by Sharpe (T. Sharpe et al., 2019) highlighted how a dMEV system failed to provide ample ventilation rates to the occupants specifically in the main bedrooms. The underlying reasons of underperformance of this system are detailed in section 3.1.2 of this thesis. Further to this in section 4.3.1, it is concluded that large proportion of the houses included in the study have unsafe levels of night-time bedroom CO_2 concentrations. Figure 4.1 provided the snapshot of the min, max and median monitored CO_2 concentration values of the whole dataset.

It is important to note that, the monitoring survey study data is from un-controlled experimentation hence the occupant behaviour would have a great influence the monitored CO_2. A comparative analysis of statistical metrices, can however provide useful insights to stipulate direction and viability of the ventilation solution proposed.

Key design parameters of the data set houses are evaluated which are following:

- Door undercut characteristic dimension.
- Bathroom door undercut characteristic dimension.

- Presence of ensuite bathroom
- Door opening (yes/no)
- Room volume
- Distance (m) from trickle vents to the closet extract.

The performance specifications of these parameters are integral elements of a dMEV setup as suggested in SGDV and the Handbook (Scottish Government, 2017, 2023). Undercuts are the purpose provided flow pathways when doors are closed. For the main bedroom having an ensuite, the distance between the trickle vents (inlet) and the extract fan (outlet) decreases. In case of opened door, the flow path resistance decreases. Larger room volume would have more dispersion of the CO_2. The last parameter concerns the distance from trickle vents and closest extract fan.

The correlation analysis of these design elements and the main bedroom occupied hours CO_2 concentrations is presented in the Appendix 1. This analysis feeds into suggesting interzone openings as potential solution to tackle elevated CO_2 concentrations in the main bedroom. This assessment of the alternative design in presented in 5.8.

4.4 Case Study House

The building under study is a 2017 built end of terrace three storey house in the North of Edinburgh. Built in accordance with 2015 building regulations which are in effect until the latest release of guidelines (Scottish Government, 2023).

In the monitoring survey study, a walkthrough was conducted to confirm the building plan, measure flow rate through extract fans (constant running) and visual condition of the trickle vents and windows and a two phased monitoring study is conducted. House is occupied by 3 children, 2 adults while third adult is reported to visit often. Two adults reported to occupy the main bedroom on the first floor, children in 2nd bedroom on the third floor while third bedroom is vacant and on the same floor as the main bedroom. Ground floor is comprised of living room, wash cabin and kitchen. 3rd floor bedroom has ensuite while main bedroom is neighboured with a washroom with entrance in the hallway.

Assessment of the trickle vent openings, door under cut and extract fans was crucial as it formulates a flow pathway which is designed to ensure safe indoor environment. For this purpose, the walkthrough of the dwelling identified following features:

- Trickle vent opening
- Window type and opening
- Extract fans
- Door undercut air passageways

- Occlusions of air flow openings

	Zone	Area*Ceiling Height (m^2*m)	Trickle Vents (5000 mm^2 each)	Windows (Top Hung)	Extract Fan Trickle (l/s)	Extract Fan Boost (l/s)	Undercut Clearance/ Height (cm)
Ground Floor	Living Room	53.2*2.4	1/4 Open	Closed	N/A	N/A	1.1
	Kitchen	17.9*2.4	N/A	Closed	3.6	7.4	1.6
	WC	11.2*2.4	N/A	Closed	3.6	6.8	1.7
First Floor	Main Bedroom	30.3*2.4	2/4 Open	Closed	N/A	N/A	1.6
	Shared Bathroom	12*2.4	N/A	Closed	4	6	0.3
	Studio	19.2*2.4	2/2 Open	Closed	N/A	N/A	0.3
	Bedroom 2	17.6*2.4	0/2 Open	Closed	N/A	N/A	1.8
Second Floor	Bedroom 3	45.9*2.7	0/2 Open	Closed	N/A	N/A	1.9
	Ensuite Bathroom	15.3*2.7	N/A	Closed	4.7	7.4	2

Table 4.2 : Data Collected Upon Walkthrough Survey

In the Table 4.2, an overview of the flow intake, pathways, and extract fan specifications is presented. The specifications are now discussed in the next section.

The dwelling construction predominantly uses timber frame construction. External walls are insulated with render systems and clad with brick. Roofs is pitched and covered with clay tiles. Windows and doors are fitted with triple glazing in uPVC frames to enhance insulation and reduce energy consumption.

4.4.1 Flow Components' Specs and Locations

As mentioned previously, the flow network for each room starts with intake from trickle vents installed on the window frame, the air intake is supposed to be extracted out of the wet room on each floor passing through door undercuts (if the door is closed).

Trickle vents provide effective area of 5000 mm^2 each. Flow passage is divided by a bridge gap while each slot measures 13 mm in height and 165 mm in length.

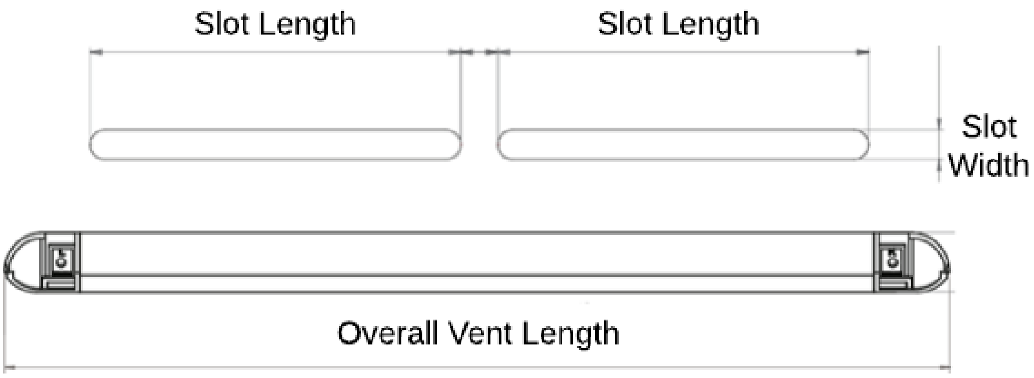

Figure 4.3: Trickle vent diagram installed in the house.

The door undercut area varied for each door. To our focal interest, the flow network on the first floor is highly hindered by the undersized bathroom door undercut which does not comply with the requirements in the building regulations. The width of all doors is 0.84m.

Identical extract fans were installed throughout the house however their extract capacity in l/s were measured to be different. These extract fans are circuited to be powered on all the time. However, the flow rate can “boost” with a switch provided next to light switch for purge ventilation when required.

4.5 Standard Occupancy - Phase I Overview

During the monitoring phase I study, occupant diary suggests that occupants of the main bedroom did not open any windows and slept with doors closed. Trickle vent settings remained unchanged as well. Main bedroom had occupancy of 2 adults however on the first day, for a part of the night, child joined the adults in the main bedroom. Although this monitoring phase was standard, no change in the flow paths was reported.

Sleeping hours for the 6 nights are:

Day 1	Day 2	Day 3	Day 4	Day 5	Day 6
0100-0700	0200-0700	0200-0700	0100-0700	0100-0600	0100-0500

Table 4.3: Main bedroom occupancy hours per occupant diary.

Occupant diary shows that for Day 1, one child accompanies parents in the main bedroom at 0500 until 0700. Rest of the nights, occupancy remained 2 adults.

For Phase I, the flow conditions remain unaltered. The inlet flow components in the main bedroom are 2 slots of trickle vents which were open during initial walkthrough when sensors were installed and second walkthrough when sensors were taken off. Hence, they are assumed to stay open during whole monitoring phase I.

The phase I CO_2 concentrations for the 6-day period shows unsafe levels consistently for a large part of the occupied period. The highlighted time periods in the plot below are from the occupant diaries. However, a closer inspection is required to confirm CO_2 concentration rise with respect to occupancy time.

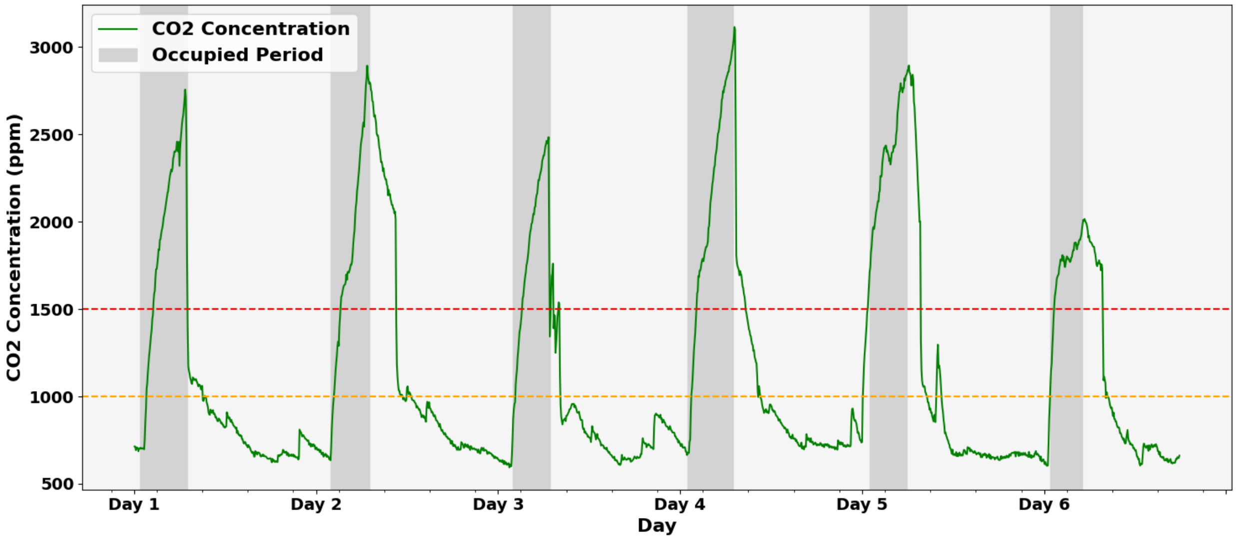

Figure 4.4: Measured CO_2 Concentrations for Phase I, 6 days period. Occupied time periods are shaded in grey. Yellow and red lines indicate “take action” and “caution” thresholds.

For the day 1, as a child joined their parents at 0500, visual inspection shows higher rate of increase of CO_2 for 0500-0700 hours. To confirm this, we will calculate rate of increase for the total occupancy period and compare it with rate of increase for the time slot when child is reported to join in the main bedroom. Linear regression equation for CO_2 concentration at time t can be written as:

$$CO2(t) = slope \times t + c \qquad 4.1$$

Where slope is the rate of change of CO_2 per hour, t is time in hours, c is y-intercept representing CO_2 at t=0.

Rate of increase for the total occupancy period is 132.9ppm/hour while for the reported increase in occupancy its 188.8ppm/hour which equates to absolute rate difference of 55.9ppm/hour.

For all the other occupied nights, there is no report of change in occupancy and according to the diary it remains 2 adults in the room.

To further confirm the occupancy schedules, we can inspect the start and end of the occupancy from the peak start and peak reach of each night.

Day	Reported Start Time	Derived Start Time	Difference in the Start	Reported End Time	Derived End Time	Difference in the End
1	01:00	01:20	20 minutes later	07:00	06:45	15 minutes earlier
2	02:00	01:55	5 minutes earlier	07:00	06:45	15 minutes earlier
3	02:00	01:30	30 minutes earlier	07:00	06:40	20 minutes earlier
4	01:00	00:55	5 minutes earlier	07:00	07:10	10 minutes later
5	01:00	0:00	1 hour earlier	06:00	06:10	10 minutes later
6	01:00	00:25	35 minutes earlier	05:00	05:20	20 minutes later

Table 4.4: Reported and derived occupancy start and end time basing upon CO_2 peaks – Phase I.

These minor discrepancies in the table above either can be due to occupant's reporting error or sensor's measurement delays or both. Hence more than one reasons of inaccuracy are present.

Possible uncertainties in the available data for Phase I listed here are not exhaustive and various other parameters could be influencing the accuracy of the data. Same is true for Phase II of the monitoring survey study data.

Data from this phase of monitoring shows that infiltration, trickle vents, door undercuts and constant running extract fan are responsible for ventilation provision. This dataset is used to investigate the variation in the model input parameters, stage-by-stage as indicated in section 4.11.

A simple base case model AFN V1 with one crack per window fitting to represent infiltration is developed. To solve flow through the purpose provided flow components i.e., trickle vents and door undercuts, a set of approaches is defined, and bedroom CO_2 concentrations are analysed. These approaches form the iterations 1 to 5 of AFN V1.

Trickle vents are modelled using the orifice equation when manufacturer advised effective area is available and using the power law if manufacturer's n and C values available.

For door undercut, the modelling parameters are unknown apart from the measurement of the physical area. Power law model's n and C values based on the geometry would give a smaller estimate of the flow solution while with C_d=0.61 in orifice equation a larger estimate of the flow (relative to each other) is expected. Literature suggests using C_d=0.35 for larger flow passages through doors. However specific flow parameters for large door undercuts are required to be researched.

The analyses for both trickle vent and door undercut are carried out via statistical and physical approaches. The five iterations of AFN – V1 are investigated for the flow solution and the final Iteration 5* is suggested to be used for further investigation stages. The key change in the inputs is the door undercut C_d. Hence Iteration 5* is the output of the AFN – V1.

The wind reduction factor which accounts for a reduced wind speed due to terrain is added to the model. This stagewise addition of detail to the model allows to evaluate the impact on the model's output. This modelling upgrade is labelled as AFN – V2 and the output is Iteration 5* Log W.

The approach to modelling infiltration is then investigated. A simple approach of placing 1 crack on each window frame is compared to distribution of cracks at top and bottom of each external window bearing facade in each room. This distribution of cracks across different heights would provide a representation of stack effect not otherwise captured. This higher level of detail in the model with distributed cracks is labelled as AFN – V3 and output is Iteration 5* Log W_d.

CO_2 generation rate has a large effect on the indoor CO_2 as would be expected and, in our case, there is no physical or physiological data for the occupants. To assess this impact, limits for sensitivity analysis are set from the literature and the values suggesting the lowest statistical error form the second output of the AFN – V3 i.e., Iteration 5* Log W_d (0.9 MET).

The same range of metabolic rates is applied to the single level, non-distributed infiltration model (Iteration 5* Log W) to determine the influence. The aim of this analysis is to gain insights and suggest a modelling approach for IAQ focussed ventilation design study.

Further investigation of ventilation design is conducted by the modelling of the interzone openings reviewed in the section 2.8. These openings are applied to Iteration 5* Log W with higher metabolic rate than standard to evaluate their impact on zone CO_2 concentrations in worst case conditions. The safe IAQ criteria is then applied to determine their effectiveness.

4.6 Interventional Occupancy - Phase II Overview

Phase II is interventional monitoring where occupants are advised to implement the certain flow conditions and steady night-time occupancy.

The results from Phase I were used to formulate Phase II. Phase I highlighted critical occupant behaviors and perceptions that influenced ventilation performance in the dwellings. One significant finding was that 71% of occupants reported closing bedroom doors at night, restricting airflow and hence leading to elevated CO_2 levels. This insight guided Phase II to prioritise the monitoring of CO_2 concentrations in main bedrooms during sleeping hours, addressing this specific concern.

Another important insight from Phase I was the discrepancy between occupant reported and actual deactivation rates of dMEV systems. Based on this, Phase II ensured that all dMEV systems were activated before monitoring began.

Phase I also highlighted the awareness of trickle vents, showing that while participants were aware of their existence, they adjusted them infrequently. This informed the setup for Phase II, where trickle vents were pre-set for each day to ensure varied airflow conditions so to analyse role of trickle vents in ventilation provision.

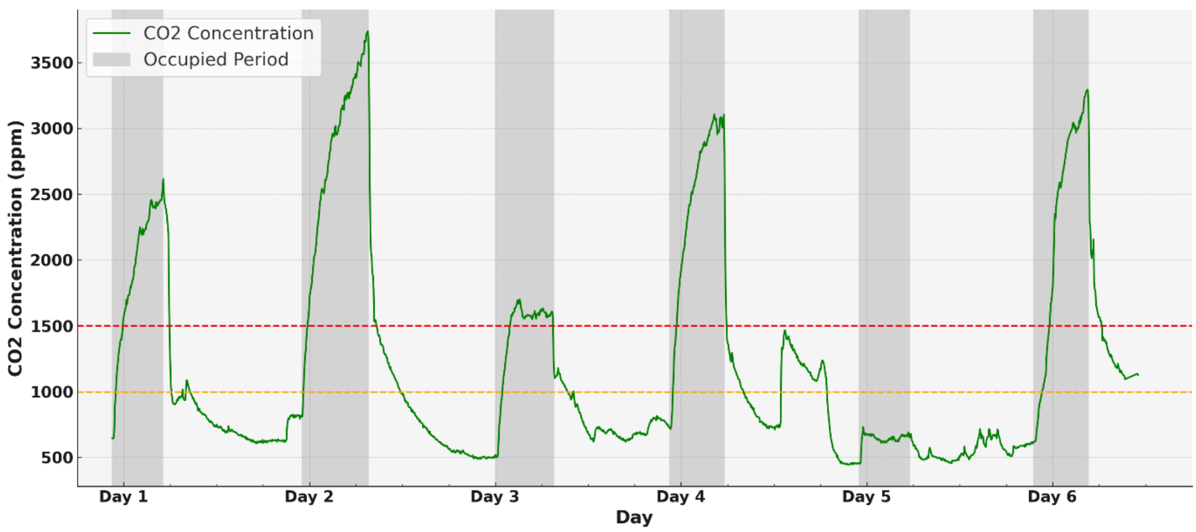

Figure 4.5: Measured CO_2 concentration for Phase II, 6 days period. Occupied time periods are shaded in grey.

The occupancy times are observed from the CO_2 peak start and end and tabulated in Table 4.5.

Day/Scenario	Start	End	Trickle Vents	Window	Door
1	22:35	05:00	Opened 4/4	Closed	Closed
2	23:00	07:30	Closed	Closed	Closed
3	00.15	07:20	Opened 4/4	Closed	10cm Open
4	22:40	05:30	Opened 4/4	Closed	Closed
5	23:10	05:40	Opened 4/4	Opened 1cm	Opened 1cm
6	21:40	04:30	Opened 1/4	Closed	Closed

Table 4.5: Occupancy start and end times and opening of ventilation components forming airflow scenarios.

Day 1 and 4 are representative of standard conditions for the dMEV system with constant running extract.

Day 2 indicates the worst-case scenario for the bedroom flow conditions as all components are kept closed and air flow is dependent upon the infiltration and door undercut.

Day 3 allows to inspect the effect of door opening which would allow additional air exchange between room and corridor.

Day 5 reduced door opening with a cracked open window.

Day 6 assesses use of a single trickle vent with the combination of door undercut.

These conditions are different from the consistent flow conditions found in phase I where 2 trickle vents were open constantly and occupants slept with closed door.

Commenting on the effectiveness of ventilation for these components, each day shows varied CO_2 peaks and the percentage of time of CO_2 between the ranges (Figure 4.5, Figure 4.6).

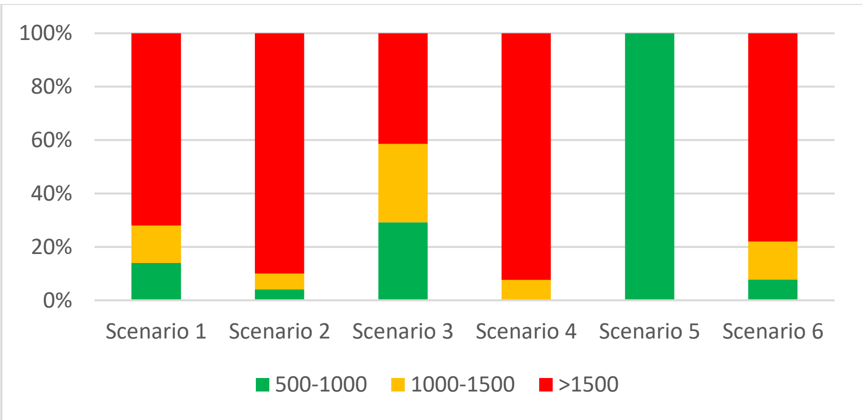

Figure 4.6: The percent of time of CO_2 concentrations (ppm) in safe, threshold and cautionary ranges as mentioned in (Scottish Government, 2017).

This varied setting would enable an assessment of the latest AFN iteration with distributed cracks and elevated metabolic rate (new base model) by modelling the different opening/closure of trickle vents rather than the continuous opening of 2/4 as in the Phase I. The closure of all trickle vents would evaluate the modelling of infiltration while on the other days different number of trickles vents openings will test the base model's respective modelling capabilities.

For opening of door (on the Day 3) in combination with trickle vents, geometric flow area formed by 0.1m of stroke length is modelled by three approaches.

1. Modelling the geometrical opening area of the door via a bi-directional flow component of modelling the door with C_d=0.61.
2. Modelling the same effective area on the top and bottom extremities of the door frame.
3. Modelling the effective area on top and bottom of the door frame using the orifice equation with the application of the correction factor given in equation 2.14.

The first approach is a simplistic approach in which the geometric area is calculated for the top triangle and the frontal rectangle of the opening, this area is modelled via a bi-directional flow door equation with C_d=0.61. In the second approach the effective area from first approach is modelled on top and bottom of the door frame to confirm the overprediction of flow rate as described in the literature review. The third approach aims to show the effect of the correction factor to tackle the overprediction. The comparison not only elaborates the possible discrepancy between measured and simulated results but also confirms the over prediction in flow solution when second approach is applied and reduction in the over predicted flow by applying the correction factor. The quantification of the difference is presented by comparing CV(RMSE) in the measured and simulated results.

The method to model door openings with the lowest CV(RMSE)% is used to model a different door opening area in combination with window openings. A visual inspection of the monitored CO_2 levels suggests a possible misreporting of the window opening area, such as the small opening of the window had a substantial effect on the monitored CO_2 concentrations. Hence a sensitivity analysis is conducted for door and window opening stroke lengths by modelling the window's geometric area with C_d=0.61 using an orifice equation. The discussion pertaining CV(RMSE)% for this analysis is produced.

4.6.1 Room Temperature

Both the monitoring phases i.e., free floating/standard and interventional were conducted in the winter months. Bedroom night-time recorded temperatures for free floating phase I (T_I) (top) and interventional phase II (T_{II}) (bottom) are given in Figure 4.7.

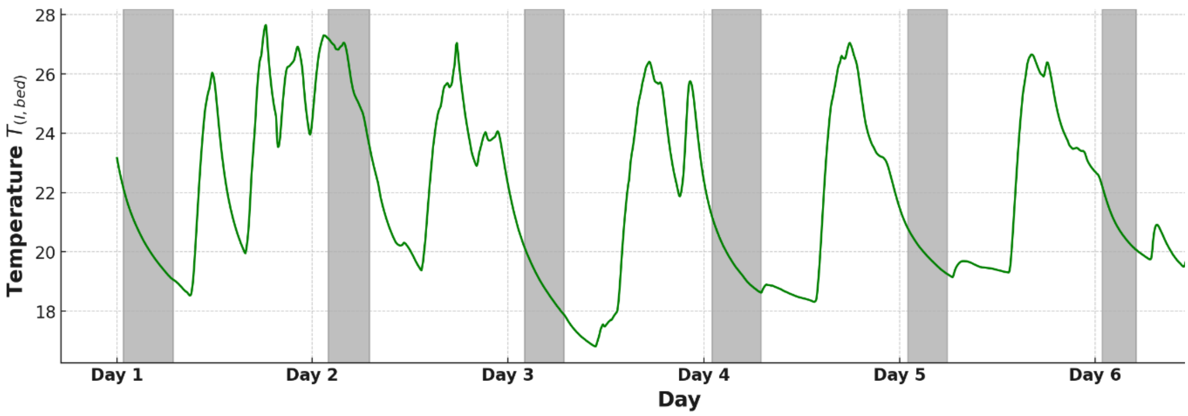

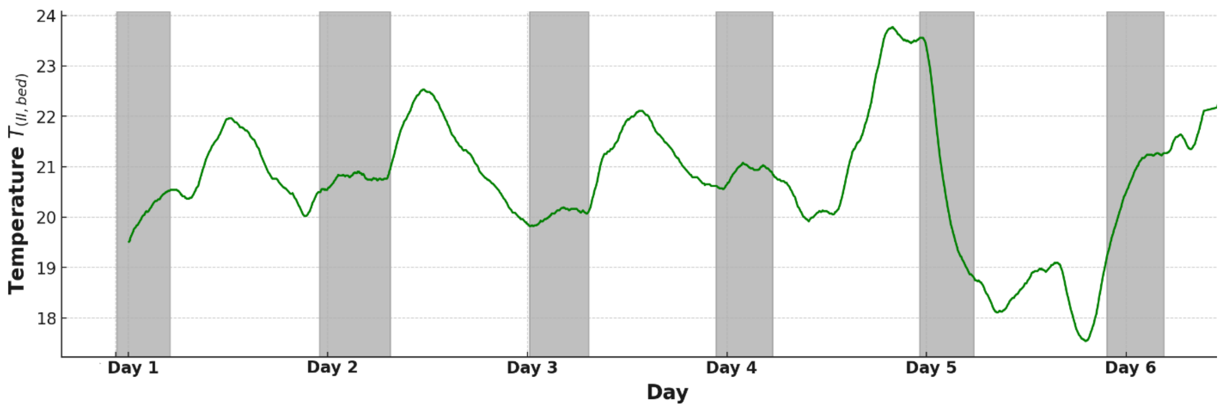

Figure 4.7: Measured indoor bedroom temperature for both phases of monitoring study. Top: Phase I, Bottom: Phase II.

Shaded grey area is for the night-time occupied sleeping hours under an investigation. The average temperatures from these time slots are given in Table 4.6.

	Average $T_{I,bed}$	Average $T_{II,bed}$
Day 1	20.26	20.09
Day 2	25.96	20.81
Day 3	18.89	20.08
Day 4	19.62	20.89
Day 5	19.92	20.36
Day 6	20.88	20.85

Table 4.6: Average bedroom temperatures for night-time occupied sleeping periods for free floating and interventional phases.

Heating setpoint was used by the occupants to keep the comfortable indoor temperature.

4.7 Modelling Inputs

In this section we will detail the use of case study data for the AFN model. Modelling tool ESP-r is used to build the geometry, flow components and internal gains. ESP-r is selected for modelling the building's Airflow Network (AFN) due to its comprehensive and integrated simulation capabilities. ESP-r also allows detailed modelling of building thermal performance, inter zone airflow and contaminant modelling within a single applet. This facilitates an accurate analysis of complex interactions between various domains. Being open source in nature and extensive validation history further support its reliability for such applications (H. Li, 2002; Strachan et al., 2008). The upcoming headings would highlight the set of inputs for each of these categories.

4.7.1 Geometry

Floor plans provided by the builders were confirmed during the monitoring survey walk through. Each zone floor areas and the ceiling heights along with the fitted flow openings, flow paths and extract fans are tabulated Table 4.2). This data is used to generate geometry of the model.

For this modelling study, the zone volumes, placement of flow openings with respect to a datum line and distance between flow components e.g., trickle vents (inlet) and extract fan (outlet) are most relevant parameters.

Although our focus is main bedroom situated on the first floor, geometry for the whole house is translated into ESP-r environment.

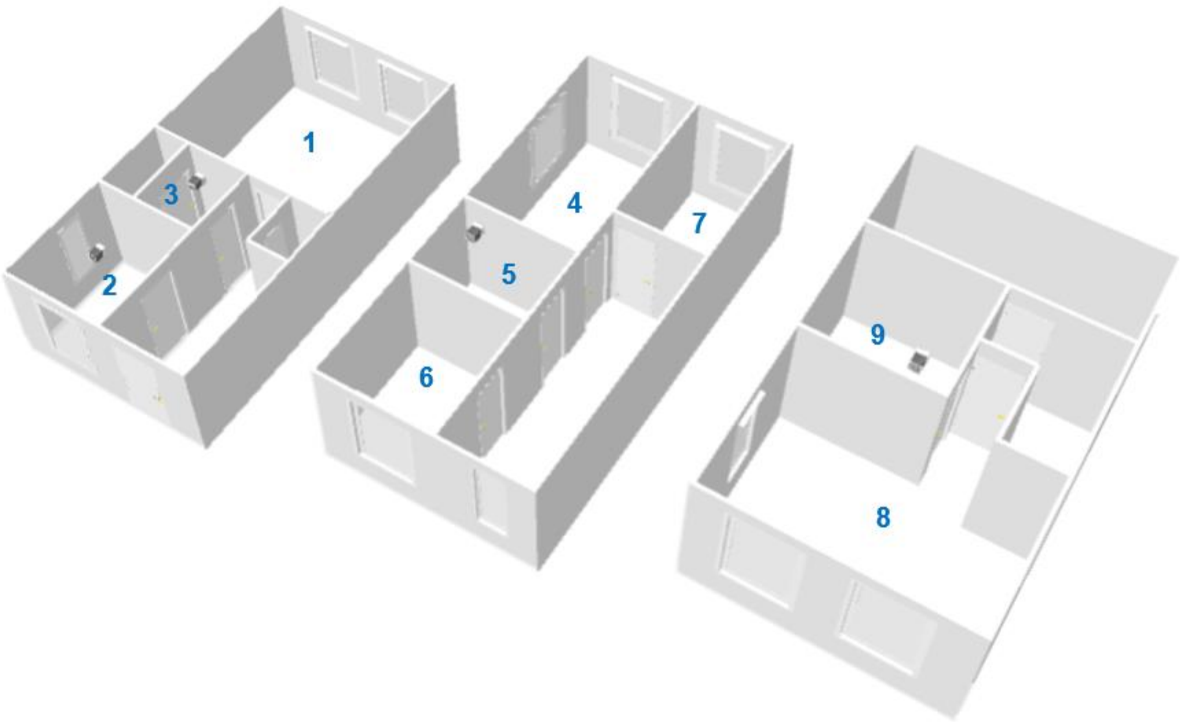

Figure 4.8: Ground, First and Second Floor of the case study house.

In Figure 4.8, all three floors of the house are presented in 3D projection view. From left to right are ground, first and second floors. The zones are numbered from 1-8.

#	Zone
1	Living
2	Kitchen
3	WC
4	Main Bedroom
5	Shared Bathroom
6	Study
7	Bedroom 2
8	Bedroom 3
9	Ensuite Bathroom

Figure 4.9: Zone numbering reference for Figure 4.8.

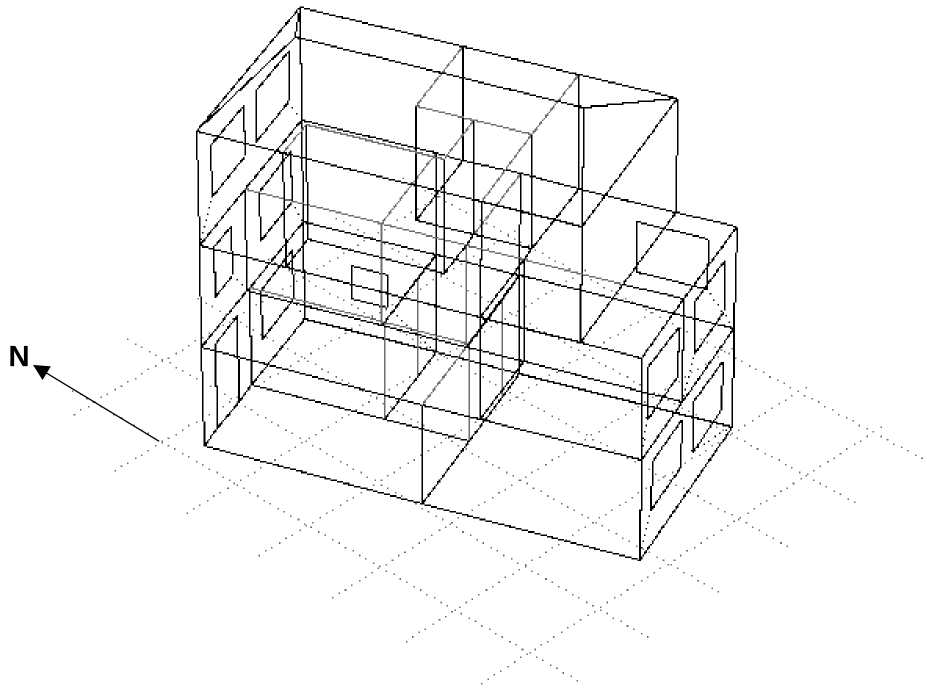

Figure 4.10: ESP-r wire frame model of the house.

The geometry of the house under study excludes furniture as part of the building's form and fabric. Inclusion of such details can introduce ambiguities and would require additional inputs. In ESP-r, furniture can be added with thermal mass assigned to materials which would contributing to heat absorption and release. However, this study does not assess energy usage nor thermal comfort. Furthermore, ESP-r does not account for airflow momentum loss caused by furniture or hinderances in the zone, making it unnecessary to include furniture or other fixtures in the model.

4.7.2 Data and Input Categorisation

Raftery (Raftery et al., 2011) has categorised types of variables into hierarchies based on reliability of the source. For example, a source which is based on direct measurement or observation will be higher in the hierarchy tree. Table 4.7 mentions available data and its source.

This table not only explains the hierarchy of the available data but also aids to form a sequence of modelling investigation as listed in the Modelling Methodology chapter.

Category	Variables	Hierarchy	Source
Weather	Ambient Temperature	2	Met Office
	Wind Speed	2	Met Office

	Wind Direction	2	Met Office
	Ambient CO_2 Concentration	2	Elevated 500ppm instead of 426ppm from NOAA-ESRL Global Monitoring for initial model.
Envelope	Geometry	2	Design Plan/On Site Confirmation
	Construction	2	Design Plan/On Site Confirmation
Ventilation and Infiltration	Airtightness	2	Building Documentation
	Crack Locations	7	Not Available
	Extract Rates	2	Measured Data
	Extract Schedules	2	Occupant's Diary
Indoor Parameters	CO_2	1	Monitoring
	Temperature	1	Monitoring

Table 4.7 : Data Categories, Hierarchies and Sources for the Whole Building Envelope.

In addition to the data inputs presented in the table above; for the main bedroom following data is available.

Category	Variables	Hierarchy	Source
Ventilation and Infiltration	Window Opening	2	Occupant's Diary
	Door Opening	2	Occupant's Diary
Occupancy	Schedules	2	Occupant's Diary
	Metabolic Rates	5	ASHRAE Guide
	Number of Occupants	2	Occupant's Diary

Table 4.8 : Additional Data Categories, Hierarchies and Sources for the Main Bedroom.

4.7.3 Occupancy Translation

To represent occupants in the main bedroom, they are modelled as a load which is a source of CO_2 generation, as detailed in literature review section 2.10.2, occupancy modelling carries high uncertainty. Due to limited information about the occupant's body factors and habits, a generalised metabolic rate for sleeping period is used. However, sensitivity analysis is conducted in the later stage of analysis to highlight the impact of metabolic rates on CO2 concentration output.

ESP-r facilitates the assignment of a schedule for occupancy of a zone which is linked to the zone node as a source of CO_2 generation. ASHRAE Fundamentals Guide (ASHRAE Fundamentals Handbook, 2021) is referred to assign metabolic rates wattage to the internal main bedroom node. For this study the selection of wattage is comparatively straightforward as occupants are sleeping during the simulation study period. However, uncertainties detailed in literature review remain part of the model. Metabolic rate is calculated from 41 W/m^2 (~1 MET) value given in ASHRAE Handbook which also indicates average body area of adult to be 1.8 m^2. For the child it is advised in the same document to be 75% of an adult. Hence a child joins their parents at 5 AM hence the total metabolic rate from 5-7AM is 203 W on the Day 1.

For the Phase II, on the 4th day, occupancy includes 2 adults, and 1 child as well and the same approach is taken to model occupancy on that day. Rest of the days have 2 adult occupancy during sleeping hours.

4.7.4 Weather Data

Real time weather station data is taken in the model as days for simulation study are known for both the phases. Weather data is downloaded from a third-party website which source the data from World Meteorological Association and MADIS weather stations. ESP-r weather file is edited for the simulation period dates for both phases of the study. Ambient temperature, wind speed (m/s) and wind direction in degrees is added to the calendar.

Solar radiation was not included in the analysis as the study is primarily focused on airflow and CO_2 concentration influenced by metabolic activity. These factors are governed majorly by indoor occupancy patterns, metabolic CO_2 generation rates, ventilation rates and external wind conditions (speed and direction). Since solar radiation primarily impacts thermal behaviour and not directly the airflow or CO_2 distribution in the building hence its inclusion was found unnecessary for this specific study.

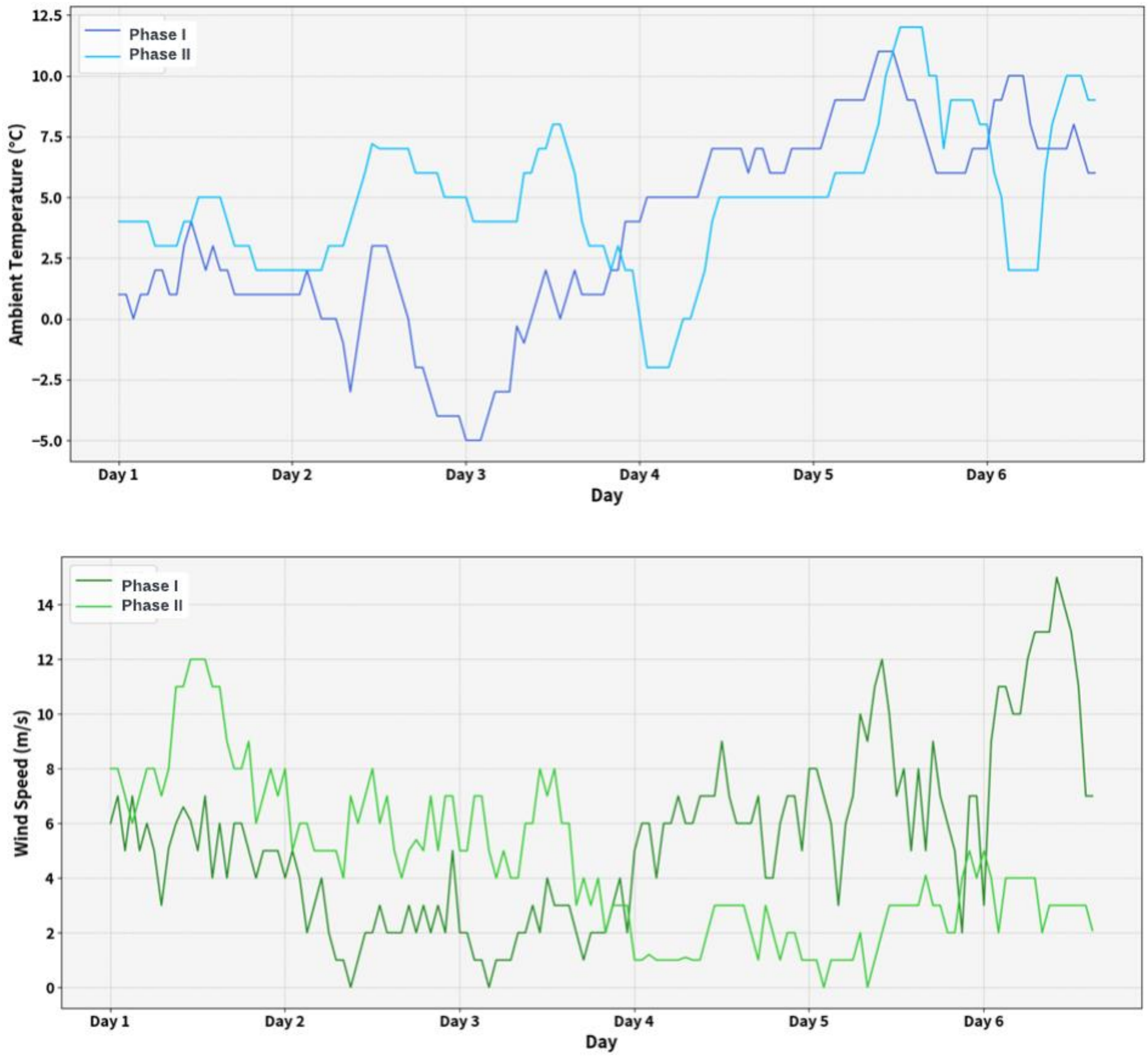

Figure 4.11: Boundary conditions data; ambient temperature (top) and wind speed (bottom) for both phases of the study.

Both phases have varied ambient temperatures and wind speeds. Values for ambient temperature and wind speed for main bedroom occupied hours will be of our interest and further insights will be assessed during the analysis of the solution for indoor CO_2 concentrations, flow through openings and cracks, and pressure difference across these flow paths.

A snapshot of the difference between indoor and ambient average temperatures ($T_{I,amb}$ and $T_{II,amb}$) during the night-time sleeping hours is given in Table 4.9.

Day	Average $T_{I,amb}$ °C	Average $T_{II,amb}$ °C	Difference of Average $(T_{I,bed} - T_{I,amb})$ °C	Difference of Average $(T_{II,bed} - T_{II,amb})$ °C
1	1.16	4.23	19.1	15.86
2	0.33	2.13	25.63	18.68
3	-3.17	4.2	22.06	15.88
4	5	-0.64	14.62	21.53
5	8.58	5.23	11.34	15.13
6	9.62	6.86	11.26	13.99

Table 4.9: Difference of average temperatures between indoor and ambient during night-time sleeping hours for each day of both phases.

Wind rose plots for the both phases are produced showing frequency of wind blowing from the directions for each day. The length of each segment depicts the frequency and colour shading for the segments refers to the legend which shows ranges for maximum wind speed for the direction. The concentric circles show the frequency percentage of the wind.

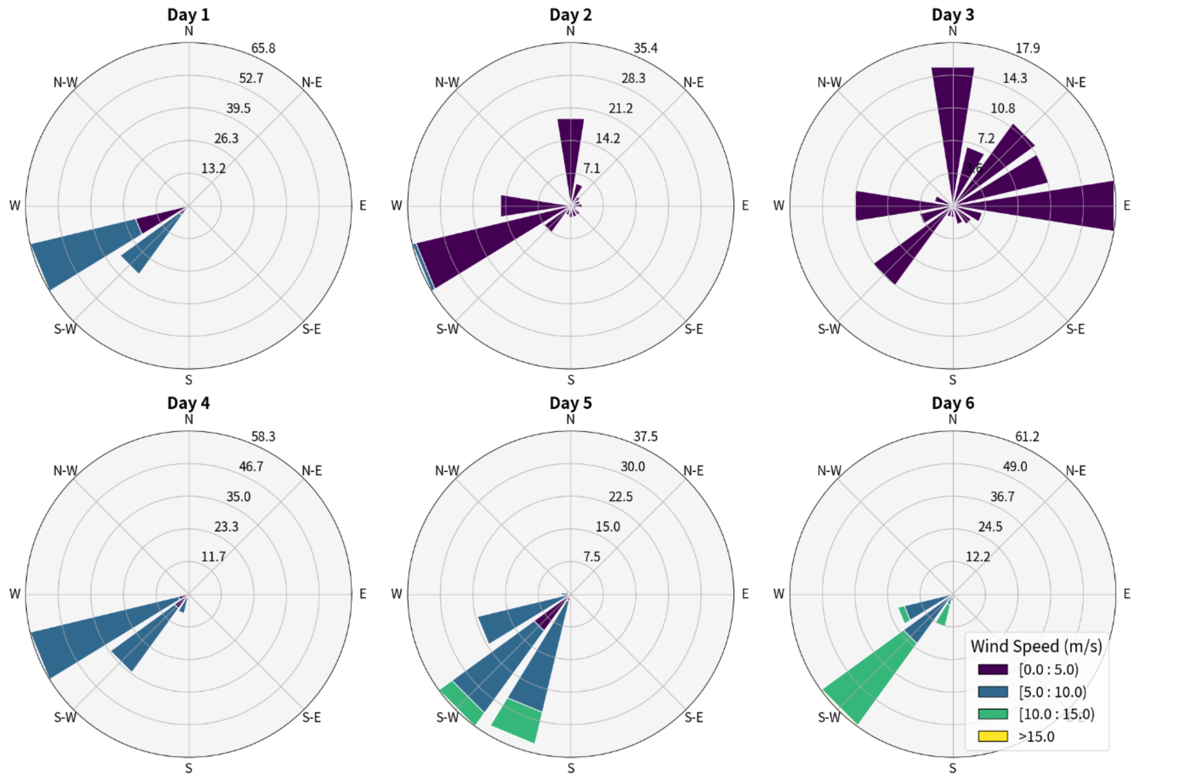

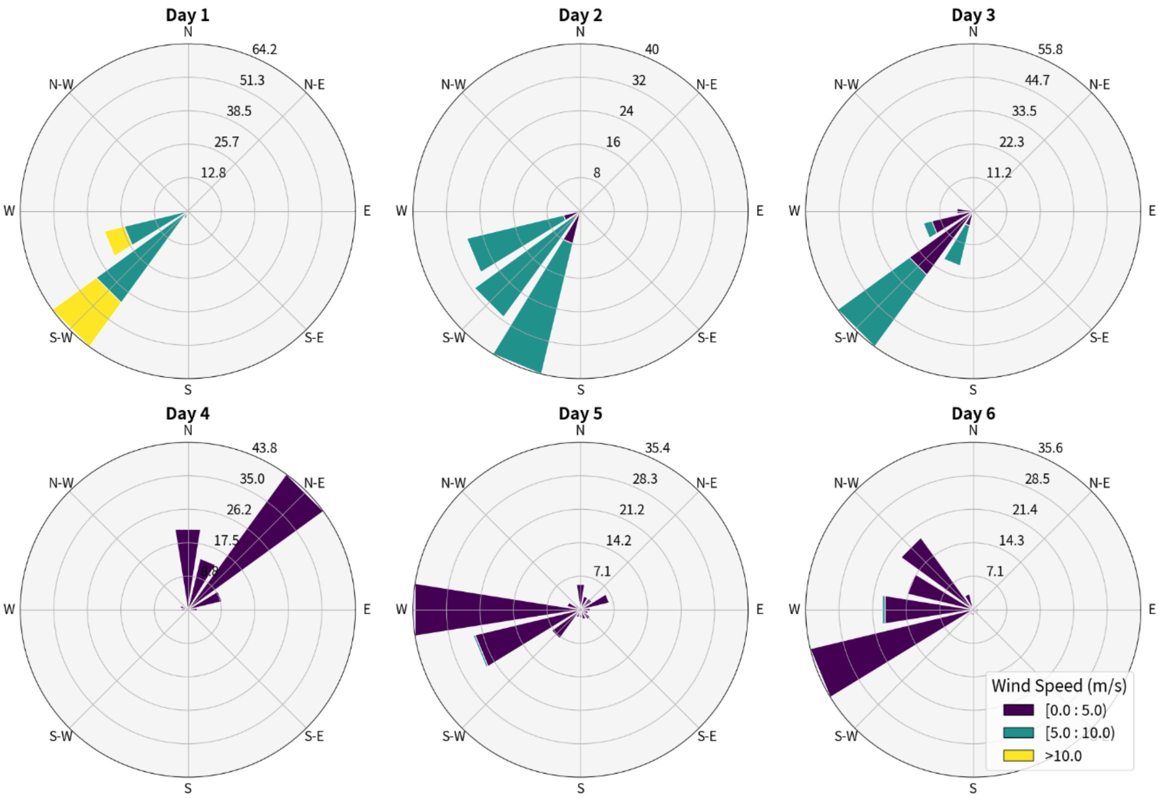

Figure 4.12: Windrose diagrams for both phases of study. Top from phase I and bottom from phase II.

The wind rose graphs for each day from phases I and II help us examine the wind data for the days of study. Phase I analysis shows that the overall average wind speed throughout 6-day period is 5.46 m/s where min speed approaches to zero and maximum recorded is 15 m/s. The predominant wind direction is 240°. Day 6 has highest average wind speed recorded to be 9.54 m/s.

For phase II as we analyse the respective weather data, this shows that average wind speed is 4.69 m/s while there are “no wind” readings, max wind speed is 13 m/s. The dominant wind direction for the 6-day period is 225°. While day 3 has highest average wind speed of 5.98 m/s. The influence of wind direction and speed on the flow is analysed in the section 5.2.11.

To account for an urban train which is determined by the distance between the neighbouring buildings, wind reduction factor is applied to the weather file in the later stage (Iteration 5* Log W). The building is situated in a comparatively dense neighbourhood with structures as high as 8m. Power law wind reduction factor is applied to represent the reduction in wind speed due to urban terrain. Appropriate coefficients from the Table 2.8 are used to find the value equal to 0.58.

4.8 Air Flow Network

The setup of internal and external nodes via flow components represents the flow paths in the case study house. A “simplistic” AFN is introduced with incremental changes to key variables suggested in the Methodology chapter and their impact on the solution is presented via comparing monitored and simulated main bedroom CO_2 concentrations.

For Phase I, three versions of AFN are summarised in the table below.

Phase I Versions	Output	Process Description
AFN – V1	Iteration 5*	Analysis of the solution of iterations 1 to 5 for the modelling of trickle vents and door undercuts.
AFN – V2	Iteration 5* Log W	Analysis of the implementation of wind reduction factor.
AFN – V3	Iteration 5* Log Wd	Introduction of further distribution of zone leakage area to introduce stack pressure due to infiltration, forming Iteration 5* Log W_d.
	Iteration 5* Log Wd (0.9 MET)	Sensitivity analysis of metabolic rates resulting into lowest error for the elevated metabolic rate of 0.9 MET.

The final version of the AFN with output Iteration 5* Log W_d (0.9 MET) is taken as base case for the next phase, Phase II. As explained earlier, Day 3 and Day 5 flow setup includes door and window openings while rest of the days have varied trickle vent openings/closures. Strategies to model door and window opening are discussed later in 5.10. The stage-by-stage process of the simulation and analysis of results would quantify the effect of selection of modelling inputs for the parameters discussed,

For phase II flow conditions, occupancy and weather conditions are changed in the final Iteration 5* Log W_d (0.9 MET).

4.8.1 Nodes, Components and Connections

To introduce the setup of an AFN comprising of the nodes, components and connections, AFN – V1 being the base case model, is taken as example to explain the network. The placement and connection of integral elements remain the same for both AFN - V1 and V2.

External nodes for each floor of the house and every façade are introduced. We have 4 external nodes per floor facing 70-, 160-, 340- and 250-degrees azimuth. The heights of these nodes are at the central distance from floor to ceiling height for each floor.

Internal nodes are also at central point of each zone. External and internal nodes are connected via infiltration cracks and trickle vent openings. Internal nodes are further connected to internal corridor node for each floor and this corridor node is further connected to bathroom/kitchen node via door cracks. This bathroom/kitchen node is then connected to external node via a constant flow extract fan component. A simplistic depiction is presented in Figure 4.13. A connection from one external node to another external node via number of components is shown in a general layout. This sequence of this layout is applicable to all floors of the house.

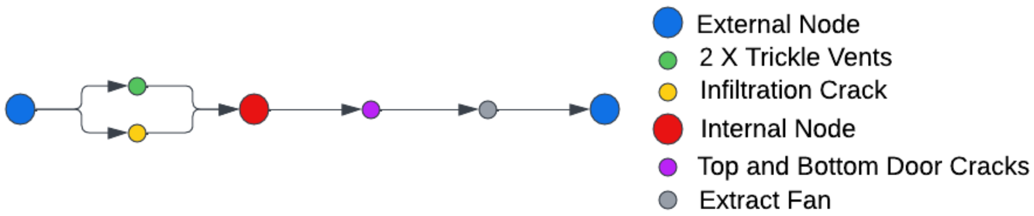

Figure 4.13: A general air flow network connection diagram featuring all flow components.

To elaborate the scheme further, flow network for the first floor of the house is presented in Figure 4.14. Similar setup of network is present in rest of the building's model and the flow components' opening and closures are mentioned previously in the section 4.4.1. The external nodes are represented by blue circles, green circle represents pair of trickle vent openings, yellow circles are infiltration cracks assigned per window fitting. While pink circle represents top and bottom fitting flow paths in a door. Extract fan is represented by a grey circle connected further to external blue node.

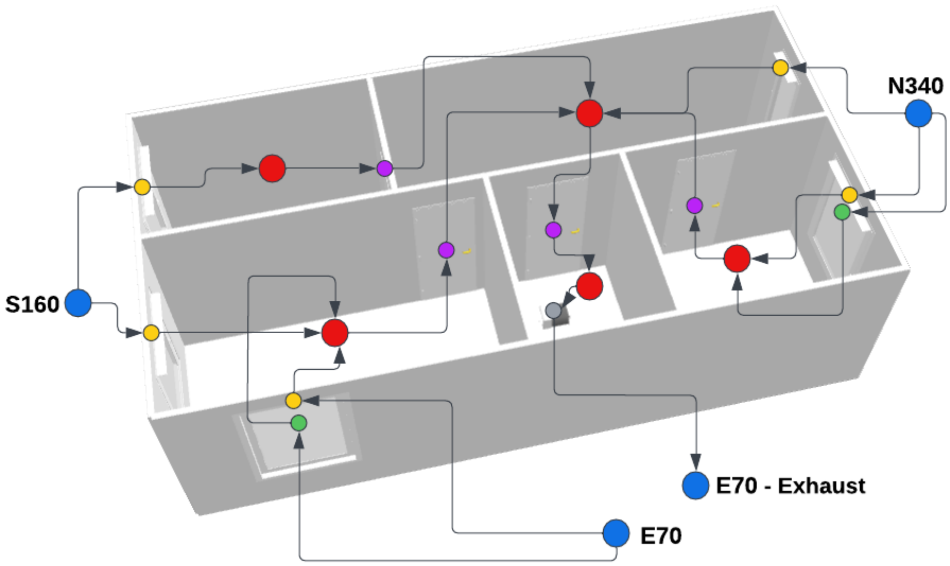

Figure 4.14: AFN (Phase I) for first floor of the case study house. S160, E70 and N340 are azimuth angles facing directions South, East and North.

The connections between nodes does not explicitly show the height difference between them. As the flow components were placed in the model in accordance with actual heights measured during the survey, the same was translated into the model. Figure 4.15 makes it further clear how components were elevated in z-axis in the AFN. Distribution of cracks is implemented in AFN – V3 which is visualised and explained in section 5.4.

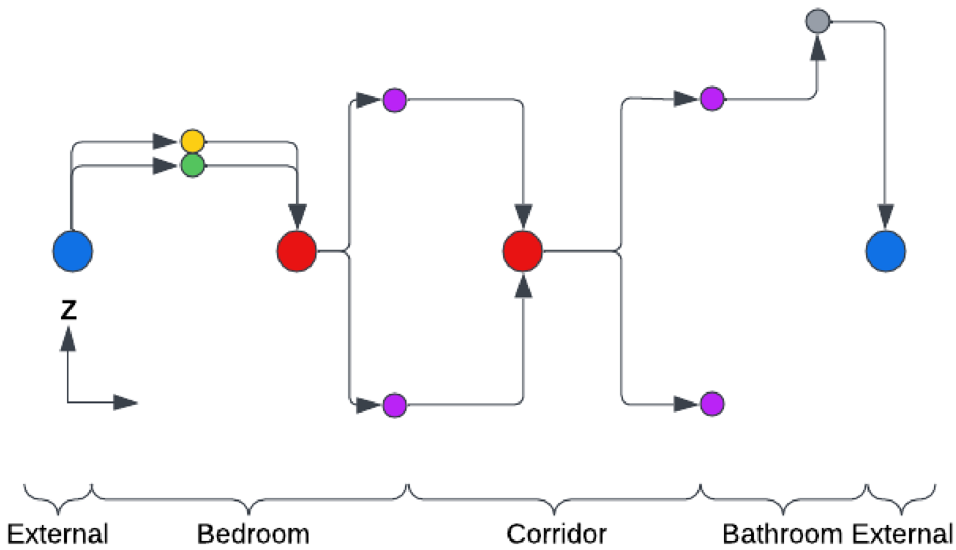

Figure 4.15: Height difference between components and nodes from E70 to E70 – Exhaust.

As it is mentioned, the flow network for the other two floors is setup and the primary linkage is between the stairwells. The flow between each floor, via this zone is explored in the section 5.2.13.

4.8.2 AFN Component Modelling Specifications

Up till this point, the nodal network setup for first two versions of the AFN for the house is explained and visualised using first floor as an example. Now equation set used for the flow solution through the components will be presented in line with the literature review. This section will lay foundation to list the iterations setup for Phase I data, present the results and compute error and effect of each component's representation in the flow solution in the main bedroom.

4.8.2.1 Modelling of Cracks and Their Distribution

First, we will start with the representation of cracks to model infiltration in the house.

For this purpose, information from the house's building documentation is used for after built and pre-occupancy airtightness i.e., 3.89 ach. This value is used to simulate blower door testing of the single zone version of the house model.

The power law model in ESP-r uses height of the crack to calculate n which is determined by the flow regime. As the crack height increases, the flow regime shifts from being fully laminar to fully turbulent. As suggested in the literature review, on average, a developing flow is observed in air tightness tests data which corresponds to the value of n to be between 0.6-0.7 while a more explicit value of 0.65 is also found. This value of n is taken by modelling the crack for a ~2mm height and length of the crack is varied to reach the airtightness number. This area of the crack (length*height) is then distributed per window in the building as a simplistic approach. This practice would eliminate the uncertainty of using unjustified height of the crack component to model infiltration.

Figure 4.16 and Figure 4.17 show the influence of change in flow rate calculation by the crack power law model for varying height and length respectively. A constant pressure difference of 2 Pa is used to visualise the solution. A non-linear relationship between the height and a linear relationship with the length of the crack with the flow rate is shown. This suggests keeping the height constant and dividing the length when distribution of crack flow area is required.

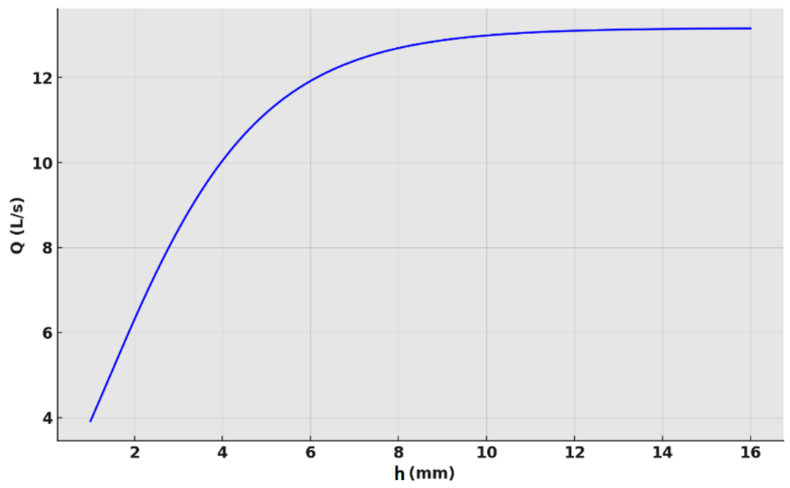

Figure 4.16:Power law relation between flow rate and height of the crack with consistent ΔP=2Pa and L=100mm.

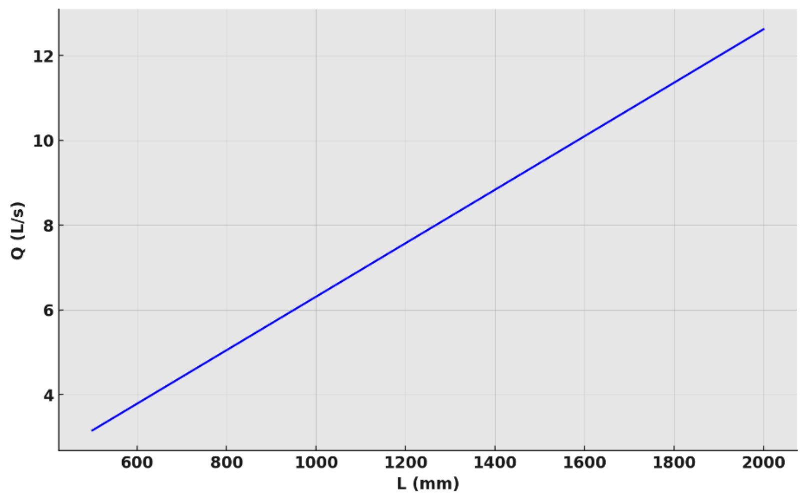

Figure 4.17:Linear relationship between Q and L of the crack with consistent ΔP=2Pa and h=2 mm.

4.8.2.2 Modelling of Trickle Vents

The monitoring survey study confirms the use of the trickle vents in the house – especially consistent opening of 2 out of 4 trickle vents in the main bedroom throughout the Phase I monitoring period. The manufacturer documentation shows effective area of the trickle to be 5000 mm^2 and physically the flow path is divided by a bridge. This divides a continuous slot each measuring height = 13 mm and length of 165 mm (Figure 4.3). As the literature review has suggested that slot shaped openings are often modelled using sharp edged orifice discharge coefficient as well as crack flow model is also used to model any horizontally elongated openings.

For the investigation for trickle vent modelling approaches, when modelling trickle vent as orifice flow component, effective area A_{eff}=0.005 m^2 is taken. While to model with the power law model, height, and sum of length of both slots is used which is suggestive of a simplistic approach and to evaluate the power law model. Later in the investigation, manufacturer testing data is used to estimate n and C values and another comparison with A_{eff} in orifice equation and n and C values in power law equation is presented.

	Approach	Inputs
TV1	Manufacturer's data in orifice equation	A_{eff}=0.005 m^2, C_d=1
TV2	Power law model data in power law equation	n=0.50, C=0.31
TV3	Manufacturer's data in power law equation	n=0.52, C=3.89

Table 4.10: Trickle vents modelling equations and inputs.

4.8.2.3 Modelling of Door Undercuts and Overcuts

Undercuts of all the doors in the house are measured and listed in Table 4.2. However, the door overcuts and any other gaps were not measured. For a detailed model such flow paths should not be excluded hence a crack on the top of the door is modelled with 2 mm height and length in accordance with door's geometry.

To model these door undercuts, as described for modelling of trickle vents, possible approaches using the orifice and power law equations are used to compare the solution. When modelling as orifice flow, default C_d=0.61 is taken along with the A=height of the undercut*0.835m. Same dimensions are used in power law equation to model the passage with an alternative approach. This way the n and C values from the power law model are examined for specific height and length of the door undercut. Later after the comparison of both these approaches and evaluation of the effect of each approach in the flow solution, C_d value of 0.35 (found in literature) is used to compare the flow solution with the approaches in the table below.

The bedroom door undercut modelling equation approach with inputs are given in the table below. BED -UC2 inputs are specified for the height of 16mm and length of 0.835m.

	Approach	Inputs
BED -UC1	Default resistance of the geometry – inputs in orifice equation.	$A_{geometric}$, C_d=0.61
BED -UC2	Power law model data in power law equation	n=0.50, C=0.78
BED -UC3	Higher resistance of the geometry – inputs in orifice equation.	$A_{geometric}$, C_d=0.35

Table 4.11: Main bedroom door undercut modelling equations and inputs.

For bathroom door undercut the height of the undercut is 3mm while length is same as main bedroom door.

	Approach	Inputs
BATH -UC1	Default resistance of the geometry – inputs in orifice equation.	$A_{geometric}$, C_d=0.61
BATH -UC2	Power law model data in power law equation	n=0.46, C=0.61

Table 4.12: First floor bathroom door undercut modelling equations and inputs.

4.8.2.4 Modelling of Extract Fans

Extract fans can be modelled using their system fan curve information as well as a constant flow component. As from the monitoring survey we have onsite measurement data for each extract fan flow rates, the constant flow equation is used by inputting the measured flow rate measurements in l/s.

4.8.2.5 Modelling of Door

In Phase II, occupant diary suggests that instructed opening of door stroke length is 10cm which equates to 7° anticlockwise from its closed position.

$$d_{stroke} = w \sin\theta$$

$$\theta = \sin^{-1}\frac{d_{stroke}}{w}$$

First approach to model this opening area as a bi-directional flow door component with effective area using C_d=0.61. Second approach used to model the door opening is spreading the same effective area on top and bottom of the door frame as a worst-case scenario due to the presence of least resistive area of flow at top and bottom of the door frame. As this approach is deemed to overestimate the flow, a correction factor is presented by Patrick Sharpe (P. Sharpe et al., 2021) which will be applied to form the third approach of modelling the door opening. This correction factor aims to reduce the overprediction of the flow when a bi-directional flow opening is modelled with a pair of orifice equations.

Unidirectional flow opening representation is not advised because of non-uniform pressure profile of the door type openings with considerable height.

On Day 5, door is reported to be opened for 1cm for which no data is available in literature. As a straightforward approach, bi-directional door component is used for the vertical slit formed taking sharp edged orifice C_d of 0.61. As proportion of stroke length is considerably smaller than undercut, a separate flow component (door undercut) is present in flow network between room and the hallway.

4.8.2.6 Modelling of Window Opening

As suggested for the door opening, window is reported to be opened for 0.01m during the phase II of the monitoring study. As stated for the door modelling, same limitation applies to the window opening of such a small stroke length. However geometric area is calculated for the window considering two side triangles and the rectangle formed by the stroke length equating to 0.02m^2. This area with a default C_d of 0.61 is used in the orifice equation.

4.9 Parameters Evaluated

1. **Ventilation flow component modelling:** The comparison of the orifice equation and power law model to model the purpose provided flow components.
2. **Door undercut modelling:** Evaluating unknown modelling parameters by comparing the flow path's discharge coefficient.
3. **Trickle vent modelling:** Using the manufacturer provided specifications to model and compare trickle vents via the orifice equation and power law equation.
4. **Wind reduction factor:** Application of a wind reduction factor to the model to account for wind speed reduction due to terrain roughness and sheltering.
5. **Infiltration modelling:** Impact of the placement of cracks and added stack pressure on the flow solution.
6. **Ventilation effectiveness:** Ability of the interzone acoustic openings to maintain CO_2 concentrations within safe thresholds.
7. **CO_2 generation and metabolic rates:** Evaluating a defined range of metabolic rates and its impact on the model output and on statistical validation of the model.
8. **Opened door modelling:** Comparing three approaches from the literature, firstly, a bi-directional flow component with a standard discharge coefficient, secondly, modelling the same effective flow area via a pair of orifice equations, and finally deploying a correction factor to tackle the expected overestimation.

9. **Window modelling:** A simplistic approach is taken to model the window and sensitivity analysis is conducted for the opening area.
10. **Stairwell flow:** Modelling of airflow between the floors using orifice and bi-directional flow equations and by varying the flow area.

4.10 Sequence of Investigation Design

The sequence of the inputs is chosen based on following justifications based on ranking of the reliability of the available data (Raftery et al., 2011).

- The base case model formation starts with the most accurately known parameters i.e., infiltration rate, trickle vent effective flow area, door undercut geometrical area, extract flow rates and occupancy numbers and schedules ensuring that the model is representative of reality. This reduces the initial uncertainty of the model.
- Following this initial model, literature-informed adjustments are made by incorporating the wind reduction factor. This step refines the boundary conditions input to the model.
- The Next stage – the distribution of cracks (placing them at wind-induced façade's extremities) accounting for infiltration represents the most uncertain feature which is added to the model.
- The final adjustments involve fine tuning of metabolic gains of the occupants to reduce discrepancy between measured and simulated CO_2 levels. Initially, metabolic gains are setup as per findings from the literature. These adjustments are based on the probability of higher activity rates of the occupants which is a highly uncertain parameter. However, a range from the literature is defined and sensitivity study is conducted.

Each stage in the sequence systematically reduces uncertainty by refining model inputs in accordance with the literature review findings. The initial stage focuses on selecting appropriate flow equations and coefficients for trickle vents and door undercuts, tackling the errors from default or unjustified values. Infiltration modelling introduces crack distribution to capture the stack effect with added flow pressure and hence addressing the oversimplifications of single crack infiltration modelling.

The inclusion of a wind reduction factor accounts for terrain and sheltering effects and introduces site specific conditions. By adjusting occupant CO_2 generation rates through sensitivity analyses reduces discrepancies between measured and modelled CO_2 levels, accounting for variability in activity rates. These rates are highly uncertain and hence sensitivity analyses in a defined range are analysed.

4.11 Stage by Stage Modelling Investigation Summary

Each stage in the modelling process is presented in a tabular form (Table 4.13). The first column has listed each iteration of the model. The first row has the AFN inputs. A legend for the superscripts (1-6) and shaded cells is given in Table 4.14.

The Table 4.13 also presents an overview of the modelling guidance suggestions generated via literature review and modelling investigation. The table would be complemented by the text under the headings 4.5 and 4.6 if read independently. The last three rows present modelling inputs for studies targeting ventilation design, overheating and energy usage in the domestic sector. An elaborated presentation of these inputs is presented in a form of the guidance document in Chapter 6.

	Dataset[1]	Process Overview	Process Outcome	Infiltration	Base CO2	Trickle Vents	Bedroom Door Undercut	Bathroom Door Undercut	Wind Reduction[2]	Cracks Distribution[3]	Metabolic Rates	Extract Fans	Door Opening[4]	Window Opening[4]	Interzone Opening	Weather[5]
Iteration 1	Standard/ Normal Conditions	Investigation into Orifice Eqn and Power Law representation of slot shapped purpose provided openings.	Door undercut modelling inputs have high impact on the flow solution.	Design/Actual	500ppm	Orifice Eqn (Manufacturer Data)	Orifice Eqn (Default Cd=0.61)	Orifice Eqn (Default Cd=0.61)	No	No	ASHRAE Fundamentals	Constant Flow Equation	N/A	N/A	No	Local Representative Weather Phase I
Iteration 2						Power Law (Model Data)	Power Law (Model Data)	Power Law (Model Data)								
Iteration 3						Orifice Eqn (Manufacturer Data)	Power Law (Model Data)	Power Law (Model Data)								
Iteration 4						Power Law (Model Data)	Orifice Eqn (Default Cd=0.61)	Orifice Eqn (Default Cd=0.61)								
Iteration 5						Orifice Eqn (Manufacturer Data)	Orifice Eqn (Default Cd=0.61)	Power Law (Model Data)								
Iteration 5*		Devised modelling representations of slot shapped openings.	Lower Cd for door undercut presents better agreement with the monitored data.		Minimum from Monitored Data	Power Law (Manufacturer Data)	Orifice Eqn (Cd=0.35)	Power Law (Model Data)								
Iteration 5* Log W		Implementation of Wind Reduction Factor	Wind reduction factor has high influence on the flow rate solution.						Yes							
Iteration 5* Log W IZ[6]		Implementation of Purpose Provided interzone openings to assess ventilation performance	Interzone openings has the capability to assist in lowering peak CO2 concentrations.								Elevated				Yes	
Iteration 5* Log Wd		Implementation of further distribution of cracks	Distribution of cracks cause higher prediction of airflow.							Yes					No	
Iteration 5* Log Wd (0.9MET)		Senstivity analysis of metabolic rates concerning CV(RMSE)%	Elevated rate of 0.9 MET gave low error hence used as base for Phase II modelling.													
Iteration 5.1* Log Wd (0.9MET)	Interventional	Analysis of three different appraoches to model door opening	Bi-directional flow component gave best fit results. Also highlights the requirement of aerodynamic data for a smaller opening of the flapped mecahnism.				N/A						Bi-Directional Flow Eqn (Default Cd)			Local Representative Weather Phase II
Iteration 5.2* Log Wd (0.9MET)													Pair of Orifice Eqn (Default Cd)			
Iteration 5.3* Log Wd (0.9MET)													Pair of Orifice Eqn (Default Cd)+Correction Factor			
Iteration 5.4* Log Wd (0.9MET)		Modelling of combination of very slight openings of door and window.	Combination of door and window opening modelling produced large errors which are tackled by senstivity analysis of opening areas. Highlights the need of design data.				Orifice Eqn (Cd=0.35)						Bi-Directional Flow Eqn (Default Cd)	Orifice Eqn (Default Cd)		
Ventilation Design	CIBSE TM59			Design/Actual	Local Weather Station	Orifice Eqn/Power Law (Manufacturer Data)	Orifice Eqn (Cd=0.35)	Orifice Eqn (Cd=0.35)	Yes	No	Elevated (0.9 MET)	Constant Flow Equation	SEAMS	SEAMS	N/A	TMY
Overheating	CIBSE TM59			Design/Actual	Local Weather Station	Orifice Eqn/Power Law (Manufacturer Data)	Orifice Eqn (Cd=0.35)	Orifice Eqn (Cd=0.35)	Yes	No	Elevated (0.8 MET)	Constant Flow Equation	SEAMS	SEAMS	N/A	DSY
Energy Usage	CIBSE TM59			Design/Actual	Local Weather Station	Orifice Eqn/Power Law (Manufacturer Data)	Orifice Eqn (Cd=0.35)	Orifice Eqn (Cd=0.35)	Yes	Yes	Elevated (0.8 MET)	Constant Flow Equation	SEAMS	SEAMS	N/A	TMY

Table 4.13: Summary table for stage-by-stage modelling investigation.

	Iterative Investigation for Trickle Vents and Door Undercuts (AFN – V1).	1	Occupants' Diaries Data for the Main Bedroom from Standard (Phase I) and Interventional (Phase II) conditions.
	Standard for Guidance Input	2	Study of Impact of Wind Reduction Factor (AFN – V2).
	Use of higher CO_2 metabolic rate via its sensitivity analysis.	3	Study of Impact of Distribution of Cracks (AFN – V3).
	Application of Interzone Openings to Evaluate their Efficacy for Bedroom Ventilation.	4	Flow Setting from the Occupants' Diary.
	Iterative Investigation for Door	5	Weather from Local Weather Station as per Phase I/II Monitoring Dates.
	Door and window opening area sensitivity analysis.	6	Investigation to assess the ability of interzone openings to reduce bedroom CO_2 concentration. Presented in the section 5.8.

Table 4.14: Legend for the summary table.

4.12 Flow of Investigation Design

A stage-by-stage summary presented in the previous section is now presented in a form of flow chart which explains the iterative process of the AFN modelling. It elaborates how the literature review and monitoring data set from the phase I and phase II are used to feed into different stages of the modelling study. Each version of the model shows the purpose and resulting outputs.

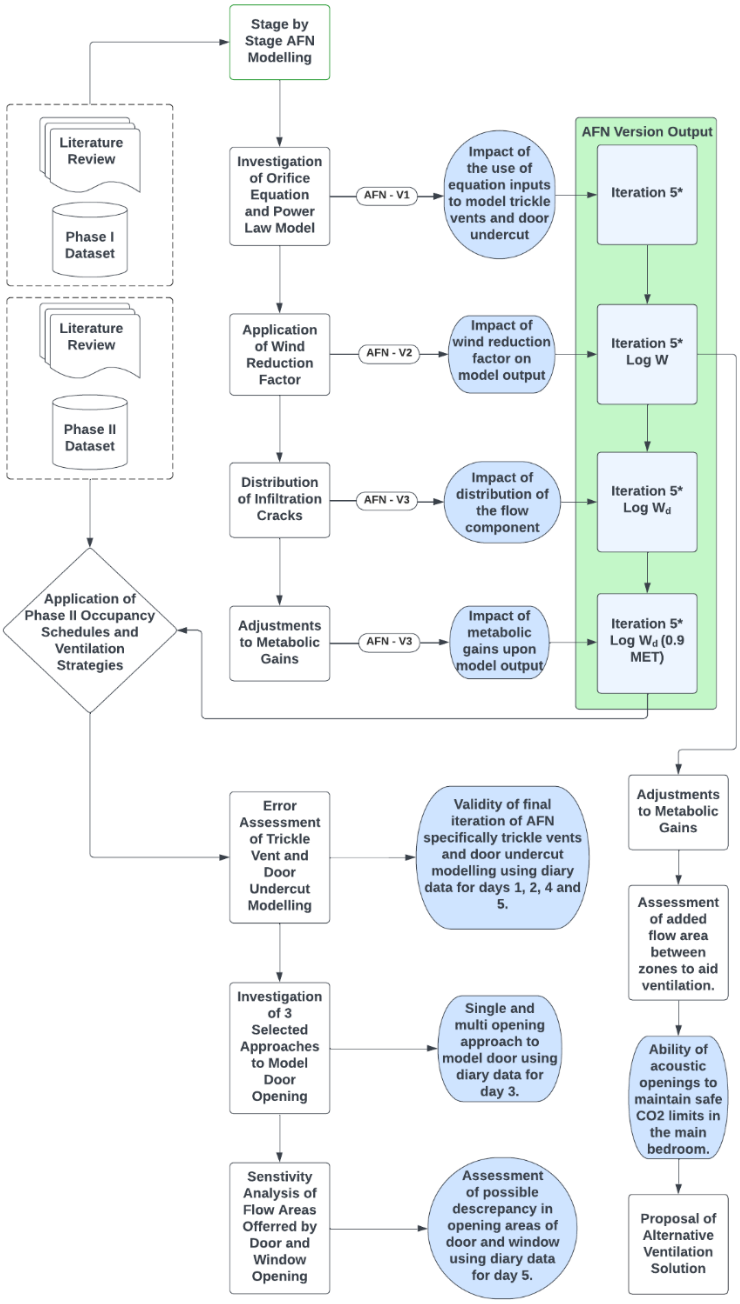

Figure 4.18: Modelling methodology.

Chapter 5 Modelling Investigation Study Results

5.1 Introduction

Building on the literature review which deals with the importance of ventilation for adequate IAQ for the occupants, the current design of domestic buildings and their translation into simulation models; this chapter will present a modelling case study to implement possible modelling approaches and evaluate their accuracy in AFN modelling.

Modelling of a real life monitored case study can provide a test bench to suggest an effective ventilation design. For this purpose, it is important to present a model with minimal inaccuracies concerning CV(RMSE)%. Possible discrepancies in the modelling output can be dealt with careful consideration of the modelling inputs. During this process, it is not only aimed to reduce the error (discrepancy in CO2 concentrations) but also provide insights which would benefit modellers to take informed decisions to undertake an AFN study.

Minimising inaccuracies would include the addressing of potential errors in the input parameters, boundary conditions, modelling assumptions, and occupant behaviour. Possible errors from simplified modelling of infiltration rates, airflow models, or variability in occupant activity levels are mitigated through sensitivity analysis, model calibration, and the use of monitored data. Adjustments, such as incorporating wind reduction factors and refining assumptions about flow coefficients, distribution of cracks would help to align the model with the dataset for accuracy.

The input specifications of the model come from the case study data of a house from a monitoring survey conducted by Sharpe (T. Sharpe et al., 2019) to assess effectiveness of ventilation in houses where inflow relies on trickle vents (as intake), door undercuts/openings (flow path) and extract (outlet) in wet rooms. The study confirms that the ventilation design in question is insufficient to maintain indoor CO_2 concentrations under suggested threshold.

As a large proportion of the time spent in domestic indoors is in the bedroom, sleeping; the focus of this study is night-time CO_2 concentration levels in the main bedroom. Furthermore, analysis specific to night-time bedroom concentrations from the monitoring survey is presented and linked with literature to confirm that the dataset from the monitoring survey study is appropriate for our modelling and subsequent design study.

From the larger data set of 41 houses, the monitoring survey study selected one case study house for detailed monitoring based on worst-case CO_2 concentrations. The suitability of this selection is inspected later in the context of our study.

Modelling inputs are extracted from the monitoring survey data available and categorised as:

- Location of the building.
- Layout and dimensions.
- Specifications and performance of flow components.
- Night-time bedroom flow conditions and occupant loads.

As mentioned earlier, the monitoring study has two phases. The first three elements of the data listed above remain the same for both phases, but the last element concerned with flow conditions in the bedroom and occupancy schedules change. The first phase (Phase I) is free-floating while second phase is interventional (concerning air flow settings and occupancy schedules). These interventions are discussed later in this chapter.

As a starting point of modelling, operational flow components and occupancy gains as per Phase I diary are modelled. At this stage, with least complexity to the model, the modelling of trickle vents and door undercuts is studied. Later, stage by stage complexity is added in the light of literature review findings. Application of wind reduction, distribution of cracks for infiltration and adjustments to occupancy metabolic gains are checked for their impact on solution.

An additional investigation of ability of interzone openings to reduce CO_2 concentration during occupancy in the main bedroom is presented. These openings from the literature are modelled one by one. This investigation is based on version of the model that incorporates non-distributed cracks with wind reduction factor as it is deemed to provide more conservative (lower) estimation of modelled CO_2 thereby offering a rigorous test of efficacy of these openings.

The final model iteration is then subjected to a varied flow settings i.e., opening/closure of trickle vents, opening of door and window, occupancy schedule and representative weather conditions. The evaluation of error % with the implementation of a varied operational and boundary conditions on the final iteration shows robustness as a base case. Additionally, the modelling of door and window opening is conducted as Phase II diary suggests opening of these two components during night-time sleeping hours. This process will allow to explore different modelling strategies of modelling door and window openings and their limitations.

5.2 Iterative AFN Results – Phase I – AFN – V1

The approaches defined for trickle vents and door undercuts in the last section are assessed for their impact on the flow solution. For this purpose, CO_2 solution from 5 iterations is analysed and compared with each other first through statistical analysis and later via physical analysis.

The nodal setup in the main bedroom suggests that the E70 node is connected to the room node via opened trickle vents. Bedroom node is then further connected to hallway node via a door undercut which is then connected to bathroom node via a bathroom door undercut. This bathroom node then connects with E70 – Exhaust outdoor node. In the described part of the network, trickle vent and door under modelling approaches presented in the last section are evaluated.

Iteration 1 to Iteration 4 models trickle vents and door undercuts in different combinations of representative flow equation. It is important to note that where orifice equation for trickle vent is used, effective area is modelled and where power law is used, geometric inputs are used. These geometric inputs are then used by power law model to approximate n and C values. For door undercuts, where orifice equation is used, C_d=0.61 is the input in the equation while in the power law representation of the undercuts, geometric data is used to approximate for the n and C values.

The 5th iteration is suggestive of the devised modelling approach. According to this approach, any flow area with height of ≥10mm should be modelled with the orifice flow equation. Hence the bedroom door undercut is modelled with orifice equation and bathroom door undercut is modelled with power law. Known effective area is used in modelling the trickle vent and approximation of C_d=0.61 is used to model the bedroom door undercut.

All 5 iterations are compared against each other via pairwise statistical analysis and a further physical analysis of the flow is undertaken in which alternative manufacturer flow testing data is used to model trickle vent using power law and using C_d=0.35 for bedroom door undercut. This further analysis forms alternative version of Iteration 5 labelled as Iteration 5*.

	Trickle Vents	**Room Door Undercut**	**Bathroom Door Undercut**
Iteration 1	TV1	UC1	UC1
Iteration 2	TV2	UC2	UC2
Iteration 3	TV1	UC2	UC2
Iteration 4	TV2	UC1	UC1
Iteration 5	TV1	UC1	UC2

Table 5.1: Inputs in the iterations for trickle vents and undercuts.

5.2.1 Indoor Temperature

The Phase I indoor temperature for main bedroom is modelled using temperature set point method in ESP-r. Sensing on temperature at bedroom node is setup and heating period times are input in accordance with measured temperature graph.

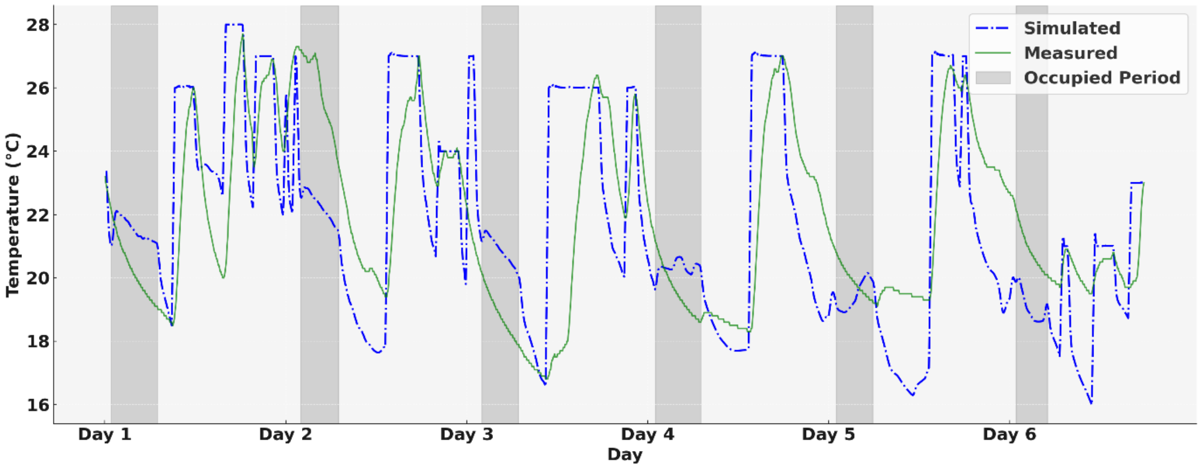

Figure 5.1: Measured and simulated indoor main bedroom temperature readings with highlighted occupied periods each night.

The Night-time occupied period is used for the calculations of CV(RMSE) and error of 9.77% remains above the acceptable range of 5% (Paliouras et al., 2015). However for a sub-hourly data, error % in the range of 10-20% is also found acceptable in the literature (O'Donovan et al., 2019). Any how a further check for difference in ambient and indoor temperatures for average measured and simulated values presented in Figure 5.2. Difference between bedroom node temperature and ambient temperature is graphed for $Avg\ T_{mb,m} - Avg\ T_{amb}$ and $Avg\ T_{mb,s} - Avg\ T_{amb}$; where:

$$Avergae\ Main\ Bedroom\ Indoor\ Temperature\ (Measured) = Avg\ T_{mb,m}$$

$$Avergae\ Main\ Bedroom\ Indoor\ Temperature\ (Simulated) = Avg\ T_{mb,s}$$

$$Avergae\ Ambient\ Temperature = Avg\ T_{amb}$$

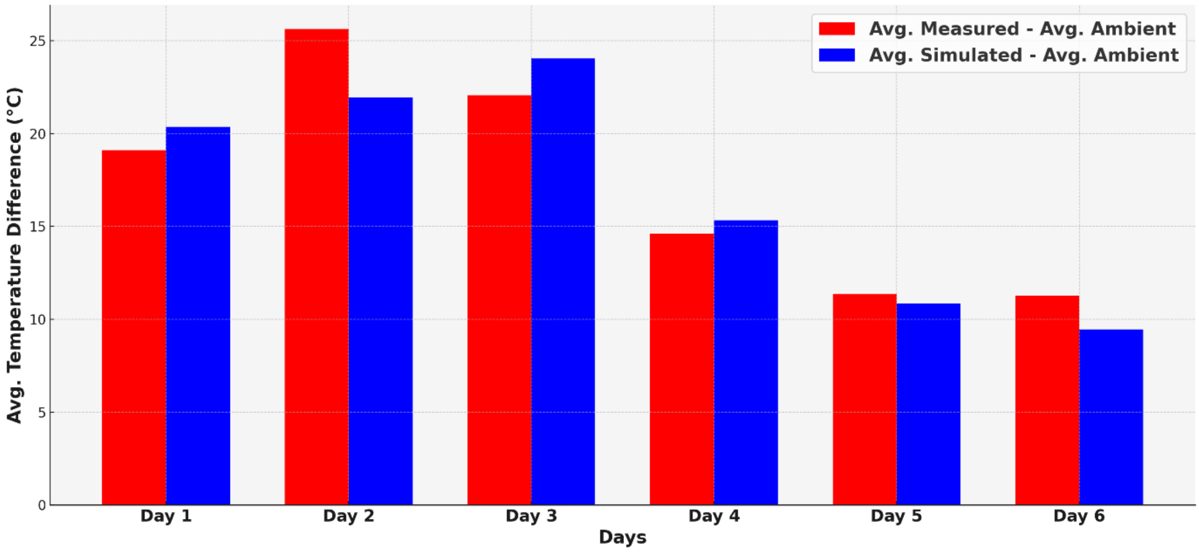

Figure 5.2: Difference in average of monitored and simulated temperatures during night-time sleeping hours with average ambient temperature.

As purpose of this study is not concerned with overheating of the living space, the small difference in the average measured and simulated ambient temperature is deemed sufficient.

5.2.2 Main Bedroom CO_2 Concentrations Results

Simulation outputs from iteration 1 to 5 are graphed below with measured CO_2 concentrations.

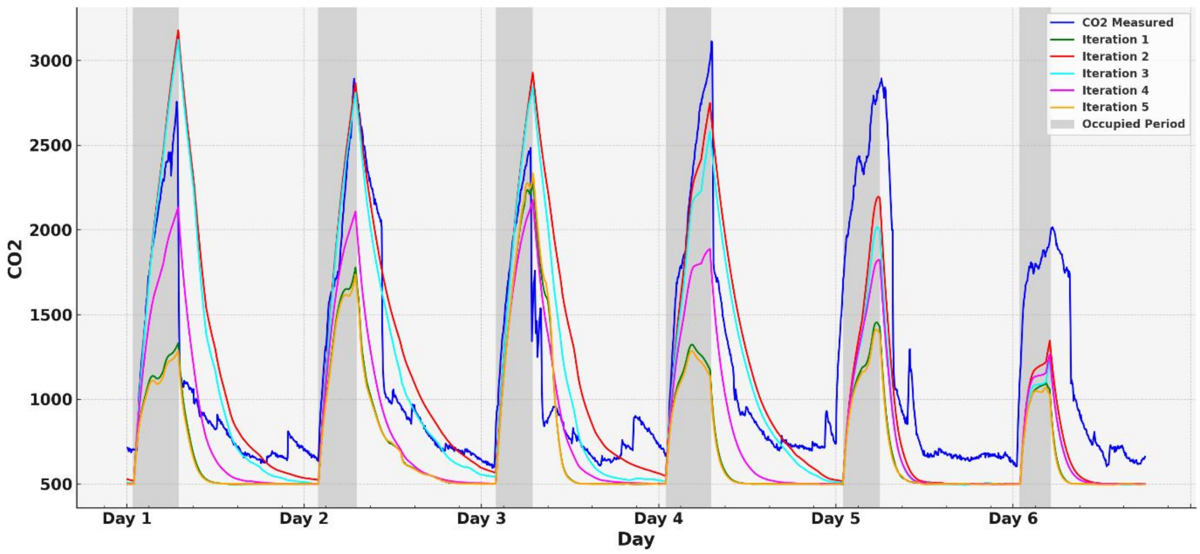

Figure 5.3: CO_2 measured vs CO_2 simulated as an output from different iterations.

First step is visual inspection of the Figure 5.3. It is evident that different iterations have varied solution for bedroom CO_2 concentrations. As the next step CV(RMSE) for each iteration during sleeping/occupied period is calculated for each day and each iteration, and then statistical analysis will be conducted to evaluate difference between iterations for the solution. As indicated in the literature review, CV(RMSE)% error under 25% is deemed suitable.

Day	Iteration 1	Iteration 2	Iteration 3	Iteration 4	Iteration 5
1	48.76%	11.42%	10.25%	20.89%	49.69%
2	31.34%	9.46%	9.26%	20.30%	32.73%
3	14.04%	18.87%	17.85%	16.03%	13.99%
4	46.07%	9.65%	14.43%	27.81%	52.50%
5	51.87%	37.72%	41.19%	43.25%	52.95%
6	44.40%	38.14%	42.30%	40.11%	44.59%

Figure 5.4: CV(RMSE) percent error for each day per iteration.

The statistical error indicates the predictive accuracy of each iteration with respect to the monitored data. However, we would like to analyse the effect of change in representation of a flow component using different equations i.e., power law and orifice equation. For this purpose, a statistical and physical approach is taken to assess the quantitative impact of the entailed coefficients. For example, Iteration 2 and 3 are closer in solution, this is due to change in modelling equation of trickle vents. This is further explored via physical analysis in 5.2.10.

To proceed with the pairwise analysis of these iteration CO_2 solutions, average and peak values are tabulated for comparisons. This comparison is per day for the average and peak values of measured and simulated CO_2 and overall CO_2 average for the whole 6-day period.

The table highlights that there is varied difference in averages and peak values. This difference is checked for significance and later effect size pairwise comparison between iterations followed by inspection of input coefficients of respective equations.

Day	Metric	Measured	Iteration 1	Iteration 2	Iteration 3	Iteration 4	Iteration 5
Day 1	Average	1869.41	1082.99	2007.12	1981.37	1538.39	1057.26
	Peak	2757.2	1331.53	3178.87	3124.47	2133.13	1287.47
Day 2	Average	1846.2	1356.35	1881.46	1844.81	1546.48	1332.68
	Peak	2893.8	1778.6	2868.33	2812.47	2108.53	1737.6
Day 3	Average	1856.36	1635.37	1914.26	1890.9	1577.92	1647.9
	Peak	2484.8	2248.13	2898.47	2821.4	2161.33	2285.4
Day 4	Average	1864.91	1140.1	1894.3	1792.15	1502.8	1111.03
	Peak	2773.7	1323	2750.07	2582.27	1888.07	1285.8
Day 5	Average	2367.64	1137.53	1478.87	1389.53	1337.08	1113.03
	Peak	2839.8	1454.27	2196.13	2016.4	1823.67	1413.2
Day 6	Average	1731.58	967.05	1078.19	1003.74	1042.05	952.49
	Peak	1961.1	1097.13	1346.73	1234.47	1263.27	1069.33
Overall	Average	1922.6833	1219.8983	1709.0333	1650.4167	1424.12	1202.3983

Table 5.2: Average and maximum CO_2 concentrations (ppm) for measured and simulation solution across iterations.

Prior to proceeding with statistical analysis, average CO_2 concentration for the whole 6-day period is compared for selected pairs to inspect the direction of solution relative to measured data in Figure 5.5. It is inferred that bedroom door undercut has largest impact for its representative equation. Trickle vent has a substantial impact while bathroom door undercut has very small impact. The upcoming analysis will further quantify this impact and present a pairwise comparison of these iterations.

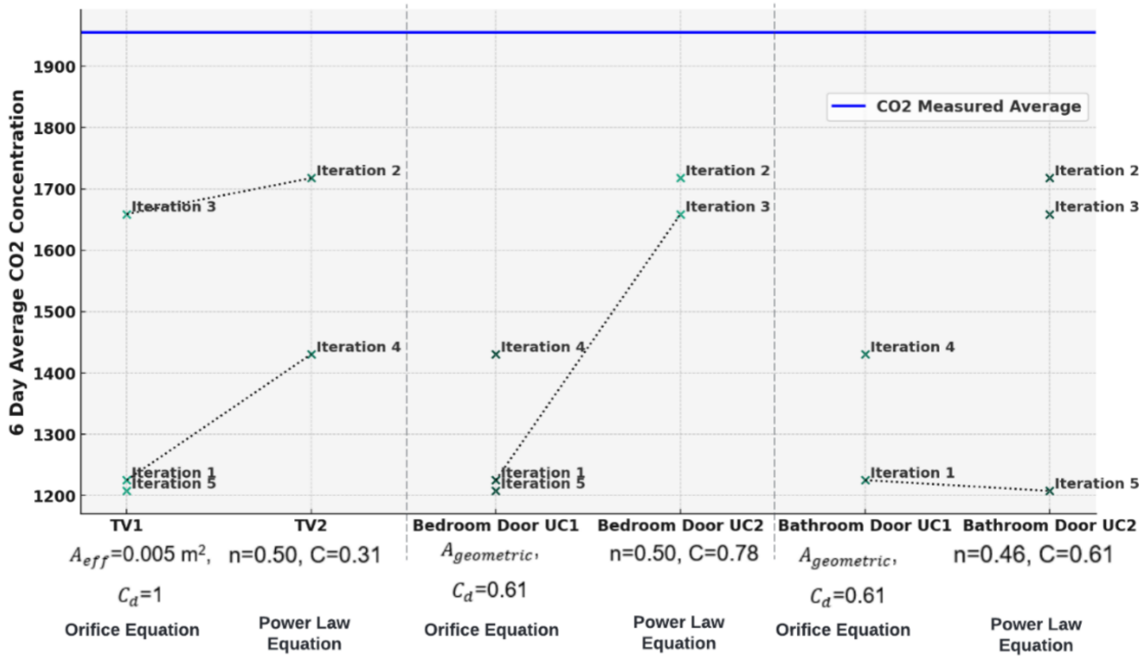

Figure 5.5: Overall 6-day CO_2 average (ppm) comparisons for measured, each iteration, and component modelling.

5.2.3 Statistical Difference between Iterations

To understand the variations in the simulated CO_2 levels across 5 iterations, a systematic statistical analysis for which a methodology is presented in section 2.12.6 is conducted. This part of the thesis focuses on analysing the statistical differences between simulated CO_2 concentrations due to varying representative equations/inputs of the flow components and paves the way for further analysis to find best suited equations to model these flow openings.

This analysis is conducted in following steps:

1. A visual inspection of the simulated CO_2 concentrations to confirm difference between the solutions of iterations.
2. The evaluation of the distribution of data to conduct suitable variance analysis.
3. The confirmation of the statistical difference between CO_2 concentrations solution by iterations.

4. A pair wise comparison of the iterations for their p-values to understand the statistically significant difference between iterations.
5. A pair wise evaluation of each iteration of simulation study informs about effect size and direction of the difference.

This exercise would allow appropriate pairwise evaluation of difference in means of iterations of AFN and confirm the significance of use of certain set of equation for the solution. This would further provide the grounds to start with the physical analysis of the flow solution concerning alternative coefficient inputs.

5.2.4 Visual Inspection of the results

Before starting with a statistical analysis of the data, first step is to graphically visualise output from all 5 iterations so to relate statistical numbers with our graphs which would further confirm the calculations of the effect of each iteration with respect to the other. Figure 5.3 shows time series plot of all the 5 iterations.

The figure shows that iterations 1 and 5 have low difference in predicting CO_2 values which is also the case when we compare iterations 2 and 3. The comparison of 1 and 5 infers that the bathroom door undercut has least effect on the concentrations while comparison of 2 and 3 suggests modelling of trickle vent as orifice or power law has a lower impact on the results. This analysis is further detailed in the upcoming sections.

5.2.5 Probability distribution Check

The visual inspection and CV(RMSE) calculations suggests different flow solution via different set of representative equations for the flow components. To quantify the difference between the iteration outputs, in a pairwise comparison, variance analysis in conducted. The choice of the analysis depends upon the probability distribution of the data. ANOVA test is suggested for the data having normal distribution while Kruskal-Wallis test is non parametric alternative to ANOVA test and does not assume data to be normally distributed. For this purpose, the histograms are plotted for each iteration (Figure 5.6) and the normality test is conducted which would confirm a non-normal distribution of the data.

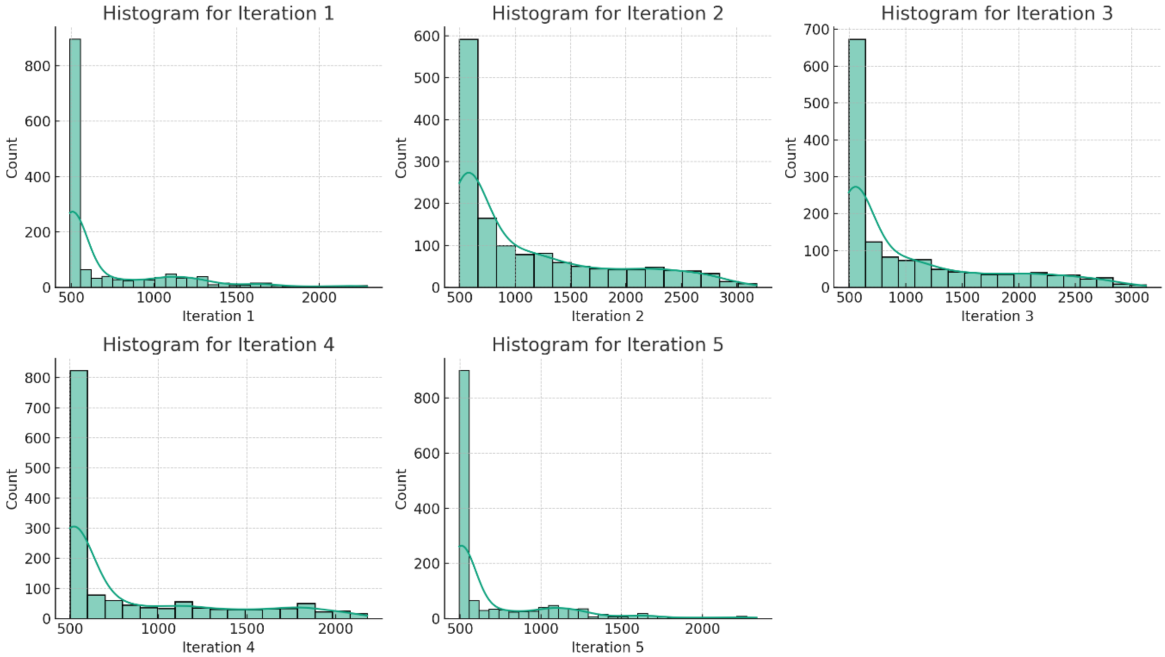

Figure 5.6: Histograms for 5 iterations showing skewed distribution of CO_2 data.

The Shapiro-Wilk test of normality calculates W statistic which ranges from 0-1; a value less than 1 indicates non-normality of the data. This null hypothesis of this test is that the data is normally distributed. Hence the distance of W-values from 1 shows the probability of non-uniformity of data.

$$W = \frac{(\sum_{i=1}^{n} a_i x_i)^2}{\sum_{i=1}^{n} (x_i - \bar{x})^2} \tag{5.1}$$

Where x_i are ordered sample values, $\bar{x}$ is sample mean and a_i constant from reference tables and number based on sample size.

	Iteration 1	Iteration 2	Iteration 3	Iteration 4	Iteration 5
W-Statistic	0.67	0.82	0.78	0.72	0.66

W-statistic values confirm non normality of the data and also confirms the visual inspection of the graph suggesting similarity between 1 and 5; and 2 and 3 while a unique distribution for iteration 4. The lesser difference in W-static between iterations is due to impact of very similar values on day 6.

5.2.6 Kruskal-Wallis Test

Given the non-normality of the data, Kruskal-Wallis test is then adopted to confirm statistical difference between the iterations. As compared to ANOVA, rather than comparing difference of means for each group, it compares the mean ranks of the groups. For this purpose, H-

Statistic is calculated using the equation below. As a first step, all data points are converted into one group and sorted in ascending order and ranks are assigned.

$$H = \frac{12}{N(N+1)} \sum_{i=1}^{g} \frac{R_i^2}{n_i} - 3(N+1) \quad 5.2$$

Where N is total number of observations across all groups, g is total number of data groups, 5 in our case, R_i is the rank sum of group i.

The table below confirms the negation of null hypothesis for Kruskal-Wallis test which states that mean ranks of the group are same.

	Iteration 1 (R_1)	Iteration 2 (R_2)	Iteration 3 (R_3)	Iteration 4 (R_4)	Iteration 5 (R_5)
Rank Sum	4060486.5	6489091	6057831.5	5246488.5	4069702.5

Given that $N = 7200$ ($n_i = 1440$ observations per iteration), H-statistic is computed to be 803.75 with p-value approaching zero and this rejects the null hypothesis. As the H-statistic is a large number with close to zero p-value, this confirms significant statistical difference amongst two or more iteration outputs.

5.2.7 Post-hoc Dunn-Bonferroni Test

Confirming the significant statistical difference between the iteration groups, it is deemed important to calculate p-values in a pair-wise analysis. This would enable us to directly compare one iteration with another to know significant statistical difference between the iterations.

$$Z = \frac{Observed\ Mean\ Rank\ Difference}{Standard\ Error\ of\ Mean\ Rank\ Difference} \quad 5.3$$

This standardised Z value is used to compute probability from available standard tables which provides p-value for each pair-wise comparison. Lower p-values (darker shade) are closer to 1 which suggest a non-significant differences between the pairwise iterations while smaller p-value (p<0.05) suggests a significant difference. It is however important to note that the p-value from this test does not indicate the effect size rather it indicates the probability of observing the data under the null hypothesis.

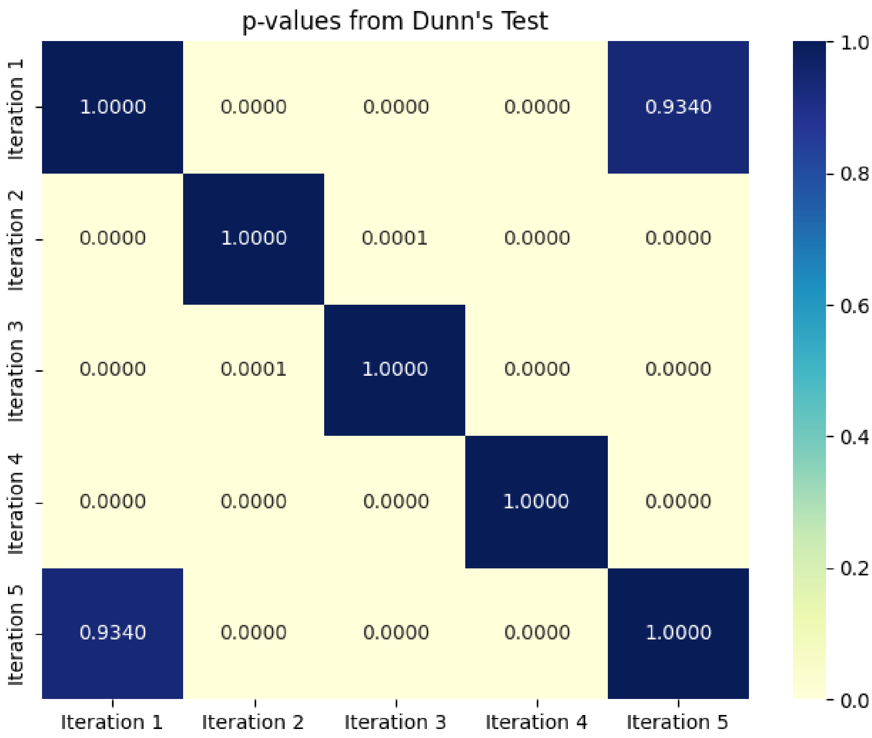

Figure 5.7: Pairwise matrix of p-values from Dunn's test confirming significant statistical difference between iteration solutions except for iteration 1 vs 5.

As evident from the heatmap Figure 5.7, iterations 1 and 5 does not show significant statistical difference. This is because the third component i.e., bathroom door undercut has minimum effect on the room's CO_2 concentration levels. Further evaluation of effect size and direction for the same pairwise comparison is required to explain the significance of solution of one equation over the other in these pairs.

5.2.8 Cohen's d Evaluation of Effect Size and Direction

After confirming the significant difference in the solution for CO_2 concentrations between iterations, Cohen's d evaluation is presented to measure the magnitude of difference in a pairwise comparison. This would present practical significance of use of power law vs orifice equation in AFN. The relation for Cohen's d is given by:

$$d_c = \frac{M_1 - M_2}{\sqrt{\frac{{SD_1}^2 + {SD_2}^2}{2}}} \tag{5.4}$$

Where M_1 and M_2 are the means of two groups being compared, SD_1 is the standard deviation for group 1 and SD_2 is standard deviation of group 2. Numerator is difference of means while denominator is the pooled standard deviation.

General interpretation of d-number is $0 \leq |d| < 0.2$ being a small effect, $0.2 \leq |d| < 0.5$ a medium effect while $0.5 \leq |d| < 0.8$ a medium-large effect and $|d| \geq 0.8$ a large effect. While for the direction, d>0 means the first group has higher mean than the second while d<0 indicates the second group has a higher mean than the first. Heatmap is presented for whole simulation period of 6 days. The heat map presented include one way comparison of Cohen's d number which implies that first iteration number should be smaller than the second iteration to look for the Cohen's d number. For example, the heatmap gives the value for the comparison of Iteration 1 with iteration 5 $d_{c(1,5)}$ but if we want comparison for 5 with 1 $d_{c(5,1)}$ we will need to multiply the Cohen's d with -1. Hence:

$$d_{c(1,5)} = -d_{c(5,1)}$$

Figure 5.8 presents Cohen's d values for pairwise comparison of the 5 iterations.

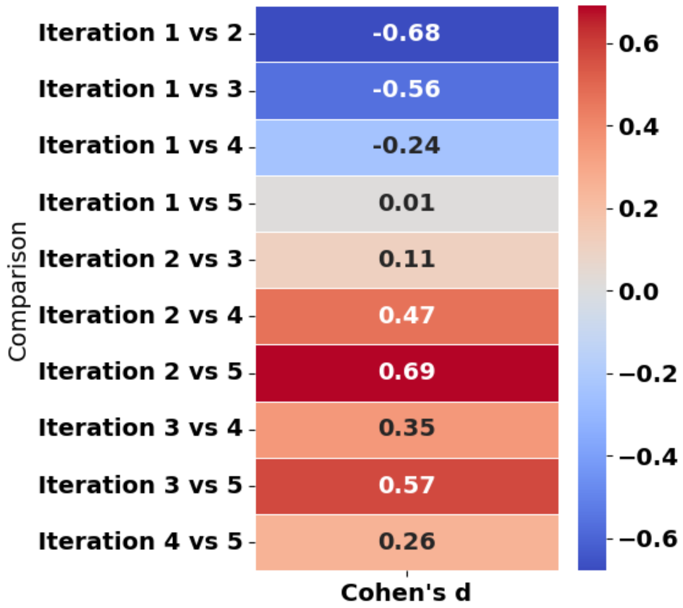

Figure 5.8: Cohen's d effect size for pairwise comparison.

A substantial variation in the CO_2 solution for the iterations is evident from the Cohen's d heat map in the figure above. To further evaluate the effect size and the direction of the solution, comparison of the time series plot Figure 5.3, Dunn's test Figure 5.7 and Cohen's d effect size Figure 5.8, confirms that Iteration 1 vs 5 and 2 vs 3 have least effect size. As mentioned earlier, comparison of 1 vs 5 shows that bathroom door undercut equation representation has minimal effect on the solution. While iteration 2 vs 3 shows that representation of trickle vent with either the power law or orifice equation has carried a smaller effect.

To further inspect the impact of trickle vent and bedroom door undercut's representation, selected iteration comparisons are re-visualised in Figure 5.9.

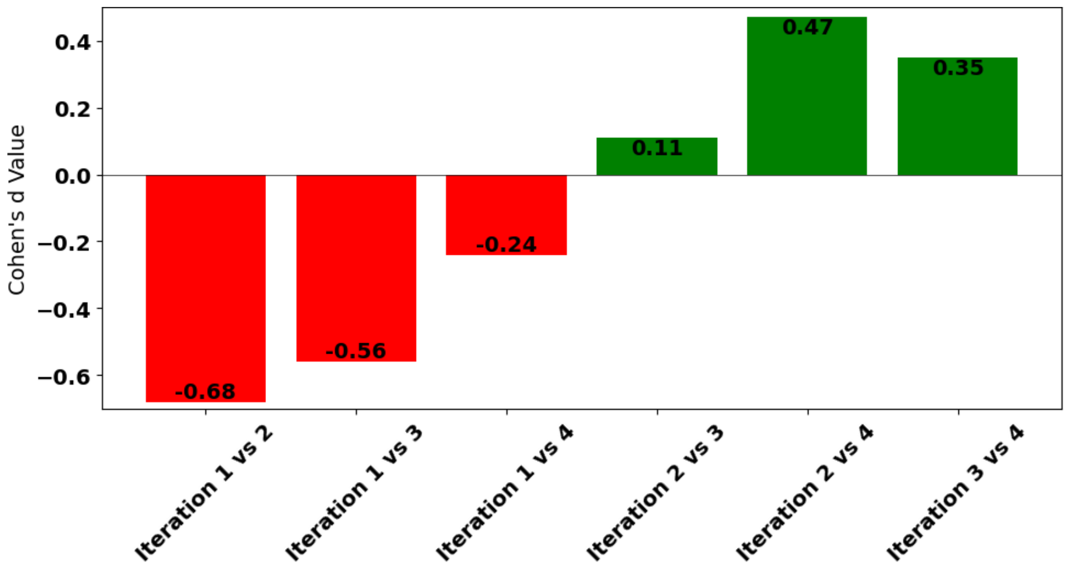

Figure 5.9: Selected comparisons of iterations to evaluate the effect of trickle vent and bedroom door undercut representation.

Low effect size for comparisons 2 vs 3, 1 vs 4 confirm lower influence of trickle vent representation while higher effect size for comparisons 1 vs 2, 1 vs 3 shows higher influence of door undercut representation in AFN solution for CO_2 concentration. It is important to note that these comparisons are not isolated, and other factors have influence on the solution.

This section has laid foundation to further investigate the impact of inputs used in the orifice and power law equations to model trickle vents and door undercuts to highlight the possible higher or lower estimation of flow.

5.2.9 Door Undercut Modelling Equation

Cohen’s d pairwise comparison for the iteration 1 vs 3 suggests medium-large effect size of door undercut representation on the CO_2 concentrations. Author will undertake a physical analysis of these 2 iterations and elaborate the difference in solution of the power law vs orifice equation. This is aided by a “sensitivity of the change” analysis to check the response of each equation to the varying ΔP and subsequent solution for the flow rates. Same procedure is taken for the undercut and trickle vent modelling.

First, the author visualises flow rate with respect to pressure difference when undercut is modelled as power law equation (left) and when modelled as orifice (right) (Figure 5.10). Standard deviation (SD) for flow rate solution via power law its 0.28 l/s and via orifice equation is 4.41 l/s which is a staggering difference.

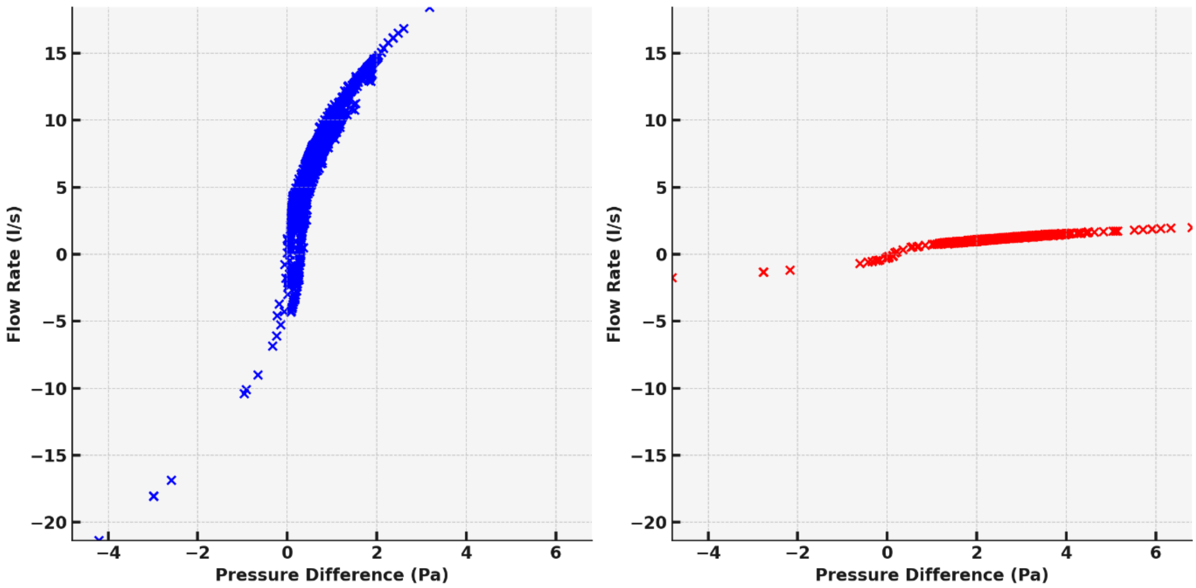

Figure 5.10: Flow rate vs pressure difference across bedroom door undercut when modelled as orifice flow (left) and power law (right).

The orifice equitation and power law model equations are re-arranged and sensitivity in terms of $\frac{dQ}{d\Delta P}$ is given by:

$$\frac{dQ}{d\Delta P} = \frac{C_d \times A}{\sqrt{\Delta P} \times \sqrt{\rho}} \tag{5.5}$$

$$\frac{dQ}{d\Delta P} = n \times C \times L \times \Delta P^{n-1} \tag{5.6}$$

Equation above, for n=0.5 can be re-written as:

$$\frac{dQ}{d\Delta P} = \frac{n \times C \times L}{\sqrt{\Delta P}} \tag{5.7}$$

$\frac{dQ}{d\Delta P}$ can be referred to as sensitivity of change in flow with the change in pressure for the orifice (5.5) and power law equations (5.7). For both equations, the use of geometric and resistive parameters directly scale sensitivity. ΔP on the other hand, exhibits decreasing sensitivity as its value increases. This behaviour is typical when inertial forces become more dominant at higher pressures.

The figure below provides a comparison for the sensitivity of solution of both orifice and power law equations over a pressure difference range. The relative comparison suggests that the use of flow coefficients in both the equations are either too large (for orifice equation) or too small (for power law). To investigate this further, we will assess the considerations taken behind input values according to the literature review presented previously.

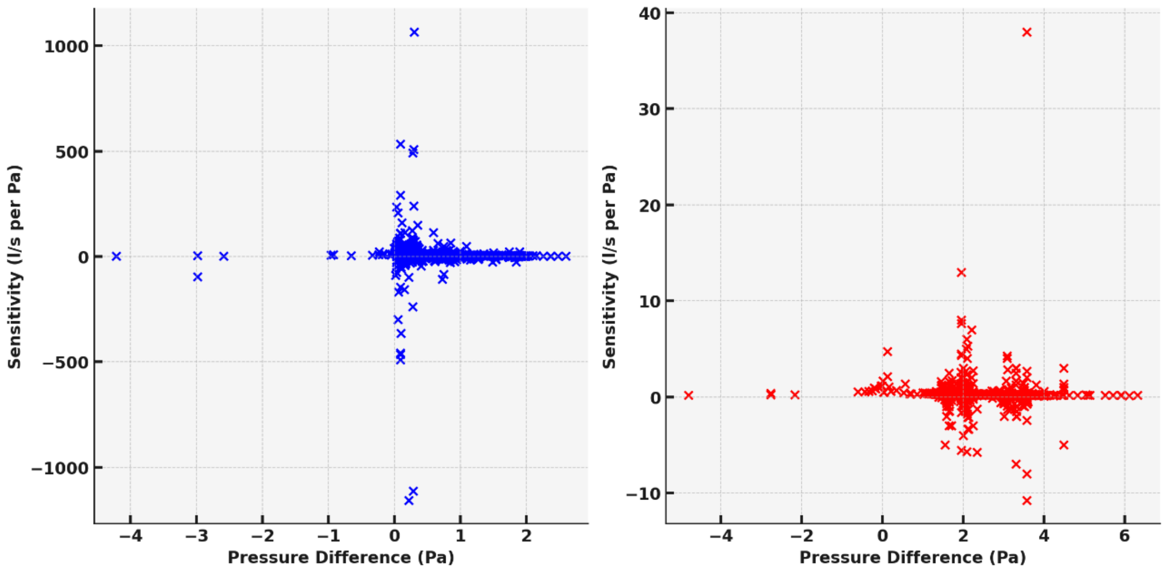

Figure 5.11: Door Undercut's sensitivity solution of orifice equation (left) and power law (right) for Q/ΔP.

In the orifice equation C_d used is 0.6 which is taken as default for shape edged orifice. As discussed in the literature, this coefficient depends upon various factors and taking such value can be erroneous and may overestimate the airflow solution. However, in Klote & Milke, (2008), use of C_d using orifice equation is suggested to be 0.35 instead of 0.65 due to formation of vortices in the opening due to turbulence and hence higher resistance is experienced by the flow.

With the limitation of use of power law model beyond 10mm of height of the door undercut and unavailability of undercut testing data, this analysis suggests using a higher resistance of the flow pathway using C_d=0.35.

5.2.10 Trickle Vent Modelling Equation

The same procedure adopted for door undercut is now applied to the trickle vent solution to understand the impact of coefficient inputs on the flow solution. Due to availability of an alternative testing data for the trickle vent, alongside the comparison of the orifice flow and power law model; solution via coefficients calculated from the trickle vent's manufacturer's testing data is also presented. This is to assess the modelling of effective area using the orifice flow equation and using test data's n and C coefficients in the power law equation.

Comparing iteration solutions for 1 vs 4, standard deviation for solution with orifice equation is 1.97 l/s and 1.53 l/s for power law. The range is much narrower as compared to door undercut when orifice equation is used for the solution.

Orifice equation has manufacturer's input of effective area while power law model has user measured geometrical area (w, h); n and C are calculated from these inputs.

This is important to note that the geometrically calculated area 4290 mm^2 which is less than the effective area of 5000 mm^2. According to the concept of effective area, in case of trickle vents, it should be less than the geometric/free area. This raise concerns implementing measured geometrical area to model using any equation, specifically power law in our case.

Comparing the iteration solutions for 1 vs 4, Q and ΔP plots show the underprediction by power law equation which is primarily due to the coefficients inputs n and C as informed by the equation 5.7. Contrary to the case of door undercut where comparison was uninformed, in case of the trickle vent the tested effective area for trickle vent is known.

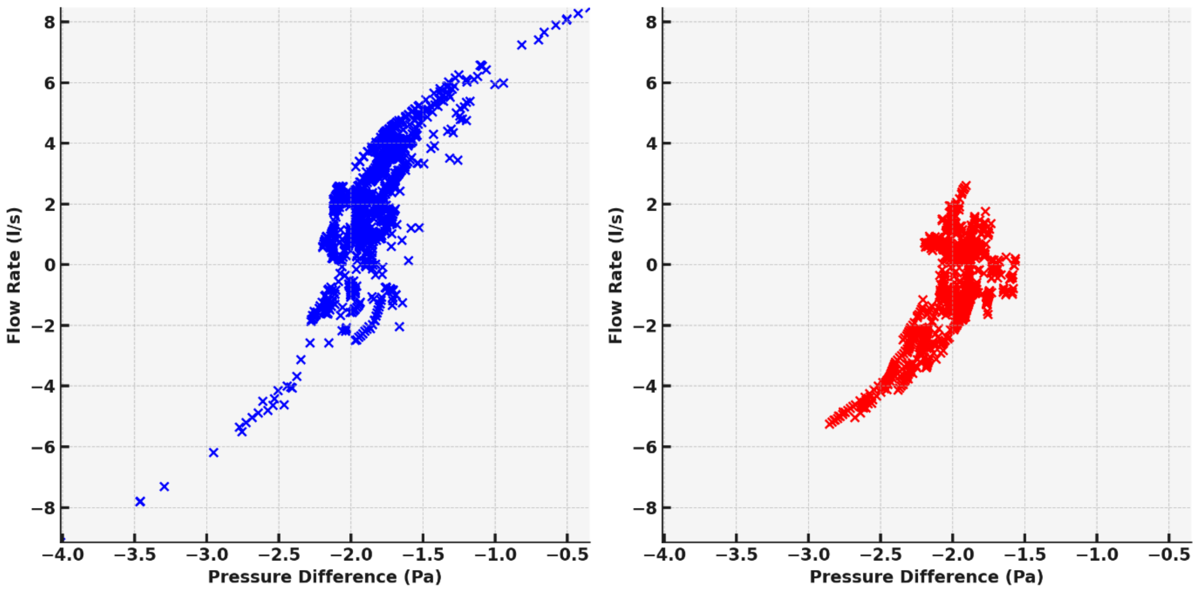

Figure 5.12: Flow rate vs pressure difference for both equations.

Figure below plots the sensitivity of both equation by following the same procedure followed in undercut's modelling evaluation.

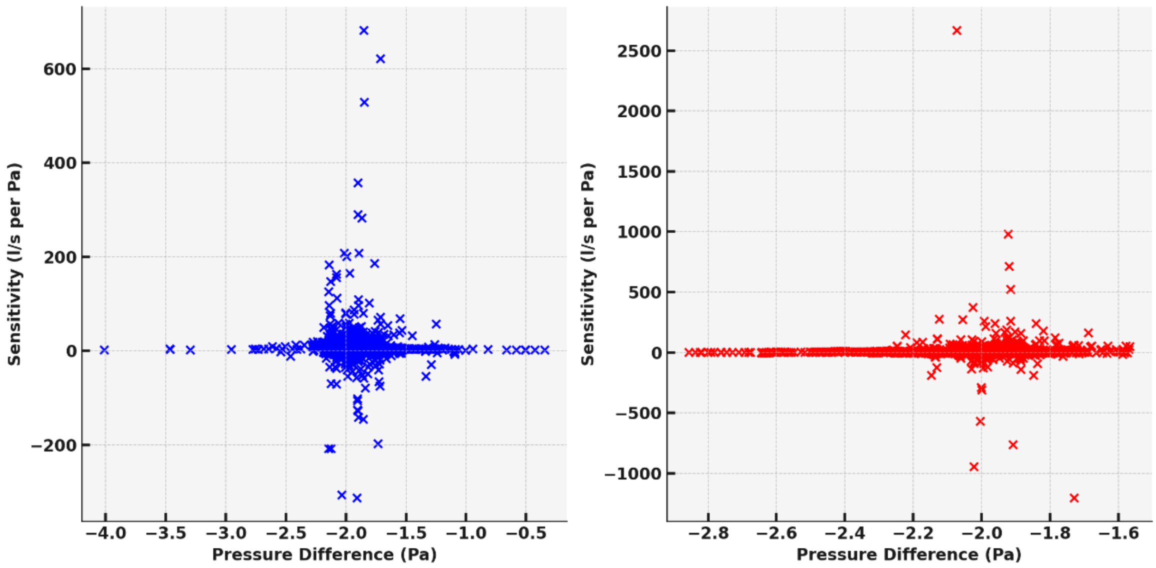

Figure 5.13: Trickle vent's sensitivity solution of orifice equation (left) and power law (right).

The relative comparison suggests that there is substantial difference between both scatter plots. Opposite to the undercut's sensitivity, when trickle vent is modelled as power law, the inputs are resulting in higher sensitivity than orifice equation. This is due to smaller $d\Delta P$ for power law equation as compared to orifice equation. The standard deviation for ΔP in case of power law is 0.19 while 0.86 for orifice flow equation. This small deviation in ΔP leads to close to zero values of $d\Delta P$ and therefore a larger sensitivity value.

The sensitivity analysis allows to inspect the behaviour of the coefficients on the flow rate solution. Additionally, it is also elaborated that both equations behave in an AFN differently despite same boundary conditions and nodal setup.

For the next stage of the analysis, the manufacturer's testing data is employed to determine n and C values and form a polynomial equation. Q and ΔP curves from previous two approaches and this third approach are visualised with response curve of the polynomial equation by inputting respective ΔP values.

To calculate n and C values from the manufacturers lab testing data is available, n is calculated by the slope of a logarithmic plot as detailed In (W.S. Dols, 2015b).

The slope of the pressure flow curve is log transformed and linear regression line in the form of $log(Q) = log(C) + n.log(\Delta P)$, intercept $log(C)$ is determined which is logarithm of C. Antilog of C gives the value equal to 3.89 while is slope is n which equals 0.52.

New power law equation to model the trickle vent from testing data from the manufacturer is given as:

$$Power\ Law^* = Q = 3.89 \times \Delta P^{0.52} \quad 5.8$$

Figure 5.14 (a) shows flow vs ΔP for orifice equation with effective area, (b) is for power law model equation $Q = 0.31 \times \Delta P^{0.50}$ and (c) is for power law equation 5.8.

From the manufacturer's specifications, 3rd order polynomial fit to data is plotted for flow rates due ΔP.

$$Q = 0.0233\Delta P^3 - 0.3300\Delta P^2 + 2.5267\Delta P + 1.6800 \quad 5.9$$

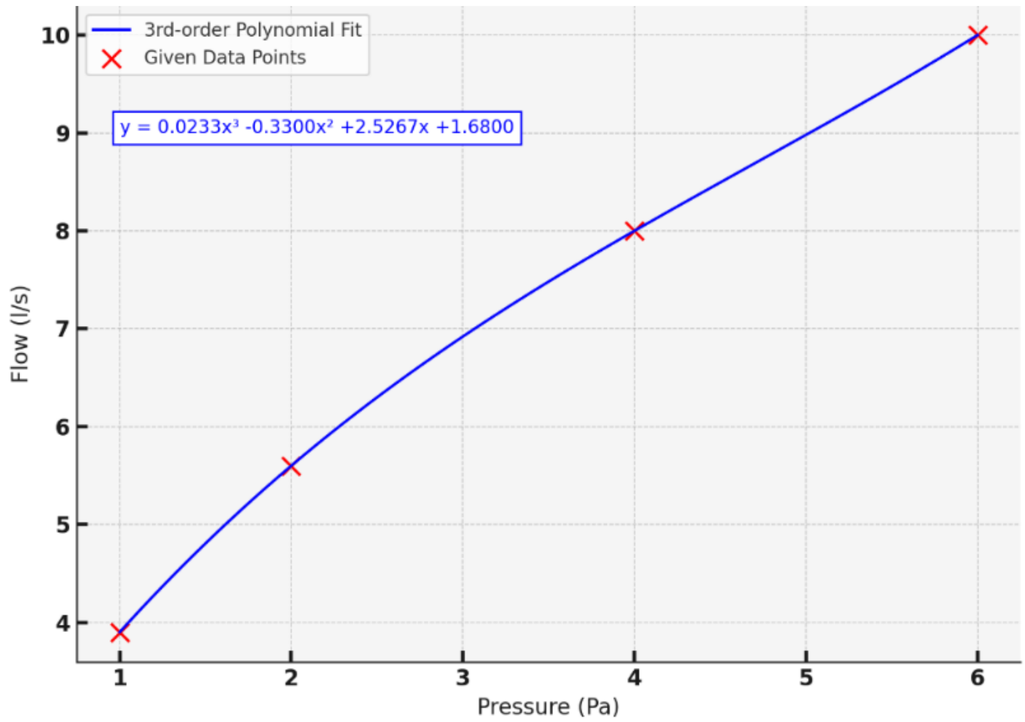

In each graph, polynomial curve is added to show the discrepancy of the solution from the laboratory tested flow trend. The polynomial equation 5.9 is further solved for residuals to assess the discrepancy between effective area (orifice equation) and Power Law* solution from equation 5.8. This comparison illustrates the difference in performance of the trickle vent in laboratory setup and simulation model.

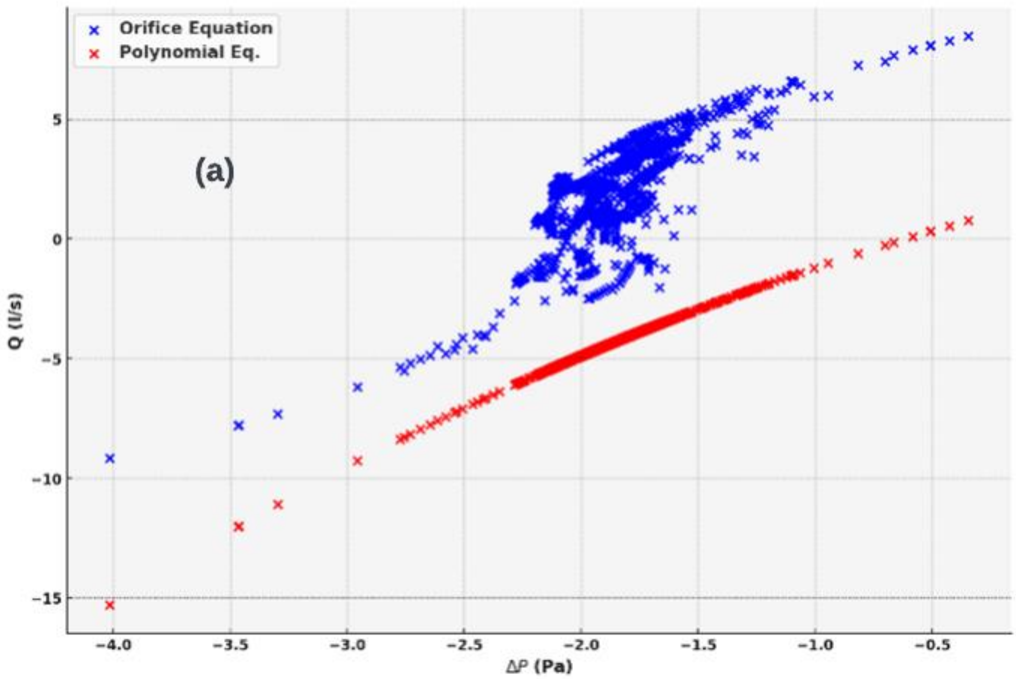
Orifice Equation
Polynomial Eq.
(a)
Q (l/s)
ΔP (Pa)

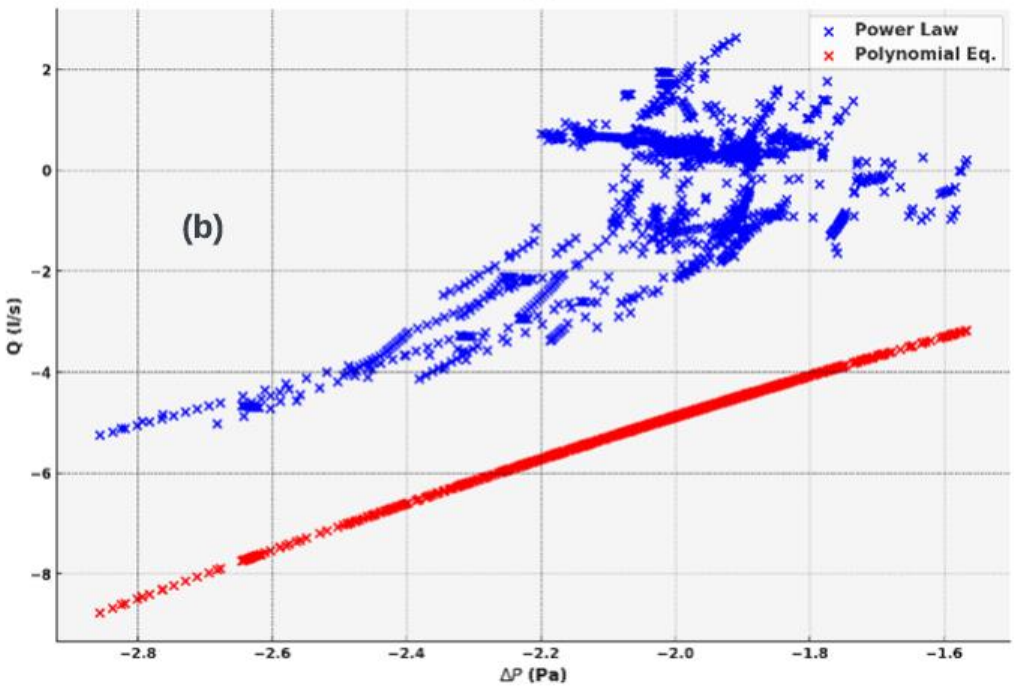
Power Law
Polynomial Eq.
(b)
Q (l/s)
ΔP (Pa)

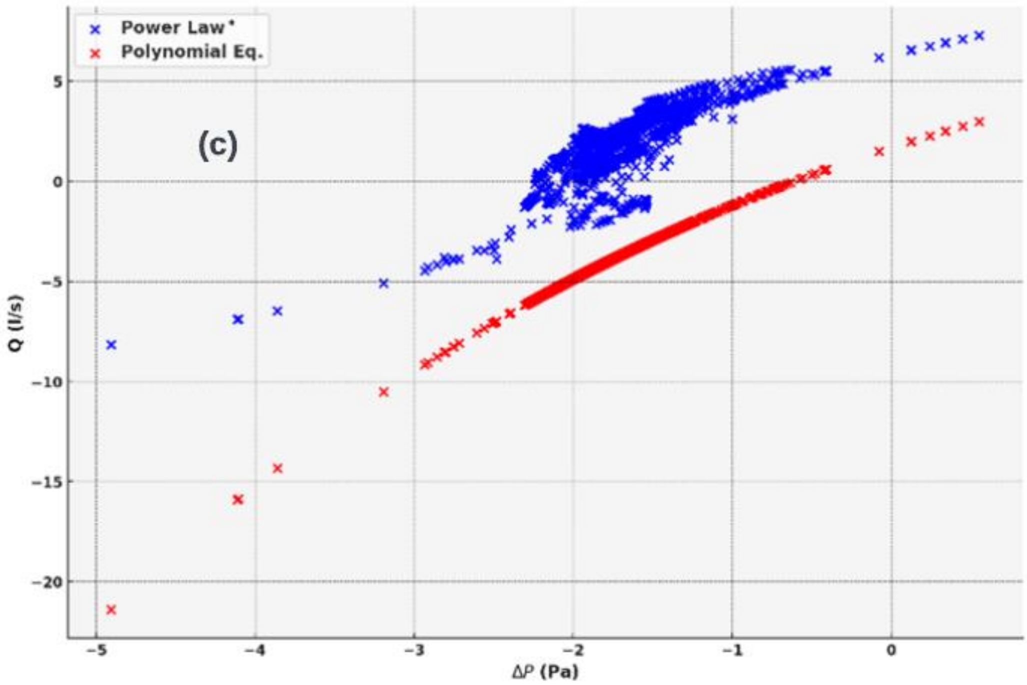

Figure 5.14:(a) Orifice equation solution with manufacturer provided effective area (b) Power Law solution using crack flow model valid up to 10mm height of the flow path (c) Power Law solution with slope of polynomial function calculated using manufacturer provided ΔP and Q values.

To compare residuals for simualted flow rate through the orifice equation and power law*, ΔP from the simulated dataset are input into polynomial equation to calculate flow rates and simulated values for flow rates for same ΔP are deducted from polynomial equation flow rate. This can be given as:

$$Residual = Q_{polynomial} - Q_{Simulated} \tag{5.10}$$

Figure 5.15 shows the residual of Q vs ΔP for effective area model using orifice equation and power law*.

When modelled using effective area, the mean residual is 6.4 l/s and standard deviation is 1.37. When modelled using power law*, mean residual is 5.66 l/s and standard deviation is 0.97. The mean residual gives an estimation of how far, on average, the simualted flow rate is from the flow rate predicted from the polynomial equation 5.9. The standard deviation of the residual show, the mangitude of deviation of simualted flow rate from the average difference. The mean residual for power law* is 11.56% lower than orifice equation. However this difference is small and insignificant difference in CO_2 solution is found when compared for both equations.

Simulated flow rates and polynomial equation predicted flow rates are different due to different data handling by power law form and polynomial form of equation. Here the purpose is to compare the orifice and power law equation inputs against a common baseline to determine the difference in their solutions.

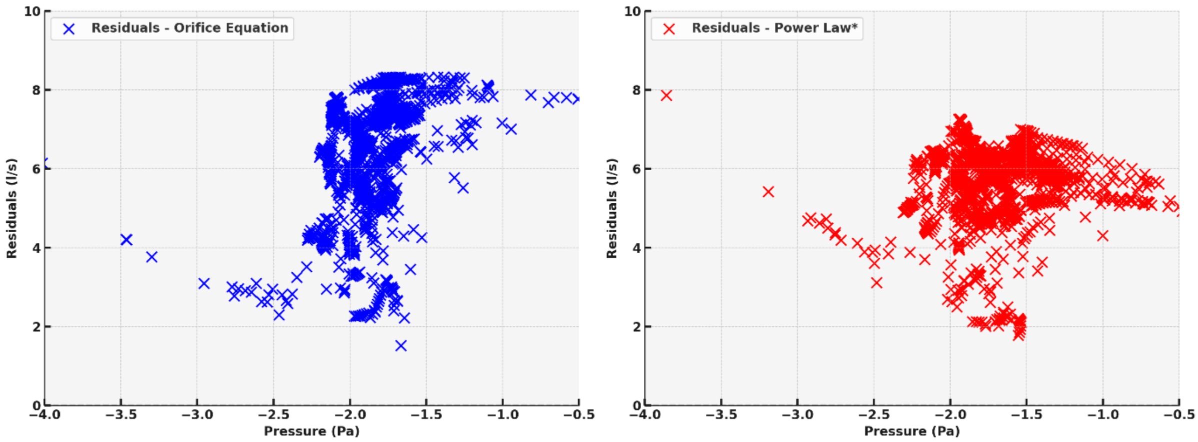

Figure 5.15: Residuals for equation solutions with respect to the polynomial equation.

In the first stage of the flow solution analysis, it was found that the flow solution via orifice equation and power law model is considerably different. Use of visually measured flow area for trickle vent must not be used. Furthermore, manufacturer design data may also present discrepancy between their respective flow rate solutions however this variation is low. Laboratory test results would differ from real life and simulation results substantially.

It is important to note that using effective area from manufacturer or n and C values from the testing data would not entail significant difference.

5.2.11 Pressure Difference and Flow Across Components

The pressure difference across the flow components is the driving force for the flow from one node to the other. In this section, ΔP and airflow across trickle vents, infiltration cracks, door undercuts and extract fan are presented and analysed. The data is from the Iteration 5 which is deemed as devised setup of equations however in the later stages Iteration 5* will be employed for the subsequent stages of the investigation. This way previously presented Q and ΔP analysis can be used for the analysis.

The pressure coefficients from AIVC are used to simulate wind pressure on each of the wind induced facades and are graphed for the study period and combined with the analysis for the airflow solution and ΔP (Figure 5.17).

Figure 5.16 shows ΔP between wind induced (South and East) nodes and internal bedroom nodes, bedroom and hall nodes and, hall and bathroom nodes. The wind speed is included in the illustration showing possible correlation with the pressure difference. A great variability in the ∆P is evident from this figure apart from Hall-Bath straight line with minute disturbance. This shows a constant pressure induction in the AFN due to constant running fan at a set flow rate. During the bedroom occupancy period of Day 1, 2 and 3, both wind-induced nodes and the internal bedroom node have very similar negative ∆P across them. East-Bed ∆P show less variability throughout the remaining occupied periods as compared to South-Bed which is highly correlated with the wind speed (0.77). A moderate correlation between East-Bed and Bed-Hall ∆P of 0.5 is evident from the plot.

Correlation between East – Bed and Bed – Hall is due to low resistance flow component on the East façade (trickle vents) which is influenced by the ∆P induced by the fan while high resistive components on South and East façade such as cracks are not influenced by the fan induced pressure.

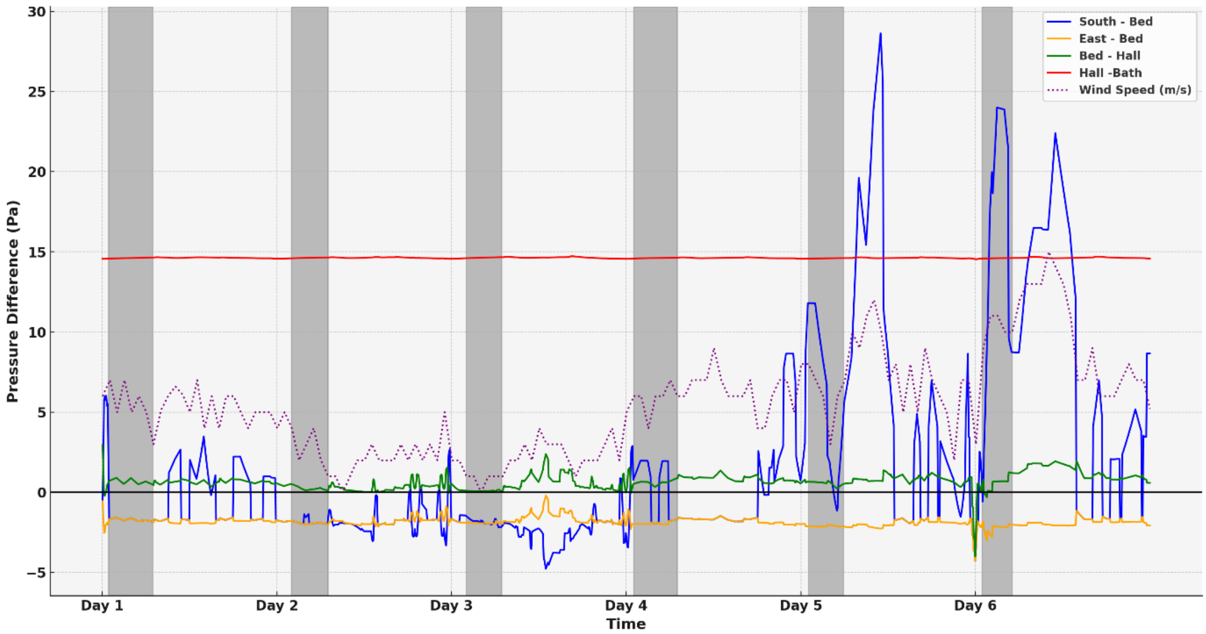

Figure 5.16: ∆P across flow components and the wind speed; cracks on 160 facade (South - Bed), one trickle vent (East - Bed) and room door undercut (Bed - Hall)

Average ∆P for the occupied time slots is tabulated in Table 5.3. Highest SD (6.56 Pa) is found for South – Bed while for rest of the nodes, it is >1 Pa.

Day	South – Bed ΔP_{avg}	East – Bed ΔP_{avg}	Bed – Hall ΔP_{avg}
1	-1.7	-1.7	0.68
2	-1.85	-1.93	0.24
3	-1.86	-1.92	0.09
4	0.33	-1.92	0.61

5	5.96	-2.11	0.55
6	16.76	-2.25	0.55

Table 5.3: Average ΔP across cracks on 160 facade (South - Bed), trickle vent (East - Bed) and room door undercut (Bed - Hall) during night-time occupied periods.

Outdoor-indoor ΔP depends upon the pressure coefficient data. To visualise temporal distribution of pressure coefficients, the dataset from AIVC (being used in ESP-r) is extracted and presented in Figure 5.17.

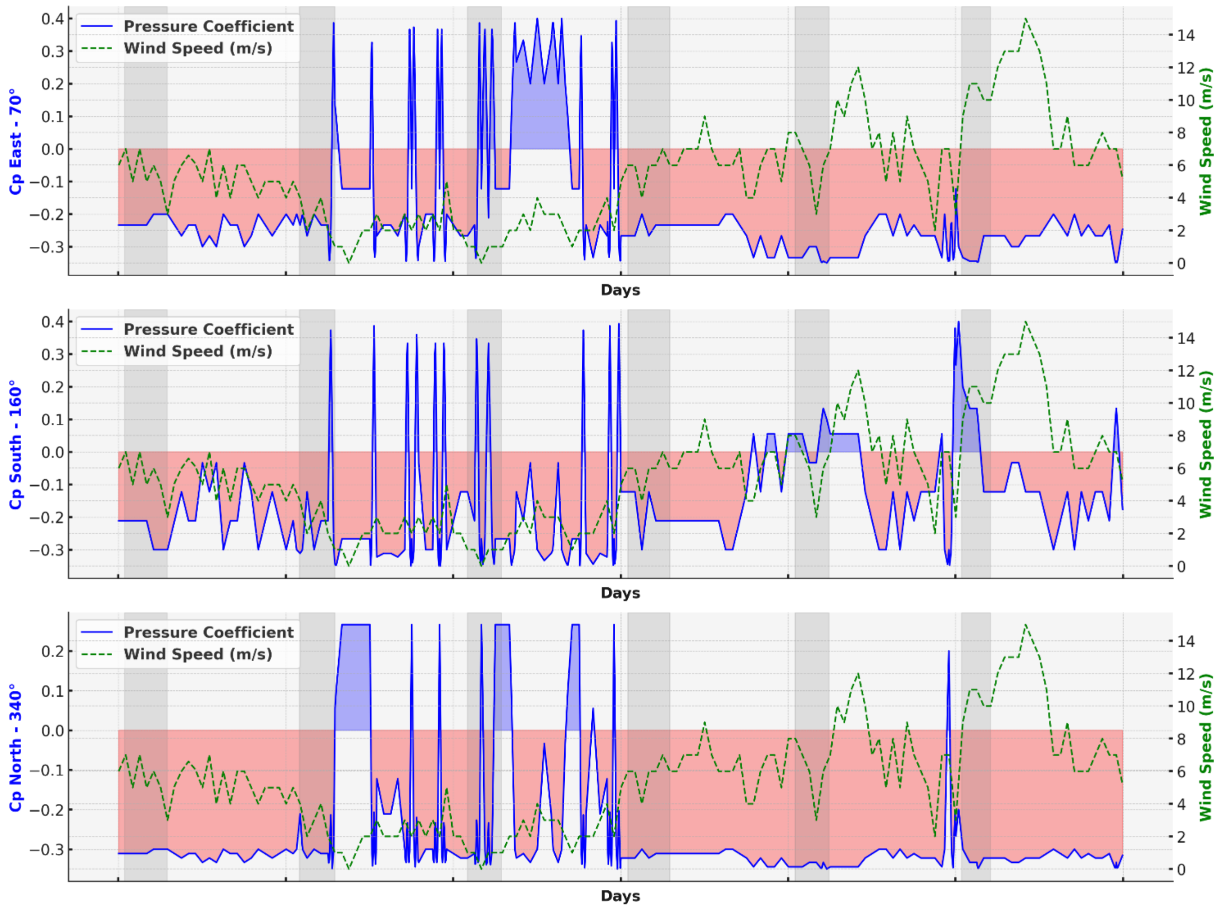

Figure 5.17: Pressure coefficients for incident wind angles, extracted from ESP-r.

The pressure coefficients are responsible for wind induced flow on the outdoor nodes however factors such as extract fan and resistive nature of the flow components also account for the variation in the pressure induced in the bedroom. Wind driven air flow being confounding in nature, however some trends can be elaborated by analysing the Figure 5.16 and Figure 5.17. During low wind speed days, ΔP is negative on the East and South façade. As the wind speed increases on Day 5 and 6, the South façade has positive ΔP.

It is interesting to see a negative spike at the start of Day 6 for ∆P for all connections shown in the ∆P plot. A further investigation into C_p values for the same time step indicates that North facing façade is subjected to positive C_p allowing inlet of the flow from the crack on that façade hence negative flow from bedroom door undercut and East and South facing flow components is evident Figure 5.18.

Bedroom door undercut is junction between bathroom, corridor window crack (North facing) and bedroom flow components on South and East façade. Flow rate graph shows high flow rate though the bedroom door undercut component and in an event of sharp pressure drop on the south and east façade, large amount of flow passes though it from the North façade in the hallway to South and East façade of the room.

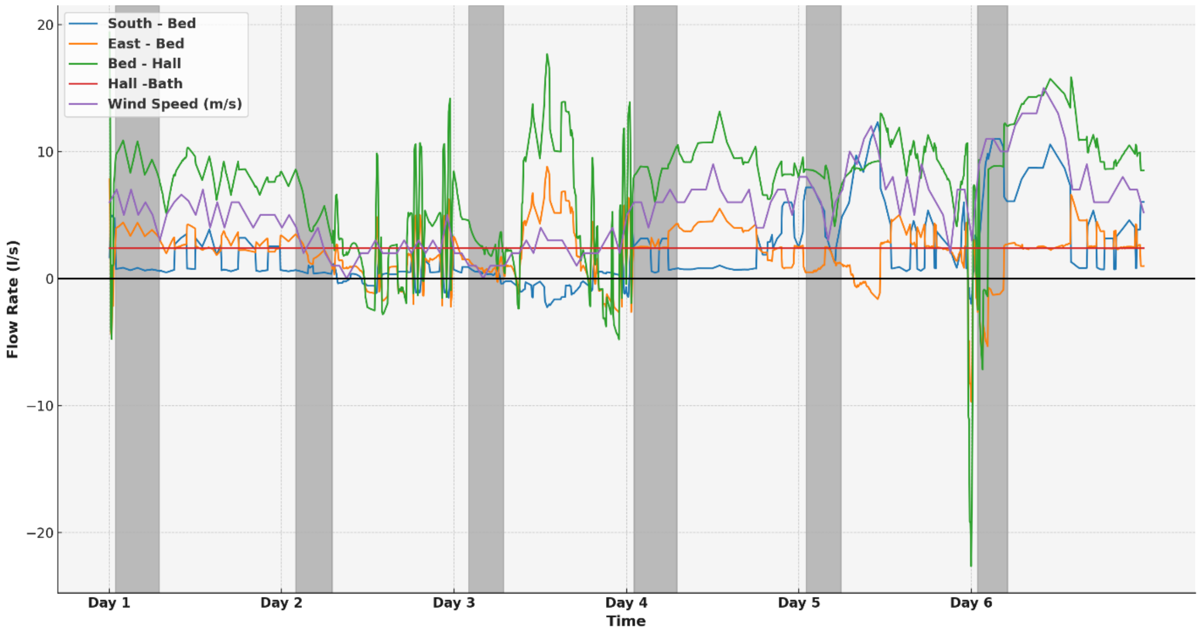

Figure 5.18: Flow (l/s) through flow components and the wind speed.

Day	South – Bed $Flow_{avg}$	East – Bed $Flow_{avg}$	Bed – Hall $Flow_{avg}$
1	0.72	3.81	9.38
2	0.53	2.02	5.23
3	0.41	0.83	2.62
4	2.10	2.83	8.45
5	4.75	1.17	7.54
6	8.6	-1.51	5.77

Table 5.4: Average flow rates (l/s) through cracks on 160 facades (South - Bed), one trickle vent (East - Bed) and room door undercut (Bed - Hall) during night-time occupied periods.

Simulation results analysis of Q and ΔP for the first floor of the case study house forms understanding of higher/lower CO_2 concentrations on certain days. Boundary conditions and modelling of flow components carry a high significance. It is learnt that appropriate set of C_p values with respect to azimuth angle of each external nodes are important to be assigned as per actual/target design attributes of the building. Please note that up till this point, wind reduction coefficient is not applied to the wind speed. This allowed a highlighted comparison of the impact of boundary conditions on the flow solution.

5.2.11.1 ∆P and Flow in context of Cohen's d Effect Size

The analysis for ∆P and flow through the components can be seen together with the Cohen's d values calculated previously. Iteration 5 which models door undercut with orifice flow equation and C_d=0.61, the greatest effect size is found when compared with power law representation of this component. In the Table 5.4 the average flow rate for each occupied period affirms that highest flow in the bedroom connections is via the door undercut. This further confirms over prediction of the flow rate from the door undercut, being highly sensitive to the pressure changes across the component. Hence suggested lower C_d value from the literature receives a backing from this analysis.

5.2.11.2 Flow Due to Buoyancy and Wind

The assessment of pressure differences across facades and the internal zones allows to evaluate the magnitude of flow and its driving forces. However, it is not elaborate enough if this flow is wind induced, or buoyancy driven. As discussed in literature review, ratio of Grashoff number to the square of Reynold's number which infers that if it is <1, the flow is primarily due to wind and if its ≥1, flow is mainly caused by buoyant forces. This ratio is called Archimedes number (Ar).

This number is calculated for each time slot of occupancy taking average wind speed and ∆T.

Day 1	Day 2	Day 3	Day 4	Day 5	Day 6
0.695	3.007	29.661	0.773	0.8768	0.299

Table 5.5: Archimedes number for occupied/sleeping time slots each day.

The values in the table above will be analysed together with CO_2 simulated results when wind reduction factor is applied. It is anticipated that with a reduction in wind speed, the CO_2 levels would rise. This percentage increase and the Archimedes number calculated will be analysed later.

5.2.12 Iteration 5*

From the previous work where we have assessed the use of coefficients in the orifice equation and power law to model trickle vents and door undercut, a new iteration 5* is introduced which uses previous analysis to solve for indoor CO_2 concentrations. Trickle vent is modelled using new flow coefficient and exponent using power law (as slightly less residual compared with polynomial equation than the orifice equation) while door undercut's C_d value is changed to 0.35.

It is also important to note that the bedroom CO_2 minimum value reaches 603ppm while in model a lower minimum value was set. The inspection of measured data informs the minimum value as 603ppm. For the subsequent iterations including iteration 5*, a higher minimum CO_2 level is set.

CV(RMSE) for the occupied period is 17.97%. The comparison of Iteration 5* and measured CO_2 is presented in Figure 5.19.

5.2.13 Modelling of Flow Between Floors in Stairwells in AFN

The literature suggests using the unidirectional flow component and orifice equation but there is some evidence that this does not correctly capture bi-directional flow which was observed in some circumstances. To investigate this the model was run with both the unidirectional and the bi-directional components, and for each component varying the opening size (2m^2 to 3m^2). It was found that this variation had no significant effect on the network flows. In a modern domestic context, where the air and surface temperature variations are small, it is then reasonable to use an unidirectional flow component with C_d=0.61 and an area the same as the base of the stairwell, similar to the common approach found in literature (Katsumichi, 2003; Wetter, 2006)

5.3 Wind Reduction Factor – Phase I – AFN – V2

Until this stage, the wind reduction factor is not introduced in the model as the sole purpose of previous work was to assess the solution of flow rates through the modelled flow paths. As discussed in the literature, wind speed at the weather station is higher as compared to a populated area. The power law wind reduction factor (0.58) is applied to the wind data and simulations are re-run. This is an important factor to be applied to the wind data to account for hinderance to the wind due to terrain and other buildings. Selection of this number is explained in the literature review and the guidance used to calculate this number is explained in the guidance chapter 6.

Figure 5.19 shows how the change in representation of trickle vent and door undercut has impacted simulated CO_2 values (iteration 5*) and then implementation of wind reduction factor (iteration 5* Log W) has a varied impact on the iteration 5* values.

Previously calculated Ar values in the Table 5.5 show a possible wind induced and buoyancy driven ventilation in the main bedroom. Alongside this metric, both visually significant and insignificant change in the CO_2 peaks is evident from the Figure 5.19. It is anticipated that for the days with a higher change in peak CO_2 with implementation of wind reduction factor should have higher possibility of wind induced ventilation. This analysis is confirmed by calculating percentage difference in CO_2 peaks.

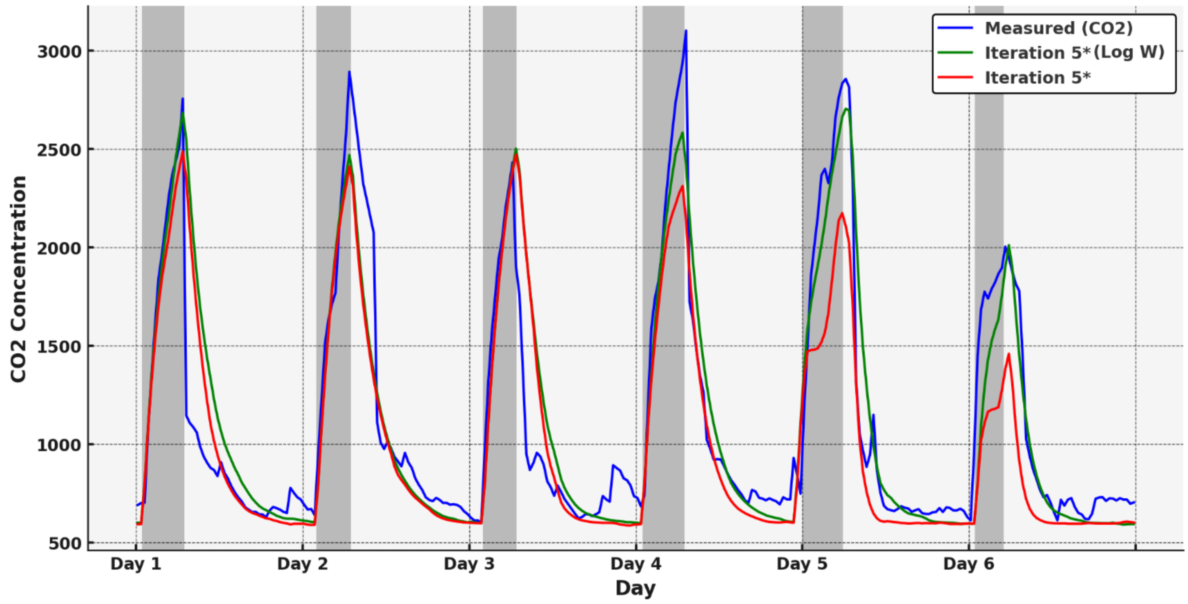

Figure 5.19: Comparison of measured CO_2 with iteration 5* and Iteration 5* Log W.

The percentage difference of peaks between Iteration 5* and Iteration 5* Log W is calculated for day i using following relation:

$$\%Difference_{Peak}(Day\ i) = \frac{Peak\ (Iteration\ 5^{*}i) - Peak\ (Iteration\ 5^{*}\ Log\ Wi)}{Peak\ (Iteration\ 5^{*}i)} \times 100$$

Where i is from 1 to 6 for each day. The calculated values for each day are tabulated in Table 5.6

Day 1	Day 2	Day 3	Day 4	Day 5	Day 6
7.91%	2.42%	1.17%	11.73%	22.50%	37.71%

Table 5.6: Percentage difference in CO_2 peaks for each day.

Comparison of data in Table 5.5 and Table 5.6 can help to evaluate the relationship between ability of wind induced ventilation and the impact of change in values with the implementation of wind reduction factor. Nonlinear regression of the data from both tables is conducted to check the best fit based on R^2 value i.e., 0.83.

$$\%Difference_{Peak} = a \times Ar^b \qquad 5.11$$

The R^2 values provide measure of how well a curve would fit the data. In our case the value is close to 1 which means that Ar effectively captures the variation in $\%Difference_{Peak}$ across both versions of iteration 5*. It further suggests that there is a non-linear relation between $\%Difference_{Peak}$ and Ar, and for the days with greater wind induced potential has higher impact of the wind reduction factor while on the days, such as Day 3 has the lowest impact. This also informs about the response of AFN model to the boundary conditions and solution of CO_2 values.

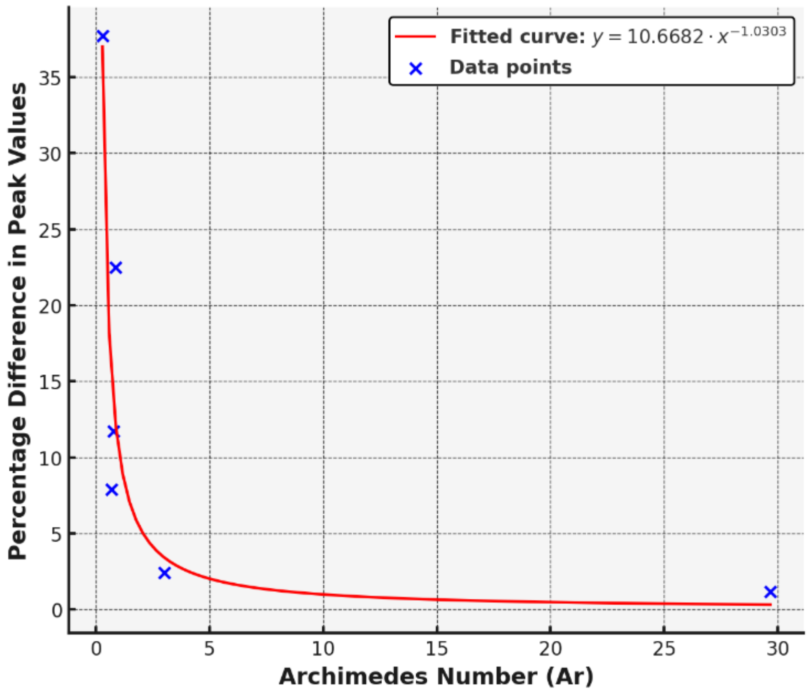

Figure 5.20: % Difference Peak vs Ar showing power law non-linear relation.

5.3.1 Influence Coefficient for Wind Reduction Factor

As discussed in literature, influence coefficient can provide a quantified measure of the difference in the output values caused by a parameter. For this calculation, average peak CO_2 value is used as the output. With decrease in wind reduction numeric value, the CO_2 output increases hence an inverse relation and ≥-0.27.

5.4 Distribution of Cracks – Phase I – AFN – V3

In the first two versions of AFN, cracks corresponding to the airtightness of the case study house were modelled using simplistic approach i.e., assigning cracks to the window frames.

Literature suggests location of cracks is a major uncertainty. The airtightness also tends to increase or decrease with time. Whichever approach we take to model cracks would be an approximation. Purpose of this exercise is to evaluate the solution with pronounced effect of stack pressure and highlight possible uncertainties. The results are then compared with non-distributed cracks AFN version AFN – V2 and the impact of is elaborated in 5.4.2. It is aimed to investigate:

- Impact of distribution of cracks in comparison with single level cracks per zone.
- Addition of stack pressure to the total ΔP.
- Influence of external factors on the flow rate.

In the context of this case study, we will distribute cracks so that the model encapsulates the effect of stack induced flow – giving us new version of Iteration 5 i.e., (Log W_d). This distribution is coupled with introduction of higher and lower levels nodes (from the central node level of the room). The top-level node is 1.2m higher while the lower is 1.2m lower than the central datum. Moreover, trickle vent is 0.7m above the datum and same height is determined for the adjacent node.

Contrary to one crack one window frame, the same crack area is distributed on top and bottom of the façade.

Figure 5.21 shows the config of AFN where top and bottom level external nodes are connected to top and bottom level wall cracks (yellow) and the trickle vents (white T). By taking this example, stack pressure equation is presented.

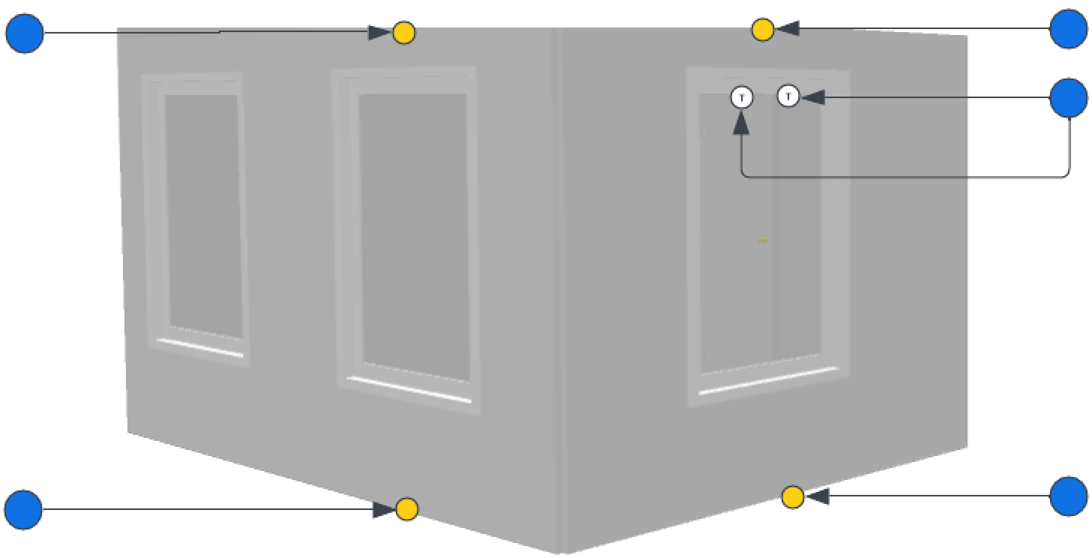

Figure 5.21: Introduction of external nodes with height difference with respect to ceiling and floor level of the room. Yellow circles represent top and bottom level cracks while white circle

represents trickle vents. Cracks and trickle vents are further connected to interior bedroom node (not illustrated).

Total pressure difference across each crack is given by:

$$\Delta P = P_{wind} - P_{room} + \rho_i g(Z_n + h_1 - Z_m - h_2) - \rho_{outdoor} g h_1 + \rho_{indoor} g h_2; i = outdoor, indoor \qquad 5.12$$

In the equation above the terms $\rho_i g(Z_n + h_1 - Z_m - h_2)$ and $-\rho_{outdoor} g h_1 + \rho_{indoor} g h_2$ represent stack pressure. While Z_n and Z_m are heights of the nodes n and m respectively. $h_1 = Z_1 - Z_n$; $h_2 = Z_2 - Z_m$ where Z_1 and Z_2 are height of openings with respect to reference level in zone n and m respectively.

Equation 5.12 can be written for the top level, bottom level crack and trickle vent opening with reference to Figure as:

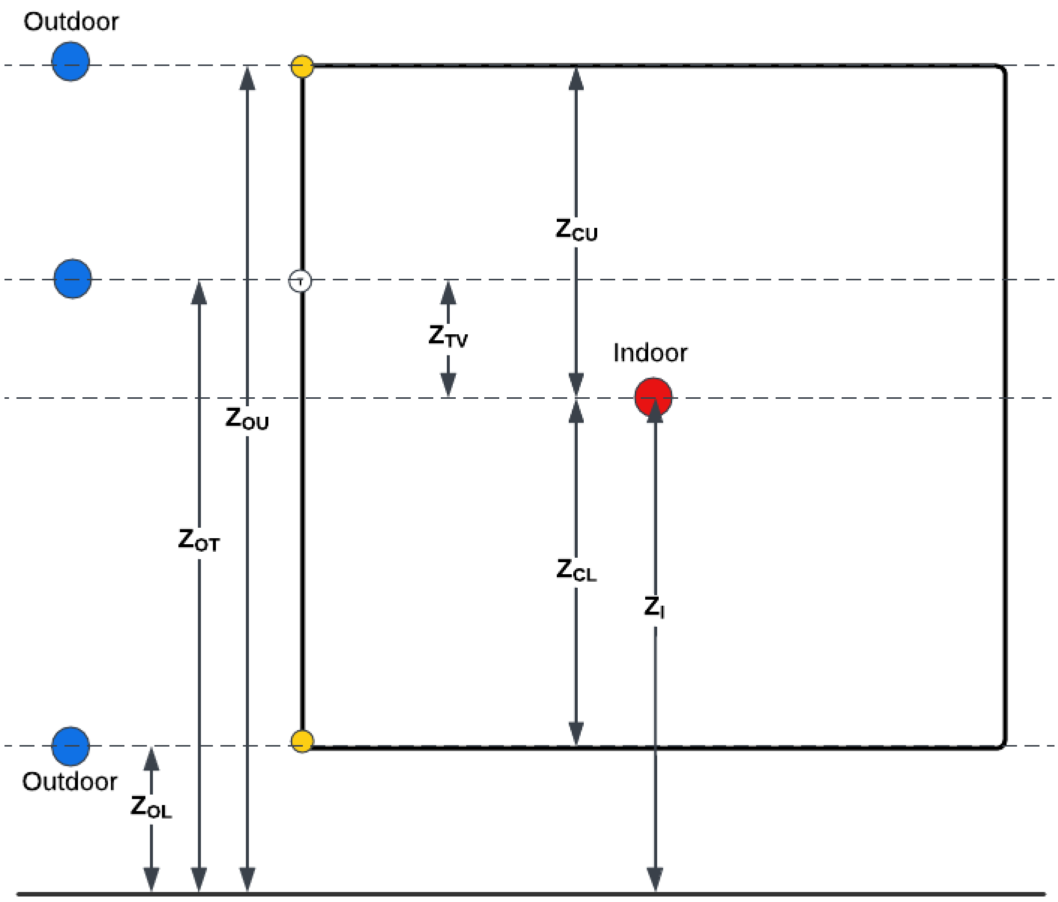

Figure 5.22: Node and flow component heights for the main bedroom for configuration 2.

$$\Delta P_{top\ crack} = P_{outdoor} - P_{indoor} + \rho_i g(Z_{OU} - Z_I - Z_{CU}) + \rho_{indoor} g Z_{CU}$$

$$\Delta P_{bottom\ crack} = P_{outdoor} - P_{indoor} + \rho_i g(Z_{OL} - Z_I - Z_{CL}) + \rho_{indoor} g Z_{CL}$$

$$\Delta P_{trickle} = P_{outdoor} - P_{indoor} + \rho_i g(Z_{OT} - Z_I - Z_{TV}) + \rho_{indoor} g Z_{TV}$$

Where $i = outdoor, indoor$.

While combined pressure at the outdoor node will be:

$$P_{total,outdoor} = C_p \times \frac{1}{2}\rho_{outdoor} {U_r}^2 - \rho_{outdoor} g h_{outdoor\ node} \quad 5.13$$

Where $P_{total,j}$ is the total pressure at outdoor node j, $C_{p,j}$ is the pressure coefficient from the database for a reference height of the node and h_j is height of the outdoor node. The element $\rho_{outdoor} g h_j$ is the static pressure addition to the total node pressure and it increases with the node's height from the reference level and at $h = 0$, total pressure on the outdoor node will be wind induced. This equation further infers that with a negative value of $C_{p,j}$, both pressure elements would add up resulting in a greater negative pressure.

5.4.1 Stack Pressure Solution for the Log W_d

Stack pressure element of Equation 5.12 are re-written for both cracks and trickle vents.

$$PS_{top_{crk}} = 1.2\rho_{indoor} g$$

$$PS_{trickle} = 0.7\rho_{indoor} g$$

$$PS_{bottom\_crk} = -1.2\rho_{indoor} g$$

The solution, which is discussed in next section, will depend on indoor density of air, height of flow component with respect to the internal node and gravitational acceleration g.

5.4.2 Effect of Distribution of Cracks on Flow Solution

Both the Iterations 5* Log W and Log W_d are compared for their flow and CO_2 concentration solutions. Purpose of this procedure is to explain the impact of added effect of buoyancy due to infiltration. In Log W model, cracks do not show any outflow due to temperature and stack pressure differences while with the distributed cracks and corresponding outdoor nodes for each flow component in Log W_d provides a more realistic approach of modelling a wind induced façade as show in Figure 5.23.

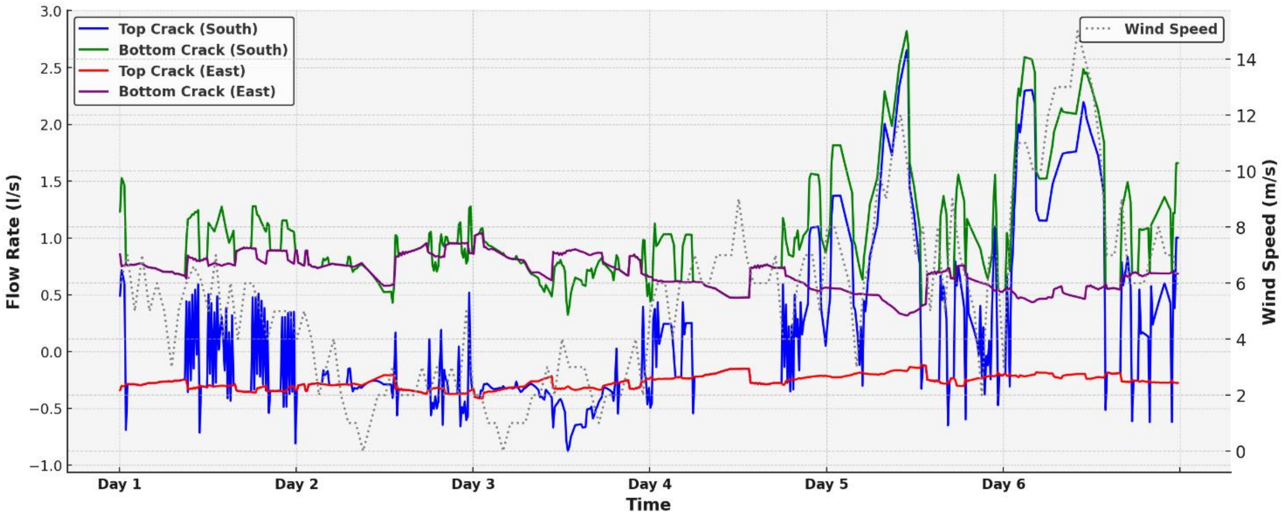

Figure 5.23: Flow through cracks in Log W_d air flow network model.

It is quite evident that South side of the room has high wind induced flow. During the high wind speed hours, flow from both top and bottom cracks is positive. On the East façade, top crack consistently exhibits a negative flow while bottom crack offers positive flow.

In Log W_d model, as the outdoor nodes are at different heights rather than just one height as in Log W, hence each component solves flow rate for a different wind induced pressure. This pressure increases with height in a linear trend given averaged pressure coefficient data for the node direction. Total ΔP, for both models, across all components which are connected between wind induced nodes and room node is plotted to visualise the impact of varied wind pressure due to node height.

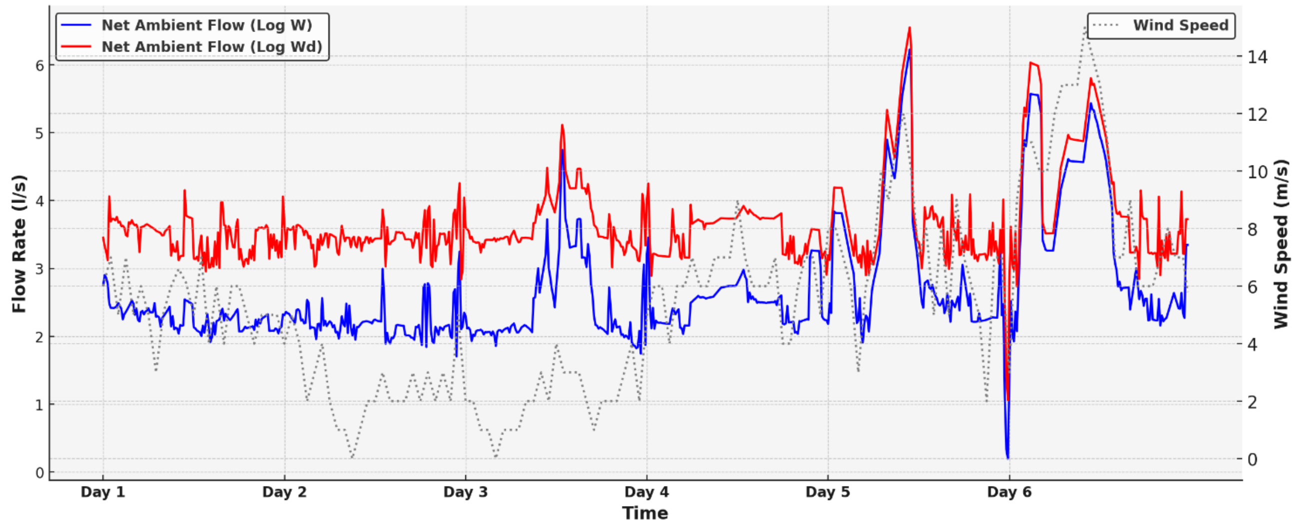

Figure 5.24: Net Flow from Ambient nodes to internal node. Comparison between Log W and Log W_d AFN model.

The shift in the increased pressure difference and flow rate is majorly due to the added stack pressure for top and bottom cracks. In real life situations, the whole façade has different pressure levels and that is inherited in the pressure coefficients values which are part of the wind pressure relation for AFN simulations. In Log W_d model, not just the effect of buoyancy is added to the flow solution, as well as the higher-level node experiences higher wind pressure and lower node a lower pressure.

Where shift in the net flow in the main bedroom is evident, this shift is not consistent e.g., Day 5 and 6 where high wind pressure is experienced by the Northen and Western facades. The flow solution is non-linear because of the power law crack and orifice trickle vent equations used. It is important to mention that the orifice flow equation also depict non-linear solution for Q and ΔP.

Now comparing CO_2 concentration solution for non-distributed and distributed cracks version of Iteration 5 i.e., Log W and Log W_d, as per flow rate analysis, lower CO_2 concentrations in the later version are evident.

This comparison provides an upper bound scenario analysis by placing the infiltration cracks at top and bottom of the façade for maximum height difference hence large stack pressure being induced. This is beneficial for a conservative estimation of the CO_2 concentrations. However as stated earlier, as location and ability of infiltration due to these cracks is unknown, any placement of cracks would carry uncertainty.

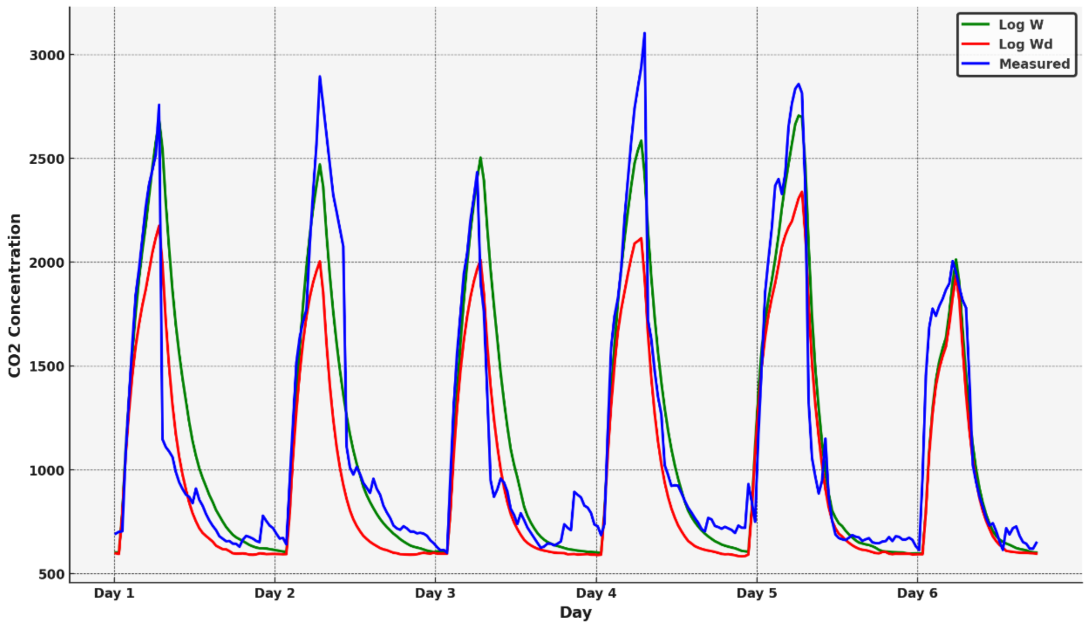

Figure 5.25: Overall lower CO_2 concentration values due to distribution of cracks and a higher stack pressure.

As far as influence coefficient is concerned, with the increase in the distribution of the cracks, a decrease in the output (average peak CO_2) is observed hence the IC=-0.16. In comparison with the application of wind reduction factor, the distribution of cracks has lower impact on the output.

Up till this point we have taken a step wise iterative approach to analyse the effects of different AFN setups and their effect on air flow solutions. CV(RMSE) for Log W is 23.51% while 26.15% for Log W_d overall and 11.27% and 19.60% for occupied period respectively. The error percentage for distributed crack in the model is close to the acceptable value of 20% as mentioned in (Paliouras et al., 2015). So far in the simulation study section, the flow related parameters and their variability is presented. The sensitivity analysis of source of the CO_2 generation i.e., occupant gains is presented in the next section, and model calibration is implemented.

5.5 CO_2 Sensitivity Analysis

The CO_2 generation rate is modelled in AFN using the equation 5.14 which relates the generation of CO_2 with the metabolic rates. In the given equation, P is CO_2 generation rate (l/s), M is the metabolic gain (Wm^{-2}) and A is the body surface area (m^2) area (CIBSE, 2018):

$$P = 4 \times 10^{-5} \times MA \qquad 5.14$$

Previously for metabolic rates, we have assumed that occupants were sleeping for the whole period of occupancy however this contains uncertainty as well. According to the ASHRAE handbook, a person sleeping or at rest have metabolic rates in the range 0.7-1.0 MET where 1 MET is 58.2 W/m^2. For all previous simulations 41 W/m^2 is used as metabolic rate for each adult in the room which is approximately equal to 0.7 MET. To assess the sensitivity of the range of metabolic rates, simulation is re-run for 0.8, 0.9 and 1.0 MET and the influence coefficient and CV(RMSE) % are calculated.

This sensitivity analysis is applied to iteration setting with one dominant crack (Log W) and distributed crack setting (Log W_d).

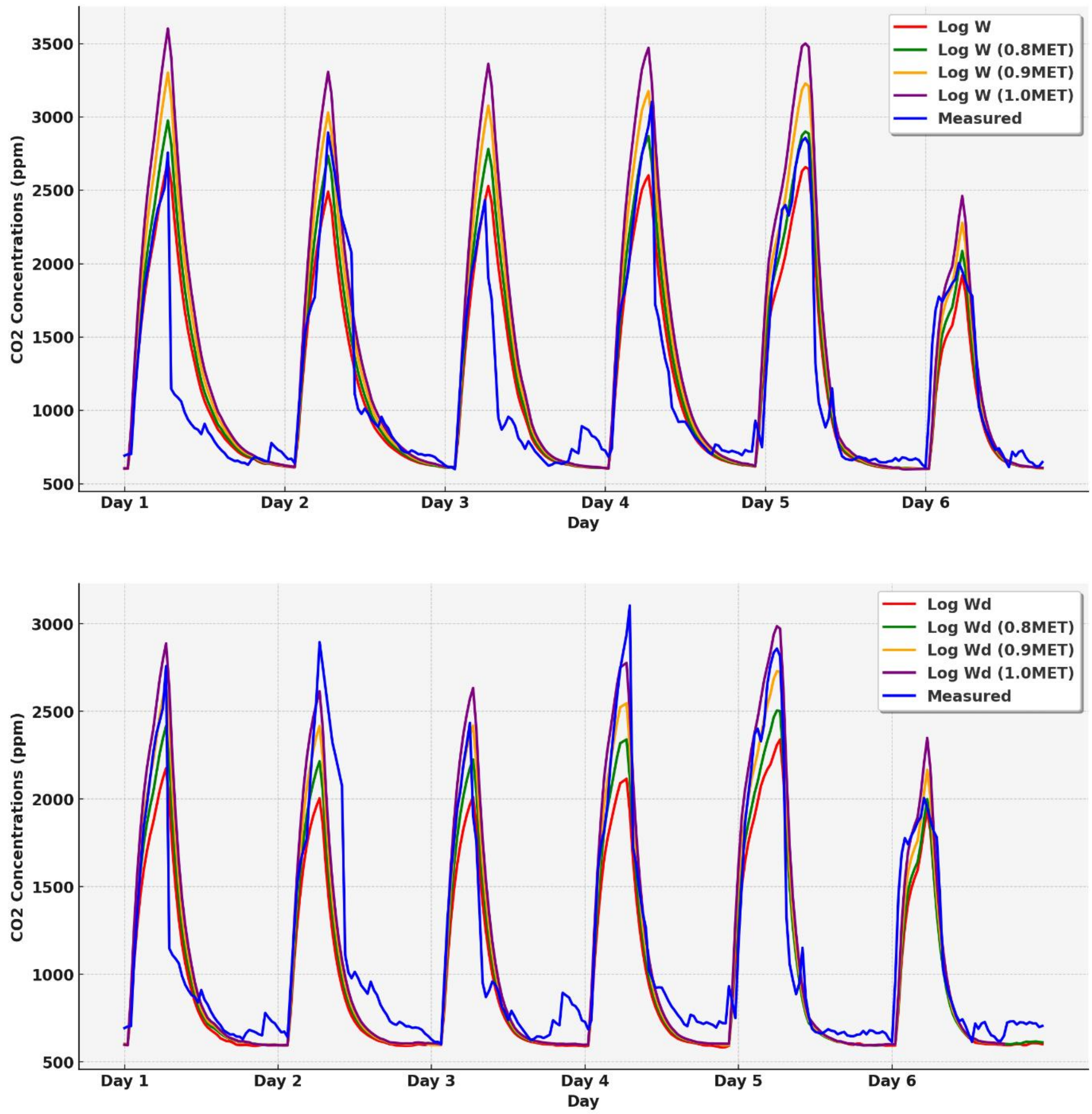

Figure 5.26: CO_2 concentrations from distributed cracks iteration with 0.7 MET and higher metabolic rates for both iterations with single dominant crack (top) and distributed cracks (bottom).

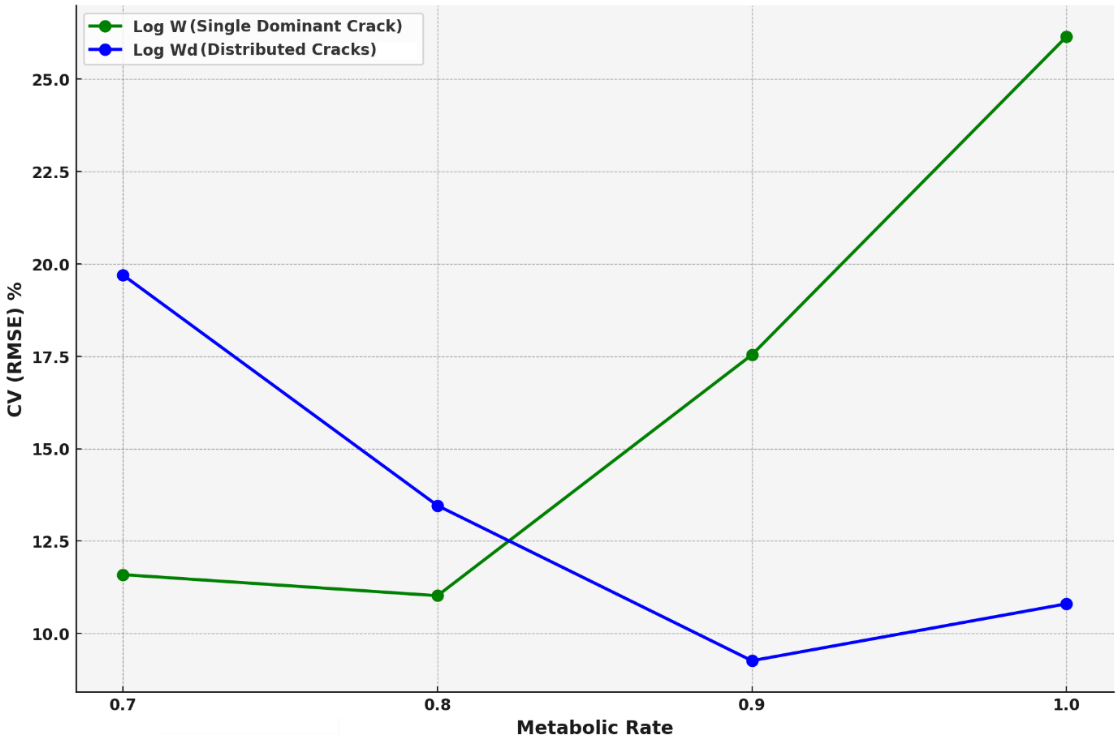

Figure 5.27:CV(RMSE) for CO_2 concentration values (occupied periods).

For the non-distributed cracks model, lowest error percentage is evident for 0.8 MET while for distributed cracks model it is for 0.9 MET input. This is relevant to the possibility that the occupants of the main bedroom collectively has higher metabolic rate as it would be for a standard person (in CIBSE and ASHRAE guidelines). Based on this, the subsequent stages of investigation will use a higher metabolic rate of the occupants. As far as the accuracy of the modelling results is concerned, the model with distributed infiltration cracks and 0.9 MET has lowest error %. While the model with non-distributed infiltration cracks with 0.8 MET has the second lowest error. These findings will be assessed together with upcoming data analysis to inform the design guidance development.

5.6 Cumulative Frequency of CO_2

CV(RMSE) suggests how well simulated model can capture variability in the monitored results and does not show the direction of the error (over or underprecition) while cummulative frequency of occurance focuses on the distribution of the frequency of occurance of the data in monitored and simualted data sets. This metric would enable to entertain the purpose of assessing a modelling strategy when it is used for ventilation design assessments.

As explained earlier in literature review, $RMSE_f$ can provide quantification of the error of the CO_2 distribution basing upon the difference in cumulative frequencies of monitored and simualted values. CO_2 values for model iteration outputs are used to calculate $RMSE_f$ and plot cumulative frequency percentage.

The previously calculated CV(RMSE) % for distributed infiltration cracks model suggested lowest error at 0.9 MET. This iteration of the model, is now assessed for this new error % metric.

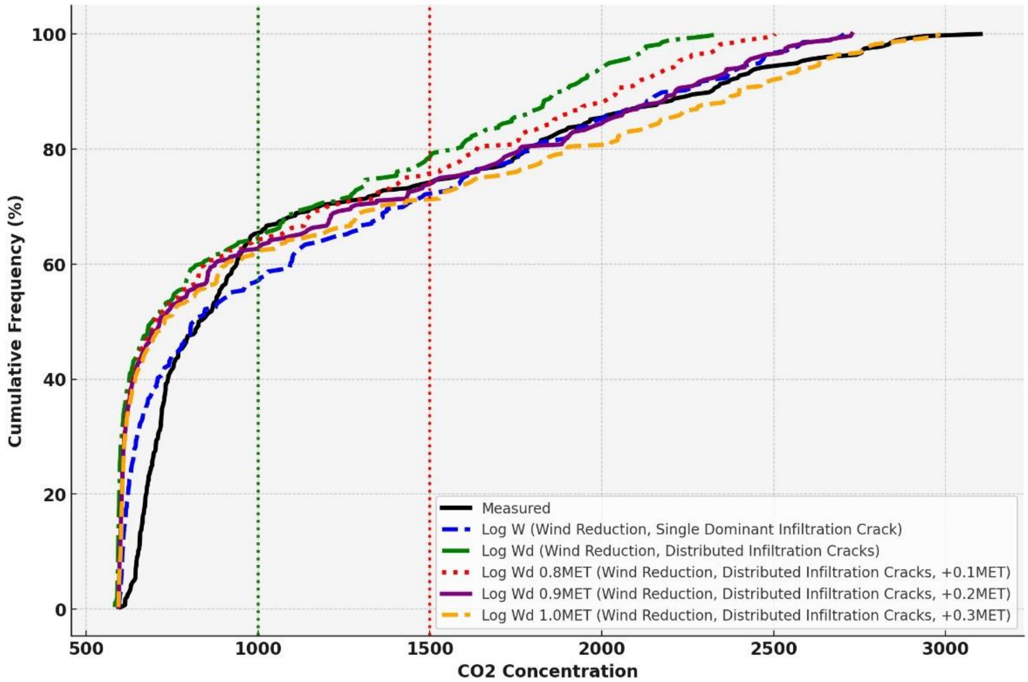

Figure 5.28: Percent cumulative frequency of occurrence of CO_2 concentrations (measured vs simulated – occupied periods in the main bedroom). The threshold lines indicate "take action" (green) and caution (red) as per SGDV.

Iteration	$\boldsymbol{RMSE_f}$ **(Occupied)**	**Cumulative Frequency (≤1000ppm)**
Log W (Wind Reduction, Single Dominant Infiltration Crack)	7.00%	56.98%
Log Wd (Wind Reduction, Distributed Infiltration Cracks)	20.68%	64.32%
Log Wd 0.8MET (Wind Reduction, Distributed Infiltration Cracks, +0.1MET)	12.14%	64.13%
Log Wd 0.9MET (Wind Reduction, Distributed Infiltration Cracks, +0.2MET)	4.79%	62.53%
Log Wd 1.0MET (Wind Reduction, Distributed Infiltration Cracks, +0.3MET)	9.03%	62.23%

Table 5.7: Overall $\boldsymbol{RMSE_f}$ and cumulative percentage for safe CO_2 threshold.

(Belmonte et al., 2019) have set the $\boldsymbol{RMSE_f}$ acceptability limit of 15% for the difference between simulated and measured CO_2 outputs. The table above shows that with the distributed infiltration cracks, there is a larger prediction of airflow causing low CO_2 output and the percentage error is greater than 15%. With an increment of higher metabolic rate, the same model is able to accurately predict with error as low as 4.79% which is under the acceptable range. Without the complexity of distributed cracks, the single dominant crack model without senstivity adjustments of metabolic rate is able to predict with an error of 7%. If this metric is seen together with percentage cumulative frequency chart, a dominant crack version of the model is well suited for higher prediction of the CO_2 concentrations. The percentage cummulative frequency at 1000ppm is also mentioned in the table above. These values indicate the percentage of CO_2 concentrations that fall below or at 1000ppm. For instance, for the Log Wd data, 64.32% of the data points are 1000ppm or lower. This further informs that the elevated MET iteration of 1.0 has lowest number of such data points.

5.7 Comparison of CO_2 Concentration Outputs from Phase I Iterations with the Measured Data

An overall comparison of CV(RMSE)% error and percentage difference between measured and modelled peak average values is presented in the table below. The inclusion of percentage difference metric is utilised to assess the peak CO_2 accumulation within a zone, this metric can inform how well a model can predict the violation of safe CO_2 limits.

Iteration	Door Undercut C_d	Wind Reduction	Distributed Cracks	Metabolic Rate	CV(RMSE)% – Occupied Periods	Average CO_2 Peak – Occupied Periods (ppm)	Percentage Difference between Measured and Iteration Peak Average
Measured	-	-	-	-	-	2674.8	-
Iteration 5	0.61	1	N	0.7	45.44%	1497.1	-44.03%
Iteration 5*	0.35	1	N	0.7	17.97%	2220.4	-16.99%
Iteration 5* Log W	0.35	0.58	N	0.7	11.27%	2493.4	-6.78%

Iteration 5* Log W (0.8 MET)	0.35	0.58	N	0.8	11.02%	2724.9	1.87%
Iteration 5* Log W (0.9 MET)	0.35	0.58	N	0.9	17.54%	3015.6	12.74%
Iteration 5* Log W (1.0 MET)	0.35	0.58	N	1	26.15%	3284.2	22.78%
Iteration 5* Log W_d	0.35	0.58	Y	0.7	19.60%	2096.2	-21.63%
Iteration 5* Log W_d (0.8 MET)	0.35	0.58	Y	0.8	13.51%	2282.7	-14.66%
Iteration 5* Log W_d (0.9 MET)	0.35	0.58	Y	0.9	9.26%	2488.3	-6.97%
Iteration 5* Log W_d (1.0 MET)	0.35	0.58	Y	1	10.80%	2706.8	1.20%

Table 5.8: Comparative analysis of CV(RMSE)% and percent difference in average of peaks in the main bedroom CO_2 concentrations between measured CO_2 and iteration solutions (occupied hours), highlighting Iterative improvements and model accuracy to predict peak CO_2 values.

The influence coefficient concerning average of CO_2 peaks is also calculated, lower wind reduction value resulted in -0.27. The negative sign indicates that with the decrease in the input shows increase in the output. In the same way by increasing the distribution of cracks, the output decreases, hence showing inverse relationship (IC=-0.16). While for the increase in the metabolic rates, there is increase in the output hence a positive influence coefficient=0.65 (changing input from 0.7 to 0.8MET). Such a high influence coefficient confirms significant influence of metabolic rate on the CO2 concentration output. This is due to the direct relationship between metabolic rate and CO2 generation.

The scatter plot (Figure 5.29) represents the comparative visualisation of the listed modelling iterations.

The black line is the measured CO_2 trend and proximity of an iteration's trend line to the measured line indicates the accuracy of that iteration for the CO_2 solution.

Data points and trend line for Iteration 5 are furthest from the measured trend. This reflects the largest deviation and highest CV(RMSE)% error when a default C_d=0.61 is used to model a door undercut in the absence of wind reduction factor.

The pairwise comparison showed great dependency of flow magnitude is on the door undercut. At this point, literature was employed which suggested greater resistivity of this flow passage and hence lower C_d of 0.35 was used (Iteration 5*). This resulted in significant improvement in the CV(RMSE) error.

Following the sequence suggested in the Methodology, wind reduction factor is then introduced (forming Iteration 5* Log W), and the impact of this addition is expressed via CV(RMSE) error as well as influence coefficient. This factor further reduced the error percentage. With the quantification of the impact of wind reduction factor, the importance of the use of correct terrain type and constant values is highlighted.

From this point, the distribution of cracks is introduced (Iteration 5* Log W_d) by modifying previous iteration. The result indicates higher estimation of flow due to increased stack pressure as the cracks are distributed at top and bottom of the wind induced facades. Literature emphasises on the probability of more than one crack at different heights. The analysis of the flow rates comparison from distributed and non-distributed crack placements also informed the overriding wind pressures over stack pressure in the event of high wind speeds. Moreover, the power law relation between the pressure and flow is confirmed. The purpose of this step is to compare the results from unit crack and distributed cracks. However, this iteration showed higher error percentage than Iteration 5* Log W. At this stage, sensitivity analysis of metabolic rates is used by defining a range which enabled lower CV(RMSE)% error and within acceptable range. The iteration with the elevated metabolic rate of 0.9MET is labelled as Iteration 5* Log W_d (0.9 MET). However elevated metabolic rate of 0.9MET sufficies the validation criteria but still underpredicts CO_2 when compared to measured data. Data lines for elevated metabolic rate of 1.0 MET show an overprediction

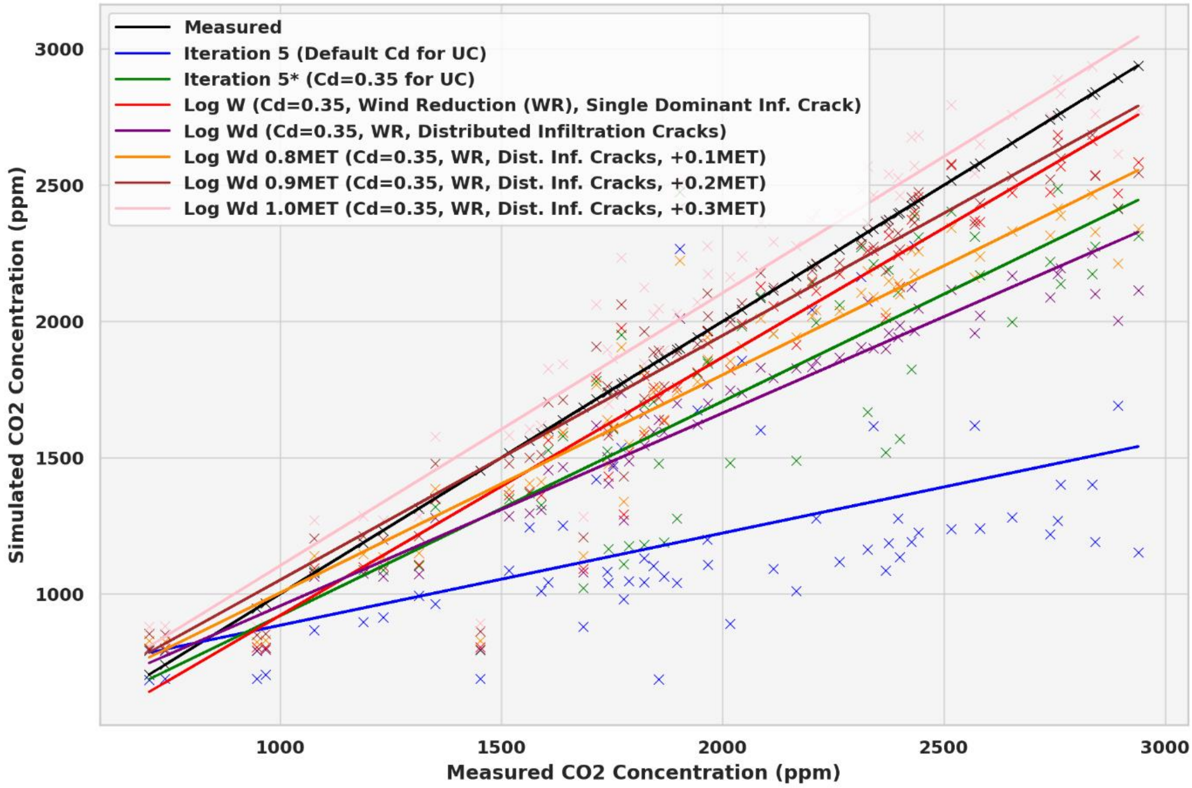

Figure 5.29: Main Bedroom CO_2 Concentrations from Occupied time-period. Data points and trend lines from measured and modelled phase I iterations.

An additional scatter plot leading from sensitivity analysis of metabolic rate with non-distributed cracks iteration is conducted for the same range i.e., 0.8-1.0 MET. As discussed earlier, with a dominant infiltration crack on a window frame, the increase in metabolic rate has higher influence on the CO_2 output as compared to the distributed cracks iteration. This is evident from the scatter plot Figure 5.30.

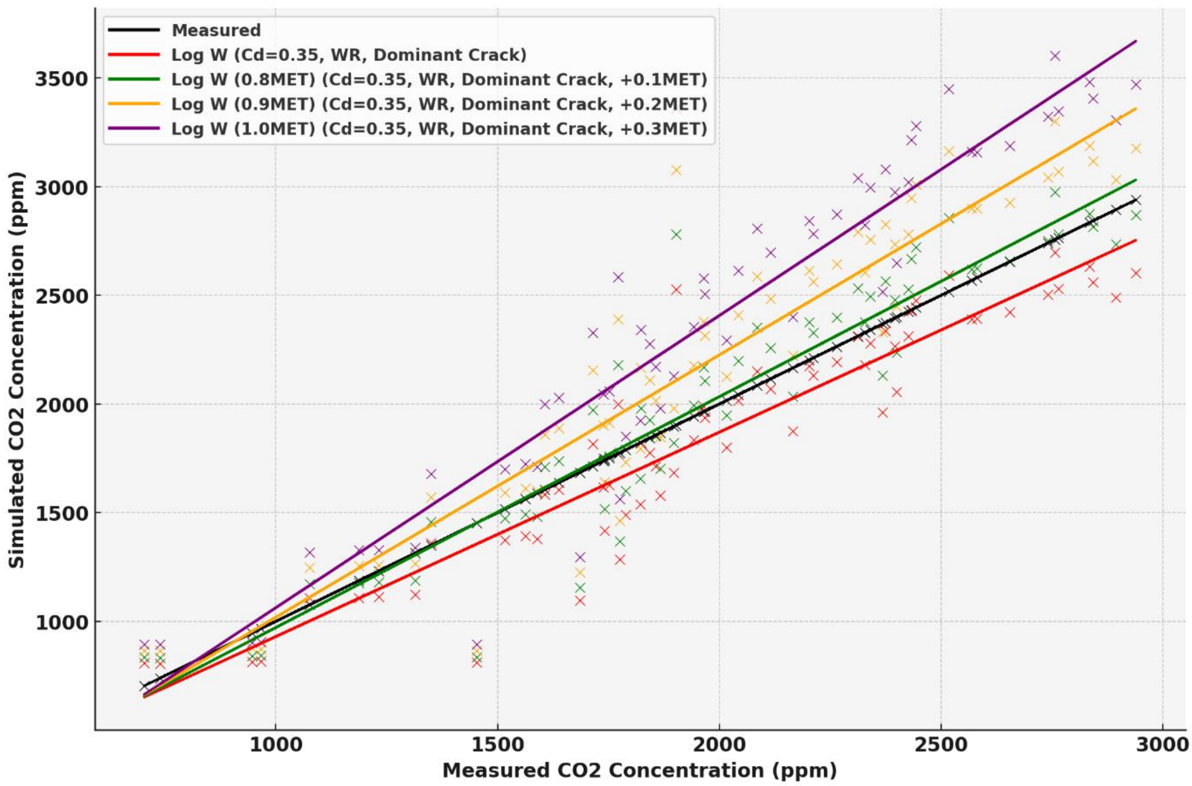

Figure 5.30: Scatter plot for metabolic sensitivity when Iteration 5* Log W as the base case showing pronounced impact of increase in metabolic rates.

Table 5.8 and scatter plots in Figure 5.29 and Figure 5.30 summarises the impact of input variations in the model. A non-distributed infiltration cracks approach gives higher estimation of CO_2 than a distributed cracks approach – with default 0.7 MET metabolic rates. However, it is learned from the sensitivity analysis of these rates that both models respond differently. Non-distributed cracks model is more sensitive to the elevation of metabolic rates than the distributed cracks model. Furthermore, it is found that the non-distributed version with metabolic rate of 0.8 MET does give a low CV(RMSE)% error while distributed cracks version give the lowest error at 0.9 MET but difference in average of peak CO_2 values suggest that the former model gives slight over prediction of CO_2 results (1.87%) while the latter underpredicts by 6.97%. Concerning a ventilation design study, in the light of this analysis, it is advisable to take a non-distributed/dominant crack approach with higher metabolic rate of 0.9 MET for the worst-case representation while for an energy demand focussed study, a distributed cracks approach with 0.8 MET would be better suited. However, moving towards a realistic translation of a built environment, the distribution of cracks is deemed to be better representation. A further extension of sensitivity analysis to other influential factors such as weather conditions, spatial occupancy variations etc can bring a more comprehensive understanding of the model.

5.8 Assessment of Acoustic Openings

The aim of this section is to incorporate interzone openings as discussed in the section 2.8.2 and compare their performance which is based on the following metrics:

- Probability of exceedance of CO_2 from safe limits.
- Percentage of time CO_2 stays in and exceeds from defined ranges – safe, threshold and cautionary.

These interzone openings are connected between the bedroom and the corridor, above the door, in the AFN.

The Phase I diary trickle vent setup suggests that, only 2/4, Eastern façade trickle vents were in use by the occupants. This investigation will introduce additional setup by introducing the opening of all 4/4 trickle vent components in the bedroom which will allow to investigate the performance of the interzone openings as well as trickle vents when full capacity of trickle vent openings are being used. To undergo this, following simulation runs are performed and results are presented.

- Base case: 2/4 trickle vents open (10000mm^2 effective area) + interzone opening.
- Best case: 4/4 trickle vents open (20000mm^2 effective area) + interzone opening.

5.8.1 Modelling Inputs

To specify these interzone openings as a part of the AFN, previous investigation of orifice equation and power law model to model trickle vents suggest that manufacturer provided testing data is necessary to model any opening. Discussion in the literature review section 2.8.2 provides 4 of such openings for which testing data is available and hence can be incorporated into the AFN by using Table 5.9 data.

To model these openings as a part of AFN, it is important to note that free and geometric area for these openings would be same expect for the overdoor grille. C_d value in combination with free area will give effective area of flow. While for overdoor grille, power law equation with n and C values from the manufacturer testing data are achieved.

For the additional trickle vents to form a best-case scenario, two components are connected between room and South outdoor node which are identical in specifications to the rest of the two trickle vents on the Eastern façade.

Modelling inputs for the openings is given in the Table 5.9:

Component	Codename	Free/Geometric Area (m^2)	C_d	n, C
Overdoor Grille	O-1	0.09	-	0.53, 4.89
Passivent	P-2	0.05	0.75	-
Gilberts	G-3	0.50	0.30	-
Hopkins	H-4	0.45	0.31	-

Table 5.9: Modelling inputs for flow components representation in the AFN.

5.8.2 Integration of Selected Components in the AFN

To introduce the interzone openings in the AFN and assess their performance, the modelling inputs in the Table 5.9 are used to model O-1 within the door frame instead of door overcut. Rest of the components are setup above the door of every bedroom on the first floor of the case study house as illustrated in the Figure 5.31.

The previously presented analysis suggested the use of higher metabolic rate of 0.9 MET for higher CO_2 predictions with a non-distributed cracks approach to represent worst case conditions. For this purpose, Log W is taken as a test bench to model these openings with metabolic rate of 0.9 MET – forming iteration 5* Log W IZ. Power law equation would be used to model O-1 while rest of the openings are modelled using orifice flow equation. Inclusion of these openings one by one would allow to add greater area of flow between the bedrooms and the corridor.

While the stage wise addition of interzone openings highlights their cumulative impact on airflow and CO_2 concentrations, the reliance on worst-case metabolic rates may lead to overly conservative predictions. The limited exploration of alternative metabolic rates under realistic scenarios would restrict the generalised use of such modelling approach. Additionally, the use of a non-distributed cracks approach might simplify infiltration solution. A comparison with distributed cracks could provide a more comprehensive understanding.

Figure 5.31: Illustration of a grille above the door - proposed design.

5.8.3 Results and Discussion

The AFN setups for the interzone openings are simulated for bedroom CO_2 concentrations using the probability of exceedance and percent of time of CO_2 falling in set thresholds.

Figure 5.32 shows that best case performs better than base case model and consequently, the interzone openings comparitively perform better in best case scenario. This is due to the provision of full capacity of effective trickle flow area.

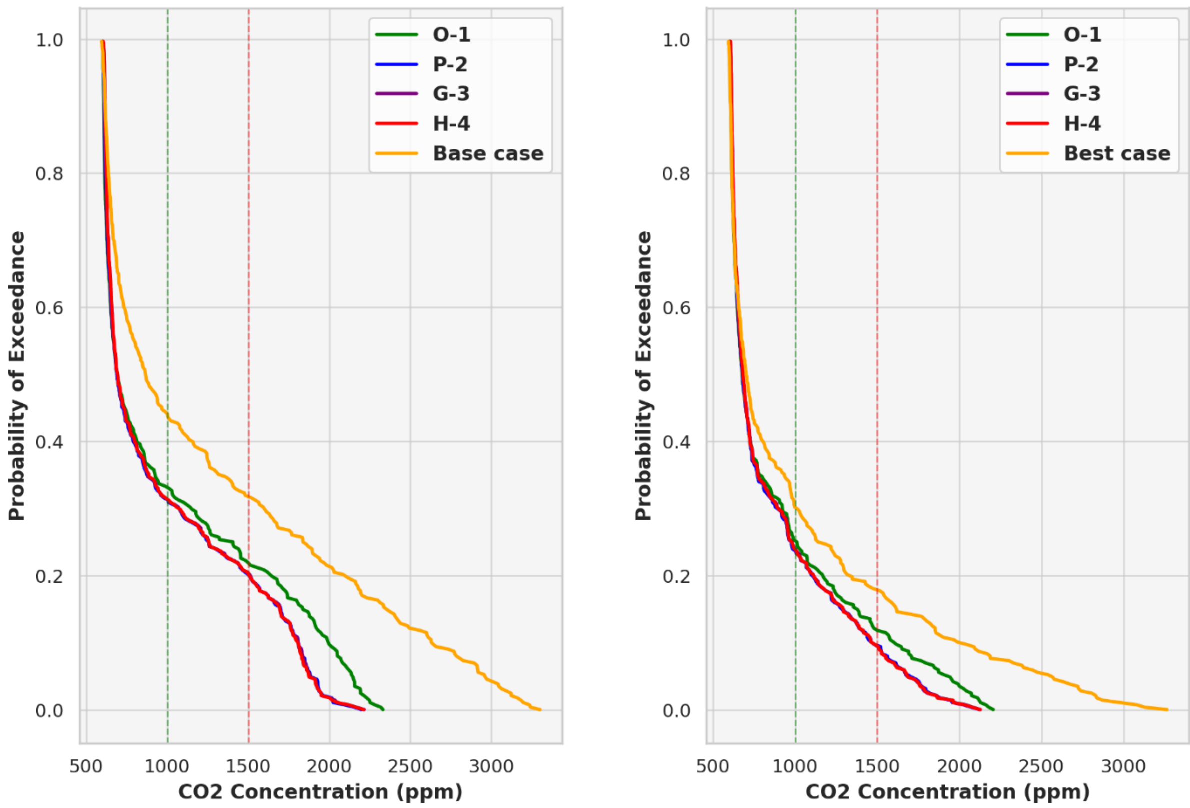

Figure 5.32: Probability of exceedance of CO_2 concentrations from the set thresholds (overall period).

This analysis provides the suitability and capacity of these openings to help in lowering CO_2 concentrations in the main bedroom. In terms of flow opening size and acoustic performance, P-2 is suggested to be best performing opening hence suggestive of larger $TL_{wall-opening}$ as area of the opening is smaller and transmission loss is higher (equation 2.42).

While P-2 is identified as the best performing opening, however the analysis primarily considers airflow and acoustic criteria only. This overlooks potential trade-offs such as flexibility in design integration and/or increased costs. Furthermore, the reliance on a single acoustic parameter, transmission loss (equation 2.42), may oversimplify the interaction noise control. By incorporating a broader set of acoustic performance indicators would provide a more balanced evaluation and can be suggested as future work.

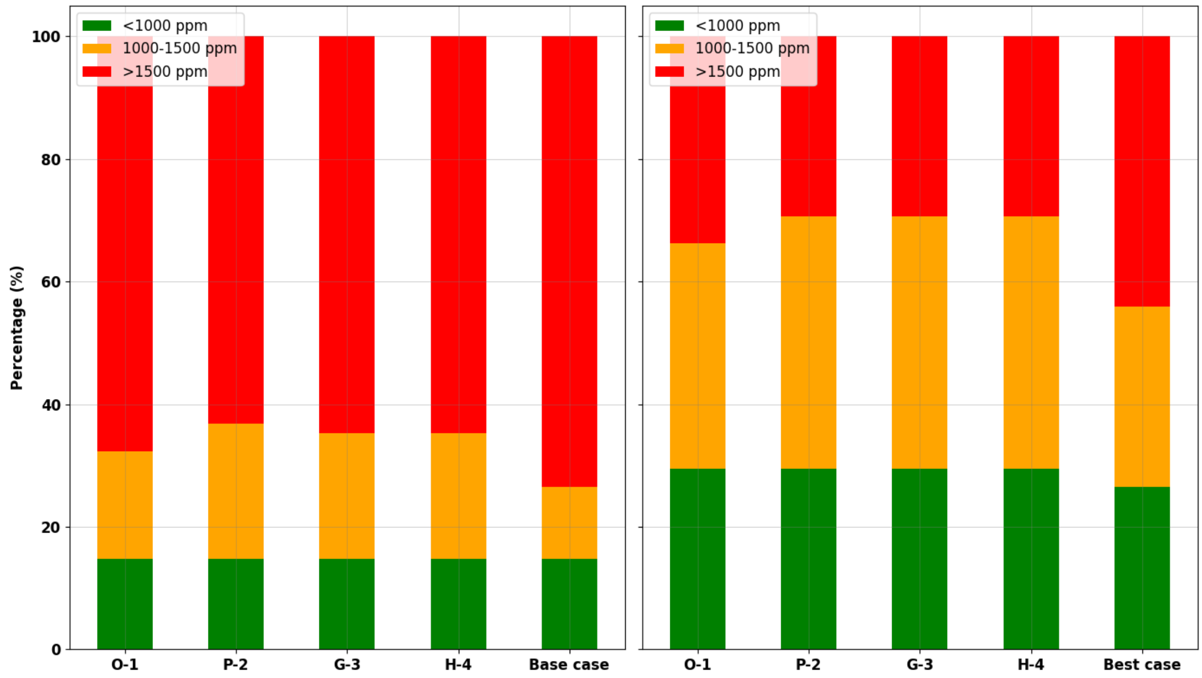

Figure 5.33: Safe, cautionary, and unsafe limits – Percent of time of CO_2 concentrations (occupied period). Left – Base case, Right – Best case.

The desired threshold of ≤1000ppm as per (Scottish Government, 2017) could not be maintained by any of the flow openings setup. However, the percent of time spend under the threshold of ≤1000ppm is higher with the opening of all 4 trickle vents in the room and added interzone openings. This further informs that the interzone openings can provide better IAQ but assistance in increased flow capacity is required via boundary level inlets/outlets.

It is important to recall that the South facing façade had high wind induced infiltration via cracks. While in the base case model, the trickle vents are present on the Eastern façade (lower wind induced flow rate potential) hence addition of trickle vents on Southern façade has large impact on the output.

This analysis will be helpful in suggesting a modified ventilation design aiming to maintain ≤1000ppm of CO_2 concentrations.

5.9 Phase I Modelling Discussion

The modelling procedure started with addressing the uncertainty in the selection of the equations and coefficients to model trickle vents and door undercut. This approach was taken as in the literature use of certain equations and coefficients is not justified. Aim of this procedure was to present comparative potential influence of using one equation/coefficient set over the other.

A step-by-step investigation approach suggested that correct use of discharge coefficient in modelling an opening with orifice equation is vital rather than using the default number 0.61.

Same is true for modelling an opening with power law model. In this case one should be aware of the fact that, without the correct selection of coefficient C and exponent n, the results can be erroneous. Crack flow component in ESP-r has limitations of use. However, in event of unavailability of data, this crack flow model can be employed to model smaller opening for which h<10mm.

Sensitivity of change in flow due to change in ΔP in case of the orifice and power law equation shows the dependency such that $\frac{dQ}{d\Delta P}$ is directly related to geometric and flow resistivity parameters.

The modelled ΔP and Q are discussed together with pressure coefficients, wind speed and direction which shows that during a high wind speed interval, especially on Day 6 of the study period, the pressure due to wind is on South façade has caused high flow rate with a strong correlation coefficient of 0.7. The monitored data also shows exceptionally low indoor CO_2 concentrations which suggests an alignment of weather data taken for simulation studies. However, the uncertainty of weather data remains the part of the model as weather station data is used rather than close to the site or onsite measurements.

This analysis is taken further to assess the model for potential of wind or buoyancy induced ventilation. Ar values suggest that on the day 3 and 6, flow is dominantly due to buoyant forces and wind induced forces respectively. This is further confirmed by applying the wind reduction factor and then comparing percentage difference in the CO_2 peaks between both versions of the AFN (with and out wind reduction factor) with Ar values for each day. This resulted in a power law curve fitting with $R^2 = 0.83$, and equation was expressed the form $\%Difference_{Peak} = a \times Ar^b$.

To address the importance of stack pressure in the total ΔP of the AFN, the Iteration with non-distributed crack with wind reduction factor is taken forward and crack heights were added for greater stack pressure. This approach was taken to evaluate the impact of increased stack pressure due to infiltration causing cracks on the flow solution.

With the increased height of the external node, wind pressure increases while with the higher flow component placement in the façade, the stack pressure increases. In the real-life situations, wind pressure varies at different points of the façade and a greater pressure is observed at the higher levels from the ground. With the inclusion of multi-level nodes and flow components, the flow network is expected to be “closer to the reality”.

At the final stage, to assess the validation of the model, CO_2 generation rate of the occupants is adjusted as per the limits found in the literature. CV(RMSE) was calculated for the occupied hours for each day. This procedure was carried out for both distributed and non-distributed cracks models i.e., Iteration 5* Log W and W_d.

Where CV(RMSE) provided insights into overall variability of the model, RMSEf was introduced to assess how accurately the model predicts CO_2 concentrations where safe/unsafe indoor CO_2 levels are a concern.

At the last stage of the investigation, to provide ground for the ventilation design study, additional interzone openings as well as full installed capacity of trickle vent opening area were utilised by using non-distributed cracks model (Iteration 5* Log W) with 0.9 MET as a base case. This analysis provided quantication of ability of these modifications to maintain safe CO_2 concentration in the main bedroom under worst case conditions.

The phase I modelling has not only highlited the importance but have also quantified the impact of inputs related to flow equations/coefficients, wind reduction and infiltration modelling for a ventialtion/IAQ study. This is done in an stage by stage manner and senstivity and the influenctial parameters are explored through statiscal and physical approaches. The outcomes of this study are utilised to form a guidance for AFN modelling.

5.10 Interventional Diary Modelling – Phase II

The previously investigated modelling parameters for the air flow and the loads are used to study a different time-period with varied airflow settings. The day 1, 4 and 5 would show the modelling of flow through the infiltration cracks, trickle vents and door undercut. While Day 3 and 6 would allow to explore the modelling for door and combination of door and window respectively.

Modelling of trickle vents is explained in detail in 4.8.2.2. The same approach is taken to model a different number of opened trickle vents in the room. The modelling of door and window is elaborated in the upcoming sections.

5.10.1 Modelling Results

The measured and simulated CO_2 plots are presented in the figure below. All days except for Day 5 show sufficient agreement with acceptable CV(RMSE) percentage.

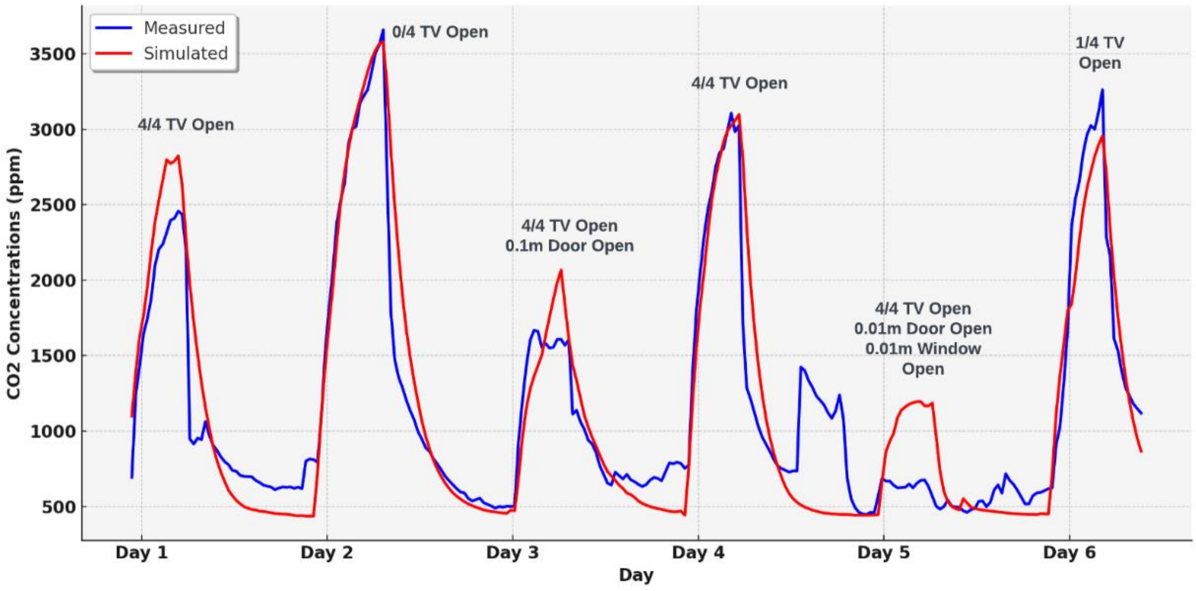

Figure 5.34: Iteration 5.1 LogW_d (0.9MET) measured vs simulated CO_2 concentrations.

	Day 1	Day 2	Day 3	Day 4	Day 5	Day 6
CV(RMSE)	17.47%	4.58%	19.02%	6.57%	66.73%	14.77%
Flow Influencing Components in the Main Bedroom	Infiltration, trickle vents and door undercut	Infiltration	Infiltration, trickle vents and door opening	Infiltration, trickle vents and door undercut	Infiltration, trickle vents and door and window opening	Infiltration, trickle vent and door undercut

Table 5.10: Iteration 5.1 LogW_d (0.8MET) CV(RMSE) and flow influencing inlet components for the main bedroom occupancy time.

The iteration 5* LogW_d (0.9MET) base case is tested for all these different combination as listed in the table above. All days have acceptable CV(RMSE)% error except for Day 5 which features a window opening. It is anticipated by observing large reduction in the measured CO_2 that the opening stroke length of 0.01m might not be accurately adhered by the occupants. Also, modelling of flow area caused by such a small stroke length of a window is not found in the literature. For this purpose, a sensitivity analysis of varied window and door opening stroke length combinations is conducted. In the next section, proposed modelling methods of door opening are evaluated via CV(RMSE)% error.

5.10.2 Modelling Methods of Door Opening on Day 3

Day 3 suggests the stroke length of the door set by occupants is 0.1cm. Three approaches were used to model this flow path.

Iteration 5.1 $LogW_d$ (0.9MET)	Bi-directional flow door component with geometric area and default C_d=0.61, $A_{eff} = 0.18\ m^2$.
Iteration 5.2 $LogW_d$ (0.9MET)	Spread of effective area at top and bottom of the door frame.
Iteration 5.3 $LogW_d$ (0.9MET)	Application of correction factor to Iteration 5.2 $LogW_d$ (0.9MET).

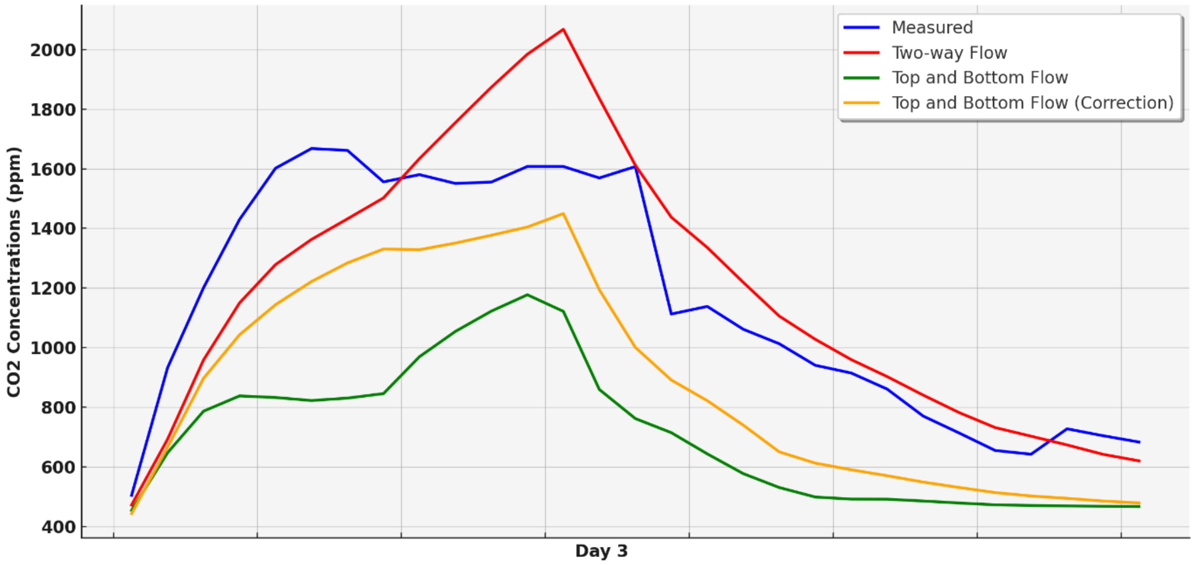

Figure 5.35: CO_2 concentration for Day 3 when door is opened for 0.1cm stroke length.

	Bi-directional Door Flow	Top and Bottom Flow	Top and Bottom with Correction Factor
CV(RMSE)	17.85%	43.35%	25.75%

The bi-directional door flow component has a lowest error while spreading the same area on top and bottom yield much greater error even though both methods offer same flow area. The third approach with correction factor is devised in the methodology.

This comparison shows how top and bottom part of an opening can behave as area of low resistance and how CO_2 peak is lower in this case as compared to the method in which a unit area is modelled using bi-directional flow component. The third approach assesses the solution in combination with correction factor.

5.10.3 Sensitivity Analysis for Day 5 Opening Areas (Iteration 5.4 Log W_d (0.9MET)

The occupants were asked to keep the door and window open for 1cm stroke length, however there is a great probability of some variation in setting this up. As this setup exceptionally exhibits high error percentage, combinations of the opening stroke lengths are applied. A range of 0.01m-0.03m stroke lengths for door and window both are set in the AFN, and 9 combinations are presented below as cartesian product of sets, door and window.

$$door = [0.01 \quad 0.02 \quad 0.03];\ window = [0.01 \quad 0.02 \quad 0.03]$$

The first number in the pair is for the door and second for the window.

$$Combinations = \begin{bmatrix} 0.01, 0.01 & 0.02, 0.01 & 0.03, 0.01 \\ 0.01, 0.02 & 0.02, 0.02 & 0.03, 0.02 \\ 0.01, 0.03 & 0.02, 0.03 & 0.03, 0.03 \end{bmatrix}$$

Figure 5.36 shows comparison plot of the 9 combinations with the measured data. It is evident by looking at combinations (0.01, 0.01), (0.02, 0.01) and (0.03, 0.01); variation in the door opening area has lower effect on the CO_2 concentrations when window stroke length is kept constant at 0.01m. While varying the window stroke length area is more effective for the dilution of CO_2.

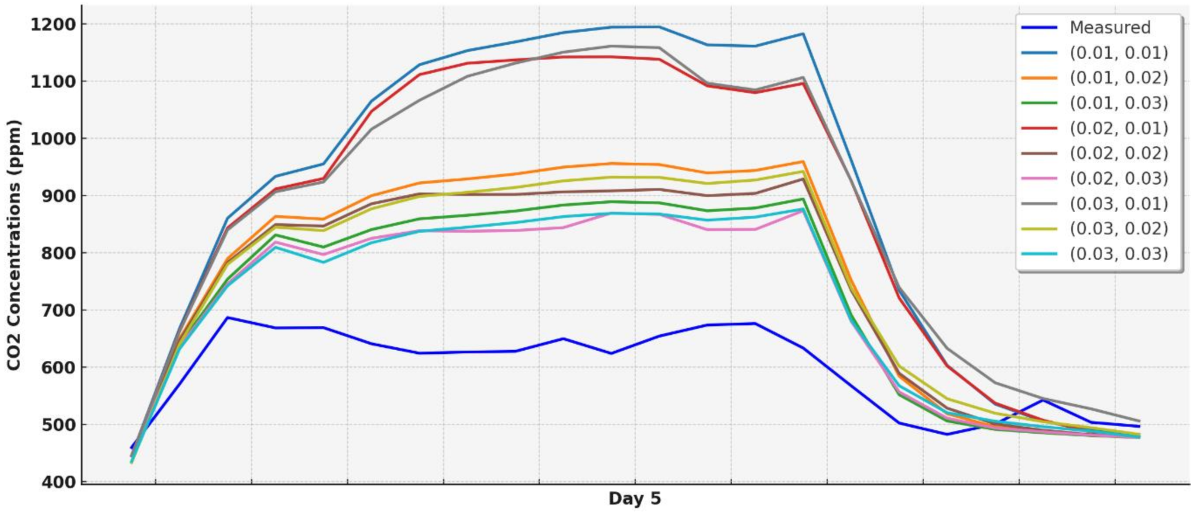

Figure 5.36: CO_2 concentration for all 9 combinations (door, window). Legend is sorted by peak values; measured plot line is exception.

The door stroke length of 0.02 m and window stroke length of 0.03 provides lowest CV(RMSE).

The analysis shows a clear trend in which increased opening sizes correlate with reduced CV(RMSE). Specifically, window opening has greater impact on the solution. The probable deviation between the instructed opening area and occupant set area is set as the base.

This exercise does not feed into any guidance aspect however provides insights into possible discrepancies in the intended and actual experimental setups. The recommendations can be generated from the analysis of Phase II modelling results such as with a greater detail available about the occupancy patterns as well as metabolic rates as well as aerodynamic properties of small slot shaped openings would provide greater accuracy in the modelling results.

Combination	0.01, 0.01	0.01, 0.02	0.01, 0.03	0.02, 0.01	0.02, 0.02	0.02, 0.03	0.03, 0.01	0.03, 0.02	0.03, 0.03
CV (RMSE) %	66.73	36.22	28.21	57.49	32.32	25.17	57.31	33.61	25.75

Table 5.11: CV(RMSE) for 9 combinations of door and window openings.

5.10.4 Phase II Modelling Discussion

The phase II simulation results, when the trickle vents and door undercut are only opened flow inlet with the infiltration cracks, are in a good agreement with measured CO_2 concentrations. For the day 3, when door opens for 0.1m stroke length, three modelling approaches are explored and their possible over and under estimation of the flow rate is proxied with simulated CO_2. It is observed that the determination of the effective flow area is a difficult task in the absence of sufficient data and contains wide range of possible uncertainties. The CV(RMSE) ranged from 17.85% to 43.35% when same opening of the door is modelled using three different approaches. These approaches were presented to further provide ground for a future work aimed at airflow through the doorways.

For the modelling of door and window combination on Day 5, the discrepancy is high. This infers either modelling equation is not able to model such small flapped opening area or the reporting of opened area by occupants is incorrect – or both. The literature does not provide flow coefficients of the flapped window opening of a 0.01m stroke length. Thus, a calculated geometric area for window is used with default C_d of 0.61. For door opening, as for Day 3, the bi-directional flow opening had good agreement with measured CO_2 results, same approach was used but for stroke length of 0.01m. Here it is important to note that for the Day 5 door modelling, door undercut is considered as flow path as opposed to Day 3. Reason being, for such small crack opened door, the door undercut would behave as a separate channel and would allow lower resistance as compared to vertical cracked opening.

5.11 Learnings and Outcomes

This chapter discusses available data set for the case study and available parameters to develop an AFN model.

A step by step, iterative approach and combination of statistical and physical analysis has enabled to gain insights into the level of uncertainty which entails in defining of flow components via different set of equations and coefficients. The statistical approach points out the magnitude of variability between iterations while the physical analysis further confirms the difference. Through this combination, efforts have been made to elaborate the importance of correct use of variables.

The learnings from a standard diary phase I modelling are applied in interventional diary phase II modelling. Trickle vent and the door undercut modelling insights from the phase I learnings were used to model different number of trickle vent openings for different weather conditions and occupancy schedules of Phase II. The CO_2 output well matched the simulated data without the need for calibration or input adjustments. This indicates that in a design study, one can safely use this method to model such openings. However, the requirement of aerodynamic testing of door undercuts remains important.

The set of approaches extracted from the literature are used to model the door opening on Day 3 and a comparison is presented. For the study's specificity, the lowest error was found by modelling door by the default technique available in the ESP-r.

For Phase II Day 5, door and window modelling had higher error percentage specially for a small opening of 0.01m of the stroke length. Unavailability of modelling specifications for such a narrowly opened flapped openings as well as uncertainty in the actual opening area by the occupants of the room possibly have caused such a large error. Hence sensitivity related to window and door opening stroke length is analysed and error percentage close to acceptable limit was achieved.

The modelling knowledge gained through the step-by-step process adopted in this chapter would lay foundation for the modelling guidance followed by example design study to be presented in the next chapter where an improved ventilation design is also assessed.

5.12 Non-Evaluated Approaches and Recommendations

In the literature review, for each integral AFN element, a set of modelling approaches were presented. Introduced case study could not evaluate them in entirety. For this purpose, an account of non-evaluated approaches is presented in this section providing grounds for the potential future work.

The review of modelling of infiltration cracks (section 2.5.2) suggest that flow exponent value n is an important parameter influenced by crack's height. Greater characteristic dimension of the crack allows turbulent flow while hairline cracks would allow a laminar nature of airflow. However, studies have shown that, overall, flow nature in a building envelop is developing in nature. The modelling case study has approximated a horizontal crack with vertical characteristic dimension to be set at 2mm. For more realistic approach to define cracks equating to leakage area, component specific coefficients can be used which are available in literature for better approximation of the air flow due to infiltration. This can be aided by sensitivity analysis of n value on the modelling outputs.

In section 2.7.4 which concerns effective area of a window related to its aspect ratio and opening angle/area. Due to small opening stroke length and unknown factors such as frame thickness and accurate opening angle, the proposed approach of using free area analytical model (SEAM) could not be applied.

For extract fan modelling (section 2.9), flow inducer equation is alternative representation of extract fan to constant flow equation. As measured flow rate data for extract fans in the case study house was available, a straightforward approach is to model such flow component with constant flow equation. However, the manufacturer supplied data fan performance curve can be interpolated for specific flow rate. Both approaches i.e., constant flow vs flow inducer can be compared for their impact on the solution of ΔP and flow rate.

As literature suggests, wind pressure can be responsible for high uncertainty to a model while modelling study confirmed that it has second highest influence coefficient after metabolic rates. In section 2.11.6, 3 different datasets for pressure coefficients are available to apply with their limitations. The study only employs built in pressure coefficients database and does not compare the impact on solution for other set of databases. Such comparison would allow to take an informed decision when using one or the other database to compute wind induced flow.

These non-evaluated approaches are further discussed with a perspective of recommendations of future work in conclusive chapter, Chapter 7.

Chapter 6 Development of Ventilation Design Guidance and Example Application to Design for IAQ.

The literature and case study analysis have shown deficiencies in current design process and can inform new guidance and methods that address these deficiencies. In this section guidance is put forward to directly inform and provide an approach for worst case ventilation design for IAQ using AFN. The application of the guidance and approach to design for IAQ is then illustrated with an example application.

6.1 Guidance on AFN Modelling for Design

The AFN models a dwelling in terms of 'nodes' that represent either outdoor or indoor physical conditions at specific locations. Nodes are then connected to each other via 'flow paths' connected through ventilation 'components' such as cracks, trickle vents, windows, ventilation openings, doors, and fans with ducts and grilles.

Pressure differentials between nodes provide the driving force for air movement along the flow paths while the components provide the resistances to that air movement. Pressures at specific nodes are influenced by air density, height, temperature, barometric pressure, wind speed and direction. Component resistances are determined by geometrical factors and material properties.

Once a representative network has been established then a solver is used to compute the pressures and mass flows at each time step. These mass flows can be used together with CO_2 background and CO_2 metabolic generation rates to compute CO_2 concentrations at each node. All of the elements involved require to be specified and modelled correctly in order to support a robust ventilation design evaluation.

The purpose behind this guidance is to build on and adapt to the domestic domain existing guidance for AFN modelling of ventilation such as in CIBSE AM10 (CIBSE AM10, 2005) and AIVC Guide 5 (Orme & Leksmono, 2002) and provide a guidance document specifically for use in the design of domestic ventilation through natural and assisted natural ventilation i.e., dMEV and intermittent extract ventilation. Initially the guidance will be offered as an addition to the ESP-r ‘Cookbook’ (Hand, 2018), however it is intended for a wider application.

The guidance is for using AFN in building simulation at design stage targeting ventilation rates and CO_2 levels which are the Key Performance Indicators (KPIs) required to meet building regulations and IAQ/IEQ standards. The use of AFN in energy performance and overheating calculations is noted and discussed in the next chapter but not the main focus of the current work.

Guidance on the correct representation of the dwelling, its surroundings, internal zones, ventilation flow paths, and ventilation components to support robust design are given in the following sections:

1. Air Flow Networks, Zoning, and the Placement of Internal and External Nodes
2. Flow Path and Components: Selection and Placement
3. Modelling of Infiltration through Unintended Openings (Internal and External) using 'Crack' Components
4. Modelling of Purpose Designed Trickle Vents
5. Modelling of Window Openings
6. Modelling of Internal Doors and Door Undercuts
7. Modelling of Purpose Designed Interzone Ventilation Openings.
8. Modelling of Stairwells
9. Extraction Fans (Zone to Zone, Internal to External, Ducts and Grilles)
10. Occupancy and Metabolic Rates
11. Weather, Design Periods and Sheltering
12. Application of AFN to IAQ, Overheating, and Energy Performance Studies
13. Example application of AFN to ventilation design for IAQ

6.1.1 Air Flow Network, Zoning and Placement of Internal and External Nodes

Zone - Definition

A 'zone' is defined as a volume of air with molecules that are free to mix and can be represented by the same physical properties. Occupying a defined physical space, they are only connected to other zones through ventilation components such as doors or ventilation openings. Zones normally correspond to individual rooms and other spaces in dwellings such as storage spaces, ensuite rooms.

Representation of Internal and External Conditions via Nodes

Internal zones are represented by a node placed at the central point. All zones within the dwelling need to be explicitly included with appropriate flow paths including insulated attics and basements (ATTMA, 2016), it is not sufficient to model an isolated room or floor unless that part of the dwelling is completely hermetically sealed (i.e. never the case in dwellings).

Stairwells, which extend over more than 1 storey in a dwelling, should be represented by 1 node for each individual storey, at the same height as nodes representing other zones on the same storey of the dwelling.

External nodes represent local outside conditions adjacent to each element of the facade with different pressure and wind conditions. The external conditions are set using a 'climate file' with 'wind speed' and 'wind direction' plus a dwelling specific 'wind reduction factor'. External conditions are referenced to the Azimuth angle measured in degrees clockwise from the North (see section 6.1.11). In a multi storey dwelling, multiple vertically extended external nodes should be placed centrally outside each distinct external facade element (according to azimuth and sheltering) at the same height as the internal zone nodes for each of the storeys of the dwelling (including attics and basements unless hermetically sealed).

It is important to consider that with the increased height of the external node, the factor of height increases the pressure solved at the node i.e., ρgh.

6.1.2 Flow-path and Component Selection and Placement

Flow paths between nodes in AFN models are associated with mass flows through explicitly defined components.

A Component is an equation with specific input parameters which can represent 'designed ventilation airflow elements’ such as trickle vents, windows, doors, door undercuts, fans, ducts, grilles, room to room ventilation openings etc. and can be directly associated with specific physical features.

A specific ‘Crack’ Component with appropriate equation and input parameters can be used to represent ‘unintended infiltration airflows'. These unintended infiltration airflows could potentially be associated with designed ventilation airflow elements e.g. leakage around edges of closed doors or windows but may also be associated with unknown flow paths related to specific construction details (plugs or light fittings, leaky loft hatches etc.) or defects (lack of sealing around soil pipe, cracks or permeable joins between building elements etc.). As infiltration flow components (cracks) are not designed there is uncertainty around their specifics, so specific assumptions need to be made depending on the purpose of the design study.

To represent the physical behaviour of components when solving flow rates and determining the nature of airflow (laminar, turbulent and developing), it is important to use a component that has correct set of equations and coefficients. This practice would tackle the inflated uncertainties in the model. The main selection criterion for component and equation is the vertical height (h) of the flow path as shown in Figure 6.1. Table 6.1 gives a summary of the selection criteria for each of the possible components and equations and describes in more detail the component types, criteria, equations and input parameters recommended in this guidance which will be explained in more detail in the following sections.

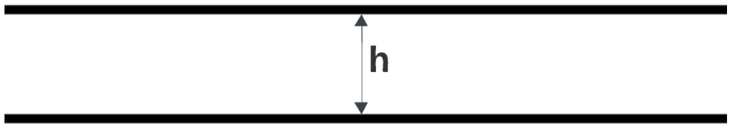

Figure 6.1: Characteristic dimension on which criterion is based.

Criteria	Equation
h<10mm	Power Law Equation 6.1
10cm>h≥10mm	Orifice Flow Equation 6.4
h≥10cm	Bi-directional Flow Equation 6.5

Table 6.1: Overview of modelling equations based on opening size.

Component	Dimension Criterion	Model/Equation	Specific Characteristic	Required Input Parameters	Referenced Sections
Crack (Infiltration)	h < 10mm	Power Law	h = 2mm	Flow exponent n, Flow Coefficient C (equation 6.2, 6.3)	6.1.3
Trickle Vent (horizontal slot)	N/A	Orifice Flow	N/A	Effective area=C_d*Geometrical Area	6.1.4
Sliding Window (Slight Opening)	h ≥ 10mm	Orifice Flow	C_d = 0.61	Geometrical Area	6.1.5
Flapped/Hinged Openings (Doors/Windows)	h ≥ 10cm	Bi-directional Flow	Use SEAM model for effective area (equations 6.6-6.8)	Aspect ratio (w/h), opening angle θ	6.1.5
Door Undercut	h ≥ 10mm	Orifice Flow	C_d = 0.35	Geometrical Area	6.1.6
Interzone Opening	N/A	Depends on specifics	N/A	Depends on specifics	6.1.7
Stairwell opening	h ≥ 10cm	Bi-directional Flow	C_d = 0.61	w, h based on stairwell specifics	6.1.8
Fan	N/A	Flow inducer equation	N/A	Fan Curve Data	6.1.9
General Opening	h ≥ 10cm	Bi-directional Flow	C_d = 0.61	w, h	

Table 6.2: Detailed modelling criteria for specific types of openings

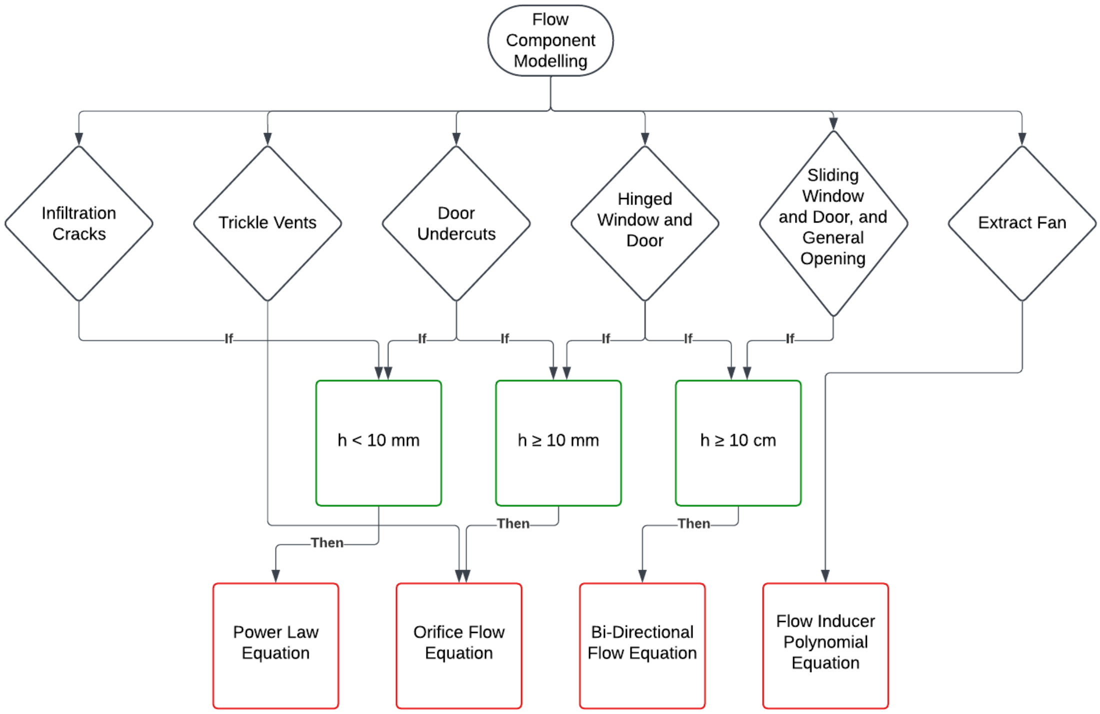

Figure 6.2: Decision tree to model a flow component. Complimenting the table above.

Overview of Equations

Starting with the unintended flow pathways accounting for infiltration, the power law equation, also known as crack flow equation, should be used with appropriate input values. The equation is given as follows:

$$Q = C \times (\Delta P)^n \qquad 6.1$$

The input parameters are the flow coefficient C and flow exponent n. Coefficient value is determined by the geometry of the pathway and flow exponent is governed by the flow regime. For infiltration flow through cracks, both of these values are approximated from geometrical factors using an analytical set of equations (J. Clarke, 2007) given as:

$$n = 0.5 + 0.5exp\left(-\frac{h}{2}\right) \qquad 6.2$$

$$C = L9.7(0.0092)^n \qquad 6.3$$

Where h (mm) is the height and L (m) is the length of the crack. This model is applicable to the openings measuring less than 10mm of height. The crack component equation is also applied to any gaps with measurable dimensions such as door undercuts if they are less than 10mm in height.

For openings with height ≥10mm but less than 10cm, the orifice flow equation should be used.

$$Q = C_d A \sqrt{\frac{2\Delta P}{\rho}} \qquad 6.4$$

The input parameters are coefficient of discharge C_d and geometric area A (m^2). If the effective area of the opening is known, then it would replace the product $C_d A$ in the equation above.

This equation is usually applicable to trickle vents, door undercuts of 10mm or above and larger slit shaped horizontally elongated openings.

As the height of an opening increases, there is a greater chance of bi-directional flow due to density difference of air between zones. For openings with height >10cm, the following equation 6.5 (Cockroft, 1979a) should be used:

$$Q = \frac{2}{3}\left[C_d \times w \times h \sqrt{\frac{2}{\rho}}\left(\frac{C_a^{\frac{3}{2}} - C_b^{\frac{3}{2}}}{C_t}\right)\right] \qquad 6.5$$

Similar to the orifice equation C_d and geometry are the key inputs however the height and width need to be explicitly entered. The opening height h is the determinant factor for bi-directional flow; hence it must be input directly. A second height parameter has to be input (h_p (m)) representing difference in height between the base of the opening and the adjacent internal node. The other coefficients in the equation are calculated in the AFN solver from h_p, h and ΔT between zones. Application of this bi-directional flow equation is relevant to doorways, windows and any other openings meeting the criteria of h≥10cm.

For the specific case of hinged/flapped openings i.e., doors and windows, the Statistical Effective Area Model (SEAM) (equations 6.6-6.8) can be used to calculate the C_d to be input to the bi-directional flow equation.

$$B = 0.18e^{-0.78\left(\frac{w}{h}\right)} + 0.61 \qquad 6.6$$

$$M = 0.016\left(\frac{w}{h} + 1\right) \qquad 6.7$$

$$C_d(\theta) = \mathrm{B}(1 - \mathrm{e}^{-M\theta}) \qquad 6.8$$

Moving from passive flow openings, mechanical extract fans are modelled using the fan curve data into polynomial equation in which ΔP is the total pressure difference, m is the mass flow rate, ρ is density of the fluid and a_i are the fit coefficients. The user must specify four points of flow and pressure so that $Q_{min} \leq \frac{m}{\rho} \leq Q_{max}$.

$$\Delta P = a_0 + a_1\left(\frac{m}{\rho}\right) + a_2\left(\frac{m}{\rho}\right)^2 + a_3\left(\frac{m}{\rho}\right)^3 \qquad 6.9$$

Further details are described in the following sections.

6.1.3 Modelling of Infiltration Through Unintended Openings (internal and external) Using 'Crack' Components.

Flow pathways involved in infiltration are unintended and their location and geometry are unknown. They can occur in external facades between internal and external nodes but also will be present between internal nodes. Their resistance to airflow between nodes can be inferred using actual or simulated blower door test results etc.

To represent these unknown pathways a 'crack' component is used. This 'crack' component represents a horizontal narrow opening with a vertical height (h) of around 2mm and with a length (L) scaled to match the required infiltration level.

As the number and locations for the actual infiltration flow path crack components is unknown some standard approaches are taken dependent on the objectives of the specific study. Figure 6.3 shows a crack component.

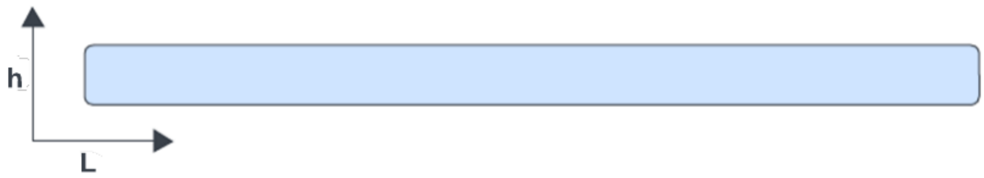

Figure 6.3: Height and length of a crack, where L×h is crack leakage area.

To represent crack components in AFN, the power law equation is used to model the relationship between the Volume Flow Rate Q (l/s) and Pressure Differential ∆P where C is the flow coefficient, and n the flow exponent (equation 6.1)

Input Parameters for crack components (h, L_{total}, L_{zone}, L_{ind} number and position of cracks):

The number and position of cracks, plus the individual crack dimensions (height h) and Individual crack Lengths L_{ind} are the inputs required to define each the individual crack components in the AFN. The following equations then use these input parameters to compute the Flow Exponent and the Flow Coefficient for individual cracks are determined from the standard equations (6.2 and 6.3):

The dimensions are of course unknown however the assumption is that infiltration flow is a mixture of laminar and turbulent and the convention is to set the vertical height (h) for the crack component to 2mm. This gives a flow exponent (n) for all cracks of 0.65 (Walker et al., 2013) from equation 6.2. Setting the vertical height of the crack for as an 'averaged' flow regime would allow to reduce uncertainty in specifying flow exponent and coefficient values.

The Total Crack Length L_{total} is set based on the target blower door airtightness. L_{total} should be determined from a blower door test simulation (50Pa of ΔP in still wind conditions) using a simple single zone model to represent the dwelling under study with only 1 single crack component of h=2mm in the dwelling external façade and adjusting the total (single) crack length to give the blower door/target air change rate.

The crack length per zone is not known, in the absence of data the approach recommended here is to distribute the crack length across zones based on the zone to total window ratio. Where L_{zone} is the length of the crack of each zone.

$$L_{zone} = \frac{Number\ of\ Windows\ in\ Zone}{Total\ Windows\ in\ the\ Building} \times L_{total} \qquad 6.10$$

The number and position of cracks per zone is not known. In the absence of data two different approaches are recommended:

(i) Maximum crack distribution over height of façade i.e. cracks at top and bottom of the facade above and below each window (best case for infiltration on still days), or

(ii) single dominant crack positioned at head of window (worst case for infiltration on still days).

The first should be used for energy analysis while the second should be used for ventilation and overheating studies.

The number and lengths for individual cracks are then determined from L_{zone} based on the view taken on crack distribution e.g. if there are 3 windows in a zone and the study is for air quality then 3 crack components each with $L_{ind} = L_{zone}/3$ and each positioned at the height of the top of the window; if there are 3 windows and the study is for energy or overheating then there are 6 crack components each with $L_{ind} = L_{zone}/6$ placed at the top and bottom of the facade above and below each of the windows.

The above approach apportions the infiltration leakage to the windows, for zones without a window (e.g. a cupboard) it is necessary to also have a crack component for correct operation of the AFN solver so a connection should be made to the outside through a small crack with h=L=0.1mm[1].

[1] Highly resistive long flow paths may result in an error for the flow solution.

Representing Inter-zone Cracks in an AFN Model

Infiltration is possible between the internal zones. Leakage paths around doors would be an obvious location for a crack but others are possible e.g. at floor / skirting board junction, associated with light fittings, sockets and other services etc. Even a fire door is fitted with clearance up to 2mm-4mm (BS 8214:2016, 2016).

There is no testing or little literature to give insight into inter-zone infiltration through unintended cracks so here it is suggested that a somewhat worst-case assumption for air movement is made with a crack of h=2mm, and L = 'width of the door opening', at the top of the door is used (J. Clarke, 2007).

Limitations

It is important to consider the limitations of this approach. Firstly, the selection of flow exponent value is an approximation which has a large impact on the flow solution. Secondly the locality of cracks is prone to vary significantly. Both of these variables are well explained in the literature review section and input suggestion should be used with caution.

6.1.4 Modelling of Purpose Designed Trickle Vents

Trickle vents are elongated, slot shaped, purpose provided aerodynamic openings which are intended to provide a flow pathway between outdoors and indoors. They are typically installed at the top of the window frame. It is less common but also possible to have vertical trickle vents, these are covered separately at the end of this section.

Representing Horizontal Trickle Vents in an AFN Model

Trickle vents are laboratory tested (Standard, 2004) and standard data for Effective Area A_{eff} is available. A_{eff} is measured in mm^2 and can be used with appropriate units in the standard orifice flow equation 6.4. Use of this parameter would allow the modeller to set the appropriate aerodynamic performance of the tricklle vents.

$$A_{eff} = C_d A$$

Size, Number and Placement of Trickle Vents

In a design evaluation, the starting point is to provide the minimum trickle vent A_{eff} for each dwelling zone according to the applicable building regulations. These should be implemented as in the actual design, this will normally be to apportion the trickle vents along the top of the windows frames with lengths to suit the frame size, and the individual trickle vent A_{eff} adjusted to give the flow area required for the zone. The size of trickle vents is a parameter can be optimised in the design process to achieve the required performance or regulatory criteria.

Special Case of Vertical Trickle Vents

In case of vertical trickle vents, due to the dimensional extent of the slot, there is a strong possibility of bi-directional flow and so the bi-directional flow equation must be used (The equation and its inputs are detailed in the section 6.1.5).

As for horizontal trickle vents, effective area is a required input. However, in this case the height, width and C_d need to be explicitly input into equation 6.5. The geometric height and width should be used, and the appropriate C_d calculated; $A_{eff}/(h \times w)$. A further input into the equation is the height difference between the base of the opening and adjacent nodes (h_p).

$$A_{eff} = C_d \times w \times h$$

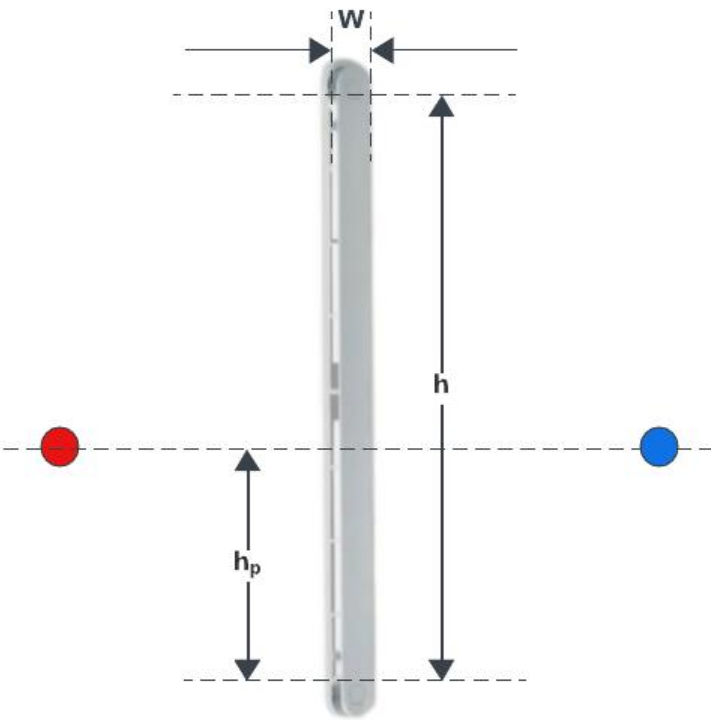

Figure 6.4: Nodal setup with height and width layout for a vertical trickle vent.

Important Considerations

- For both horizontal and vertical trickle vents the geometric cross-sectional area of trickle vent slots must not be used in combination with C_d=0.61. This approach can overestimate the flow by ~100% as indicated by (Karava et al., 2003) via an experimental study.
- h_p is the difference in height expressed as a positive number. (A negative h_p will lead to a negative neutral height i.e., below the base level which is not physically possible for a bi-directional opening).

- The height of nodes on either side of a bi-directional component should be the same specially when representing a vertical flow component.

6.1.5 Modelling of Window Openings

A window opening is normally a glazed and framed panel fitted in a frame which can be adjusted to allow airflow, aimed to provide ventilation allowing the occupant (or an automated control system) to adjust the indoor environment. Flow through such an opening varies with wind speed and direction, sheltering, temperature differences, aspect ratio of the frame and angle of the opening (Grabe, 2013; Heiselberg et al., 2001; P. Sharpe et al., 2021). A categorisation of popular window mechanisms is shown in Figure 6.5 and their modelling in AFN is explained in the next section.

Note that for worst case IAQ design these window openings are normally closed (only trickle vents can normally be assumed to be open). For energy performance and for summer overheating studies different assumptions would be made e.g. there may be an assumption that there is a 'secure opening' that can be left constantly open, or an assumed 'occupant opening' schedule based on some algorithm around occupancy, comfort, and temperatures.

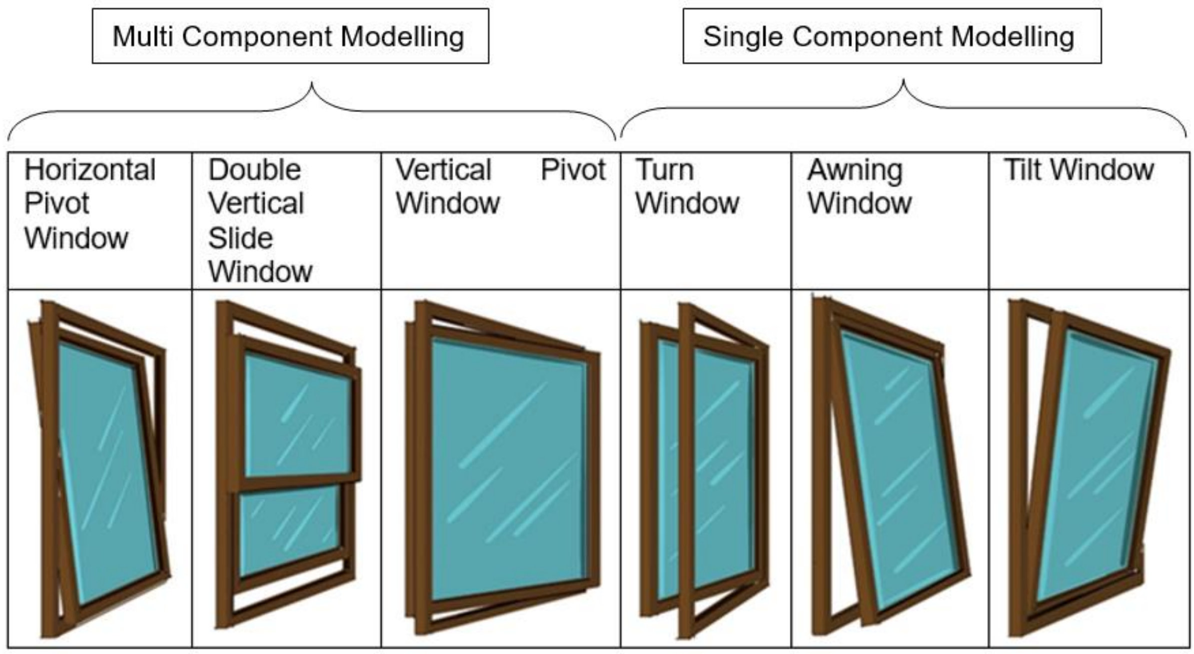

Figure 6.5: Categorisation of windows based on symmetry.

Translating Window Openings into an AFN Model

Six of the most used window mechanisms are identified in Figure 6.5. The 3 on the right (turn, awning and tilt) are hinged at an edge and there is a single window opening made up of two triangular and one rectangular element modelled together and categorised here as Single Component Modelling. The other 3 on the left (horizontal pivot, double vertical slide window, and vertical pivot) effectively create two separated openings and can best be represented by 2 separate components in an air flow network - categorised as Multi Component Modelling.

Representing a Double Vertical Slide Window in an AFN Model

The Double Vertical Slide window has a simple sharp edged rectangular geometry for each of the paired top and bottom openings. Each of these two individual openings should be modelled using the appropriate equation and input parameters based on the height of the centre of the individual opening.

If the individual opening has a height greater than 10mm and less than 10cm then an orifice flow component (equation 6.1) is appropriate, where A = geometric open area, and C_d=0.61. Larger heights (>10cm) should be modelled with a bi-directional component (equation 1.2). Each of the 2 components should be positioned in the network at their centre height, usually towards the top and bottom of the frame. Where a vertical slide window is only open at the top or the bottom then a single component is used to represent that situation.

Placement of this individual component in the façade is by specifying the centre height of each opening with respect to outdoor and indoor nodes e.g. as show in Figure 6.6.

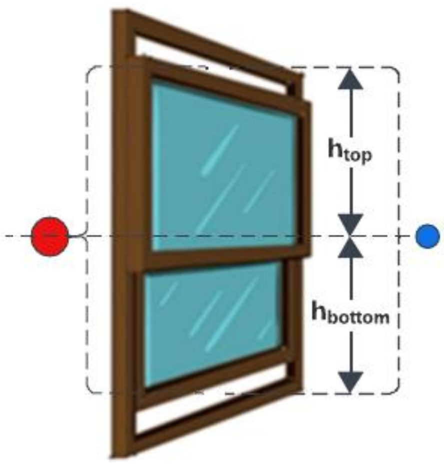

Figure 6.6: Nodal setup determining the placement of openings for double vertical slide window.

Representing Single Component Hinged Windows (Turn, Awning and Tilt) in an AFN Model

There are triangular element to the sides of the opening which must be taken into account, also, these types normally have a vertical extent >10cm which will support 'two-way' flow so the bi-directional flow equation component (6.5) should must be used, the input parameters are C_d, w and h.

To model such windows, the gross extents w and h are input into the equation as depicted in the Figure 6.7. C_d is then calculated using the ratio of w and h in equations 6.6 and 6.7 and the angle of opening input into equation 6.8 to calculate the appropriate C_d. This equation set is from the Statistical Effective Area Model (SEAM) (P. Sharpe et al., 2021). It is found important to be mindful of the measurements of w and h and only use moveable flap's measurements rather than the window frame.

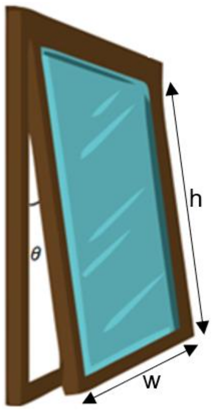

Figure 6.7: Aspect ratio of the flap and opening angle for an awning window.

The placement of the flow component in the network is represented by the h_p parameter which captures the differential height magnitude (and pressure differential) relative to the reference nodes as shown in Figure 6.8.

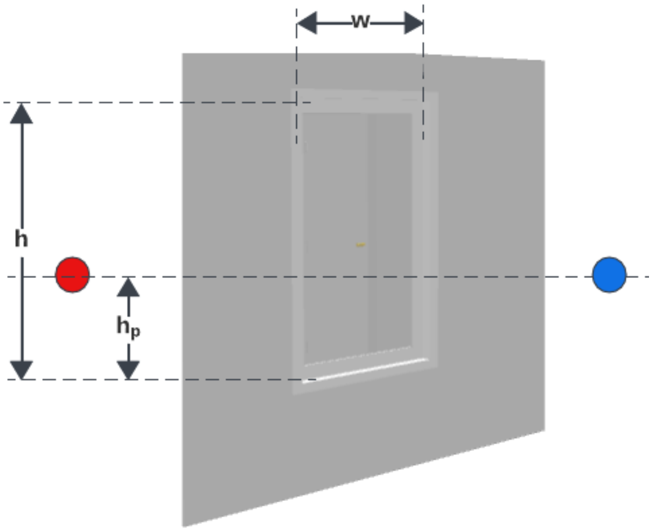

Figure 6.8: Nodal setup, aspect ratio and hp to elaborate the placement of a window in AFN.

Representing Multi Component Hinged Windows (Horizontal or Vertical Pivot) in an AFN Model

For multicomponent windows with more complex hinged geometry i.e. the horizontal and vertical pivot in Figure 6.5 where a plane divides the opening area to effectively form two single component windows, each of the two single components are considered separately in determining the appropriate component type and placement in the AFN network. Figure 6.9 shows the dividing plane for horizontal and vertical pivot windows.

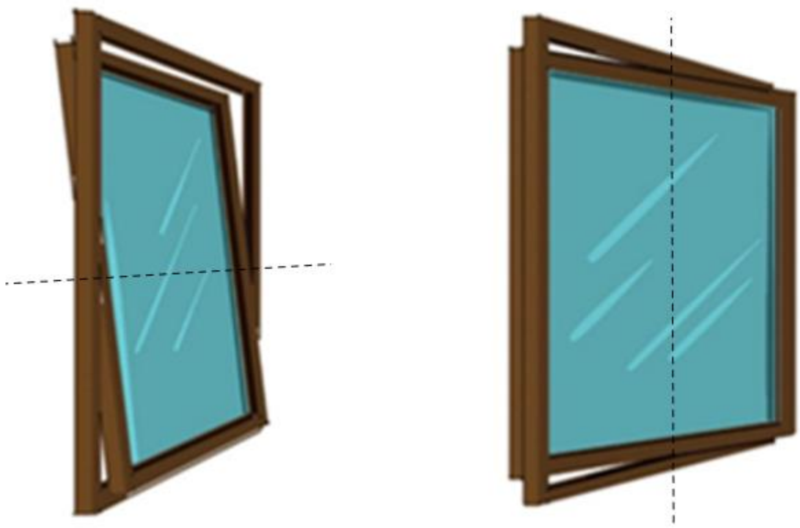

Figure 6.9: Dividing planes for multicomponent window mechanisms; left: horizontal pivot window, right: vertical pivot window.

For the example shown in Figure 6.9, the bi-directional flow component equation 6.5 is used for each of the two individual opening components. Each opening component in this example would follow the same approach as for the hinged single component window described in the previous section.

For example, for the horizontal pivot window shown in Figure 6.10, where the pivot is half the whole window vertical height, each component will have a height half of the whole window height input to equations 6.6 and 6.7.

The h_p inputs for these hinged multi-component windows are shown in Figure 6.10. A horizontal pivot window would have two separate flow components with h_p and h_p' for the 2 components as shown. While a vertical pivot window also has two components, but each has the same value i.e. $h_p *$ in the figure.

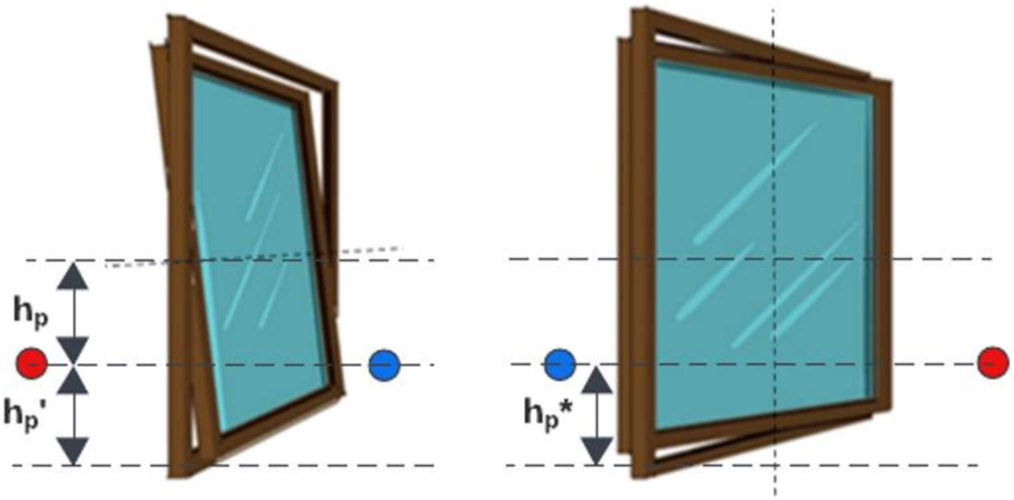

Figure 6.10: Distances between window component(s) base and zone nodes; left: horizontal pivot window, right: vertical pivot window.

Modelling tools also offer controls feature to set open or closed state of a flow component. It is advisable to set appropriate control setting for windows as well as other flow components as per the TUS data.

6.1.6 Modelling of Internal Doors and Undercuts

An internal door is a flapped inter zone opening which is used to close off an entrance or passage within a dwelling which is capable of bi-directional flow due to temperature difference between zones and the vertical dimension of the opening.

Representation of an Opened Door in an AFN Model

Doors are normally > 10cm in height and therefore modelled using the bi-directional flow component (equation 6.5). For a regular hinged door the input parameters are obtained from the SEAM model[2] in a similar way to the side hinged 'Turn' window described in the section above (P. Sharpe et al., 2021). In the case of sliding doors or doorway passages with a sharp geometric shape, the geometric width and height of opening, and C_d=0.61 should be used similar to the case of sliding windows.

Representing Door Undercuts in an AFN Model

A door Undercut is a deliberate gap left under an interior door which allows air to flow between zones. In the context of dMEV and MVHR systems undercuts are normally required to facilitate the adequate distribution of fresh air.

Door undercuts are key components in dwelling ventilation schemes and must be carefully modelled in an AFN. Typically, the height of an undercut is >10mm and an orifice flow component is appropriate. There is currently no standard method for determining Effective Area A_{eff} for a specific situation e.g. taking account of door thickness and construction, floor finish etc. In the absence of a standard test for effective area it is recommended that the geometric cross-sectional area L×h (Figure 6.11) must be used, together with an appropriate C_d. There is a shortage of literature but a value of C_d=0.35 is suggested (Klote & Milke, 2008; Mckeen & Liao, 2019) (lower than for a sharp-edged orifice). Door undercuts, in practice and in modelling, is an area where standards could be improved.

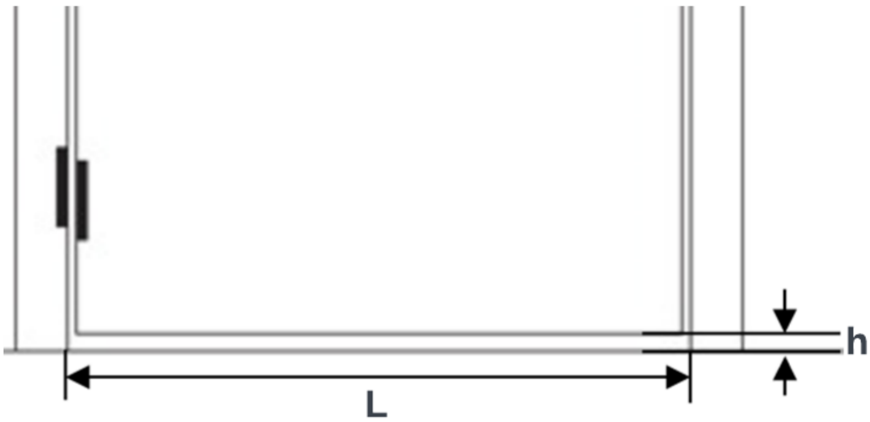

Figure 6.11: Height and length of a door undercut, where L×h is Geometric Cross Section Area.

6.1.7 Modelling of Purpose Designed Interzone Ventilation Openings

Purpose provided interzone openings between zones within a building are becoming more common, aimed at facilitating airflow while mitigating ingress of unwanted sound. These

2 As this model is based on window opening data and takes account of reduced flow efficiency of the side triangles of the window however to apply it to doors, this efficiency is not identical for both triangles formed (top and bottom) by a door opening. Hence application of SEAM to a door entails greater approximation.

openings are normally introduced in internal walls at a height such that visual privacy is not compromised. Such openings are normally tested to standards for acoustics and aerodynamics; hence data is available to allow their representation in AFN.

Aerodynamic test data for such openings is normally available, the same approach as for trickle vent components can be used in which the standard test effective area A_{eff} is input into the orifice equation component, or alternatively the standard test values for n and C values for the power law equation component can be used if these are available. The situation when aerodynamic values are not available, it is highly advisable to refer to literature for closely resembling opening types.

6.1.8 Modelling of Stairwells

In the case of stairwells, each storey is to be modelled as a separate zone with a node at the same height as the other nodes on that storey. The vertical flow between one storey and the next is, in reality, through a complex 3D geometry. The normal convention is to model this as a simple unidirectional orifice flow component between the adjacent vertically separate nodes, with the area equal to the footprint of the base of the stairwell. In the context of domestic building, the ΔT between the floors is small enough to support use of C_d=0.61 (Wetter, 2006).

6.1.9 Fans (Zone to Zone, Internal to External)

Care must be taken to correctly represent fan performance in ventilation modelling. It is critically important to ensure that actual fan performance in the application is correct. In design it is straightforward to use a fixed flow component to represent a fan however a fan curve data should be used for realistic fan flow representation as per (equation 6.9). When using constant flow equation, this would place the onus on the specifier and supplier of the actual system to ensure it does indeed deliver at least this flow rate in the application (including ducts, bends, grilles, filters, etc.) under varying conditions (weather, sheltering, specific heights and orientations etc.).

6.1.10 Occupancy and Metabolic Rates

Use and inhabitation of the living spaces by people is termed as occupancy. In terms of building energy simulation relevant to ventilation performance, occupancy is defined by presence (occupancy schedules, number of people, time in each zone, use of controls e.g. windows etc.) and activity level and associated metabolic rate in watts. Both occupancy and activity level are both directly related to the metabolic output of CO_2 in a specific zone. Occupancy and therefore CO_2 production rates are highly uncertain as there are a wide range of people with different metabolic rates, plus a wide range of household characteristics driving occupancy patterns. Occupancy patterns and metabolic rates can be quite different due to age, health, employment, and other personal and social factors. It is important that ventilation design of buildings is robust to a realistic range of normal occupancy patterns. Ventilation design should also allow for adequate ventilation capability for ‘non normal’ occupancy through provision of ‘purge’ ventilation capability. The ‘normal’ ventilation scheme should support healthy, comfortable, and low energy use of the building under ‘normal’ circumstances.

CIBSE TM59 provides a range of occupancy schedules. Metabolic rates for different activities are listed in the ASHRAE Fundamentals and CIBSE Guide A, metabolic production rate of CO_2 is given in CIBSE KS17 (Clancy, 2011), there is however a need to establish standardised occupancy patterns to be used for regulatory purposes in the domestic context. Furthermore, it should be considered that these schedules are generic, and location specific variability and temporal changes are possible.

The focus in this work has been on bedrooms, CIBSE suggests ‘normal’ bedroom sleeping occupancy is 2 average people from 11pm to 8am while total occupancy is from 10pm to 8am, and ASHRAE suggests 0.7 to 1.0 MET for resting and a standard body size. A typical schedule and percent occupancy is tabulated below. The ‘normal’ behaviour that is assumed in regulations in terms of ventilation component control is to have the trickle vents open, but the windows and doors closed.

Time Period	Occupancy (%)	Source/Reference
00:00 - 06:00 AM	100%	Typical nighttime occupancy (all occupants sleeping).
06:00 - 08:00 AM	75%	Morning activity before leaving for work/school.
08:00 - 12:00 PM	30%	Daytime low occupancy, reflective of work/school.
12:00 - 01:00 PM	40%	Midday break, occasional returns to home.
01:00 - 05:00 PM	30%	Low occupancy during work/school hours.
05:00 - 07:00 PM	85%	Evening return, household activities resume.
07:00 - 10:00 PM	95%	Peak occupancy during family time or leisure.
10:00 - 12:00 AM	100%	Nighttime, all occupants at home and preparing for bed.

In lieu of a standard it is recommended in this document that for a double bedroom an occupancy schedule of 10pm to 8am is used with 2 occupants with a metabolic rate of 0.9 MET and standard body size, trickle vents open but doors and windows closed. This would represent a slightly worst case but realistic scenario according to the single case study example used in this thesis.

The extent to which the bedroom occupancy as described above is sufficient for a 'robust design' approach to provide a healthy indoor environment under all normal occupancy scenarios should be a focus for a future standardisation committee should also consider other zones of the dwelling.

Addition to occupant's presence, the motivation to open windows is found to be highest at ~23.4°C while 4°C is considered as deadband which refers to minimised frequency of adjustment from closed to open state.

6.1.11 Weather, Design Periods and Sheltering

Definition

Key components of a weather data file are wind speed, wind direction, temperature, and humidity.

Types of Datasets

Typical (TMY) weather data is suggested to be used as the method for generate the dataset gives appropriate representation of weather variability based on a wide range of years. The TMY then needs to be filtered for Winter Months and representative periods with lowest average wind speed (Energy Plus Documentation, 2020) to give a worst-case period. The generic nature of the dataset should be considered and may cause uncertainty.

Wind Reduction Factor

This factor determines the reduction in the weather station recorded wind speed by taking into account the general effect of the surrounding terrain. To implement this, the standard power law wind profile relationship and coefficient values is presented in (ASHRAE Fundamentals Handbook, 2021).

$$W_r = \frac{U_l}{U_{lo}} = K z_l^a \qquad 6.11$$

Where U_l is local wind speed, U_{lo} is either speed measured in the open countryside or at a certain height i.e., 10 m at the meteorological station, z_l is the local site height while K and a are terrain dependent constants which vary for flat, rural, urban, and dense city types.

Terrain Type	**Description**	**Coefficient K**	**Exponent a**	$\boldsymbol{W_r}$
Country	Open terrain, low rise buildings (<10m). Open flat areas.	0.68	0.17	0.99

Suburban/Urban	Encompassing suburban and urban areas. Numerous obstructions comparable to low rise residential buildings.	0.35	0.25	0.62
City	Large city centre areas where at least half of the buildings are taller than 20 meters.	0.21	0.33	0.45

Table 6.3: Common terrains and their relevant inputs in the wind reduction factor equation. Example wind reduction factors are calculated for a typical low rise building in UK context z_l=10m.

The calculated wind reduction factor is multiplied with the wind speed value from the weather data file. This number would not be suitable for a special case of terrain such as fully isolated or mountainous terrain and other special cases.

Exposure and Sheltering

The local wind conditions at each external node representing a façade element will depend on the orientation of the façade element with respect to the wind speed and direction, plus the extent to which the façade element is sheltered from the wind due to surrounding structures.

Sheltering effects including those appropriate for domestic low-rise buildings are captured in the AIVC database[3] (CIBSE, 2021) with associated methods. Exposure is categorised based on exposure and also based on geometrical factors, e.g. exposed, semi-exposed, sheltered, heights, lengths and aspect ratios of walls etc. The database then provides pressure coefficients to be applied in AFN tools to modify weather driven conditions at each façade element.

It is important to consider urban microclimates which are localised climatic conditions influenced by factors such as building density, surface materials, vegetation, and human activity. These effects would significantly impact thermal comfort, energy use, and environmental sustainability in such environments.

[3] Caution should be taken when using default pressure coefficient data. With the advancements in the field, more accurate models are being developed.

6.1.12 Approach for IAQ Performance Evaluation

To implement the previously described modelling guidance of AFN modelling to study the effectiveness of a ventilation design, safe IAQ indicator of indoor concentration of CO_2≤1000ppm can be used. This section aims to present a clear and concise AFN modelling approach for IAQ performance evaluation of a ventilation design in worst case conditions.

- Set up AFN zoning, and the placement of internal and external nodes as elaborated in the section 6.1.1.
- Set up crack components and paths to outside to meet worst case (lowest) target design infiltration with worst case cracks distribution (e.g. 3 $m^3/h/m^2$ and one crack per window frame as per section 6.1.3.
- Set up trickle vents components and paths (as per section 6.1.4) (e.g. in all living spaces with effective are as per (Scottish Government, 2023))
- Set up windows as closed (for IAQ assessment window openings that are closed can be omitted from the AFN).
- Set up doors as closed with appropriate components and paths i.e. undercut at base and inter-zone crack at the top of the door frame (as per section 6.1.6).
- Set up inter-zone designed ventilation opening components and paths (as per section 6.1.7)
- Set up stairwell component and paths (as per section 6.1.8).
- Set up fan components and paths (as per section 6.1.9)
- Set up worst case occupancy (as per 6.1.10) (e.g. occupancy patterns per CIBSE Guide TM59 (Bonfigli et al., 2017) and CIBSE Guide A (CIBSE, 2021) for metabolic rates adjusted by + 0.2 MET).
- Set up worst-case weather period and appropriate wind reduction and sheltering per façade element (as per 6.1.11).
- Carry out simulations, inspect results validate against a reference, iterate design to achieve KPIs (sensitivity/parametric, optimisation), validate outputs against reference documentation.

For IAQ the KPI can be for example % of time during a worst-case period that CO_2 ≤ 1000ppm.

It is important to be mindful of the validation of the model outputs. Modelling of flow components for which aerodynamic data is available, simulation results must be compared with the available lab test results which are usually ΔP-Q curves. However, as indicated for door undercuts, no such data is available hence relevant guidance can be followed using a lower discharge coefficient number and validation would not be possible.

6.2 Example Ventilation Design Guidance Application

The monitoring study by (T. Sharpe et al., 2019) carried out during a winter period suggests that the dMEV system was inadequate to ensure safe IAQ for the occupants in a domestic bedroom environment. The dwelling that was subject to detailed monitoring in that work has plans and other details available making it suitable as an example application for the AFN guidance and design approach outlined in the previous sections.

The local TMY weather dataset was analysed for the worst case 3 consecutive days in winter with least wind induced ventilation potential combined with highest dry bulb temperature. A base model of the dwelling was modelled following the above approach for the case study with specifications set in compliance with the applicable Scottish Regulation with dMEV. The base and 4 modified designs were evaluated to illustrate the proposed process in Table 6.4.

Setup	Trickle Vents Effective Area (mm^2)	Designed Inter-zone Opening (Yes/No)	Door Undercut heights (mm)	Extract Fan Flow Rate (l/s)	Change Log
Base (Worst Case)	11000	N	10mm	4	Standard dMEV design.
1	11000	Y	10mm	4	Added inter-zone opening (IZO).
2	11000	Y	10mm	8	IZO + 2X Extract Rate.
3	20000	Y	10mm	8	IZO + 2X Extract + Increased trickle ventilation.
4	20000	Y	10mm	10	IZO + 2.5X Extract + Increased trickle ventilation.

Table 6.4: Ventilation setups to illustrate IAQ design approach.

Table 6.5 shows peak CO_2 (ppm) values and % Occupied Hours > 1000ppm for the base (worst case) and each option. Figure 6.12 and Figure 6.13 further illustrate the range in CO_2 levels for each ventilation setup. It is clear that in this case only option 4 would consistently achieve ≤1000ppm under the TMY worse case weather conditions. The results indicate that the current regulations are insufficient and that improvement options are available which can deliver better results.

With standard dMEV system, it is not possible to maintain safe IAQ levels in case of CO2 as a proxy. It is evident that 42% of the occupied hours exceed the threshold. However, with the increases interzone flow capacity, there is more than 50% reduction in those hours. Later increments only have marginal impact on the CO2 levels. Hence for a design perspective, the flow resistivity between the inlet and extract should be reduced.

	Base	Option 1	Option 2	Option 3	Option 4
CO_2 Peak (ppm)	3105	1412	1135	1081	994
Occupied Hours Exceeding 1000ppm.	42%	18%	15%	13%	0.0%

Table 6.5: Peak CO_2 concentrations and percentage of occupied hours above the 1000ppm threshold in main bedroom for the ventilation setups.

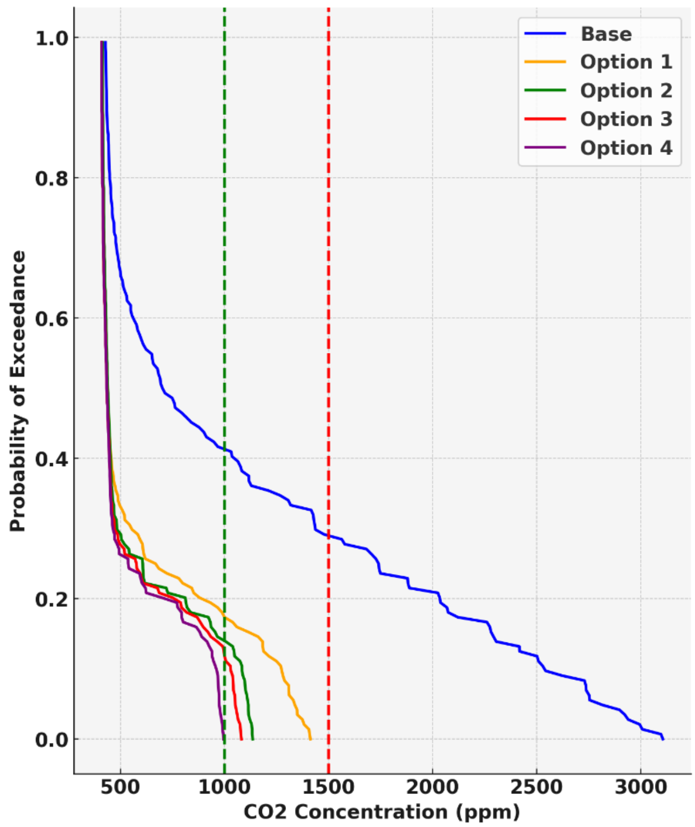

Figure 6.12: Probability of exceedance for ventilation setups suggesting higher probability of exceedance for worst case setup to surpass 1500ppm limit.

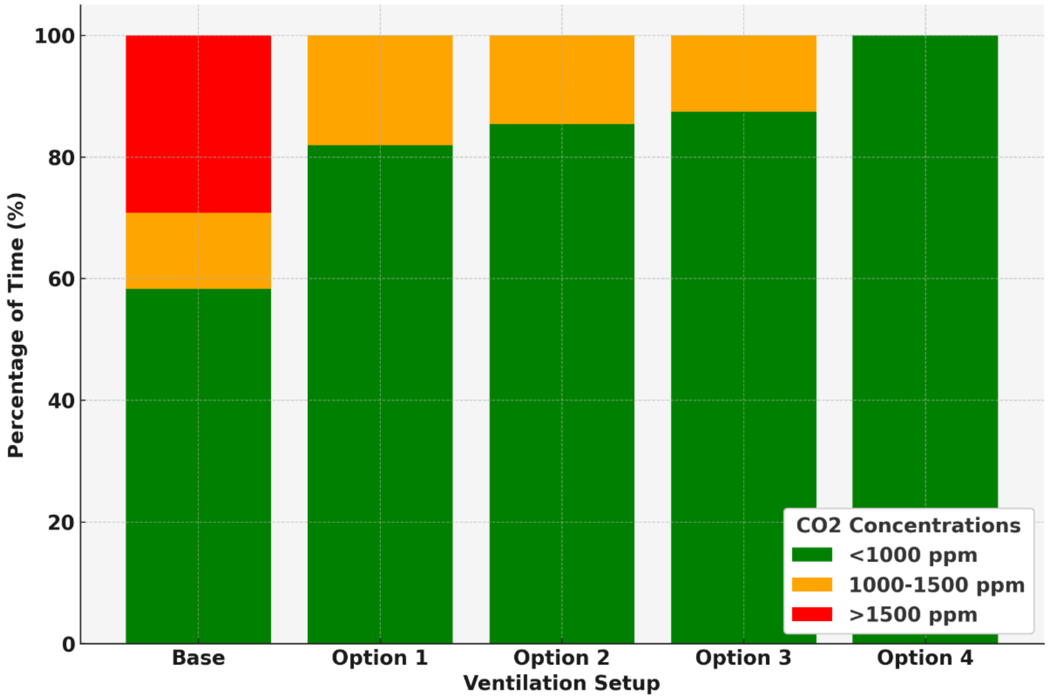

Figure 6.13: Percentage of instances CO_2 concentrations for each ventilation setup.

Chapter 7 Discussion and Conclusions

7.1 Overview

The ventilation inefficacies of current low energy houses equipped with dMEV is the key motivation of this work. Therefore, the modelling and analysis of core air flow network elements (described in the previous chapters) has been executed via a simulation case study that was informed by a literature review. The literature review and analysis of the study data (T. Sharpe et al., 2019) confirmed the underperformance of this system – features of which are detailed in the Domestic Technical Handbook (Scottish Government, 2023).

Air Flow Network (AFN) modelling is commonly used to tackle the implications of ventilation design, while a detailed literature review identified the ambiguities and vast range of approaches used to conduct a simulation study. A review of the outcomes was presented and the proposed approaches to model key elements of an AFN model were extracted.

Additionally, a review of statistical methods was presented that compared the metrices used to evaluate error between the measured and simulated outputs (specifically metabolic CO_2). This was developed into a framework by extracting a stage-wise process to quantify the impact of multiple modelling strategies. This impact was expressed in effect size values termed as Cohen's d number.

A stage-wise iterative modelling methodology was then applied to the case study house for which a limited set of data was available. This modelling aimed to implement the approaches suggested in the literature. As mentioned, the data was limited and collected in uncontrolled conditions, while several approaches were not evaluated. Despite this limitation, these approaches were critically examined through a literature review and presented as guidance to offer valuable insights for modellers focusing on domestic ventilation design.

Based upon the literature review and modelling study, this work presented a guidance document (Chapter 6) which included both evaluated and non-evaluated approaches. This output provides directions to model the worst-case building ventilation design using AFN. The modelling parameters for key elements of the network (including boundary conditions and loads) were explicitly defined, while their representative equations and inputs were fully explained. This was followed by the key performance metrices of the ventilation design study using AFN modelling. The guidance chapter concluded with a sample application on the worst-case scenario in which a standard ventilation system with modified setups was assessed for bedroom ventilation for night-time sleeping hours.

The study provides modellers and designers with sufficient information on which to make informed decisions on using one approach over another. These aspects are further detailed in next section of this chapter. However, there are limitations to this work which relate to the availability of the dataset, the level of detailed information about the case study, and the scope of the work. This chapter also discusses suggestions for future research to build upon the findings of this thesis.

7.2 Key Outcomes and Contributions to Knowledge

The objectives of this study were outlined in Chapter 1 which informed the research question, *“How to conduct an effective Air Flow Network modelling study to devise improvements in ventilation design of energy efficient dwellings?”* A research methodology was developed to achieve the aim, and a set of objectives were defined. These objectives are revisited in this section to identify the key outcomes and contributions to knowledge.

7.2.1 Objective 1: To understand domestic ventilation design and the occupant's influence on its effectiveness

The first research objective was to understand and identify the problem of low IAQ in domestic living spaces due to a lack of sufficient design and/or the occupant’s influence on the effectiveness of ventilation design. To address the insufficiency of ventilation design, building design literature was reviewed. A comparison of the literature informed the following outcomes:

- The installation of a ventilation system in a house is subjective to its airtightness. For example, a dMEV system is advised when house airtightness is 3-5 $m^3/hr/m^2$. It was found important to take account of the fact that, over time, the structural integrity of a building can be compromised
- The advised effective flow area for a trickle vent is insufficient to ensure safe indoor CO_2 levels for occupied periods.
- Door undercuts are not defined by their effective flow area. Rather, they are defined by a geometric dimension i.e., the height of the component is advised.
- Co-existence of extract fans and trickle vents were deemed suitable in a wet room but not in a decentralised system.
- The Scottish Building Regulatory Handbook describes a very generalised approach and requires an update.

These key outcomes from the comparative review yielded the following contribution to knowledge:

It was established that current building regulations in the Scottish Handbook (section 3.14) are sensitive to small alterations to the ventilation component specifications and/or deficiencies in the setup. A decentralised system on its own is unable to provide up to the mark ventilation to the occupants of an airtight house as it relies on the occupant's operation and discretion. This contribution can offer set of improvement to current guidance and support a move away from a fragile decentralised system.

7.2.2 Objective 2: To identify the shortcomings and ambiguities in building airflow modelling practices

The second research objective was to determine current approaches to model key airflow components as per the specifications for ventilation design outlined in the guidance documents. By reviewing the literature and current practice of AFN modelling, the following key outcomes were identified and informed the guidance chapter:

- Infiltration modelling is governed by the inputs in the crack flow/power law equation. The power law analytical model was found in the literature to further inform the length of the crack.
- Ambiguity was found in the definition of large cracks and small openings.
- The ability of an opening to exhibit a bi-directional flow was also identified.
- The aerodynamic properties of hinged openings were discussed in detail, and it was found that the discharge coefficient value varied significantly. The use of a state-of-the-art analytical model is advised.
- Modelling of large openings between the floors in a stairwell of a dwelling was found a challenge and accurate modelling via these horizontal flow openings is an area of further research.
- The review helped to categorise modelling of extract fans according to the required complexity in the modelling study.
- Occupancy was found to greatly affect the AFN study when metabolic CO_2 concentrations were used to proxy the ventilation performance of the system. To sufficiently model the occupancy via spatial presence and metabolic gains, recommended approaches were outlined in the absence of specific data.
- The use of an appropriate weather database was also noted as important. Additionally, the wind reduction factor and its available models were explained, and the choice of any model would depend upon the availability of building site data. Insufficient guidance was found on selecting an appropriate terrain and differentiating between relevant constant values.
- A statistical approach to evaluate the impact of one set of inputs over another was presented.
- The purpose of this review was to form a list of openings for application in the modelling stage and evaluate their ability to tackle the issue of low IAQ. These openings were

modelled in the later stage of the thesis and found to be helpful in mitigating high CO_2 levels.

These outcomes from the detailed review of AFN modelling yielded the following contribution to knowledge:

To support the development of guidance for AFN-assisted ventilation design study, it was found that, current modelling practices carry ambiguities while a clear method and a definition for flow components as well as specifications of weather-related boundary conditions were not found. More than one approaches was present without clear justification for the use of one over the other. These learnings from the literature review were fed into the guidance and were partially tested to determine the impact of one approach over the other. Non-evaluated approaches were listed at the end of Chapter 5.

7.2.3 Objective 3: To compare the solutions for a simplistic and proposed airflow modelling approaches

The third objective was to compare the modelling approaches found in the literature via a simulation study. This was enabled by a case study dataset for a house representing a worst-case, main bedroom ventilation performance. Metabolic CO_2 from the AFN solution was used to validate the modelling approaches. The following were the key outcomes from the stage-by-stage modelling study:

- The study highlighted the importance of choosing an appropriate equation set and their coefficients to model trickle vents and door undercuts. This selection significantly influences the accuracy of a simulated airflow. A simplified approach would be to use geometric data in either power law or orifice equation which is shown to exhibit upto 53% It was also concluded that using aerodynamic performance data in either orifice or the power law equation shows a small difference in the flow solution.
- Despite its limitations, the crack flow model in ESP-r is a viable tool to model smaller openings (where height < 10mm) in scenarios where limited data is available. For a larger opening (height > 10mm), the magnitude of flow prediction was significantly lower (~35% less) than modelling the same geometric area via an orifice flow equation.
- The analysis showed the significant impact of wind and buoyancy forces on airflow solutions. The quantified impact of the use of a wind reduction factor is well informed. With no use of wind reduction factor errors are up to 6%.
- By modelling the same leakage area at the top and bottom of the facades, the distribution of infiltration cracks on the wind induced facades of the model was adjusted.

- To assess the impact of incorporating interzone openings on metabolic CO_2 in the case study main bedroom, the modelling data extracted in the review was modelled on top of the two base models. Both models exhibited actual and best-case trickle vent settings. The analysis showed that such openings were capable of significantly increasing the interzone flow rates and a larger number of hours (37% compared to 24%) were spent in safer CO_2 concentrations.
- The modelling of slight door openings was found to be challenging. Translating a bi-directional flow component via two orifice equations overestimated the flow rate compared with a single bi-directional flow component.
- However, a simplistic window modelling method showed a substantial discrepancy. This step emphasised the need for further study to inform guidance on the modelling of such opening pathways.

These key outcomes from the stage-by-stage AFN modelling yielded the following contribution to knowledge:

By integrating statistical and physical approaches, the study uncovers the complexities of modelling ventilation components which are integral to current domestic building design. A comparison of modelled and measured CO_2 concentrations and flow rate predictions highlighted the difference in using the power law model versus the orifice equation. This informed the guidance to model small slot-shaped openings.

By knowing the possible impact on the flow solution, a quantified analysis of the wind reduction factor and the distribution of cracks would further inform guidance and allow modellers to implement these features within their AFN models.

Furthermore, the capability of interzone openings to assist current decentralised systems showed a possible solution to address the fragility of the design.

7.2.4 Objective 4: To formulate guidance for "close-to-reality" AFN simulations which will help to suggest an effective ventilation design in dwellings

The findings and analysis from the literature and modelling study provided insights that informed AFN modelling guidance. Chapter 6 presented the key components of modelling aimed at assessing a dMEV design, and the following contributions to knowledge are described:

The guidance defines these key components and suggests appropriate equation sets and inputs to the equations. It starts by describing the set-up of the nodes, the flow paths and their representative criteria, appropriate equations, specific characteristics, and the required input parameters. The equations and their usage are described, and the modelling of infiltration is described in a step-by-step process. Two approaches are presented to set up the infiltration and users are encouraged to use a relevant approach according to the purpose of the AFN simulation study. Similarly, the modelling of trickle vents, door undercuts, interzone openings and extraction fans is described. To model occupancy, existing guidance documents are considered for both the spatial scheduling and metabolic gains. As far as boundary conditions are concerned, weather databases are categorised for their relevant usage as per the study's purpose. The use of a wind reduction factor is recommended; the terrain types are defined along with suitable constant values which are input to the sheltering model. Pressure coefficient guidance is limited, like the occupancy modelling, and hence existing guidance is considered. At the end, the key performance metrics for conducting a ventilation design study are explained. Additionally, thermal comfort and evaluation criteria for energy-use centric designs are also presented.

7.2.5 Objective 5: To propose an alternative solution for adequate ventilation provision to the occupants - concerning widely adopted and current dMEV system

An example of a design study is presented based on a bedroom in a house which is representative of a current domestic dMEV system. Guidance inputs are used to model the evaluation of a ventilation design. As the system underperforms and does not guarantee safe IAQ, implementing various scenarios featuring interzone openings shows that changes to the stock system are required.

The contribution from this objective is the presentation of an alternative ventilation design to assist the current dMEV system. A stage-wise increment in the design components show the impact of each change, while the probability of the exceedance metric informed the performance of these settings. This exercise would greatly help to improve ventilation design.

7.3 Limitations of the Work and Future Recommendations

The limitations of this work stem from the defined scope and focus of this thesis, and the limited data available for modelling the case study.

The study's approach to modelling infiltration via cracks, by approximating a horizontal crack with a 2mm vertical dimension, may oversimplify the complex nature of airflow through cracks of varying sizes. This approximation neglects the potential for both laminar and turbulent flows. Such flows are associated with different building components. Future work could benefit from incorporating component-specific coefficients determined from a full-scale pressurisation study.

Both literature review and modelling study suggested that there is a need for specific testing data to determine effective flow area for door undercuts. For future work, it is vital to conduct aerodynamic testing to understand the resistance to airflow through door undercuts across varied settings. The settings would address varied setting of a door undercut such as undercut area and the interfacing floor surfaces such as carpet, wood, marble, or metal strips used for carpet fixation.

Limitations related to modelling the effective area of window/flapped openings, especially with small stroke lengths where frame thickness hindered the flow. Such small openings prevented the application of the free area model, SEAM. This gap suggests the need for refined analytical models and empirical data to better account for these factors.

The guidance to model different window opening mechanisms presented in the guidance chapter are not validated as these set of recommendations are directly informed by the literature. It is much advised to employ a dataset to model and validate these AFN setups.

Where literature showed potential error in flow rate predictions when horizontal planer openings are modelled by vertical planer openings, it is recommended that further research effort is put into modelling of horizontal planar openings such as roof mounted windows and flow area between the floors in a stairwell. All AFN modelling components are vertical planar openings; hence, to model large horizontal planar openings capable of multi-directional flow, no flow component was found.

While the study employed the constant flow equation based on the measured/target flow rate from the extraction fans, an alternative approach using a flow inducer equation component with inputs from the manufacturer-supplied performance curves was not explored. A comparative analysis of these methods could further highlight their respective impacts on modelling outcomes, specifically in terms of ΔP and flow rate.

This study focussed on occupancy in a single room as well as only during sleeping hours. It would be recommended to analyse whole house occupancy variation and ventilation performance.

Alongside metabolic rates, the uncertainty associated with wind pressure is acknowledged as a key influence on AFN modelling. The research did not compare the effects of employing different pressure coefficient datasets. For a study concerning wind loads on facades, a comparison of these pressure coefficient datasets could provide valuable insights to select the most appropriate dataset. Additionally, an insight into the quantified impact of choosing one terrain over the other when including wind reduction factor in the model would further allow to emphasise the careful selection of respective constant values.

By the perspective of current ventilation design, a review is recommended to transform the guidance documents into a more robust framework which is widely applicable. Ensuring safe IAQ is the main objective of current design guidance documents, but they are found to lack in delivering this sufficiently. It is recommended to move away from the dependence on passive intake and mechanical extract of the design and introduce mechanical inlet and extraction of air; ideally equipped with heat recovery.

The guidance chapter of this thesis is aimed to have broader applications when commonalities across various ventilation systems are focussed. Although the dMEV system served as the primary case study, the constituent modelling elements have wider applicability to advanced systems such mechanical inlet and extract assisted with heat recovery (MVHR). The respective elements of the guidance further empower modellers and designers to address various crucial consideration for a sustainable building design e.g., mitigating overheating risk and optimising building energy efficiency.

7.4 Overview of Existing Guidance for Thermal Comfort and Energy Usage

7.4.1 Design Evaluation for Thermal Comfort

The challenge of designing thermally comfortable and energy efficient building is more critical than ever. In this context it is important to ensure a comprehensive framework to assess the risk of overheating in residential building. This needs to encompass factors such as solar gains, ventilation strategies and thermal mass.

CIBSE TM59 guidance provides such a framework by emphasising on the importance of design factors such as building layout, shading and ventilation methods. For example, the document highlights the need to assess the impact of high proportion of glazing and reduced natural ventilation opportunities. These factors are contributing towards significant overheating risks.

TM59 provides reasonable usage patterns of houses – including occupancy schedules and internal gains from the equipment and lighting. The data includes specific gains profile tables for various room types and occupancy scenarios. This data can be integrated into a simulation study for overheating.

CIBSE TM59, TM52, CIBSE AM10 and Environmental Guide A suggest use of Design Summer Year (DSY) weather database to assess the building for overheating risks with consideration of future weather scenarios. This would allow realistic simulation study of thermal conditions during summer months by using typical summer weather conditions based on location.

Table 7.1 presents the thermal comfort criteria when evaluating a real life or simulation scenario. The occupiable spaces of a house (categorised as naturally or mechanically ventilated) should comply with the criteria. This approach behind the criteria recognises that the occupants of naturally ventilated houses can adapt to wider range of temperatures by controlling windows and other adjustable openings. While mechanically ventilated houses provide limited opportunity for such adjustments. Hence the criterion for these houses is a fixed temperature approach.

Criteria Type	Room Type	Criterion
Naturally Ventilated Homes	Living Rooms, Kitchens, Bedrooms	ΔT>1°C Not more than 3% of occupied hours from May to September should exceed this temperature rise.
	Bedrooms (specifically)	Not to exceed 26°C for more than 1% of occupied hours.
Mechanically Ventilated Homes		Not to exceed 26°C for more than 3% of the annual occupied hours.

Table 7.1: Thermal comfort criteria for assessing overheating in residential buildings.

7.4.2 Design Evaluation for Energy Usage

At design and post occupancy stages, a careful assessment of operational energy performance is conducted. CIBSE document TM61 addresses the performance gap specifically for energy performance of buildings. This guidance is mainly concerned with non-domestic and large apartment buildings however the key contributors to energy performance gap are highlighted. These factors are recommended to be addressed by following guidance available in TM54 to undertake a modelling study focussed on predicting energy performance of a building in its design stage.

TM54 emphasises the necessity of a holistic approach and categorises regulated and unregulated energy consumption. Regulated energy consumption term is used for heating and cooling while unregulated term refers to appliance usage and occupant behaviour.

The methodology in the document takes into account both fixed and variable occupant reliant factors. For example, detailed guidance on inclusion of specific energy usage from non-regulated consumption.

To develop a good energy simulation model, one should first acquire available information about the building and its usage. Second stage is to undertake simulation with accurate modelling i.e., by factoring in all energy usages (regulated, non-regulated). This factoring should adhere to reasonable and context-based assumptions. TM54 does provide clear guidance for these two stages related to design. However, later stages of construction, commissioning and maintenance also interfere with the proposed design. Such implications can be addressed by undertaking a calibration and sensitivity study of the model. TM63 provides framework to calibrate the variable inputs to help understand the performance issues can be caused in the stages coming after the design.

Guidance in TM54 in conjunction with TM63 can be implemented in 5 stage which are described as follows:

Stage	**Description**
Stage 1: Base case model development	Create or use an existing base case model reflecting all design stage input parameters. This can be achieved using TM54 guidance. • Weather inputs using TRY/DSY database. • Occupancy and building usage as per TM59.
Stage 2: Model modification	Modify the base case model with real weather data/appropriate synthetic weather database. Further modification is via information from realistic building operations data obtained from audits, post-occupancy evaluations, monitoring, and/or metering. This results in adjusted model.
Stage 3: Comparison and calibration	Compare the simulation outputs of the adjusted model with actual metered energy use. Use calibration criteria presented in ASHRAE Guideline 14. If criteria not met,

	proceed to the next stage to calibrate the adjusted model.
Stage 4: Iterative improvements	Implement iterative improvements by obtaining new operational data. When no further data is available and calibration criteria are not met, the output will be semi-calibrated model.
Stage 5: Uncertainty and sensitivity analysis	Conduct an uncertainty analysis to identify the impact of input uncertainty on outputs. At later stage, perform sensitivity analysis to identify the most influential input variables.

Energy usage threshold assessment tools such BREEAM or documentations for energy benchmarking i.e., CIBSE TM46 can be targeted by following the stage wise modelling procedure in the table above.

7.5 Overall Conclusions

The comprehensive analysis presented in this thesis highlights several important conclusions that collectively advance the understanding of AFN modelling concerned with domestic ventilation systems.

Firstly, the adoption of a step-by-step, iterative approach, combined with the implementation of statistical and physical analyses, has shown its effectiveness in tackling the complexities of AFN modelling. This method facilitated a clearer understanding of the influence of various parameters and coefficients, highlighting the importance of care in the selection of accurate simulation outcomes. Secondly, the research shows the role that specific modelling decisions play in determining the ability of an AFN simulation to accurately predict CO_2 concentrations. Hence, the equations and coefficients are proven to impact the assessment and optimisation of ventilation designs.

The implementation of a wind reduction factor was found to be crucial. A high prediction for infiltration flow was found in the absence of this sheltering feature. The analysis concluded that the wind reduction factor was more influential when the wind induced flow probability was higher.

The distribution of infiltration cracks in a building's façade was found to be the most uncertain parameter. The study could quantify the impact of this distribution by showcasing two modelling approaches with the conclusion that either approach could be used according to the specific aim of the AFN study.

Moreover, this study highlights key limitations and uncertainties within current modelling practices. The identified gaps show the need for further research that aims to refine the AFN modelling techniques. Additionally, the insights derived by applying these modelling approaches to a real-world design study have provided a framework to evaluate and optimise domestic ventilation designs. This also demonstrates the potential for AFN modelling to offer a valuable tool for design studies without extensive calibration procedures.

In conclusion, this research contributed significantly to the field of building physics, simulation, and ventilation design by clarifying the critical factors which influence AFN modelling - specifically buildings which aim to achieve energy efficient designs. It clarifies a pathway for future investigations to build upon with the aim of simplifying the complexities of ventilation modelling and hence guiding the development of more effective, sustainable building designs.

References

Abdul-Wahab, S. (2011). *Sick Building Syndrome: in Public Buildings and Workplaces*. https://doi.org/10.1007/978-3-642-17919-8

Adams, J. (2006). Socioeconomic position and sleep quantity in UK adults. *Journal of Epidemiology \& Community Health*, *60*(3), 267–269.

Afshari, R. (2020). *Indoor Air Quality and Severity of COVID-19 : Where Communicable and Non-communicable Preventive Measures Meet*. *March*, 1–2.

Aganovic, A., Hamon, M., Kolarik, J., & Cao, G. (2017). Indoor air quality in mechanically ventilated residential dwellings/low-rise buildings: A review of existing information. *38th AIVC Conference*.

Ahmed Abdul–Wahab, S. A., En, S. C. F., Elkamel, A., Ahmadi, L., & Yetilmezsoy, K. (2015). A review of standards and guidelines set by international bodies for the parameters of indoor air quality. *Atmospheric Pollution Research*. https://doi.org/10.5094/APR.2015.084

Air Quality Expert Group. (2022). *Indoor Air Quality*.

AKINS, R. E., PETERKA, J. A., & CERMAK, J. E. (1980). AVERAGED PRESSURE COEFFICIENTS FOR RECTANGULAR BUILDINGS. In J. E. CERMAK (Ed.), *Wind Engineering* (pp. 369–380). Pergamon. https://doi.org/https://doi.org/10.1016/B978-1-4832-8367-8.50041-3

Al horr, Y., Arif, M., Katafygiotou, M., Mazroei, A., Kaushik, A., & Elsarrag, E. (2016). Impact of indoor environmental quality on occupant well-being and comfort: A review of the literature. *International Journal of Sustainable Built Environment*, *5*(1), 1–11. https://doi.org/10.1016/j.ijsbe.2016.03.006

Allard, F., Dorer, V. B., Feustel, H. E., Infiltration, A., & Ventilation Centre, C. (United K. (1990). Fundamentals of the multizone air flow model - COMIS. *Measurements*, *208*, 760Kb.

Amasyali, K., & El-Gohary, N. M. (2021). Real data-driven occupant-behavior optimization for reduced energy consumption and improved comfort. *Applied Energy*, *302*, 117276.

Andrea Saltelli, Stefano Tarantola, Francesca Campolongo, M. R. (2004). *SENSITIVITY ANALYSIS IN PRACTICE. A GUIDE TO ASSESSING SCIENTIFIC MODELS*. John Wiley and Sons, Ltd.

ANSI/ASHRAE. (2002). ASHRAE Guideline 14-2002 Measurement of Energy and Demand Savings. *Ashrae*, *8400*, 170.

Aragon, V., Gauthier, S., Warren, P., James, P. A. B., & Anderson, B. (2019). Developing English domestic occupancy profiles. *Building Research \& Information*, *47*(4), 375–393.

Arendt, K., Krzaczek, M., & Tejchman, J. (2017). Influence of input data on airflow network accuracy in residential buildings with natural wind- and stack-driven ventilation. *Building Simulation*, *10*(2), 229–238. https://doi.org/10.1007/s12273-016-0320-5

Ashrae, A., & others. (2019). Standard 62.1-2019, Ventilation for Acceptable Indoor Air Quality. *American Society of Heating, Refrigerating, and Air-Conditioning Engineers: Atlanta, GA, USA*.

ASHRAE Fundamentals Handbook. (2021). ASHRAE: Atlanta. *GA, USA*.

ASTM. (2013). E413,"Classification for Rating Sound Insulation." *American Soc for Testing and Materials, Philadelphia*.

ATTMA. (2016). *Measuring Air Permeability of Dwellings*. *44*(1), 0–25.

Auffhammer, M., & Mansur, E. T. (2014). Measuring climatic impacts on energy consumption: A review of the empirical literature. *Energy Economics*, *46*, 522–530. https://doi.org/https://doi.org/10.1016/j.eneco.2014.04.017

Awbi, H. B. (1994). Design considerations for naturally ventilated buildings. *Renewable Energy*, *5*(5–8), 1081–1090.

Awbi, H. B. (2003). *Ventilation of buildings*. Taylor & Francis.

Azevedo, L., Gomes, R., & Silva, C. (2021). Influence of model calibration and optimization techniques on the evaluation of thermal comfort and retrofit measures of a Lisbon household using building energy simulation. *Advances in Building Energy Research*, *15*(5), 630–661. https://doi.org/10.1080/17512549.2019.1654916

Baba, F. M., Ge, H., Zmeureanu, R., & Wang, L. (Leon). (2022). Calibration of building model based on indoor temperature for overheating assessment using genetic algorithm: Methodology, evaluation criteria, and case study. *Building and Environment*, *207*, 108518. https://doi.org/https://doi.org/10.1016/j.buildenv.2021.108518

Baeumle, R., & Hunt, G. R. (2018). Capturing the needs of architects: a survey of their current information requirements for natural ventilation design. *International Journal of Ventilation*, *17*(2), 120–147. https://doi.org/10.1080/14733315.2017.1351737

Baghoolizadeh, M., Rostamzadeh-Renani, M., Dehkordi, S. A. H. H., Rostamzadeh-Renani, R., & Toghraie, D. (2022). A prediction model for CO2 concentration and multi-objective optimization of CO2 concentration and annual electricity consumption cost in residential buildings using ANN and GA. *Journal of Cleaner Production*, *379*, 134753. https://doi.org/https://doi.org/10.1016/j.jclepro.2022.134753

Baghoolizadeh, M., Rostamzadeh-Renani, M., Hakimazari, M., & Rostamzadeh-Renani, R. (2023). Improving CO2 concentration, CO2 pollutant and occupants' thermal comfort in a residential building using genetic algorithm optimization. *Energy and Buildings*, *291*, 113109. https://doi.org/https://doi.org/10.1016/j.enbuild.2023.113109

Bailey, B. J., Montero, J. I., Parra, J. P., Robertson, A. P., Baeza, E., & Kamaruddin, R. (2003). Airflow Resistance of Greenhouse Ventilators with and without Insect Screens. *Biosystems Engineering*, *86*(2), 217–229. https://doi.org/https://doi.org/10.1016/S1537-5110(03)00115-6

BBC. (2011). *People's showering habits revealed in survey*. https://www.bbc.co.uk/news/science-environment-15836433

Belmonte, J. F., Barbosa, R., & Almeida, M. G. (2019). CO 2 concentrations in a multifamily building in Porto, Portugal: Occupants' exposure and differential performance of mechanical ventilation control strategies. *Journal of Building Engineering*, *23*(October 2018), 114–126. https://doi.org/10.1016/j.jobe.2019.01.008

Benesty, J., Chen, J., Huang, Y., & Cohen, I. (2009). Pearson Correlation Coefficient. In *Noise Reduction in Speech Processing* (pp. 1–4). Springer Berlin Heidelberg. https://doi.org/10.1007/978-3-642-00296-0_5

Bibby, C. (2011). *Investigation of the acoustical and airflow performance of interior natural ventilation openings*. University of British Columbia.

Bibby, C., & Hodgson, M. (2014). Field measurement of the acoustical and airflow performance of interior natural-ventilation openings and silencers. *Applied Acoustics*, *82*, 15–22. https://doi.org/10.1016/j.buildenv.2013.05.025

Bietry, J., Sacré, C., & Simiu, E. (1978). Mean wind profiles and change of terrain roughness. *Journal of the Structural Division*, *104*(10), 1585–1593.

Biler, A., Unlu Tavil, A., Su, Y., & Khan, N. (2018). A review of performance specifications and studies of trickle vents. *Buildings*, *8*(11), 152.

Bitnun, A., & others. (2009). Bonferroni Correction. *J Clin Viro. L*, *44*, 262–267.

Bocanegra-Yanez, M. del C. (2018). *Detailed simulation of the indoor environment to aid ventilation system design in low energy houses*.

Bonfigli, C., Chorafa, M., Diamond, S., Eliades, C., Mylona, A., Taylor, B., & Virk, D. (2017).

TM59: Design methodology for the assessment of overheating risk in homes. CIBSE, London.

Bouvier, J. L., Bontemps, S., & Mora, L. (2019). Uncertainty and sensitivity analyses applied to a dynamic simulation of the carbon dioxide concentration in a detached house. *International Journal of Energy and Environmental Engineering*, *10*(1), 47–65. https://doi.org/10.1007/s40095-018-0291-7

Box, G. E. P. (1953). Non-Normality and Tests on Variances. *Biometrika*, *40*(3/4), 318–335.

Bradwell, S. C. (2014). Standard, quiet and super quiet-The modelling of flow and the reduction of turbulences. *INTER-NOISE and NOISE-CON Congress and Conference Proceedings*, *249*(8), 137–156.

BRE. (1994a). *BRE Digest 399: Natural ventilation in non-domestic buildings*.

BRE. (1994b). Continuous mechanical ventilation in dwellings: design, installation and operation. *Digest 398*.

BRE. (1998). *Trickle ventilators in offices*.

Brönnimann, S., Martius, O., Rohr, C., Bresch, D. N., & Lin, K.-H. E. (2019). Historical weather data for climate risk assessment. *Annals of the New York Academy of Sciences*, *1436*(1), 121–137. https://doi.org/https://doi.org/10.1111/nyas.13966

Bruce-Konuah, A. (2014). *Occupant window opening behaviour: the relative importance of temperature and carbon dioxide in university office buildings*. University of Sheffield.

BS 8214:2016. (2016). *Timber-based fire door assemblies-Code of practice BSI Standards Publication Publishing and copyright information*.

BS EN ISO 9972. (2015). *Thermal performance of buildings--determination of air permeability of buildings--fan pressurization method*.

BSI. (2019). *BSI Standards Publication Energy performance of buildings — Assessment of overall energy performance*.

Building (Scotland) Regulations. (2019). *Technical handbook: Domestic*.

Building Standards Division. (2023). *Building standards technical handbook June 2023: domestic*.

Buonanno, G., Stabile, L., & Morawska, L. (2020). Estimation of airborne viral emission: Quanta emission rate of SARS-CoV-2 for infection risk assessment. *Environment International*, *141*(May), 105794. https://doi.org/10.1016/j.envint.2020.105794

Burman, E., Rigamonti, D., Kimpain, J., & Mumovic, D. (2012). Performance gap and thermal modelling: a comparison of simulation results and actual energy performance for an academy in North West England. *First Building Simulation and Optimization Conference*.

Cakyova, K., Figueiredo, A., Oliveira, R., Rebelo, F., Vicente, R., & Fokaides, P. (2021). Simulation of passive ventilation strategies towards indoor CO2 concentration reduction for passive houses. *Journal of Building Engineering*, *43*, 103108. https://doi.org/https://doi.org/10.1016/j.jobe.2021.103108

Cao, G., Awbi, H., Yao, R., Fan, Y., Sirén, K., Kosonen, R., & Zhang, J. (Jensen). (2014). A review of the performance of different ventilation and airflow distribution systems in buildings. *Building and Environment*, *73*, 171–186. https://doi.org/https://doi.org/10.1016/j.buildenv.2013.12.009

Casini, M. (2022). Chapter 5 - Building performance simulation tools. In M. Casini (Ed.), *Construction 4.0* (pp. 221–262). Woodhead Publishing. https://doi.org/https://doi.org/10.1016/B978-0-12-821797-9.00004-0

Cavanaugh, W. J., Farrell, W. R., Hirtle, P. W., & Watters, B. G. (1962). Speech privacy in buildings. *The Journal of the Acoustical Society of America*, *34*(4), 475–492.

Chai, T., & Draxler, R. R. (2014). Root mean square error (RMSE) or mean absolute error (MAE)?--Arguments against avoiding RMSE in the literature. *Geoscientific Model Development*, *7*(3), 1247–1250.

Chatzidiakou, L., Mumovic, D., & Summerfield, A. J. (2015). Is CO2 a good proxy for indoor air quality in classrooms? Part 1: The interrelationships between thermal conditions, CO2 levels, ventilation rates and selected indoor pollutants. *Building Services Engineering Research and Technology*, *36*. https://doi.org/10.1177/0143624414566244

Chen, C.-Y., Chen, P.-H., Chen, J.-K., & Su, T.-C. (2021). Recommendations for ventilation of indoor spaces to reduce COVID-19 transmission. *Journal of the Formosan Medical Association*, *120*(12), 2055–2060.

Chiu, Y. H., & Etheridge, D. W. (2002). Calculations and Notes on the Quadratic and Power Law Equations for Modelling Infiltration. *International Journal of Ventilation*, *1*(1), 65–77. https://doi.org/10.1080/14733315.2002.11683623

Chu, C. R., Chiu, Y.-H., Chen, Y.-J., Wang, Y.-W., & Chou, C. (2009). Turbulence effects on the discharge coefficient and mean flow rate of wind-driven cross-ventilation. *Building and Environment*, *44*(10), 2064–2072. https://doi.org/https://doi.org/10.1016/j.buildenv.2009.02.012

CIBSE. (2016). *CIBSE Guide B2 Ventilation and ductwork*.

CIBSE. (2018). *A Handbook of Sustainable Building Design and Engineering*. https://doi.org/10.1201/9781315172026-20

CIBSE. (2021). *Environmental Design: Guide A*. https://doi.org/10.4324/9781315671796

CIBSE AM10. (2005). CIBSE Applications Manual AM10 - Natural ventilation in non-domestic buildings. *Cibse Am10*.

Clancy, E. (2011). *Indoor air quality and ventilation*. CIBSE.

Clarke, J. (2007). Energy simulation in building design. *Energy Simulation in Building Design*, 1–362. https://doi.org/10.4324/9780080505640

Clarke, J. A. (2001). 5 - Fluid flow. In J. A. Clarke (Ed.), *Energy Simulation in Building Design (Second Edition)* (Second Edi, pp. 126–156). Butterworth-Heinemann. https://doi.org/https://doi.org/10.1016/B978-075065082-3/50005-X

Coakley, D., Corporation, M. E., & Raftery, P. (2012). *Calibration of Whole Building Energy Simulation Models : Detailed Case Study of a Naturally Ventilated Building Using Hourly Measured Data CALIBRATION OF WHOLE BUILDING ENERGY SIMULATION MODELS : DETAILED CASE STUDY OF A NATURALLY VENTILATED BUILDING USIN*. *September*.

Coakley, D., Raftery, P., & Keane, M. (2014). A review of methods to match building energy simulation models to measured data. *Renewable and Sustainable Energy Reviews*, *37*, 123–141.

Cockroft, J. P. (1979a). *Heat transfer and air flow in buildings. PhD thesis*. 240. https://core.ac.uk/download/pdf/9655076.pdf

Cockroft, J. P. (1979b). *Heat transfer and air flow in buildings. PhD thesis*.

Cominola, A., Spang, E. S., Giuliani, M., Castelletti, A., Lund, J. R., & Loge, F. J. (2018). Segmentation analysis of residential water-electricity demand for customized demand-side management programs. *Journal of Cleaner Production*, *172*, 1607–1619.

Cóstola, D., Blocken, B., & Hensen, J. L. M. (2009). Overview of pressure coefficient data in building energy simulation and airflow network programs. *Building and Environment*, *44*(10), 2027–2036. https://doi.org/https://doi.org/10.1016/j.buildenv.2009.02.006

Crawley, D. B., Lawrie, L. K., & others. (2015). Rethinking the TMY: is the ‘typical’meteorological year best for building performance simulation. *Conference:*

Building Simulation, 2655–2662.

D'Oca, S., Corgnati, S., Pisello, A. L., & Hong, T. (2016). *Introduction to an occupant behavior motivation survey framework*.

DCLG. (2015). *Technical housing standards--nationally described space standard*. Department for Communities and Local Government London.

de Jong, T., & Bot, G. P. A. (1992). Flow characteristics of one-side-mounted windows. *Energy and Buildings*, *19*(2), 105–112. https://doi.org/https://doi.org/10.1016/0378-7788(92)90004-Z

De Salis, M. H. F., Oldham, D. J., & Sharples, S. (2002). Noise control strategies for naturally ventilated buildings. *Building and Environment*, *37*(5), 471–484.

DOE, U. S. (2008). M\&V guidelines: measurement and verification for federal energy projects version 3.0. *US Department Of Energy*.

Dubois, D., & Dubois, E. F. (1989). A formula to estimate the approximate surface area if height and weight be known. *Nutrition*, *5*(5), 303 – 311.

Ehsan, A., Gameiro, M., & Costa, J. (2010). *Measurement and Simulation if Indoor Air Quality and CO2 Concentration in a Hotel Room*. *60*, 1–10.

Ekren, O., Karadeniz, Z. H., Atmaca, I., Ugranli-Cicek, T., Sofuoglu, S. C., & Toksoy, M. (2017). Assessment and improvement of indoor environmental quality in a primary school. *Science and Technology for the Built Environment*, *23*(2), 391–402.

Elharidi, A. M., Tuohy, P. G., Teamah, M. A., & Hanafy, A. A. (2017). Energy and indoor environmental performance of typical Egyptian offices: Survey, baseline model and uncertainties. *Energy and Buildings*, *135*, 367–384. https://doi.org/https://doi.org/10.1016/j.enbuild.2016.11.011

Energy Plus Documentation. (2020). *EnergyPlus Documentation Engineering Reference*.

Etheridge, D. (2011). *Natural ventilation of buildings: theory, measurement and design*. John Wiley \& Sons.

Etheridge, D., & Ford, B. (2008). Natural ventilation of tall buildings--options and limitations. *CTBUH 8th World Congress*, 3–5.

Etheridge, D. W. (1984). Air leakage characteristics of houses—a new approach. *Building Services Engineering Research and Technology*, *5*(1), 32–36. https://doi.org/10.1177/014362448400500105

Etheridge, D. W. (2000). Unsteady flow effects due to fluctuating wind pressures in natural ventilation design—mean flow rates. *Building and Environment*, *35*(2), 111–133. https://doi.org/https://doi.org/10.1016/S0360-1323(99)00007-4

Etheridge, D. W., & Sandberg, M. (1996). *Building ventilation: theory and measurement* (Vol. 50). John Wiley & Sons Chichester, UK.

Fabi, V., Andersen, R. V., Corgnati, S. P., Olesen, B. W., & Filippi, M. (2011). Description of occupant behaviour in building energy simulation: state-of-art and concepts for improvements. *Proceedings of Building Simulation*, 2882–2889.

Fabrizio, E., & Monetti, V. (2015). Methodologies and Advancements in the Calibration of Building Energy Models. *Energies*, *8*(4), 2548–2574. https://doi.org/10.3390/en8042548

Favarolo, P. A., & Manz, H. (2005). Temperature-driven single-sided ventilation through a large rectangular opening. *Building and Environment*, *40*(5), 689–699.

Feng, X., Yan, D., & Hong, T. (2015). Simulation of occupancy in buildings. *Energy and Buildings*, *87*, 348–359.

Ferdyn-Grygierek, J. (2014). Indoor environment quality in the museum building and its effect on heating and cooling demand. *Energy and Buildings*, *85*, 32–44. https://doi.org/https://doi.org/10.1016/j.enbuild.2014.09.014

Fernandes, L., Friedrich, M., Cóstola, D., Matsumoto, E., Labaki, L., & Wellershoff, F. (2020). *Evaluation of discharge coefficients of large openable windows using full-scale samples in wind tunnel tests*. *35*, 203–214.

Feustel, H. E. (1999). COMIS—an international multizone air-flow and contaminant transport model. *Energy and Buildings*, *30*(1), 3–18. https://doi.org/10.1016/S0378-7788(98)00043-7

Few, J., & Elwell, C. (2021). Open or Closed? Use of Windows and Doors at Home: Ventilation Rates in Occupied Dwellings. *INDOOR ENVIRONMENTAL QUALITY PERFORMANCE APPROACHES (IAQ 2020), PT 1*.

Few, J., Shipworth, M., & Elwell, C. (2024). Ventilation regulations and occupant practices: undetectable pollution and invisible extraction. *Buildings & Cities*, *5*(1).

Fisk, W. J., Mirer, A. G., & Mendell, M. J. (2009). Quantitative relationship of sick building syndrome symptoms with ventilation rates. *Indoor Air*, *19*(2), 159–165. https://doi.org/10.1111/j.1600-0668.2008.00575.x

Flett, G., & Kelly, N. (2021). Modelling of individual domestic occupancy and energy demand behaviours using existing datasets and probabilistic modelling methods. *Energy and Buildings*, *252*, 111373.

Foldvary, V. (2016). *Assessment of indoor environmental quality in residential buildings before and after renovation. PhD thesis.*

Fox, J. (2008). *A study of occupant controlled ventilation within UK dwellings*. University of London, University College London (United Kingdom).

Fracastoro, G. V., Mutani, G., & Perino, M. (2002). Experimental and theoretical analysis of natural ventilation by windows opening. *Energy and Buildings*, *34*(8), 817–827. https://doi.org/10.1016/S0378-7788(02)00099-3

Gilberts. (2022). *Gilberts*. https://gilbertsblackpool.com/wp-content/uploads/2022/02/Gilberts-Series-VNS-Feb-2022.pdf

Gonzalez, M. A. (1984). On the aerodynamics of natural ventilators. *Building and Environment*, *19*(3), 179–189.

Gonzalo, F. del A., Griffin, M., Laskosky, J., Yost, P., & González-Lezcano, R. A. (2022). Assessment of indoor air quality in residential buildings of New England through actual data. *Sustainability*, *14*(2), 739.

Government, H. (2010). *Approved document F: Ventilation*.

Government, H. M. (2018). *Conservation of fuel and power: Approved Document L*. HM Government London.

Grabe, J. Von. (2013). Flow resistance for different types of windows in the case of buoyancy ventilation. *Energy & Buildings*, *65*, 516–522. https://doi.org/10.1016/j.enbuild.2013.06.035

Continuous Extract / dMEV Regulation-ready fan designed to deliver Guaranteed Installed Performance, (2016). https://www.greenwood.co.uk/product/577/unity-cv21

Grosso, M. (1992). Wind pressure distribution around buildings: a parametrical model. *Energy and Buildings*, *18*(2), 101–131.

Gu, L. (2007). *Airflow network modeling in EnergyPlus*.

Gupta, R., & Chandiwala, S. (2010). Understanding occupants: feedback techniques for large-scale low-carbon domestic refurbishments. *Building Research \& Information*, *38*(5), 530–548.

Guyot, D., Giraud, F., Simon, F., Corgier, D., Marvillet, C., & Tremeac, B. (2020). Building energy model calibration: A detailed case study using sub-hourly measured data. *Energy and Buildings*, *223*, 110189. https://doi.org/https://doi.org/10.1016/j.enbuild.2020.110189

Guyot, G., Geoffroy, H., Ondarts, M., Migne, L., Bobee, M., Gonze, E., & Woloszyn, M. (2019). Modelling the impact of multizone airleakage on ventilation performance and indoor air quality in low-energy homes. *Building Simulation*, *12*(6), 1141–1159. https://doi.org/10.1007/s12273-019-0557-x

Haldi, F., & Robinson, D. (2011). Modelling occupants' personal characteristics for thermal comfort prediction. *International Journal of Biometeorology*, *55*, 681–694.

Hall, I. J., Prairie, R. R., Anderson, H. E., & Boes, E. C. (1978). *Generation of a typical meteorological year*.

Hand, J. W. (2018). Strategies for deploying virtual representations of the built environment. *Glasgow: University of Strathclyde*.

Hasan, M. H., Alsaleem, F., & Rafaie, M. (2016). Sensitivity study for the PMV thermal comfort model and the use of wearable devices biometric data for metabolic rate estimation. *Building and Environment*, *110*, 173–183. https://doi.org/https://doi.org/10.1016/j.buildenv.2016.10.007

Havtun, H., & Bohdanowicz, P. (2011). *Sustainable Energy Utilisation*. KTH Royal Institute of Technology.

Heiselberg, P., Iqbal, A., & Afshari, A. (2015). *Discharge coefficient of centre-pivot roof windows*. *92*, 635–643. https://doi.org/10.1016/j.buildenv.2015.05.034

Heiselberg, P., & Sandberg, M. (2006). *Evaluation of Discharge Coefficients for Window Openings in Wind Driven Natural Ventilation*. *3315*. https://doi.org/10.1080/14733315.2006.11683723

Heiselberg, P., Svidt, K., & Nielsen, P. V. (2001). Characteristics of airflow from open windows. *Building and Environment*, *36*(7), 859–869. https://doi.org/https://doi.org/10.1016/S0360-1323(01)00012-9

Hensen, J. L. M. (1991). *On the thermal interaction of building structure and heating and ventilation system - (Dissertation) - Technische Universiteit Eindhoven, Netherlands*.

Hensen, J. L. M. (1995). Modelling coupled heat and airflow: ping pong vs. onions. *DOCUMENT-AIR INFILTRATION CENTRE AIC PROC*, 253.

Hopkin, C., Spearpoint, M., Hopkin, D., & Wang, Y. (2022). Using Probabilistic Zone Model Simulations to Investigate the Deterministic Assumptions of UK Residential Corridor

Smoke Control Design. *Fire Technology*, *58*(3), 1711–1736. https://doi.org/10.1007/s10694-022-01221-6

Hopkins, C. (2004). A prototype ventilator for cross ventilation in schools: Sound insulation and airflow measurements. *Building Research Establishment Ltd*.

Hove, M. Y. C. Van, Delghust, M., & Laverge, J. (2023). Uncertainty and sensitivity analysis of building-stock energy models: sampling procedure, stock size and Sobol' convergence. *Journal of Building Performance Simulation*, *0*(0), 1–23. https://doi.org/10.1080/19401493.2023.2201816

Hunt, G. R., & Coffey, C. J. (2010). Emptying boxes – classifying transient natural ventilation flows. *Journal of Fluid Mechanics*, *646*, 137–168. https://doi.org/10.1017/S0022112009993028

Hyun, S.-H., Park, C.-S., & Augenbroe, G. (2007). Uncertainty and sensitivity analysis of natural ventilation in high-rise apartment buildings. *BUILDING SIMULATION, China*.

Idel'čik, I. E. (1966). *Handbook of hydraulic resistance: coefficients of local resistance and of friction*. Israel Program for Scientific Translations.

IES MacroFlow User Guide. (2014). *MacroFlo User Guide*. http://iesve.com/content/downloadasset 7285.

International Organization for Standardization. (2005). ISO15927-4: Hygrothermal performance of buildings—Calculation and presentation of climatic data—Part 4: Hourly data for assessing the annual energy use for heating and cooling. *International Organization for Standardization, Geneva*.

Ipsos-RSL, & of National Statistics, O. (2003). United Kingdom Time Use Survey 2000 (computer file). *Colchester, Essex: UK Data Archive (Distribuitor)*.

ISO. (2004). ISO 8996: Ergonomics of the thermal environment—determination of metabolic rate. *ISO Geneva*.

ISO. (2005). ISO 7730: Ergonomics of the thermal environment Analytical determination and interpretation of thermal comfort using calculation of the PMV and PPD indices and local thermal comfort criteria. *Management*, *3*, 605–615. https://doi.org/10.1016/j.soildyn.2004.11.005

Izadyar, N., Miller, W., Rismanchi, B., & Garcia-Hansen, V. (2020). Impacts of façade openings' geometry on natural ventilation and occupants' perception: a review. *Building and Environment*, *170*, 106613.

Jaggs, M., & Scivyer, C. (2006). Achieving airtightness: Part 1: General principles. Part 2: Practical guidance on techniques: floors, walls and roofs. Part 3: Practical guidance on techniques: windows and doors, sealing methods and materials. *BRE Good Building Guide*, *67*, 1–8.

Jiang, Y. (2002). *Study of Natural Ventilation in Buildings with Large Eddy Simulation*. 196.

Jin, M., Bekiaris-Liberis, N., Weekly, K., Spanos, C. J., & Bayen, A. M. (2016). Occupancy detection via environmental sensing. *IEEE Transactions on Automation Science and Engineering*, *15*(2), 443–455.

Johnson, M. H., Zhai, Z. J., & Krarti, M. (2012). Performance evaluation of network airflow models for natural ventilation. *HVAC and R Research*, *18*(3), 349–365. https://doi.org/10.1080/10789669.2011.617291

Jones, B. M., Lowe, R. J., Davies, M., Chalabi, Z., Das, P., & Ridley, I. (2014). Modelling uniformly porous facades to predict dwelling infiltration rates. *Building Services Engineering Research and Technology*, *35*(4), 408–416. https://doi.org/10.1177/0143624413499354

Jose, R. S., & Perez-Camanyo, J. L. (2023). Modelling infiltration rate impacts on indoor air quality. *International Journal of Thermofluids*, *17*, 100284. https://doi.org/https://doi.org/10.1016/j.ijft.2023.100284

Kalamees, T., Kurnitski, J., Korpi, M., & Vinha, J. (2007). The distribution of the air leakage places and thermal bridges of different types of detached houses and apartment buildings. 2nd European BlowerDoor-Symposium, 16-17 March. *Kassel, Germany, 11p*.

Kalliomäki, P., Saarinen, P., Tang, J. W., & Koskela, H. (2016). Airflow patterns through single hinged and sliding doors in hospital isolation rooms – Effect of ventilation, flow differential and passage. *Building and Environment*, *107*, 154–168. https://doi.org/https://doi.org/10.1016/j.buildenv.2016.07.009

Kanthila, C., Boodi, A., Beddiar, K., Amirat, Y., & Benbouzid, M. (2021). Markov chain-based algorithms for building occupancy modeling: A review. *2021 3rd International Conference on Smart Power & Internet Energy Systems (SPIES)*, 438–443.

Kapsalaki, M. (2022). *AIVC's Technical Note 71: Durability of building airtightness*.

Karava, P., Stathopoulos, T., & Athienitis, A. K. (2003). Investigation of the performance of trickle ventilators. *Building and Environment*, *38*(8), 981–993.

Karava, P., Stathopoulos, T., & Athienitis, A. K. (2004). Wind Driven Flow through Openings

– A Review of Discharge Coefficients. *International Journal of Ventilation*, *3*(3), 255–266. https://doi.org/10.1080/14733315.2004.11683920

Kasam, A. A., Lee, B. D., & Paredis, C. J. J. (2014). Statistical methods for interpolating missing meteorological data for use in building simulation. *Building Simulation*, *7*, 455–465.

Katsoyiannis, A., & Cincinelli, A. (2019). 'Cocktails and dreams': the indoor air quality that people are exposed to while sleeping. *Current Opinion in Environmental Science & Health*, *8*, 6–9. https://doi.org/https://doi.org/10.1016/j.coesh.2018.12.005

Katsumichi, N. (2003). Modeling of the flow resistance of the stairwell on the ventilation network calculation. In *Research in Building Physics* (pp. 719–727). CRC Press.

Kim, H., Hong, T., & Kim, J. (2019). Automatic ventilation control algorithm considering the indoor environmental quality factors and occupant ventilation behavior using a logistic regression model. *Building and Environment*, *153*, 46–59.

Klote, J. H., & Milke, J. A. (2008). *Principles of smoke management*. РГБ.

Kolokotroni, M., & Littler, J. (1995). Effectiveness of extractor fans in reducing airborne moisture in homes. *Indoor Air*, *5*(1), 69–75.

Kramer, R., Workman Jr., J., & Reeves III, J. B. (2004). Qualitative Analysis. In *Near-Infrared Spectroscopy in Agriculture* (pp. 175–206). John Wiley & Sons, Ltd. https://doi.org/https://doi.org/10.2134/agronmonogr44.c8

Kravchenko, I., Kosonen, R., Jokisalo, J., & Kilpeläinen, S. (2022). Performance of Modern Passive Stack Ventilation in a Retrofitted Nordic Apartment Building. *Buildings*, *12*(2). https://doi.org/10.3390/buildings12020096

Kurnitski, J., Boerstra, A., Franchimon, F., Mazzarella, L., Hogeling, J., Hovorka, F., & Seppänen, O. (2020). *REHVA COVID-19 guidance document*. *2020*(i), 1–6.

Kwok, H. H. L. (2021). *Multi-zone IAQ Assessment, Monitoring and Control in Buildings Leveraging BIM Technology*. Hong Kong University of Science and Technology (Hong Kong).

Lam, J. C., & Hui, S. C. M. (1996). Sensitivity analysis of energy performance of office buildings. *Building and Environment*, *31*(1), 27–39. https://doi.org/10.1016/0360-1323(95)00031-3

Larsen, T. S. (2006). *Natural Ventilation Driven by Wind and Temperature Difference*. 158. http://vbn.aau.dk/da/publications/natural-ventilation-driven-by-wind-and-temperature-difference(63925380-8137-11db-8b97-000ea68e967b).html

Lee, Y. S., & Malkawi, A. M. (2014). Simulating multiple occupant behaviors in buildings: An agent-based modeling approach. *Energy and Buildings*, *69*, 407–416.

Lelyveld, T., Livingstone, M., & Ross, D. (2018). *Good practice in the design of homes*. UK: Chartered Institute of Building Services Engineers.

Levermore, G. J., & Parkinson, J. B. (2006). Analyses and algorithms for new Test Reference Years and Design Summer Years for the UK. *Building Services Engineering Research and Technology*, *27*(4), 311–325.

Li, H. (2002). *Validation of three multi-zone airflow models*.

Li, Z. (2007). *Characteristics of byoyancy driven natural ventilation through horizontal openings*. Aalborg University.

Liao, J., Stankovic, L., & Stankovic, V. (2014). Detecting Household Activity Patterns from Smart Meter Data. *2014 International Conference on Intelligent Environments*, 71–78. https://doi.org/10.1109/IE.2014.18

Liddament, M. (1986). Air Infiltration Calculation Techniques - An Applications Guide. *AnnexINTERNATIONAL ENERGY AGENCY Energy Conservation in Buildings and Community Systems Programme*, *Discussion*.

Liddament, M. W., & Diff, T. (1987). *Power Law Rules- OK ? I*(2), 4–6.

Linden, P. F. (1999). THE FLUID MECHANICS OF NATURAL VENTILATION. *Annual Review of Fluid Mechanics*, *31*(1), 201–238. https://doi.org/10.1146/annurev.fluid.31.1.201

Liu, J., Dai, X., Li, X., Jia, S., Pei, J., Sun, Y., Lai, D., Shen, X., Sun, H., Yin, H., & others. (2018). Indoor air quality and occupants' ventilation habits in China: seasonal measurement and long-term monitoring. *Building and Environment*, *142*, 119–129.

Lorenzetti, D. M. (2002). Computational aspects of nodal multizone airflow systems. *Building and Environment*, *37*(11), 1083–1090. https://doi.org/https://doi.org/10.1016/S0360-1323(02)00011-2

Lu, Y., Dong, J., & Liu, J. (2020). Zonal modelling for thermal and energy performance of large space buildings: A review. *Renewable and Sustainable Energy Reviews*, *133*, 110241.

Macbeth, G., Razumiejczyk, E., & Ledesma, R. D. (2011). Cliff's Delta Calculator: A non-parametric effect size program for two groups of observations. *Universitas Psychologica*, *10*(2), 545–555.

Mai, J. (2023). Ten strategies towards successful calibration of environmental models. *Journal of Hydrology*, *620*, 129414. https://doi.org/https://doi.org/10.1016/j.jhydrol.2023.129414

McKay, S., Ross, D., Mawditt, I., & Kirk, S. (2010). Ventilation and indoor air quality in Part F 2006 Homes. *Department for Communities and Local Government Report BD*, *2702*.

Mckeen, P., & Liao, Z. (2019). The influence of building airtightness on airflow in stairwells. *Buildings*, *9*(10), 1–25. https://doi.org/10.3390/buildings9100208

Menberg, K., Heo, Y., & Choudhary, R. (2019). Influence of error terms in Bayesian calibration of energy system models. *Journal of Building Performance Simulation*, *12*(1), 82–96. https://doi.org/10.1080/19401493.2018.1475506

Mewomo, M. C., Toyin, J. O., Iyiola, C. O., & Aluko, O. R. (2023). Synthesis of critical factors influencing indoor environmental quality and their impacts on building occupants health and productivity. *Journal of Engineering, Design and Technology*, *21*(2), 619–634.

Ministry of Housing, C. and L. G. (2019). *Ventilation and indoor air quality in new homes*.

Mochida, A., Yoshino, H., Takeda, T., Kakegawa, T., & Miyauchi, S. (2005). Methods for controlling airflow in and around a building under cross-ventilation to improve indoor thermal comfort. *Journal of Wind Engineering and Industrial Aerodynamics*, *93*(6), 437–449. https://doi.org/10.1016/j.jweia.2005.02.003

Morris, M. D. (1991). Factorial Sampling Plans for Preliminary Computational Experiments. *Technometrics*, *33*(2), 161–174. https://doi.org/10.1080/00401706.1991.10484804

MOSER, A., SCHÄULIN, A., DAVIDSON, L., CORRADO, V., DORER, V., & KOSCHENZ, M. (2001). 11 - DESIGN WITH MODELING TECHNIQUES. In H. Goodfellow & E. Tähti (Eds.), *Industrial Ventilation Design Guidebook* (pp. 1025-p3). Academic Press. https://doi.org/https://doi.org/10.1016/B978-012289676-7/50014-X

Moutzouri, E. (2011). *Comparison between PHPP and SAP & Elaboration of monitored data for two dwellings with different insulation levels*.

Muehleisen, R. T., & Patrizi, S. (2013). A new parametric equation for the wind pressure coefficient for low-rise buildings. *Energy and Buildings*, *57*, 245–249.

Musser, A., & Yuill, G. K. (1999). Comparison of residential air infiltration rates predicted by single-zone and multizone models. *TRANSACTIONS-AMERICAN SOCIETY OF HEATING REFRIGERATING AND AIR CONDITIONING ENGINEERS*, *105*, 951–963.

Nevander, L. E., & Kronvall, J. (1978). Air tightness of buildings—research in Sweden. *IEA Seminar on R&D Projects in the Area of Infiltration in Buildings, Paris, France*.

NICE. (2020). *Indoor air quality at home*.

O'Brien, W., Gunay, H. B., Tahmasebi, F., & Mahdavi, A. (2017). A preliminary study of representing the inter-occupant diversity in occupant modelling. *Journal of Building Performance Simulation*, *10*(5–6), 509–526. https://doi.org/10.1080/19401493.2016.1261943

O'Donovan, A., O'Sullivan, P. D., & Murphy, M. D. (2019). Predicting air temperatures in a naturally ventilated nearly zero energy building: Calibration, validation, analysis and approaches. *Applied Energy*, *250*, 991–1010.

Oke, T. R. (1988). Street design and urban canopy layer climate. *Energy and Buildings*, *11*(1), 103–113. https://doi.org/https://doi.org/10.1016/0378-7788(88)90026-6

Organisation, E. V. (2012). International performance measurement and verification protocol. Concepts and options for determining energy and water savings. *Efficiency Valuation Organisation: Toronto, ON, Canada*.

Organisation, W. H. (2009). *WHO guidelines for indoor air quality: dampness and mould*. WHO Regional Office Europe.

Organization, W. H., & others. (2010). *WHO guidelines for indoor air quality: selected pollutants*.

Orme, M., & Leksmono, N. (2002). Ventilation modelling data guide. *AIVC Guide*, *5*(2002), 80.

Orme, M., Liddament, M. W., & Wilson, A. (1994). *An analysis and data summary of the AIVC's numerical database*. Oscar Faber.

Orme, M., Liddament, M., & Wilson, A. (1998). *Numerical data for air infiltration and natural ventilation calculations*. Air Infiltration and Ventilation Centre.

Page, J., Robinson, D., Morel, N., & Scartezzini, J.-L. (2008). A generalised stochastic model for the simulation of occupant presence. *Energy and Buildings*, *40*(2), 83–98.

Paliouras, P., Matzaflaras, N., Peuhkuri, R. H., & Kolarik, J. (2015). Using measured indoor environment parameters for calibration of building simulation model - A passive house case study. *Energy Procedia*, *78*, 1227–1232. https://doi.org/10.1016/j.egypro.2015.11.209

Park, H. K., Bradley, J. S., & Gover, B. N. (2008). Evaluating airborne sound insulation in terms of speech intelligibility. *The Journal of the Acoustical Society of America*, *123*(3), 1458–1471.

Passivent. (2019). *Passivent*.

Pennycook, K. (2009). *The illustrated guide to ventilation*. Bsria.

Peppes, A. A., Santamouris, M., & Asimakopoulos, D. N. (2001). Buoyancy-driven flow through a stairwell. *Building and Environment*, *36*(2), 167–180.

Perera, M., Marshall, S. G., & Solomon, E. W. (1993). Controlled background ventilation for large commercial buildings. *Building Services Engineering Research and Technology*, *14*(3), 81–86.

Persily, A. K., & Gorfain, J. (2004). *Analysis of ventilation data from the US Environmental Protection Agency building assessment survey and evaluation (BASE) study*. US Department of Commerce, Technology Administration, National Institute of~….

Pivac, N., Nižetić, S., Bajc, T., Zanki, V., & Papadopoulos, A. (2019). The use of the wearable sensory devices for metabolic rate estimation. *Zbornik 50. Me{\dj}unarodnog Kongresa o KGH*, 417.

Qadir, Z., Khan, S. I., Khalaji, E., Munawar, H. S., Al-Turjman, F., Mahmud, M. A. P., Kouzani, A. Z., & Le, K. (2021). Predicting the energy output of hybrid PV--wind renewable energy system using feature selection technique for smart grids. *Energy Reports*, *7*, 8465–8475.

Raftery, P., Keane, M., & O'Donnell, J. (2011). Calibrating whole building energy models: An evidence-based methodology. *Energy and Buildings*, *43*(9), 2356–2364. https://doi.org/10.1016/J.ENBUILD.2011.05.020

Ramponi, R., Costola, D., Angelotti, A., Blocken, B. J. E., Hensen, J. L. M., & others. (2011). Evaluation of wind-driven ventilation in building energy simulation: sensitivity to pressure coefficients. *Cleantech for Sustainable Buildings Conference. Lausanne, Switzerland*, 949–954.

Refsgaard, J. C., van der Sluijs, J. P., Højberg, A. L., & Vanrolleghem, P. A. (2007). Uncertainty in the environmental modelling process – A framework and guidance. *Environmental Modelling & Software*, *22*(11), 1543–1556. https://doi.org/https://doi.org/10.1016/j.envsoft.2007.02.004

Renson. (2023). *Invisido 469*. http://www.aluplasto.pt/uploads/pdfProdutos/renson/grelha469.pdf

Reynolds, A. J., Mokhtarzadeh-Dehghan, M. R., & Zohrabian, A. S. (1988). The modelling of stairwell flows. *Building and Environment*, *23*(1), 63–66. https://doi.org/https://doi.org/10.1016/0360-1323(88)90019-4

Richardson, I., Thomson, M., & Infield, D. (2008). A high-resolution domestic building occupancy model for energy demand simulations. *Energy and Buildings*, *40*(8), 1560–1566.

Rida, M. (2020). *Towards an improved representation of building occupant's thermal interaction, integrating detailed occupant thermal models within building simulation*.

Riffat, S. B. (1991). Domestic kitchen exhaust systems: Performance assessment. *Building Services Engineering Research and Technology*, *12*(1), 45–48.

Roetzel, A., Tsangrassoulis, A., Dietrich, U., & Busching, S. (2010). A review of occupant control on natural ventilation. *Renewable and Sustainable Energy Reviews*, *14*(3), 1001–1013.

Rojas, G., Fletcher, M., Johnston, D., & Siddall, M. (2024). A review of the indoor air quality in residential Passive House dwellings. *Energy and Buildings*, *306*, 113883. https://doi.org/https://doi.org/10.1016/j.enbuild.2023.113883

Royapoor, M., & Roskilly, T. (2015). Building model calibration using energy and environmental data. *Energy & Buildings*, *94*, 109–120. https://doi.org/10.1016/j.enbuild.2015.02.050

Ruxton, G. D., & Beauchamp, G. (2008). Time for some a priori thinking about post hoc testing. *Behavioral Ecology*, *19*(3), 690–693. https://doi.org/10.1093/beheco/arn020

Sahal, N., & Lacasse, M. A. (2005). Water entry function of a hardboard siding-clad wood stud wall. *Building and Environment*, *40*(11), 1479–1491.

Saini, N., Shiel, P., West, R. P., Kerrigan, R., & Pyburn, I. (2020). *Impact of occupant behaviour on indoor environment of A-rated dwellings*.

Sakiyama, N. R. M., Mazzaferro, L., Carlo, J. C., Bejat, T., & Garrecht, H. (2021). Natural ventilation potential from weather analyses and building simulation. *Energy and Buildings*, *231*, 110596.

Salvati, A., Palme, M., Chiesa, G., & Kolokotroni, M. (2020). Built form, urban climate and building energy modelling: case-studies in Rome and Antofagasta. *Journal of Building Performance Simulation*, *13*(2), 209–225. https://doi.org/10.1080/19401493.2019.1707876

Samuel, A. A., & Strachan, P. (2006). An integrated approach to indoor contaminant modeling. *HVAC and R Research*, *12*, 599–619. https://doi.org/10.1080/10789669.2006.10391197

SAP DECC. (2023). *The Government's Standard Assessment Procedure for Energy Rating* *of Dwellings (SAP)*.

Sarna, I., Ferdyn-Grygierek, J., & Grygierek, K. (2022). Thermal Model Validation Process for Building Environment Simulation: A Case Study for Single-Family House. *Atmosphere*, *13*(8). https://doi.org/10.3390/atmos13081295

Satish, U., Fisk, W. B., Mendell, M. J., Eliseeva, K., Hotchi, T., Sullivan, D., Cleckner, L. B., Shekhar, K., & Teng, K. (2011). Impact of CO2 on human decision making and productivity. *Journal of Applied Social Psychology*, *23*, 847–866.

Satish, U., Fisk, W. B., Mendell, M. J., Eliseeva, K., Hotchi, T., Sullivan, D., Cleckner, L. B., Shekhar, K., Teng, K., Berkeley, L., & Laboratories, N. (2005). *Impact of CO 2 on human decision making and productivity*. 2–3.

Savage, N. H., Agnew, P., Davis, L. S., Ordóñez, C., Thorpe, R., Johnson, C. E., O'Connor, F. M., & Dalvi, M. (2013). Air quality modelling using the Met Office Unified Model (AQUM OS24-26): model description and initial evaluation. *Geoscientific Model Development*, *6*(2), 353.

Schweiker, M. (2017). Understanding occupants' behaviour for energy efficiency in buildings. *Current Sustainable/Renewable Energy Reports*, *4*, 8–14.

Scottish Government. (2017). *Supporting Guidance Domestic Ventilation 2nd Edition*.

Scottish Government. (2023). *Building Standards Collections*. https://www.gov.scot/collections/building-standards

Selamet, A., Xu, M. B., Lee, I.-J., & Huff, N. T. (2005). Analytical approach for sound attenuation in perforated dissipative silencers with inlet/outlet extensions. *The Journal of the Acoustical Society of America*, *117*(4), 2078–2089.

SeppĘnen, O. (2008). Ventilation Strategies for Good Indoor Air Quality and Energy Efficiency. *International Journal of Ventilation*, *6*(4), 297–306. https://doi.org/10.1080/14733315.2008.11683785

Sharpe, P., Jones, B., Wilson, R., & Iddon, C. (2021). What we think we know about the aerodynamic performance of windows. *Energy and Buildings*, *231*, 110556. https://doi.org/10.1016/j.enbuild.2020.110556

Sharpe, T., Farren, P., Howieson, S., Tuohy, P., & McQuillan, J. (2015). Occupant interactions and effectiveness of natural ventilation strategies in contemporary new housing in Scotland, UK. *International Journal of Environmental Research and Public Health*, *12*(7), 8480–8497. https://doi.org/10.3390/ijerph120708480

Sharpe, T., McGill, G., Dancer, S. J., King, M.-F., Fletcher, L., & Noakes, C. J. (2020). Influence of ventilation use and occupant behaviour on surface microorganisms in contemporary social housing. *Scientific Reports*, *10*(1), 11841.

Sharpe, T., McGill, G., McQuillan, J., Lantschner, B., Morgan, C., & Tuohy, P. (2019). *Ability of decentralised mechanical ventilation to act as 'whole-house'ventilation systems in new-build dwellings*.

Sherman, M. H. (1980). *Infiltration-pressurization correlation: Simplified physical modeling*.

Sherman, M. H., & Grimsrud, D. T. (1980). *Measurement of infiltration using fan pressurization and weather data*.

Shree, V., Marwaha, B. M., & Awasthi, P. (2019). Assessment of indoor air quality in buildings using CFD: A brief review. *International Journal of Mathematical, Engineering and Management Sciences*, *4*(5), 1154.

Silva, H. E., & Henriques, F. M. A. (2021). The impact of tourism on the conservation and IAQ of cultural heritage: The case of the Monastery of Jerónimos (Portugal). *Building and Environment*, *190*, 107536.

Simiu, E., Scanlan, R. H., Sachs, P., & Griffin, O. M. (1980). *Wind effects on structures: an introduction to wind engineering and wind forces in engineering*.

Singh, M., & Sharston, R. (2022). A literature review of building energy simulation and computational fluid dynamics co-simulation strategies and its implications on the accuracy of energy predictions. *Building Services Engineering Research and Technology*, *43*(1), 113–138. https://doi.org/10.1177/01436244211020465

Standard, B. (1991). BS EN 5925: Code of practice for design of buildings: ventilation principles and designingfor natural ventilation. *British Standards Institution, London*, *1991*.

Standard, B. (2004). EN13141-1: 2004 Ventilation for buildings--Performance testing of components/products for residential ventilation--Part 1: Externally and internally mounted air transfer devices. *BSI London*.

Stanke, D. A., Danks, R. A., Muller, C. O., Hedrick, R. L., Fisher, F. J., Osborn, J. E., Butler, D. S., Gallo, F. M., Rasmussen, R. D., Alevantis, L. E., Girman, J. R., Rogers, L. J., Schoen, L. J., Bellenger, L. G., Houston, T. P., Howard, E. P., Sheinman, H. M., Howard, R. L., Siano, D. M., … Marriott, C. E. (2007). Ventilation for acceptable indoor air quality. *ASHRAE Standard*, *2007*(62.1-2007), 1–41.

Strachan, P. A. Ã., Kokogiannakis, G., & Macdonald, I. A. (2008). *History and development of validation with the ESP-r simulation program*. *43*, 601–609. https://doi.org/10.1016/j.buildenv.2006.06.025

Strøm-Tejsen, P., Zukowska, D., Wargocki, P., & Wyon, D. P. (2016). The effects of bedroom air quality on sleep and next-day performance. *Indoor Air*, *26*(5), 679–686. https://doi.org/10.1111/ina.12254

Sun, K., Yan, D., Hong, T., & Guo, S. (2014). Stochastic modeling of overtime occupancy and its application in building energy simulation and calibration. *Building and Environment*, *79*, 1–12.

Sundell, J., Levin, H., Nazaroff, W. W., Cain, W. S., Fisk, W. J., Grimsrud, D. T., Gyntelberg, F., Li, Y., Persily, A. K., Pickering, A. C., Samet, J. M., Spengler, J. D., Taylor, S. T., & Weschler, C. J. (2011). Ventilation rates and health: multidisciplinary review of the scientific literature. *Indoor Air*, *21*(3), 191–204. https://doi.org/10.1111/j.1600-0668.2010.00703.x

Swami, M. V, & Chandra, S. (1988). Correlations for pressure distribution on buildings and calculation of natural-ventilation airflow. *ASHRAE Transactions*, *94*(1), 243–266.

Tamura, Y. (2012). Aerodynamic database for low-rise buildings, Global Center of Excellence Program, Tokyo Polytechnic University. *Database*.

Tan, G. (2005). *Study of natural ventilation design by integrating the multi-zone model with CFD simulation*. Massachusetts Institute of Technology.

Thomas, D. A., & Dick, B. A. (1953). Air infiltration through gaps around windows. *Journal of the Institution of Heating and Ventilating Engineers*, *21*, 85–97.

Titon. (n.d.). *Titon Technical Information*.

Toledo, L., Sharpe, T., McGill, G., Howieson, S., McElroy, L. B., Tuohy, P. G., & McQuillan, J. (2023). *Research to identify if changes to guidance in standard 3.14 ventilation in 2015 have been effective in improving ventilation and indoor air quality*.

Tomczak, M., & Tomczak, E. (2014). *The need to report effect size estimates revisited. An overview of some recommended measures of effect size*.

Torresin, S., Albatici, R., Aletta, F., Babich, F., Oberman, T., & Kang, J. (2019). Acoustic design criteria in naturally ventilated residential buildings: New research perspectives by applying the indoor soundscape approach. *Applied Sciences*, *9*(24), 5401.

UK Government. (2015). *Approved Document F: Ventilation (2010 Edition Incorporating 2010* *and 2013 Amendments)*. Riba Enterprises. https://books.google.co.uk/books?id=XFztjgEACAAJ

UK Government. (2023). *PM recommits UK to Net Zero by 2050*. Press Release. https://www.gov.uk/government/news/pm-recommits-uk-to-net-zero-by-2050-and-pledges-a-fairer-path-to-achieving-target-to-ease-the-financial-burden-on-british-families

UNFCCC. (2015). *Paris Agreement: Convention on Climate Change*.

Urquhart, R., Richman, R., & Finch, G. (2015). The effect of an enclosure retrofit on air leakage rates for a multi-unit residential case-study building. *Energy and Buildings*, *86*, 35–44.

Van Den Bossche, N., & Janssens, A. (2016). Airtightness and watertightness of window frames: Comparison of performance and requirements. *Building and Environment*, *110*, 129–139. https://doi.org/10.1016/j.buildenv.2016.09.034

Vardoulakis, S., Giagloglou, E., Steinle, S., Davis, A., Sleeuwenhoek, A., Galea, K. S., Dixon, K., & Crawford, J. O. (2020). Indoor exposure to selected air pollutants in the home environment: a systematic review. *International Journal of Environmental Research and Public Health*, *17*(23), 8972.

Vargha, A., & Delaney, H. D. (1998). The Kruskal-Wallis Test and Stochastic Homogeneity. *Journal of Educational and Behavioral Statistics*, *23*(2), 170–192. https://doi.org/10.3102/10769986023002170

Virk, D., & Eames, M. (2016). CIBSE weather files 2016 release: Technical briefing and testing. *CIBSE, London*.

Voigt, E., & Pelikan, J. (2010). *CO2-Measurement during Ventilation*. Dräger Medical Incorporated.

Von Grabe, J., Svoboda, P., & Bäumler, A. (2014). Window ventilation efficiency in the case of buoyancy ventilation. *Energy and Buildings*. https://doi.org/10.1016/j.enbuild.2013.10.006

W.S. Dols, B. J. P. (2015a). *NIST Technical Note 1887 CONTAM User Guide and Program Documentation*. https://nvlpubs.nist.gov/nistpubs/TechnicalNotes/NIST.TN.1887.pdf

W.S. Dols, B. J. P. (2015b). *NIST Technical Note 1887 CONTAM User Guide and Program Documentation*.

Walker, I. S., Sherman, M. H., Joh, J., & Chan, W. R. (2013). Applying Large Datasets to Developing a Better Understanding of Air Leakage Measurement in Homes. *International*

Journal of Ventilation, *11*(4), 323–338.

Walker, I. S., & Wilson, D. J. (1990). *AIM 2: The Alberta air infiltration model.*

Walker, I. S., & Wilson, D. J. (1998). Field Validation of Algebraic Equations for Stack and Wind Driven Air Infiltration Calculations. *HVAC\&R Research*, *4*(2), 119–139. https://doi.org/10.1080/10789669.1998.10391395

Walker, I. S., Wilson, D. J., & Sherman, M. H. (1998). A comparison of the power law to quadratic formulations for air infiltration calculations. *Energy and Buildings*, *27*(3), 293–299. https://doi.org/https://doi.org/10.1016/S0378-7788(97)00047-9

Walton, G. N. (1989). *AIRNET-a computer program for building airflow network modeling.*

Wang, J., Wang, S., Zhang, T., & Battaglia, F. (2017). Assessment of single-sided natural ventilation driven by buoyancy forces through variable window configurations. *Energy & Buildings*, *139*, 762–779. https://doi.org/10.1016/j.enbuild.2017.01.070

Wang, L. (Leon), & Chen, Q. (2008). Evaluation of some assumptions used in multizone airflow network models. *Building and Environment*, *43*(10), 1671–1677. https://doi.org/10.1016/j.buildenv.2007.10.010

Wang, L., & Chen, Q. (2007). Validation of a coupled multizone-CFD program for building airflow and contaminant transport simulations. *HVAC&R Research*, *13*(2), 267–281.

Wang, Q., Pan, Y., Zhu, M., Huang, Z., Tian, W., Zuo, W., Han, X., & Xu, P. (2017). A state-space method for real-time transient simulation of indoor airflow. *Building and Environment*, *126*, 184–194.

Wang, W., Li, S., Guo, S., Ma, M., Feng, S., & Bao, L. (2021). Benchmarking urban local weather with long-term monitoring compared with weather datasets from climate station and EnergyPlus weather (EPW) data. *Energy Reports*, *7*, 6501–6514. https://doi.org/https://doi.org/10.1016/j.egyr.2021.09.108

Wargocki, P., Porras-Salazar, J. A., & Bahnfleth, W. P. (2017). Quantitative relationships between classroom CO 2 concentration and learning in elementary schools. *Aivc*.

Wargocki, P., Sundell, J., Bischof, W., Brundrett, G., Fanger, P. O., Gyntelberg, F., Hanssen, S. O., Harrison, P., Pickering, A., Seppänen, O., & Wouters, P. (2002). Ventilation and health in non-industrial indoor environments: Report from a European Multidisciplinary Scientific Consensus Meeting (EUROVEN). *Indoor Air*, *12*(2), 113–128. https://doi.org/10.1034/j.1600-0668.2002.01145.x

Wei, S., Jones, R., & De Wilde, P. (2014). Driving factors for occupant-controlled space heating in residential buildings. *Energy and Buildings*, *70*, 36–44.

Wei, T. (2013). A review of sensitivity analysis methods in building energy analysis. *Renewable and Sustainable Energy Reviews*, *20*(December 2012), 411–419. https://doi.org/10.1016/j.rser.2012.12.014

Wetter, M. (2006). Multizone airflow model in Modelica. *Proc. of the 5-Th International Modelica Conference*, *2*, 431–440.

Williams, L. J., & Abdi, H. (2010). Post-hoc comparisons. *Encyclopedia of Research Design*, 1060–1067.

Wills, A. D., Berquist, J., Macdonald, I. A., & Banister, C. (2022). *Using Fan Depressurization Test Data in Building Detailed Air Flow Network Models: Approach and Impacts*.

Wong-Parodi, G., Dias, M. B., & Taylor, M. (2018). Effect of Using an Indoor Air Quality Sensor on Perceptions of and Behaviors Toward Air Pollution (Pittsburgh Empowerment Library Study): Online Survey and Interviews. *JMIR MHealth and UHealth*, *6*(3), e48. https://doi.org/10.2196/mhealth.8273

Wu, Y., Liu, Z., & Kong, Z. (2023). Indoor Environmental Quality and Occupant Comfort. *Buildings*, *13*(6). https://doi.org/10.3390/buildings13061400

Yang, C., Shi, H., Yang, X., & Zhao, B. (2010). Research on flow resistance characteristics with different window/door opening angles. *HVAC and R Research*, *16*(6), 813–824. https://doi.org/10.1080/10789669.2010.10390936

Yang, L., Ye, M., & others. (2014). CFD simulation research on residential indoor air quality. *Science of the Total Environment*, *472*, 1137–1144.

Yazici, B., & Yolacan, S. (2007). A comparison of various tests of normality. *Journal of Statistical Computation and Simulation*, *77*(2), 175–183. https://doi.org/10.1080/10629360600678310

Yi, Q., Wang, X., Zhang, G., Li, H., Janke, D., & Amon, T. (2019). Assessing effects of wind speed and wind direction on discharge coefficient of sidewall opening in a dairy building model – A numerical study. *Computers and Electronics in Agriculture*, *162*, 235–245. https://doi.org/https://doi.org/10.1016/j.compag.2019.04.016

Younes, C., Shdid, C. A., & Bitsuamlak, G. (2012). Air infiltration through building envelopes: A review. *Journal of Building Physics*, *35*(3), 267–302. https://doi.org/10.1177/1744259111423085

Yu, S., Eder, B., Dennis, R., Chu, S.-H., & Schwartz, S. E. (2006). New unbiased symmetric metrics for evaluation of air quality models. *Atmospheric Science Letters*, *7*(1), 26–34. https://doi.org/10.1002/asl.125

Zero Carbon Hub. (2016a). *Services Guide*. B.

Zero Carbon Hub. (2016b). *Ventilation in New Homes*. A.

Zhang, B., Liu, Y., Rai, R., & Krovi, V. (2017). Invariant probabilistic sensitivity analysis for building energy models. *Journal of Building Performance Simulation*, *10*(4), 392–405. https://doi.org/10.1080/19401493.2016.1265590

Zhao, Z., Amasyali, K., Chamoun, R., & El-Gohary, N. (2016). Occupants' perceptions about indoor environment comfort and energy related values in commercial and residential buildings. *Procedia Environmental Sciences*, *34*, 631–640.

Zheng, X., & Wood, C. J. (2020). On the power law and quadratic forms for representing the leakage-pressure relationship – Case studies of sheltered chambers. *Energy and Buildings*, *226*, 110380. https://doi.org/https://doi.org/10.1016/j.enbuild.2020.110380

Zou, P. X. W., Wagle, D., & Alam, M. (2019). Strategies for minimizing building energy performance gaps between the design intend and the reality. *Energy and Buildings*, *191*, 31–41. https://doi.org/https://doi.org/10.1016/j.enbuild.2019.03.013

Appendix 1

Correlation Analysis of Monitored CO_2 Dataset from the Survey Study for Occupied Hours in the Main Bedrooms

From the survey study, night-time CO_2 concentrations for the whole dataset for the occupied hours are filtered and means are calculated. These means are used to calculate Pearson Correlation with parameter variables.

Figure Appendix.1 shows the scatter plots for the listed parameters providing a snapshot suggesting that ensuite bathroom has strongest correlation with mean CO_2 values. Lower values are expected for the bedrooms with an ensuite. It is evident from the correlations that the flow path area and distance between inlet and outlet is of higher importance.

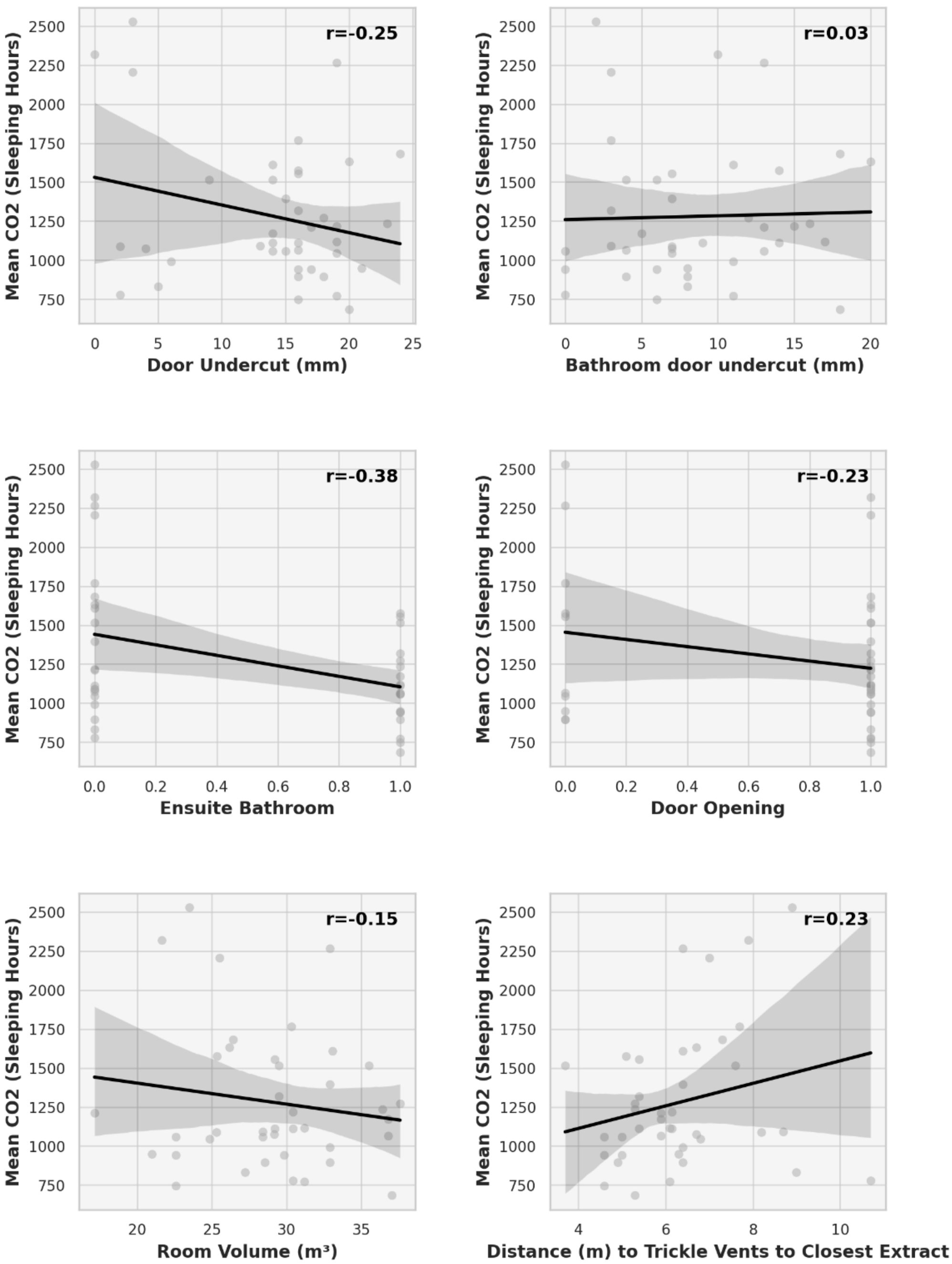

Figure Appendix.1: Pearson correlation for listed parameters with mean CO_2 in each bedroom during night-time sleeping hours.

This analysis suggests that both flow area between zones and distance between inlet and outlet carry high significance for safer CO_2 concentrations. It can be implied that by an inclusion of an added flow area/reduced airflow resistance between zones such that it minimised the distance between trickle vents and the extract would significantly reduce the occurrence of unsafe CO_2 levels. This has further informed the implementation of interzone openings to tackle such CO_2 levels.